AN EXPERIMENTAL STUDY OF THE DYNAMICS OF CATENARY MOORING LINES

JOHN F. CROSS, B.Sc.

An Experimental Study of the Dynamics of Catenary Mooring Lines

by

© John F. Cross BSc.

A thesis submitted to the School of Graduate Studies
in partial fulfillment of the requirements for the degree of
Master of Engineering

Faculty of Engineering and Applied Science
Memorial University of Newfoundland
June, 1992

St. John's Newfoundland Canada

ISBN 0-315-78102-5

Abstract

This work examines the dynamic forces that are generated in catenary mooring lines when the top part of the line is subjected to a forcing function. The forcing function consists of a sinusoidal motion of fixed amplitude but varying frequency and varying angle in the vertical plane. The effect of changes in the pretension in the chain is also examined.

Four different areas of response are classified by the response of the line and the characteristics of the force in the line observed over time. The force in each area is examined and the mechanism that generates these forces is discussed. The change of these forces with changes in the forcing function at the top end of the line is also examined.

The model parameters for the catenary mooring system are identified and model tests performed. From these model tests it is possible to conclude that large structures such as oil rigs and large vessels will cause mooring lines to respond in a range where dynamic forces need not be taken into account. However, smaller objects such as buoys will suffer significant dynamic forces.

Dedication

To my mother Jessica Margaret Eyre Ford Cross (1928-1990). From whom I learned the most about engineering.

Acknowledgements

Although my name is the sole name on the cover of this thesis I have incurred the aid of many in bringing it to a successful conclusion. First and foremost I would like to thank my supervisor Dr. M. Booton for his excellent guidance and advice. His calm approach to problem solving helped me many times.

I am grateful for financial support from the Center for Cold Ocean Resources Engineering in the form of a C-CORE fellowship and also to the Natural Science and Engineering Research Council for support in the form of an NSERC post-graduate scholarship.

I am also indebted to many others such as Mr. Hussein and Dr. Marshall who helped me perform my experiments. I am also grateful to the staff of the wavetank, the machine shop and the Center for Computer Aided Engineering for their help and guidance. Ginny as she usually does sorted me out when I became entangled in mathematical expressions. And also, my thanks to the Engineering Graduate Student Body for their advice and support.

Contents

List of Figures

List of Tables

List of Symbols

T_h	horizontal component of line tension
T_v	vertical component of line tension
H	water depth
S	scope of the mooring line
w	weight per unit length of line
ψ	tangent angle at the top end of the line
θ	angle of inclination of the line of action
R	the amplitude of the motion of the forcing function
ω	the frequency of the forcing function
μ	water dynamic viscosity
ρ_f	water density
m_c	modified mass of the chain
E	effective Young's modulus
D	parameter for chain diameter
g	gravitational acceleration
T	the total tension in the line
ν	water kinematic viscosity
V	velocity amplitude of the forcing function

Chapter 1

Introduction

In the ocean environment there are many forces that act on a moored object. Because it is difficult to design a system to maintain an object completely stationary when facing these forces, most mooring systems allow a degree of movement. The catenary mooring system is the most common system of this type.

The techniques for the static analysis of a catenary mooring are well established. However the dynamic analysis can be quite complicated because of the contributions from pretension, hydrodynamic drag (and related factors such as vortex shedding), inertial effects and added mass. Although some analytical models exist, there is a shortage of experimental data. This thesis will provide some data on the properties of the dynamics of mooring chains.

Some of the previous studies indicate that there are very large dynamic loads generated in mooring lines. Published data indicate that these loads can reach a magnitude of ten times that of the static load. At the present time, moorings are designed based on expected static tension and on previous experience. The accurate prediction of dynamic loads would improve the selection process.

This thesis describes experiments that will examine the dynamics of catenary

mooring systems. Experiments took place in the Memorial University of Newfoundland wave tank. A support structure on which a motor was mounted was placed just above the water surface. The motor oscillated a block in a straight line. One end of the chain was attached to this block through a tension measuring device.

The motor speed was varied to provide specified excitation frequencies. The support structure could be tilted allowing the translational oscillations to occur at different orientations in the vertical plane. The static tension could also be varied.

The work had several objectives which were composed of two primary objective and several secondary objectives. These objectives are listed below with the primary objectives given first. In summary, the objectives of the experiment were to determine:

1 the magnitude of the dynamic forces present in an oscillating mooring chain (primary objective),

2 whether the dynamic forces were more prominent in one particular orientation (primary objective),

3 how the static tension affects the dynamic tension (secondary objective),

4 if the four conditions that Suhara et al, (1981) identified could be found in the slack condition (secondary objective),

5 what the model scale effects are; *ie* how the experiment relates to the ocean environment (secondary objective).

To introduce the topic, a brief description of the catenary mooring system is given in Chapter 2. Past work in this field and related fields is examined in Chapter 3, followed by the derivation of a dimensionless equation describing an oscillating mooring chain in Chapter 4. The apparatus and procedure will be examined in Chapter 5. Chapter 6 will discuss the results from this work and Chapter 7 will draw conclusions about the experiments. Some recommendations regarding future work will be made in Chapter 8.

Chapter 2

The Catenary Mooring System

The catenary mooring system takes its name from the shape of the curve formed by the mooring line (the word catenary is from the latin catena or chain). This curve is characteristic to any line which is suspended from two points and which has a uniform weight per unit length and negligible bending stiffness. The derivation of the basic equations for the catenary line is given in Appendix A. The length of the line from the top to where it touches the bottom is called the scope of the line. The scope and other terminology relating to the catenary mooring system is shown in Figure 2.1.

The catenary mooring system has been traditionally used by ships and other sea going vessels for several reasons. The system can be easily and compactly stowed when not in use, it requires little maintenance, it uses simple easily obtainable materials, and in spite of its simplicity, it provides a remarkably effective way to position a floating object. If the top end of the chain is moved, a restoring force is created. The restoring force is small at first but increases very rapidly. A descriptive analysis of the mooring system would be as follows.

If there are no displacing forces on the moored object, the mooring chain will

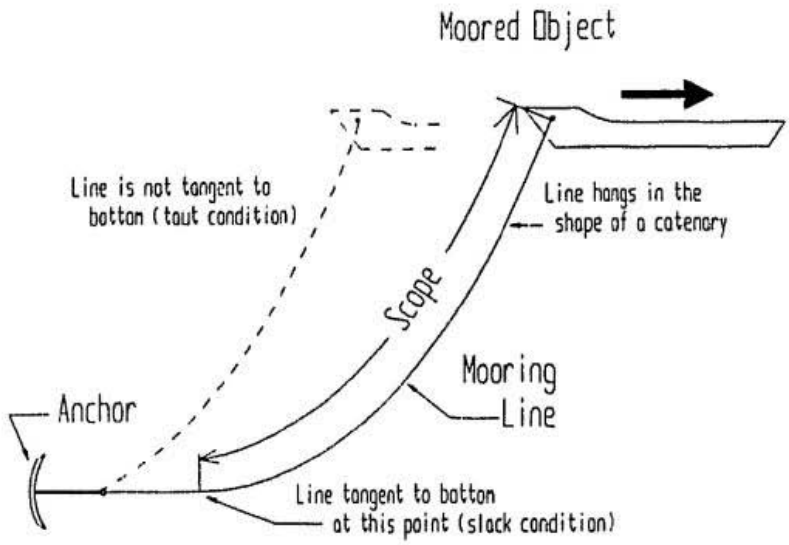

Figure 2.1: The Catenary Mooring System

hang in a vertical line as shown in Figure 2.2. As soon as the moored object is displaced, two events will take place. First, some of the chain will be picked up from the bottom. Second, the chain will start to make an angle with the moored object away from the vertical. It is a combination of these effects that cause the chain to apply a restoring force on the moored object.

As chain is picked up off the bottom more weight needs to be supported at the top. This will show up as an increase in the tension. Also, since the line makes an angle with the vertical, there will now be a component of force generated in the horizontal direction. This horizontal force is what counteracts the displacing force. To hold the chain against horizontal forces an anchor is used.

The effectiveness of the mooring system can be seen in Figure 2.2. The diagram is drawn to scale and it shows that as the displacing force increases from 0.2 units

to 20 units, the actual displacement increases by a factor of about 4. The force unit in this case is the weight of a length of mooring line equal to the depth of the water.

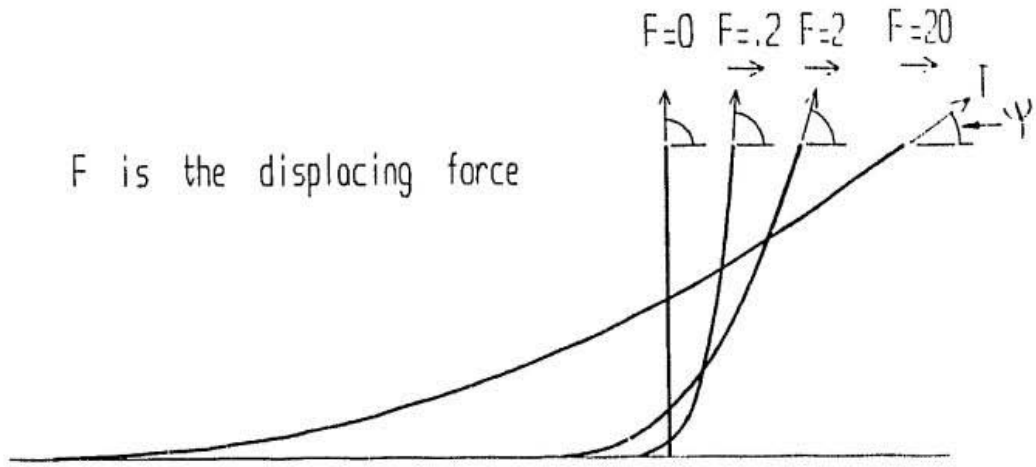

Figure 2.2: A Catenary Mooring System Under Horizontal Loads

Catenary systems can be classified as either taut or slack. In the slack case the lower end of the chain is tangent to and touching the bottom. At this point there are only horizontal forces in the chain which must be resisted by the anchor and the friction of the sea bed. In the taut case, the chain is never tangent to the bottom and stops at the anchor forming an angle with the bottom. In this circumstance, the anchor must resist a vertical force as well as a horizontal one. In this experiment, the chain is maintained in the slack condition at all times.

The basic equations for the catenary mooring system are given below. There is no explicit equation for tension and so an iterative technique must be used. These equations solve for T_x and T_y (the horizontal and vertical components of

the tension in terms of: water depth, H; scope, S; and weight per unit length, w. The derivation for these equations can be found in Appendix A. Other equations using different input variables can be derived depending on what values you wish to use as input.

$$\begin{aligned} T_x &= T\cos\psi \\ T_y &= T\sin\psi = wS \end{aligned} \tag{2.1}$$

$$H = \frac{T\cos\psi}{w}\cosh\left(\sinh^{-1}\frac{Sw}{T\cos\psi}\right) - \frac{T\cos\psi}{w} \tag{2.2}$$

Chapter 3

Review of Previous Work

The study of the dynamics of mooring chains has received a great deal of attention, at least in theoretical developments. Parnell and Hicks (1976) state that over 500 papers have been published that deal with cable dynamics. However they go on to say that experimental data are limited. Pattison (1974) agrees with this and states that although analytical models exist, data are scarce.

This review will be divided into four sections. The first will discuss the simple static problem as it applies in the marine environment. Then, experimental work will be reviewed, followed by an examination of various numerical and computer techniques for finding dynamic forces in mooring lines. Finally, a brief review of a relatively new topic, statistical treatment of dynamic forces in mooring lines, will be undertaken.

3.1 The Static Problem

A good place to start looking at the dynamics of mooring lines is with the static problem. The static analysis has been fairly well studied and can be found in several books on differential calculus (Fox (1950) and Edwards and Penney (1982)

for example.) The basic approach is to solve the geometric catenary equations.

One of the earliest and best analysis of catenary problems as they apply to the ocean environment is given by Collipp et al(1962). They use the geometric approach to derive the basic catenary equations which are then used to draw up tables that give properties such as tension, angle the cable makes in the vertical plane and potential energy in the cable. However the parameter they use for entry into the tables may, in some cases, be awkward. Their parameter requires knowing the depth of water, the scope of the cable and the horizontal distance that the scope covers. The equations shown in Chapter 2 give the same result, but require just the scope and depth of water.

Because of the non-linear relation between the displacement and restoring force the use of tables and charts figure prominently in the analysis of mooring systems. Adams (1969) and Radwan et al (1986) use tables as an aid to the design of mooring systems. Even today when computers can give exact solutions the speed and ease of use of tables still make them popular.

Along with tables, there was some attempt to linearize the equations. Ogawa (1984) tried this and used a linearization coefficient matrix to represent line tensions as a linear function of displacement. However, as with all such methods, it is inaccurate outside certain limits.

The use of numerical techniques to solve the equations became popular with the wide spread use of computers. Nielsen (1976) used a Newton-Raphson root solving algorithm to match restoring forces to external loads. The shape of the force versus displacement curve lends itself well to solution by the Newton-Raphson technique.

A program which solves the static problem of a catenary system has been written and is included in Appendix B. It uses the equations derived by Collipp et al (1962) along with a Newton-Raphson algorithm. The results generated by this program are identical to those published by Collipp, Borgman and Miller.

3.2 Experimental Work

Some of the earliest thoughts given to designing experiments were directed towards scale model tests. Collier (1972) attempted to derive scale laws for a moored buoy in an ocean current by using the governing equations. Constants were introduced to relate the model and the prototype properties such as mass, force and length. Substitution of these constants into the governing equations allow a relationship between the constants to be determined. Dimensionless numbers were then drawn up. Collier used a distorted scale to achieve dynamic similarity in his model laws. While this does have the advantage of avoiding problems that are typical in hydroelastic models (*ie* the inability to scale all the relevant parameters), it does have the disadvantage that the cable oscillatory velocity must be small compared to the current speed which in the majority of cases is an unrealistic assumption. Unfortunately, Collier did not do tests using this idea and no record of any tests with a distorted scale can be found.

Parnell and Hicks (1976) also use the governing equations to derive their dimensionless numbers. However their analysis differs from Collier in that they do not use a distorted scale. They ignore the hydrodynamic force tangent to the cable by stating that it is small compared to the normal force. The normal force is accounted for by a 'hydrodynamic force parameter' which is the drag coefficient

for a cylinder multiplied by the ratio of cable length to diameter. Parnell and Hicks go on to state that it is difficult to scale all the relevant parameters. Their solution was to do the tests in a fluid with a much higher viscosity than water. This solution is well known to hydraulic modelers, but it appears that no one has used this idea to model a catenary.

Experimental examination of the dynamics of mooring cables seems to have started in the mid 1970's with the work of two projects. Pattison (1974) seems to have been the first to publish experimental work followed by van Sluijis and Blok (1977) several years later.

Pattison's purpose was to perform experiments on several different kinds of mooring line material and develop these into a data base for analytical model validation. The method was to oscillate a slider sinusoidally in the vertical plane by means of a drive cable attached to a rotating crank arm. The mooring line was joined to the slider via a two way force dynamometer. Five different mooring line materials were tested with scope to depth ratios between 1.1 and 1.6 and a frequency of motion between 0.1 and 2.2 Hz. Dynamic tensions up to 1.2 times that of the static tension were recorded. Higher loads were recorded but were ignored as being unrealistic of conditions at sea.

Unfortunately Pattison had some problems with his experiment. He reported problems with the two way force transducer that he used in his experiments. It appears that the transducers were coupled and he spent quite a bit of his analysis trying to decouple the forces. Also, although he reported sinusoidal oscillations, from the way his equipment was set up he would actually produce motion with two sinusoidal components. It would be impossible to say what the effect of the

second component would be without knowing more about his equipment.

van Sluijs and Blok (1977) also preformed similar experiments except that they oscillated the cable in a horizontal plane. They reported an increase of dynamic tension with an increase of frequency up to a maximum. After this maximum, increasing the frequency caused a decrease in the tension. They also reported that there was no significant scale error in the dynamic effect. (More will be said about this in Chapter 6).

In the mid 1980's there were also two published reports of experimental work. These were done by van den Boom (1985) and Suhara et al (1981).

van den Boom conducted experiments involving the harmonic oscillation of mooring lines. He does not say if the oscillations were horizontal or vertical but the impression is that they were horizontal. No scaling parameters for the experiment were given but it is stated that the scaling was carried out according to Froude's law of similitude.

It is hard to see how Froude's law would be applicable in a case like this and other analysis do not have the Froude number as an important consideration. Thus it would seem that van den Boom's attempts at modelling were in error. However, the experimental results do show the expected rise and drop off in dynamic tension with increasing frequency of the forcing function.

Suhara et al did their tests with both horizontal and vertical oscillations and used scope to depth ratios between 2.8 and 8.3. They also used a wide range of frequencies for the forcing oscillations and several different amplitudes.

One important outcome from their work was the classification of the results by the means of several dimensionless parameters. The static condition is determined

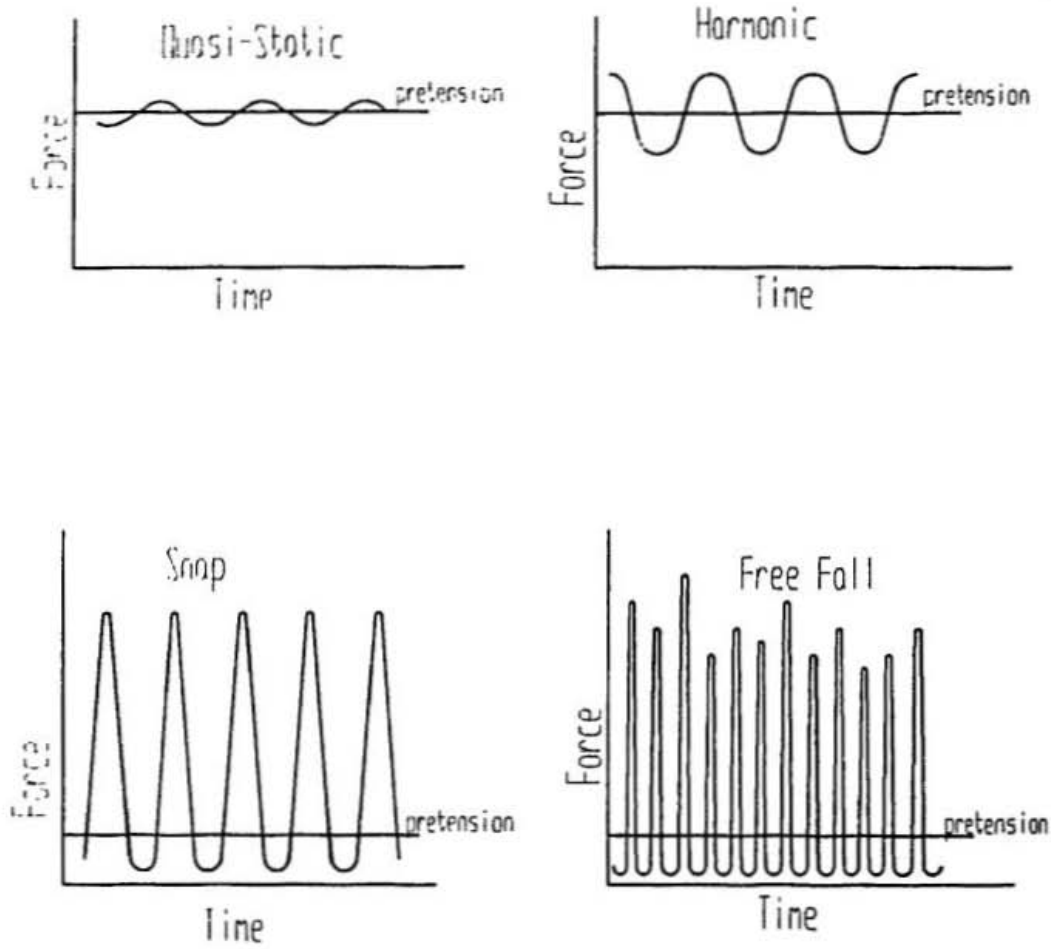

Figure 3.1: Force-time traces for the four conditions

by the ratio wX_0/T_{H0} where w is the weight per unit length, X_0 is the amplitude of motion of the top part of the chain, and T_{H0} is the static horizontal tension. The dynamic characteristics are determined by two ratios: 1) Z_m/D_c where Z_m is the vertical displacement of the center of gravity of the catenary part and D_c is the diameter of a cylinder with the same volume as the chain, and 2) the ratio $Z_m\omega^2/g$ where ω is the frequency of the oscillation and g is gravitational acceleration.

Using these parameters they identified four conditions. The first is a quasi-

static condition where the dynamic tensions can be calculated by the position of the top end and the static formula. Second is a harmonic oscillation condition. The third is called a snap condition and shows what happens when the cable goes taut. The last is a free-fall condition and in it parts of the chain actually fall until brought up by the rest of the chain generating impact forces. The first two conditions seem to be what Pattison (1974) recorded.

Since part of this work was to identify these four stages, some time should be taken here to examine what happens in the four stages. The first stage was described above and nothing more needs to be said except that the primary contribution to the line tension is from the static pre-tension. In the harmonic oscillation region, the force trace in the time domain appears close to sinusoidal. In this area the inertial forces of the chain and the fluid properties of added mass and drag are the primary contributors to the line tension.

In the snap region, a new mechanism come into play. The minimum tension in the chain, which until this time has been greater than zero, becomes zero (since a chain cannot support compressive loads, the tension can never be less than zero). This means that for a brief amount of time, the links of the chain are not supporting any load. This takes place while the top of the chain is moving in a direction towards the anchor (in a direction that slackens the chain). When the direction reverses (so that the top part is now moving in a direction that increases the tension of the chain), the slackening suddenly stops. This sudden stopping of the links as they fall generates impact loading. The magnitude of the impact loads are dependant upon the time that the links had no tension on them. It is these impact loads that cause the extremely high tensions that are associated with

dynamic forces. Because of the shape of the catenary and the length of the line, not all the links take part in this phenomena. However, as the speed of the top part increases, more and more links come into play and this causes the increasing impact forces.

Eventually a time comes where the top is moving so fast that it is able to reach the end of its run and start back before the remainder of the chain can respond. Now, fewer and fewer links are involved and the time the links are allowed to fall, free of forces in the chain, becomes smaller so the dynamic forces start to decrease. This is the free-fall region characterised by the decrease in the dynamic forces.

Suhara et al (1981) also compared their results to a theoretical prediction method called the lumped mass method. Agreement was good in conditions 1 and 2 but was significantly off for conditions 3 and 4.

Another paper discussing the derivation of the dimensionless parameters relevant to oscillating mooring lines is by Papazoglou et al(1990). They used the method of governing equations to derive the important parameters. They also recognized that for deep water moorings the elasticity of the cable is an important consideration in the calculation of dynamic forces.

They have proposed a modeling scheme where all parameters except for the elasticity parameter are met as well as possible and then the elasticity is modelled with springs.

The idea of using springs to compensate for the inability to correctly model the scaling parameters is also presented in a report by Faure (1989). Faure used a set of springs that best simulated the catenary effect and the elasticity of the missing section as well as compensated for the elasticity of the remaining model.

Unfortunately no mention of the modelling parameters is made except to say that line lengths and weights were scaled correctly.

3.3 Numerical Calculations of Mooring Line Dynamics

Numerical simulations of the dynamics of mooring lines have been abundant in the past. Due to non-linear materials, non-linear drag coefficients, non-linear forcing functions and non-linearities due to the nature of the catenary, a purely analytical approach was impossible. There was some thought given to linearizing the equations of motion and using other types of analysis such as perturbation expansions, however these methods were inaccurate outside certain limits. Computer run numerical simulations seemed to provide the best tool for analyzing the problem.

Computer programs to solve the quasi-static problem are relatively easy to create and very inexpensive in CPU time to run and these were the first attempt to solve the problem. However, using the quasi-static approach meant that the most interesting phenomena were ignored. Sometimes the quasi-static method is still used but this is usually for a special application (Nakajima (1986)) and, even so, it can be misleading.

To handle the non-linearities of the system several numerical techniques were derived. The most powerful of these proved to be some sort of discrete element technique. There are two main types of discrete element algorithms used to analyze the motions of mooring lines. They are the known as the finite element method and the lumped mass method and a good review of the two methods is

given by van den Boom (1985). There have been a large number of schemes for either method proposed.

In the finite element method the cable is broken into a number of segments with a set of assumed behaviour functions. These equations are applied to the kinematic and dynamic equilibrium equations as well as the equations describing the material properties.

Johansson (1978) proposed a finite element model with linearly elastic material properties and a constant drag coefficient. Webster (1981) developed a program called SEADYN based on the finite element method. SEADYN broke the problem into two parts, one dealing with the quasi-static solution, the other handling the dynamic aspects. The program could handle non-linear materials and it attempted to model fluid forces as well as strumming phenomena. One of the best finite element models is that proposed by Hwang (1986). As well as an improved method of accounting for drag, it was able to handle composite lines (lines where two or more materials are joined together) and clumped weights. It also used a 3-dimensional analysis of the line.

The other main method used was the lumped mass method. The lumped mass method was first proposed by Walton and Polacheck (as reported in van den Boom (1985)). It involves the lumping of the mass and the external and internal forces of the line at a number of discrete points. Equations of equilibrium and continuity at these points or nodes can be derived and then solved using numerical methods. Several authors note that the lumped mass method seems to be more computationally efficient than the finite element method (van den Boom (1985), Faure (1989)).

The simplest implementation of the lumped mass method would be to work with just one node. Suhara et al (1983, 1987) did this and obtained reasonable results for the smaller frequencies (ie where the dynamic forces were relatively small). Liu (1973) had more elements in his model but the numerical modelling of the fluid drag and added mass was poor and the material was assumed to follow Hooke's law (except when the chain went into compression).

van den Boom (1985) proposed a lumped mass model which he incorporated into a program called DYNLIN. He proposed that the fluid loading of a line is due to the orbital motion of the waves, the current and the motions of the line (it should be noted that his model neglected the wave motions). His 2-dimensional model also included sea floor reaction forces. He reported good agreement with experimental data.

Recently, Faure proposed a model based on van den Boom's model (Faure (1989)). This model had a better representation of bottom reaction forces and bottom friction. It also used Morison's equation to calculate the fluid loading on the lines.

There have also been several attempts to develop computer packages that assist in the design of whole mooring systems, *eg* Owen and Linfoot (1976).

All the numerical methods mentioned above needed some values for the various hydrodynamic coefficients. Some experimenters used previously published data where others such as Faure (1989) came up with their own. It should be mentioned here that the coefficients needed are those that occur in oscillating fluids. While these values are needed for the harmonic oscillating condition, the case is different for the snap and free-fall conditions. In these cases the chain motion is

not harmonic so coefficients measured from random oscillation tests such as those reported by Longoria et al (1991) should be used.

3.4 Statistical Analysis Techniques

With the realization of the existence and magnitude of oscillatory forces and the increased knowledge of metal wear and fatigue, attention was naturally turned to these effects in mooring lines. Shaw (1989) analyzed the problem using wave statistics and a mooring line tension transfer function which he obtained from matching model tests to a numerical simulation. However he was interested in obtaining a method of calculating the cyclic loading that a mooring line would experience and not in determining the mooring line's maximum load.

Sincock and Lalani (1990) were interested in developing guidelines for fatigue analysis of anchor chains. They state that there are two ways to calculate loads in the mooring line: the quasi-static approach and a dynamic procedure. They also go on to talk about some of the design codes in effect for semi-submersibles and floating production units.

The American Bureau of Shipping and Lloyd's make no mention of guidelines for mooring system and leave the specification up to the owner. The UK's guide on offshore installations makes no mention of any specific design methodology by which to calculate loads. The Norwegians allow either a quasi-static or dynamic analysis. The newly drafted American Petroleum Institute's "Recommended Practices for Design, Analysis and Maintenance of Catenary Mooring for Floating Production Systems" does acknowledge the significance of dynamic loading and recommends a time domain dynamic mooring load analysis.

A very good review of general techniques for tension response statistics can be found in Luo (1990). Luo shows that a Gaussian distribution cannot account for the nonlinearities in the system. He goes on to state that significant improvement in the tension ranges can be obtained by using the Weibull distribution.

Computer applications of this method are usually written to solve this specific problem and thus allow more versatility on the part of the person deriving the equations.

Chapter 4

Dimensionless Analysis of a Catenary

The first step in developing an experiment is to determine what is to be measured and the parameters that affect the experiment. Dimensional analysis can show ways in which the parameters can be grouped together. The dimensionless equation is derived here for an oscillating catenary system and then the groups in it are compared to the dimensionless groups found by other experimenters.

4.1 Definition of Physical Parameters

The parameters necessary to describe the system can be divided into three groups. The first group consists of the quantity to be measured in the experiment. The second group contains the input parameters for the experiment. The last group holds the parameters describing properties of the system.

In this experiment the quantity that is to be measured is the tension, T, in the cable. Since the tension is changing along the length of the chain, a position for the tension measurement must be chosen. The two logical places to measure tension are at either end of the chain. The tensions at the bottom are of interest

to those designing anchor systems. In this experiment the forces that the chain would exert on an object are important so tension is measured at the top.

The input parameters describe the initial conditions of the system and the forcing function that will move the top end of the chain. The initial conditions consists of the scope of the chain S, the depth of water H and the angle of inclination the line of action makes with the water, θ. Although the static tension or pre-tension is an important consideration it is not included here because it is set once the scope and depth of water are set.

To describe the forcing function that acts on the cable end, two parameters are needed. First, the frequency at which the oscillation occurs, ω, is important. Second the amplitude of the oscillation, R, is important. Since the oscillation is assumed to be a pure sinusoid, the amplitude can be either a velocity amplitude or a displacement amplitude. Once one is fixed, the other is set. In this case displacement is chosen because it gives a better physical understanding of the model.

The system parameters describe various properties of the physical set up. For the fluid, the important properties are the viscosity, μ, and the density, ρ_f. For the cable the descriptive parameters are a measure of the mass of the chain, m_c, and the effective Young's modulus, E. The measure of the mass of the chain is defined as the density of the chain material minus the fluid density. Thus m_c is seen to have the same units as density but is modified to account for buoyancy. E is called the effective Young's modulus because it is not the Young's modulus of the material but the slope of the stress strain curve for the whole chain.

A final property of the chain that must be described is its drag. Suhara et al

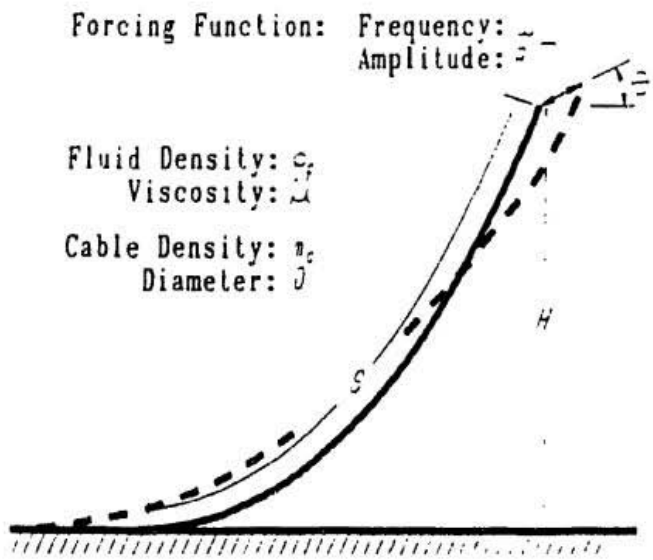

Figure 4.1: Parameters for the catenary mooring system

(1981) used for their parameter the diameter of a cylinder D, having the same volume as the chain parameter. This quantity is just to give a characteristic length to the chain. A last physical parameter that must be included is the gravitational acceleration, g. Figure 4.1 shows these variables.

4.2 Derivation of the Dimensionless Equation

Note that under the properties of the cable, no account was made of the bending stiffness. This is consistent with the catenary analysis which assumes that the bending stiffness of the cable is zero.

These parameters form the functional relation for the system. To start the derivation of the functional relation, the tension is assumed to be a function of the other properties:

$$T = \phi \{\rho_f, \mu, m_c, E, D, S, H, g, R, \omega, \theta\}. \tag{4.1}$$

The quantity θ is already dimensionless and thus may be left out of the analysis for now. Including T in the expression on the right hand side of Equation 4.1 and reordering this expression the following is obtained.

$$\phi \{\rho_f, m_c, \mu, E, T, g, \omega, R, D, H, S\} = 0 \tag{4.2}$$

To allow the greatest amount of control in deriving the functional expression, the method of synthesis with linear proportionalities is used by Sharp (1981). Either the fluid density or the modified cable density is used to cancel the mass dimensions where they appear. The parameters that have units of mass in them are μ, E and T. μ is divided by ρ_f to get ν and E and T are divided by m_c. Also, m_c is divided by ρ_f.

$$\phi \left\{ \nu, \frac{E}{m_c}, \frac{T}{m_c}, g, \omega, S, D, H, R, \frac{m_c}{\rho_f} \right\} = 0. \tag{4.3}$$

Linear proportions are created from the first five parameters $\nu, E/m_c, T/m_c, \omega$ and g, the rest already having dimensions of length except for the term m_c/ρ_f which is dimensionless and, like θ, will be left out from the analysis for now. It is noted that E has the same units as pressure and T is a force. All the possible linear proportions are listed below.

$$\left\{ \frac{\nu^{2/3}}{g^{1/3}}, \frac{E}{m_c g}, \left(\frac{T}{m_c g}\right)^{1/3}, \frac{g}{\omega^2}, \left(\frac{\nu}{\omega}\right)^{1/2}, \left(\frac{T}{E}\right)^{1/2}, \right.$$

$$\left(\frac{E}{m_c\omega^2}\right)^{1/2}, \left(\frac{T}{m_c\omega^2}\right)^{1/4}, \left(\frac{\nu^2 m_c}{E}\right)^{1/2}\Bigg\}.$$

The five parameters should give 10 linear proportions (4 + 3 + 2 + 1) but we only have 9 because linear proportions can not be formed from the parameters ν and T. From the 9 groups only 4 are needed, however each of the variables must be chosen at least once and they must all be interrelated.

A little art and instinct is needed here to select appropriate groups although the groups selected can be compounded to form any of the non-selected groups. However a good place to start is to select the term with T in it. Since T is the quantity we are interested in, only one term with it should be selected. We have a choice of three but the term with T as a ratio of the tension to the weight of the cable figures prominently in the static analysis. Thus the group $(T/m_c g)^{1/3}$ is chosen.

Also, it would be most useful to have E in terms of properties of the cable so $E/m_c g$ is chosen.

The forcing frequency is an important consideration so it should appear in only one factor. This gives a choice of selecting one of the following: g/ω^2, $(E/m_c\omega)^{1/2}$, $(\nu/\omega)^{1/2}$ or $(T/m_c\omega^2)^{1/4}$. The terms with ν and E are eliminated because they are not as relevant to the experiment as the other two terms.

It is possible that the term $T/m_c\omega^2$ could prove to be a very useful parameter, however the other term is selected as g/ω^2 because it is desirable to have T in only one term.

The last term selected is $\nu^{2/3}/g^{1/3}$ and it is chosen to provide the missing parameter, ν. Thus the list of linear proportionalities becomes:

$$\left\{\frac{\nu^{2/3}}{g^{1/3}}, \left(\frac{T}{m_c g}\right)^{1/3}, \left(\frac{E}{m_c g}\right)^{1/2}, \frac{g}{\omega^2}, R, S, H, D\right\}.$$

Now each term is divided by one of the four lengths to make the expression dimensionless. Again, suitable selections must be made that will allow useful parameters to be formed. The term $\nu^{2/3}/g^{1/3}$ is the only term that has both the fluid viscosity and density, so it would make sense that it should be divided by the drag parameter, D. The term $(T/m_c g)$ needs to be divided by three lengths to make it dimensionless. Choosing the terms D^2H will give the ratio of tension to the mass of a length of chain equal to the depth of the water. (Actually, the term differs from this value by a factor of $\pi/4$, however constants, or lack of them do not harm the validity of a dimensional analysis.) The term $E/m_c g$ needs to be divided by only one length to make it dimensionless and S is chosen. It would seem to make sense to have a parameter that contains both the amplitude of motion and the frequency, so g/ω^2 is divided by R. Finally, the length terms are made dimensionless to give R/H, S/H and D/S. Also, the θ term and the m_c/ρ_f are reintroduced into the equation to give:

$$\frac{T}{m_c g D^2 H} = \phi\left\{\frac{\nu^{2/3}}{g^{1/3}D}, \left(\frac{E}{m_c g S}\right), \frac{g}{\omega^2 R}, \frac{R}{D}, \frac{S}{H}, \frac{D}{S}, \frac{m_c}{\rho_f}, \theta\right\}. \qquad (4.4)$$

Several of the parameters in this equation are familiar. The tension term and the ratio S/H are used in the static analysis. The term $\nu^{2/3}/g^{1/3}D$ is a form of the Froude-Reynolds number. Also the term R/D is similar to the Keulegan-Carpenter number.

Parnell and Hicks (1976) gave as their dimensionless parameters: ρ_f/ρ_c, T/mgL, $C_D L/D$, $E/\rho_c g L$ and U_o^2/gL. All the terms except for $C_D L/D$ and U_o^2/gL are

found in equation 4.4. $C_D L/D$ is not there because of the way that the drag is defined (C_D is a measure of the drag) and U_o^2/gL is not there because the experiment is based on the displacement amplitude not the velocity amplitude.

Suhara et al (1981) have as their parameters $wX_o/T_{HO}, Z_m/D_c$ and $Z_m\omega^2/g$. The first parameter listed is just a measure of the static tension. The terms Z_m/D_c and $Z_m\omega^2/g$ can be found in equation 4.4 except that the amplitude of the forcing function is used instead of Z_m which is the motion of the center of gravity of the chain. $g/\omega^2 R$ is very similar to the α term used by Suhara.

4.2.1 Dimensional Analysis Using a Velocity Amplitude

As was mentioned in the previous section the forcing function can be given in terms of a velocity amplitude as well as a displacement amplitude. It is interesting to repeat the dimensional analysis of catenary using this. The equation for tension is now as shown below.

$$T = \phi\{\rho_f, \mu, m_c, E, D, S, H, g, V, \omega, \theta\} \tag{4.5}$$

The initial part of the analysis is carried out exactly as before. This gives the equation as shown below.

$$\phi\left\{\nu, \frac{E}{m_c}, \frac{T}{m_c}, g, \omega, V, S, D, H, \frac{m_c}{\rho_f}\right\} = 0. \tag{4.6}$$

There are now six variables from which linear proportions can be derived. The six variables should give 15 groups of linear proportions, however no groups can be made from the combinations ν and T and E and V so there are actually only 13 groups. These groups are listed below.

$$\left\{\frac{\nu^{2/3}}{g^{1/3}}, \frac{E}{m_c g}, \left(\frac{T}{m_c g}\right)^{1/3}, \frac{g}{\omega^2}, \left(\frac{\nu}{\omega}\right)^{1/2}, \left(\frac{T}{E}\right)^{1/2}, \frac{\nu}{V}, \left(\frac{T}{m_c V^2}\right)^2 \right.$$
$$\left. \frac{V^2}{g}, \frac{V}{\omega}, \left(\frac{E}{m_c \omega^2}\right)^{1/2}, \left(\frac{T}{m_c \omega^2}\right)^{1/4}, \left(\frac{\nu^2 m_c}{E}\right)^{1/2} \right\}.$$

The same rules are used to select the parameters as before except this time five groups are needed. Some of the groups are the same as in the previous method and are still significant parameters so they are selected again. These are the groups $(T/m_c g)^{1/3}$, $(E/m_c g)$ and g/ω^2. There are still two more groups to select, at least one of which must contain ν and one V. There are two groups that fulfill this condition and are familiar. These are the group ν/V (which can be developed into a Reynolds number) and the group V^2/g (which can be developed into a Froude number).

To complete the analysis all terms are divided by one of the lengths in the system to obtain the dimensionless equation below.

$$\frac{T}{m_c g D^2 H} = \phi\left\{\frac{VD}{\nu}, \left(\frac{E}{m_c g S}\right), \frac{g}{\omega^2 R}, \frac{V^2}{Dg}, \frac{S}{H}, \frac{D}{S}, \frac{m_c}{\rho_f}, \theta\right\}. \tag{4.7}$$

There are other groups that can be found here that are familiar. Compounding the group g/ω^2 with V^2/g and taking the square root will give the Keulegan- Carpenter number. Combining the Reynolds number with the Keulegan-Carpenter number will produce the frequency parameter, $\nu/\omega^{\frac{1}{2}}$.

The analysis based on the velocity amplitude gives more of the numbers familar to hydrodynamics. However this is just because of the way that the forcing function is defined. It would be equally possible and valid to repeat the analysis using an acceleration amplitude instead of the velocity amplitude but no new

insights would be gained from this exercise.

4.3 Validation of the Model Using the Static Case

As with many problems in hydrodynamics, it is difficult to prove that the dimensionless equation derived is indeed valid. However, an expression for the dynamics of a catenary mooring system must include the parameters for the static system. Thus, if all the terms that contain information about the dynamics of the system are set equal to zero, the remaining terms must describe the static situation.

To start, examine equation 4.4. The most obvious terms that contain dynamic information are the terms involving frequency of the forcing function and the amplitude of the motions. Thus the term $g/\omega^2 R$ is dropped from the equation. Also since there is no motion, the viscosity of the water is not relevant. The angle θ, the angle that the forcing function acts at is also irrelevant now. The diameter of the cable was important as a drag parameter as was the ratio m_c/ρ_f so they can be removed. The removal of these expressions leaves the following equation that describes the tension in a static catenary.

$$\frac{T}{m_c g D^2 H} = \phi\left\{\left(\frac{E}{m_c g S}\right), \frac{S}{H}\right\}. \tag{4.8}$$

Usually the catenary is assumed to have infinite axial stiffness so the term $E/m_c g S$ is ignored but in some cases (as in Collipp et al (1962)) it is included. Thus the static tension is dependent upon the weight per unit length of chain and the ratio S/H.

Looking at the catenary equation as shown in Chapter 2, we find that this is

the case. This is not surprising, since we started with this equation, however if this had not worked it would have pointed out that there was something wrong with the theory.

4.4 Selection of the Experimental Parameters

From the functional equation (equation 4.4) three parameters were chosen to be the variables in the experiment. These parameters are: $T/m_c g D^2 H, g/\omega^2 R$, and θ . Several notes should be made at this time explaining why these parameters were chosen and why others were not.

It might seem inappropriate to include the tension term in this list since that is what is to be measured, however this is due to the fact that the force that we actually measure is a combination of the static and dynamic force and one of the parameters that is varied is the static tension. These two forces could be separated, however this serves no useful purpose since the dynamic tension that we are interested in is a combination of both.

Since the system will be operating in water and since the constant g will not change significantly, there is no need to change the fluid property ν. Also, the material used to make the model chain is steel which is also the most common material for commercial chains, thus the material property m_c does not need to be changed. This is also true to a certain extent for the Young's modulus of the chain E. However, as E is defined as the Young's modulus for the whole chain, the geometry of the chain becomes important. Nonetheless, this was considered a small effect in shallow water mooring and thus no attempt was made to model it.

This left the following parameters that were important to the experiment:

$T/m_c g D^2 H, g/\omega^2 R$, and θ . To do a complete analysis of the system, these parameters would need to be changed, one at a time, while the others remained constant. However, this soon means that total number of tests needed is too large to be accommodated. Thus some limits had to be imposed.

From previous work it was found that frequency is the single most important parameter, thus it must be varied throughout the tests. Also, the experiment was initially designed to examine response as the forcing function was applied at various angles. Thus the angle that the line of action makes with the water is also important. Finally, as mentioned before, the pre-tension in the chain was changed.

With the experimental parameters selected, the experiment and the necessary equipment could be designed.

Chapter 5

Experimental Work

The experimental portion of the work had as its goal the measurement of tension at the top end of the chain, while the chain underwent different forcing functions with different pre-tensions. Experiments took place between September 26 and October 3 1990, in the wave/towing tank at Memorial University of Newfoundland. The wave/towing tank was selected because it provided the largest depth of water while having sufficient length for the chain to be stretched out.

5.1 Equipment

The main item of equipment needed for the tests was a device that could apply a forcing function to the top end of the chain at different frequencies and at different orientations in the vertical plane. The forcing function had to be sinusoidal and the device also had to be capable of supporting the chain near the water and attaching to the catwalk. A schematic of the equipment is shown in Figure 5.1.

Since this was a very specialized item of equipment, there was nothing suitable readily available. Thus the apparatus had to be designed and built. The device designed was a variation of a scotch yoke. A variable speed electric motor rotated

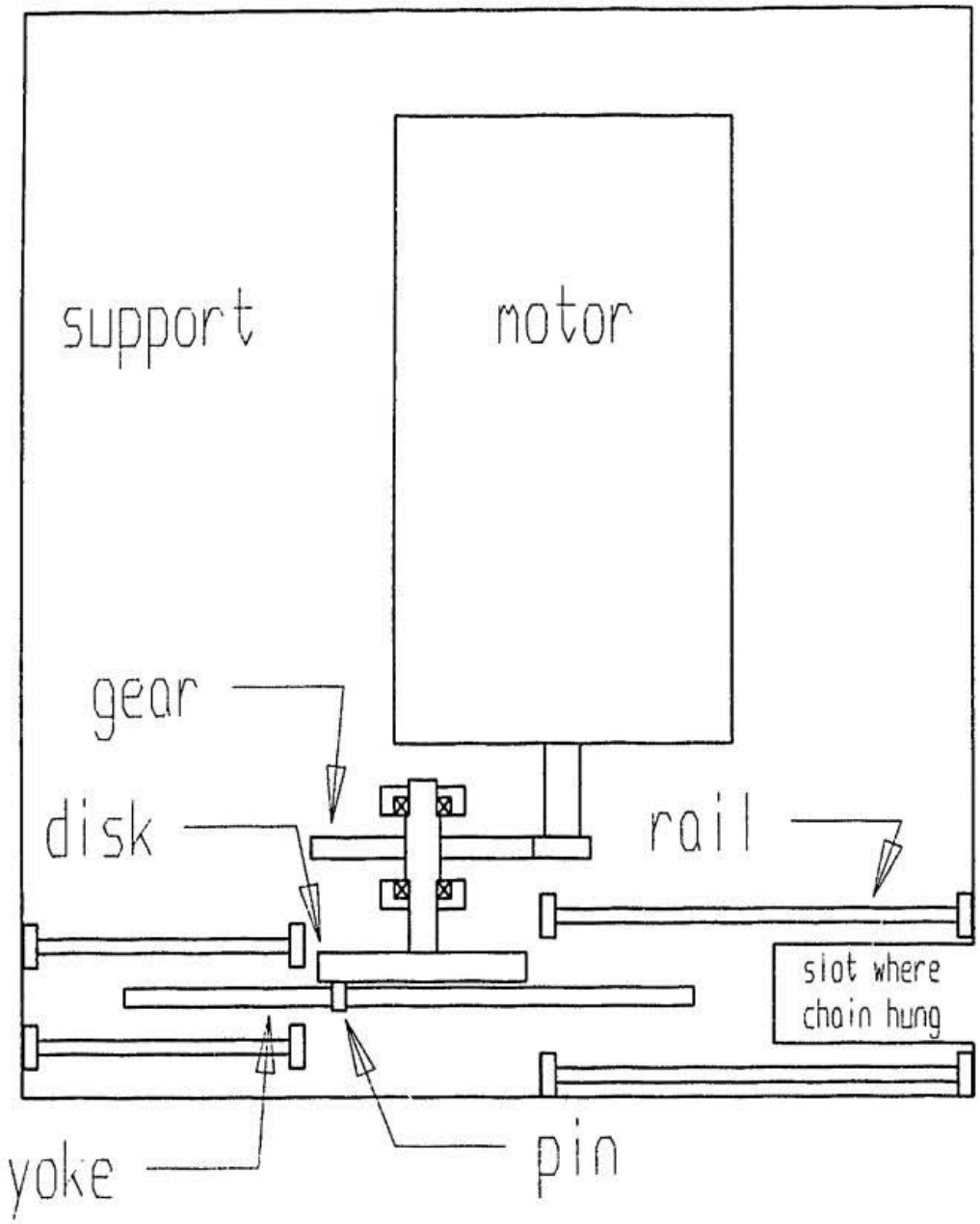

Figure 5.1: Overview of equipment for imposing a forcing function on a catenary mooring system

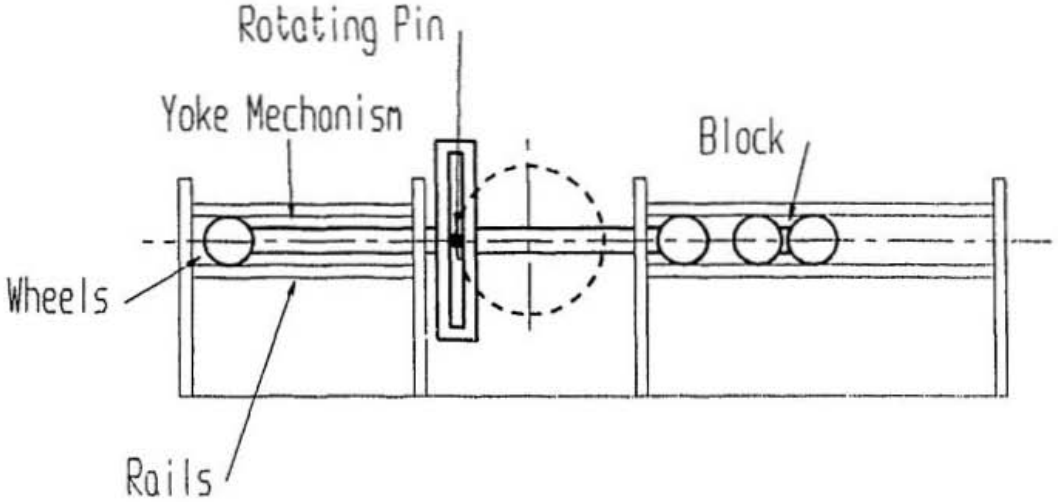

Figure 5.2: Side view of the equipment

a disk on which was mounted an eccentric pin. The yoke had a vertical slot in which the pin would fit. The pin was free to move in the vertical slot but would force the yoke to follow its horizontal motions (see Figure 5.2). Horizontal and vertical in this description mean parallel and perpendicular to the base plate.

The motor selected for the experiment was a 1/3 Hp variable speed electric motor. The output shaft was attached to a gear reducer which caused a 4:1 reduction in speed and a consequent 4:1 increase in torque. On the output shaft of the gear reducer was located the rotating disk. The output shaft was supported by bearings at each end. The disk was made of steel while the rest of the assembly

was made of aluminum. The reason for using steel was to add inertia to the system. Since the pretension in the chain would add energy to the system over half the stroke and subtract energy for the other half, the inertia was needed to smooth the motion out. The calculation for the force required to move the chain was based on the classic mechanical design problem of a continuously operating punch.

The block was attached to the front of the yoke and ran on rails. It provided a support for the two way force transducer and, through it, the chain. Under the block, a slot was cut in the support plate through which the chain hung.

The support plate was mounted under the catwalk and was free to tilt relative to the water as shown in Figure 5.3. Once at the desired angle it was held in place by bolts from the side frame to the mounting frame. It could be placed in one of six angles: 0, 15, 30, 45, 60, 75, and 90°.

The pivot point of the base plate was located at the center of the line of motion experienced by the top link of the chain. The reason for this was to make sure that the motion of the chain for all tests took place about a common center.

Most of the device was made from 3/8 inch aluminum plate although steel was used in some places like the shaft in the gear reducer and the disk as mentioned above.

Frequency was changed through the controller on the variable speed motor. The speed control for the variable speed motor was a simple dial with 10 graduations on it. After the runs, the actual speed was calculated by examining the accelerometer trace, however during the tests the speed was set to approximately the desired value through the dial which was calibrated with a strobe light.

Since the design of most of the device was unique, complete technical drawings

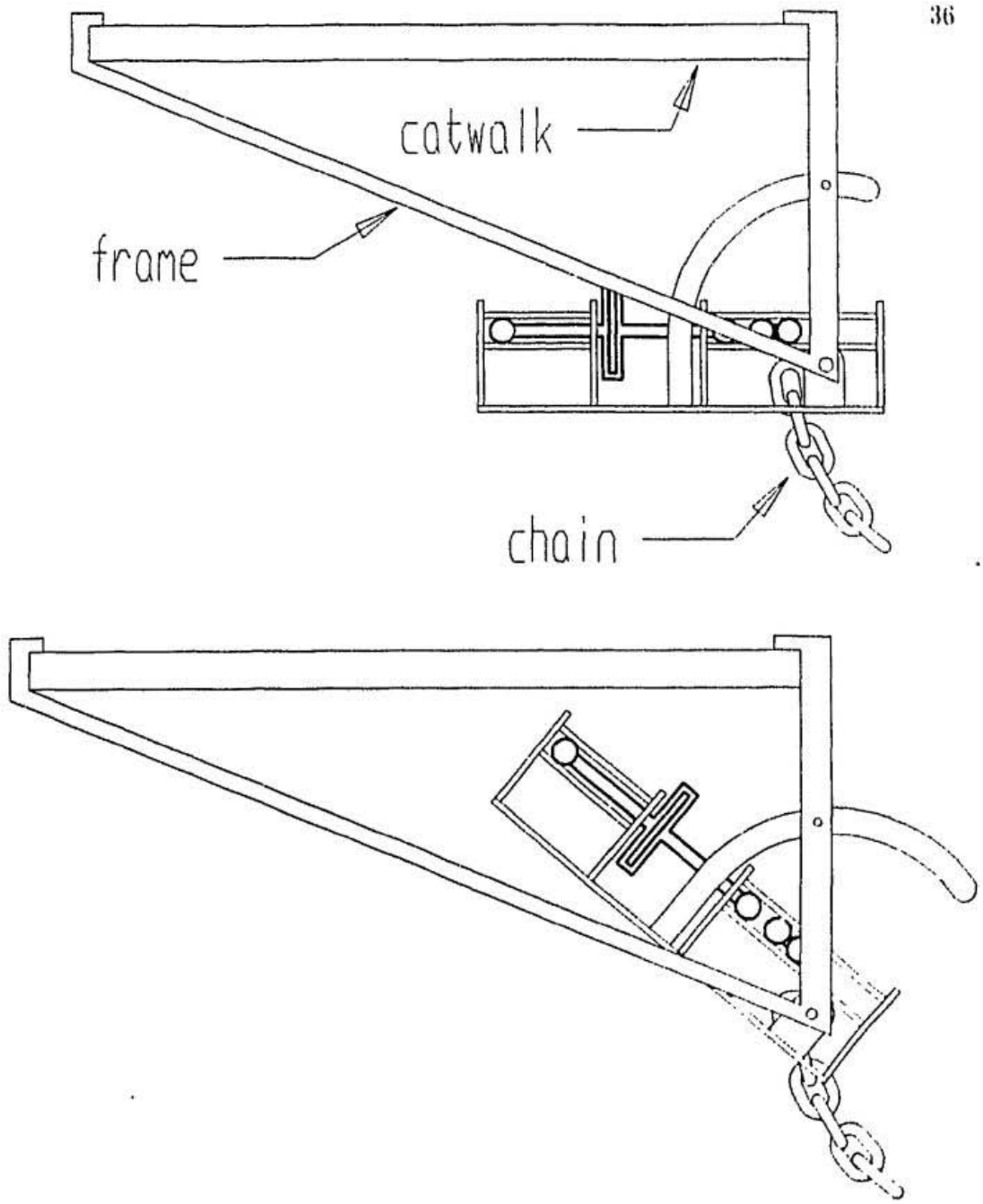

Figure 5.3: The equipment mounted in place both level and tilted

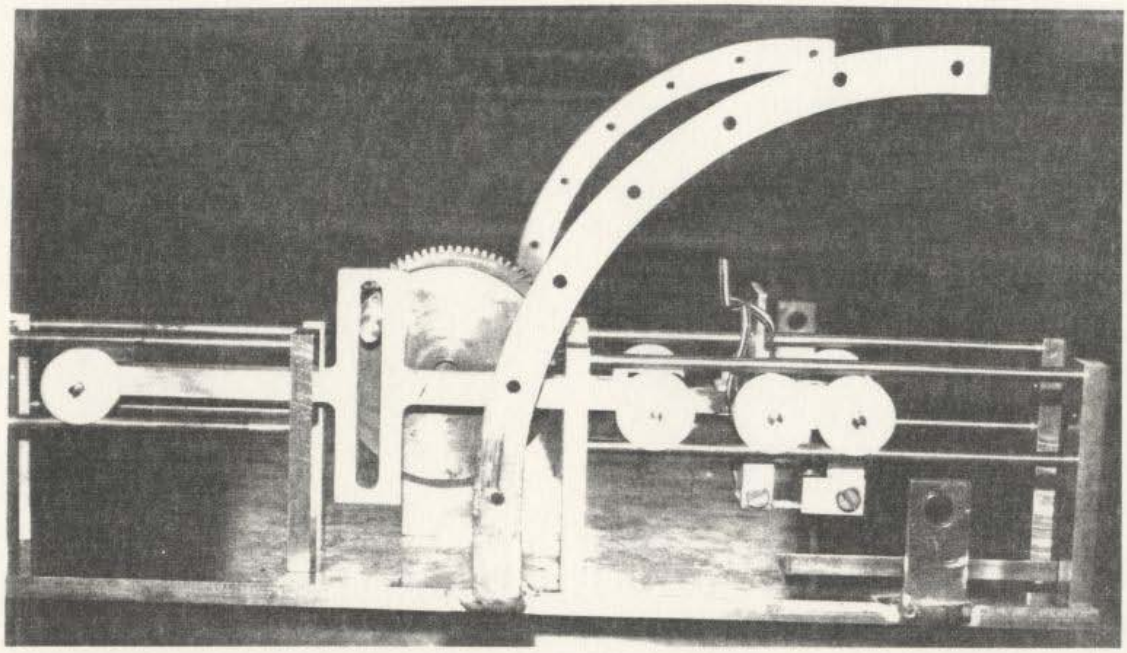

Figure 5.4: Photograph of the equipment

and assembly drawings are given in Appendix C. Overall the performance of the equipment was very good. Wear was noticed on the pin/yoke interface, however that was to be expected and the wear during the tests was negligible. The only improvement that could be made would be to allow either the top rail or the bottom rail to move and be set in place after the wheels were mounted. This would allow a better fit in between the rails for the wheels on the yoke and the block.

Figure 5.4 shows a photograph of the side view of the device. A close up view of the two way force transducer (described in the next section) is shown in Figure 5.5. The equipment mounted in place is shown in Figure 5.6.

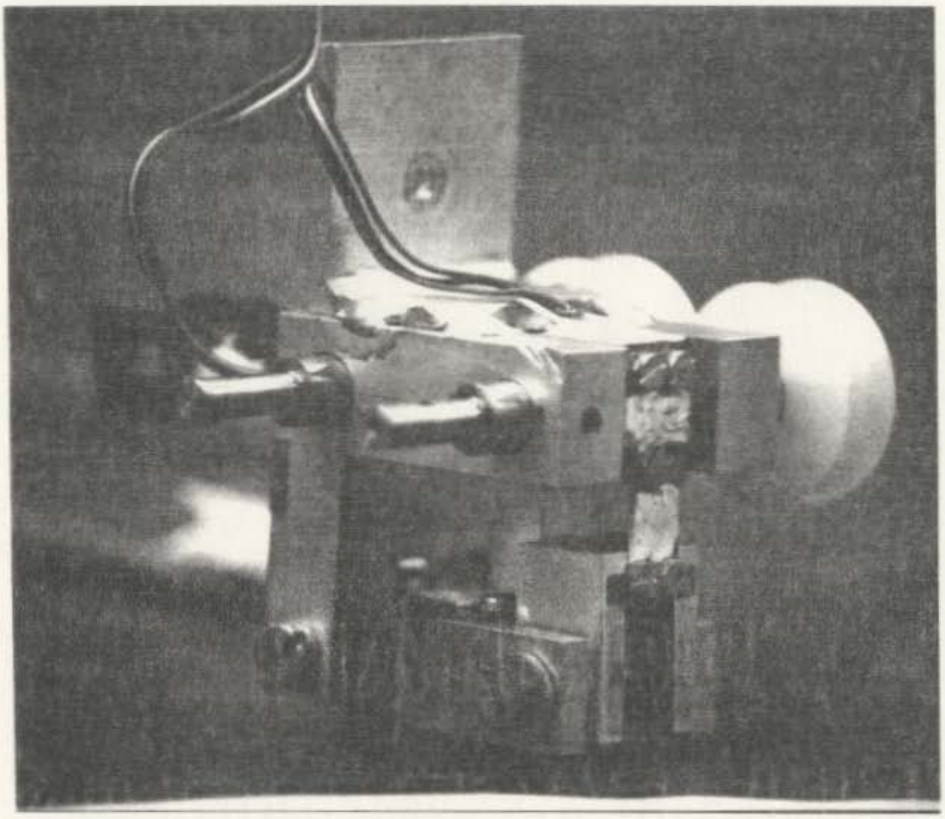

Figure 5.5: Close up of the force transducer

5.2 Instrumentation

Figure 5.7 shows the instrumentation set up and the flow of information. At the start is the physical apparatus (*ie* the accelerometer and two way force transducer), at the end is a VAX 8530, and in between were amplifiers, filters, a Keithley data acquisition system and a 286 PC computer. Figure 5.8 shows the actual location of the instrumentation.

The data gathering apparatus for the experiment consisted of an accelerometer and a two way force transducer. The accelerometer was a Bruler and Koch 4378 accelerometer with the characteristics shown in Table 5.1.

The two way force transducer was designed and built at Memorial University. What was needed was an instrument that could measure the force that the chain

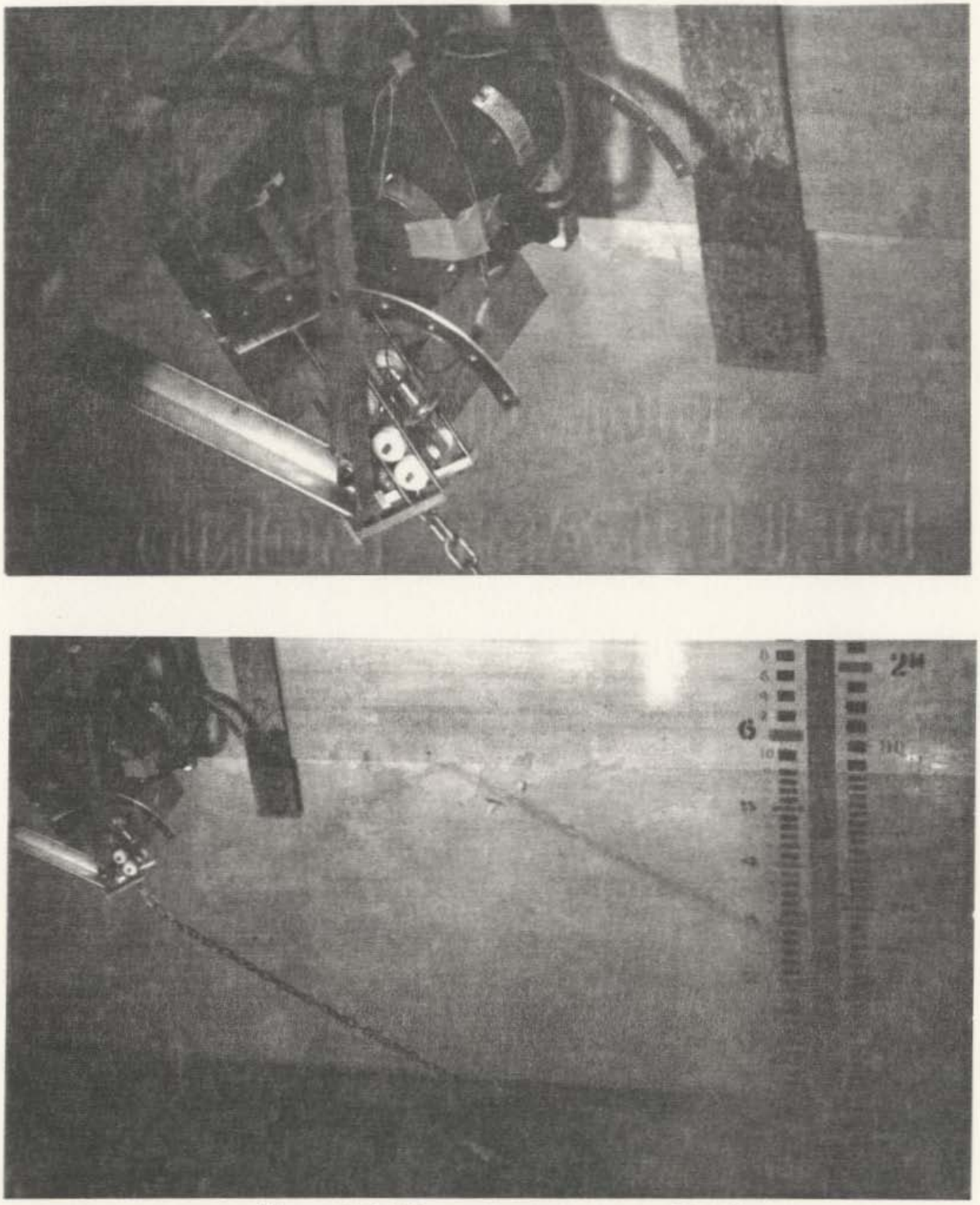

Figure 5.6: The equipment mounted in place

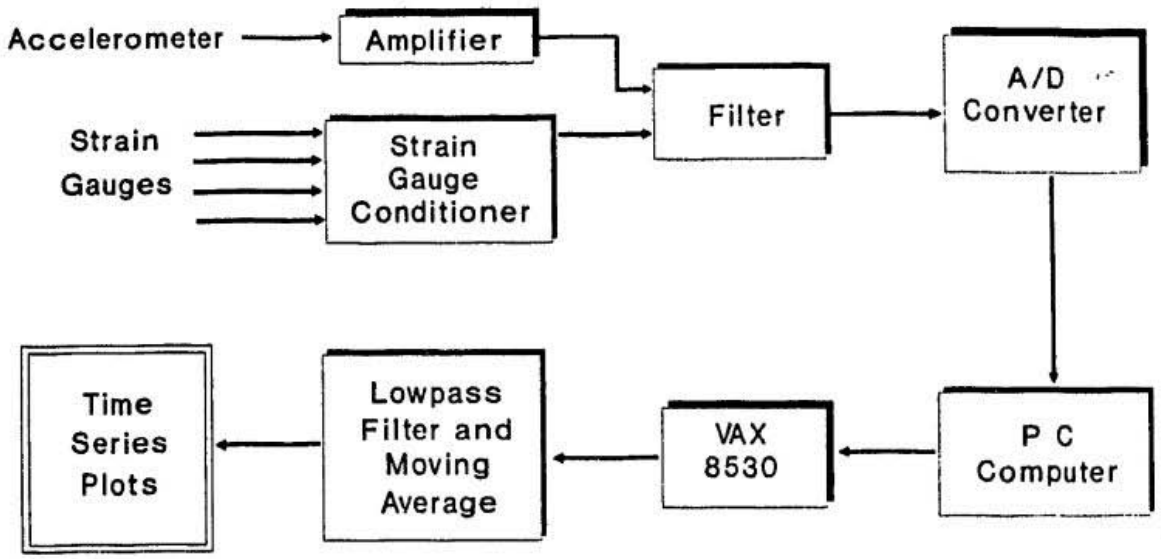

Figure 5.7: Information gathering system

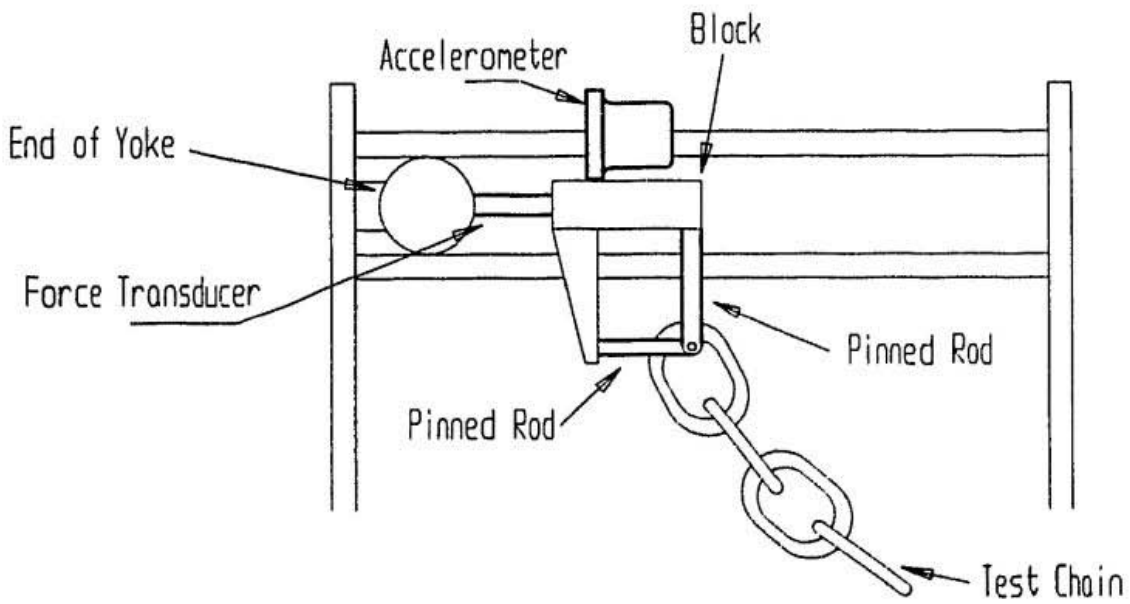

Figure 5.8: The location of the instrumentation

Serial number	1426469
Charge sensitivity	315 Pc/g
Voltage Sensitivity	258 mV/g
Natural Frequency	13 kHz

Table 5.1: Parameters for the accelerometer

Configuration	Wheatstone Bridge
Type	Student EA-06-120LZ-120
Resistance	120 Ω $\pm$.03%
Gage factor	2.05 $\pm$ 0.5%
Strain limits	5%

Table 5.2: Parameters for the strain gages

exerted on the driving mechanism (the block) while allowing the top link of the chain to pivot freely. Since the angle of the top link was not known and always changed, force had to be measured in two directions which could then be added vectorially to get the total force.

The two way force transducer measured force both parallel and perpendicular to the plate. It was made of two sets of thin plates instrumented with strain gauges. One set was parallel to the support plate and the other was perpendicular to it (see Figure 5.9). Each set was made of two identical plates with each plate having two strain gauges fixed in perpendicular directions. Properties of the strain gauges are shown in Table 5.2. The four strain gauges in each set were connected in a Wheatstone Bridge configuration. See Figure 5.10 for the circuit diagram.

Each plate was fixed by machine screws to a support at either end. At one end, the support was fixed to the block through a pivot and at the other end the

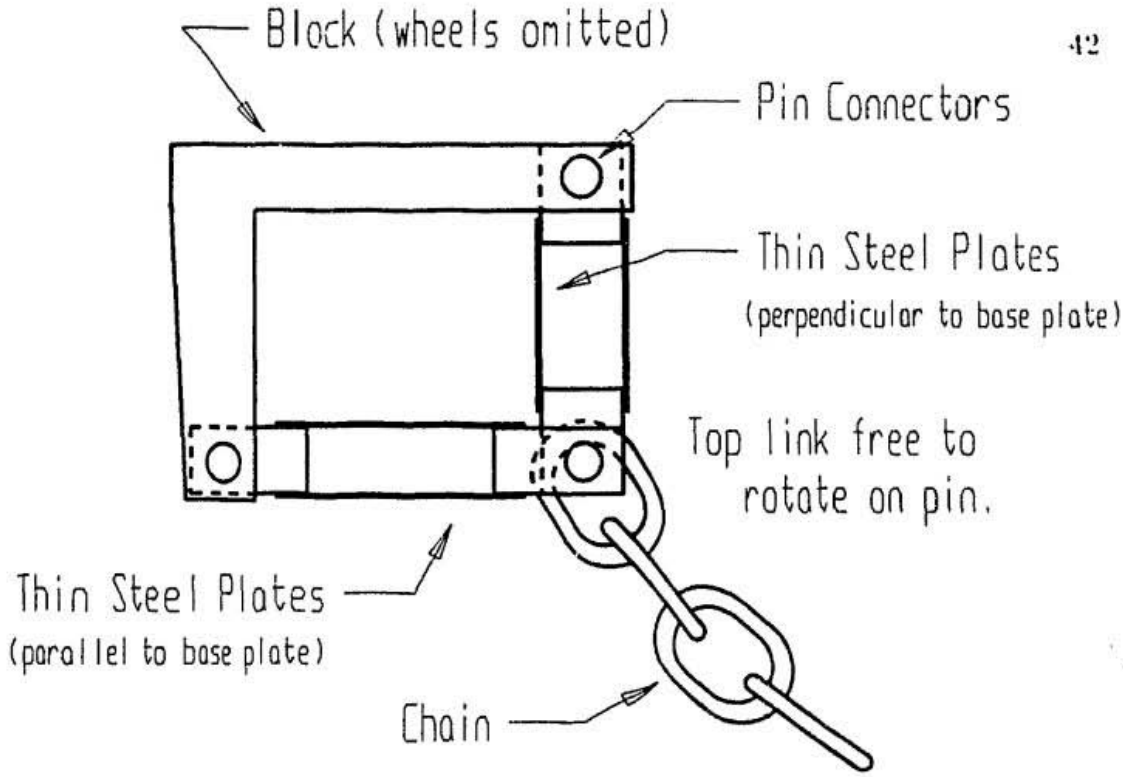

Figure 5.9: The two way force transducer

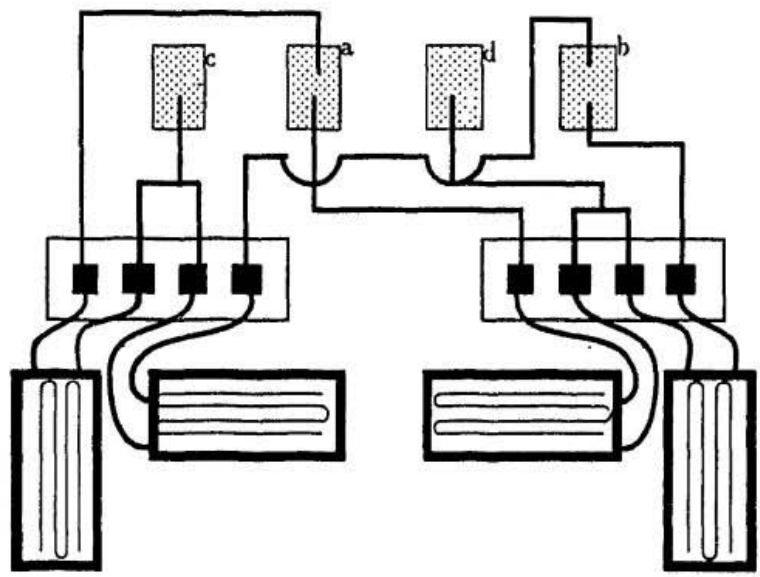

Figure 5.10: The circuit diagram for the strain gauges in the force transducer

supports from the two transducers were joined together. The pivot connections allowed the axial forces to be measured without introducing the problems that bending forces would cause.

The transducer was calibrated by clamping it to a rigid structure and loading it with known weights. The parallel and the perpendicular transducers were calibrated independently, and checks for one set interfering with the other were made. There was no interference observed and thus it can be concluded that the forces were decoupled. The data acquisition system was used to check on the linearity of the voltage-force curve. In general, the correlation coefficient, r, for the trials was .999 indicating a good linear fit.

The transducer was designed to withstand a maximum force of 500 N. However, in actual tests, the force never went above 150 N.

Although for most of the tests the force transducer measured tensile stress, there were occasions when compressive forces were important. This occurred when the test apparatus was tilted at 90° as can be seen in Figure 5.11. The transducer functioned well in compression, however in this configuration the top link put a bending stress on the perpendicular set of plates and this caused an error in the readings. The error was eliminated by using a small piece of wire to attach the chain to the force transducer, however this solution was implemented only after the first run had been made.

The accelerometer was powered by a charge amplifier and the signal from it was fed into a filter. The strain gauges were connected to a strain gauge conditioner and amplifier and then also to the same filter. This filter was a lowpass filter set to filter out frequencies above 250 hz. From the filter the signals, one for

In this case the top link placed a bending moment on the bottom force transducer

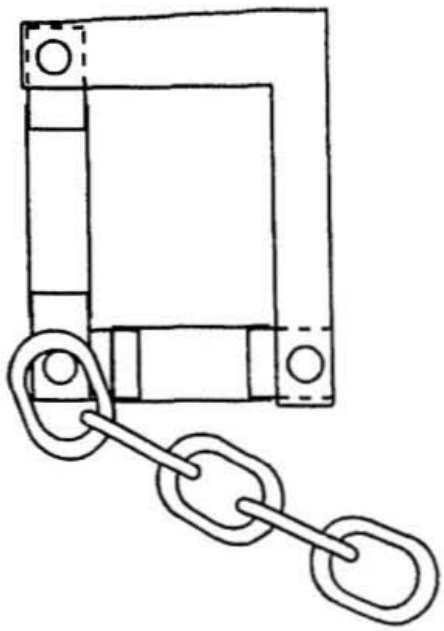

This problem was solved by inserting a small length of wire to keep the chain clear of the transducer

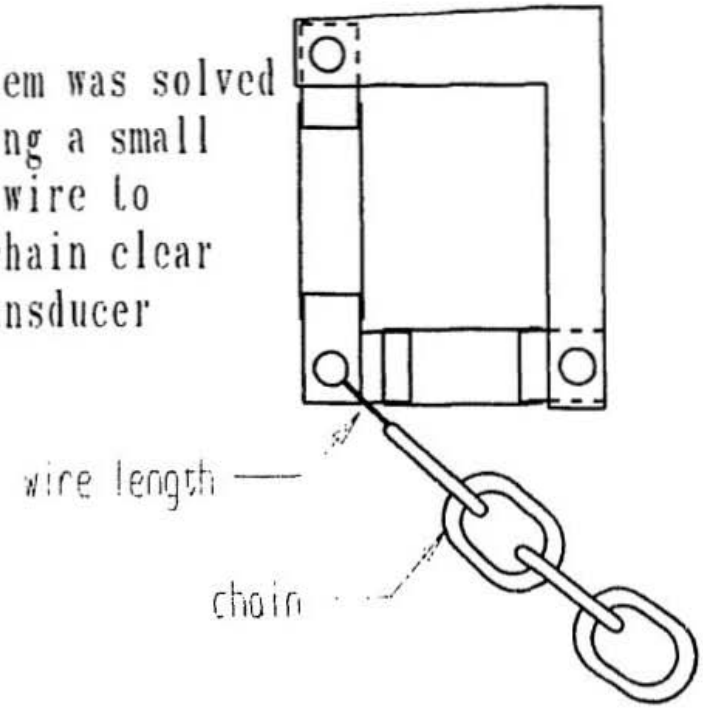

Figure 5.11: The equipment tilted at 90

Type	Open link, galvanized stainless steel
Specific Gravity	7.88
Mass per unit length	.768 Kg/m
Hardness	90 RB
Equivalent Young's Modulus	29 GPa

Table 5.3: Properties of the chain

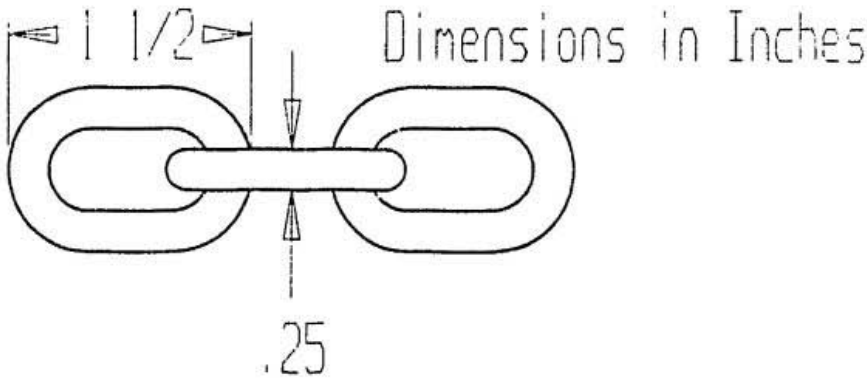

Figure 5.12: The test chain

the accelerometer and two for the force transducer, went to a Keithley analog to digital converter. From here it went to the 286 PC computer and then was transferred to the VAX 8530 for further filtering and analysis.

5.3 The Test Chain

The chain selected was an open link steel chain. Properties of the chain are found in Table 5.3 and the dimensions of the chain are shown in Figure 5.12.

There was no effort made to model a particular chain since many different kinds are used. However the modelling laws dictate that the density ratio between the

working fluid and the mooring line material must be the same in both model and prototype. Since water is used in both instances (the density difference between salt water as used in the prototype and fresh as used in the model is negligible for this experiment) the mooring line material density should also be the same in model and prototype. This justifies the use of a steel link chain.

5.4 Procedure

As was derived in Chapter 4, the variables to be changed in this experiment were the pre-tension, and the frequency and angle of the forcing function. The frequency was very easy to change through the controller of the variable speed motor. Angle was a little more difficult to change because the base plate had to be tilted and then fastened in place at the new angle. The pre-tension was the most difficult to change because it involved moving a 30kg anchor.

With this in mind, the following procedure was followed. The apparatus was initially set up in a configuration with the base plate level to the water and the anchor set to give the smallest pre-tension in the chain. The first test was then run with the lowest frequency, followed by tests with increasing frequencies up to a maximum. At this point, the angle of the base plate was changed and the frequencies run through again. This continued until all the angles were run through and then the pre-tension was changed.

Frequencies were started initially at 0.5 Hz. and then increased to a maximum of about 4.0 Hz. Frequencies below 0.5 Hz. were not significant since they were well into the quasi-static area. Frequencies greater than 4.0 Hz. were not used because the equivalent scaled frequencies are not encountered in nature.

The start frequency, the cut off frequency and the number of frequencies sampled underwent small changes through out the series of experiments. For example it was found that under the largest pre-tension condition and at an inclined angle, the motor could not provide enough torque to produce pure sinusoidal motion at a frequency of 0.5 Hz. so the tests started at 1 Hz.

The equipment was run for about 10 seconds before data recording began to allow transients to die off. Also, observations were made during the first series of tests to make sure that neither the equipment nor the catwalk vibrated to a significnat amount

There were four angles used in this experiment: 0, 30, 60 and 90°, although as mentioned before, some problems were found at 90°. There were also three pre-tensions used: 15N, 20N and 30N.

5.5 Data Analysis

As mentioned before the signals from the accelerometer and the strain gauges were filtered at 250 Hz. before the A/D converter. After the data were collected, they were sent to the VAX 8530 computer for further analysis.

The analysis consisted of two stages. First, the signal was run through a program which applied a moving average with a window of 10 to the data set. This removed much of the random noise in the signal.

However it was observed that there was still some noise in the system. An examination of the signal revealed that much of this noise was found in the 40 to 90 Hz. range. This is possibly due to the electrical noise from the motor, or the mechanical noise (vibrations) from the machinery operating (*eg* gears meshing).

It is interesting to note that there was not a significant contribution at the 60 Hz. frequency; a common frequency for interference. Thus it was decided to filter the signal again to remove components of higher frequency.

To perform this a Yule-Walker filter was designed. Looking at the signal it was determined that the significant portion of it was composed of frequencies less than 25 Hz. for the high frequency tests decreasing to less than 10 Hz. for the low frequency tests. Consequently, two filters were designed, one that cut out frequencies of more than 25 Hz. and one that cut out frequencies of more than 15 Hz.

The signal from the lower frequency tests appeared to be noisier than that from the high frequency tests. The reason for this is that the force in the small frequency tests was on the order of a tenth of a Newton and thus the signal output from the strain gauges was quiet weak. For the higher frequency tests the forces involved went as high as 100 Newtons and effectively drowned out the random noise.

A graph showing the results from a low frequency test with and without filtering is shown in Figure 5.13. Graphs of the signal versus the frequency for the two Butterworth filters used are shown in Figure 5.14.

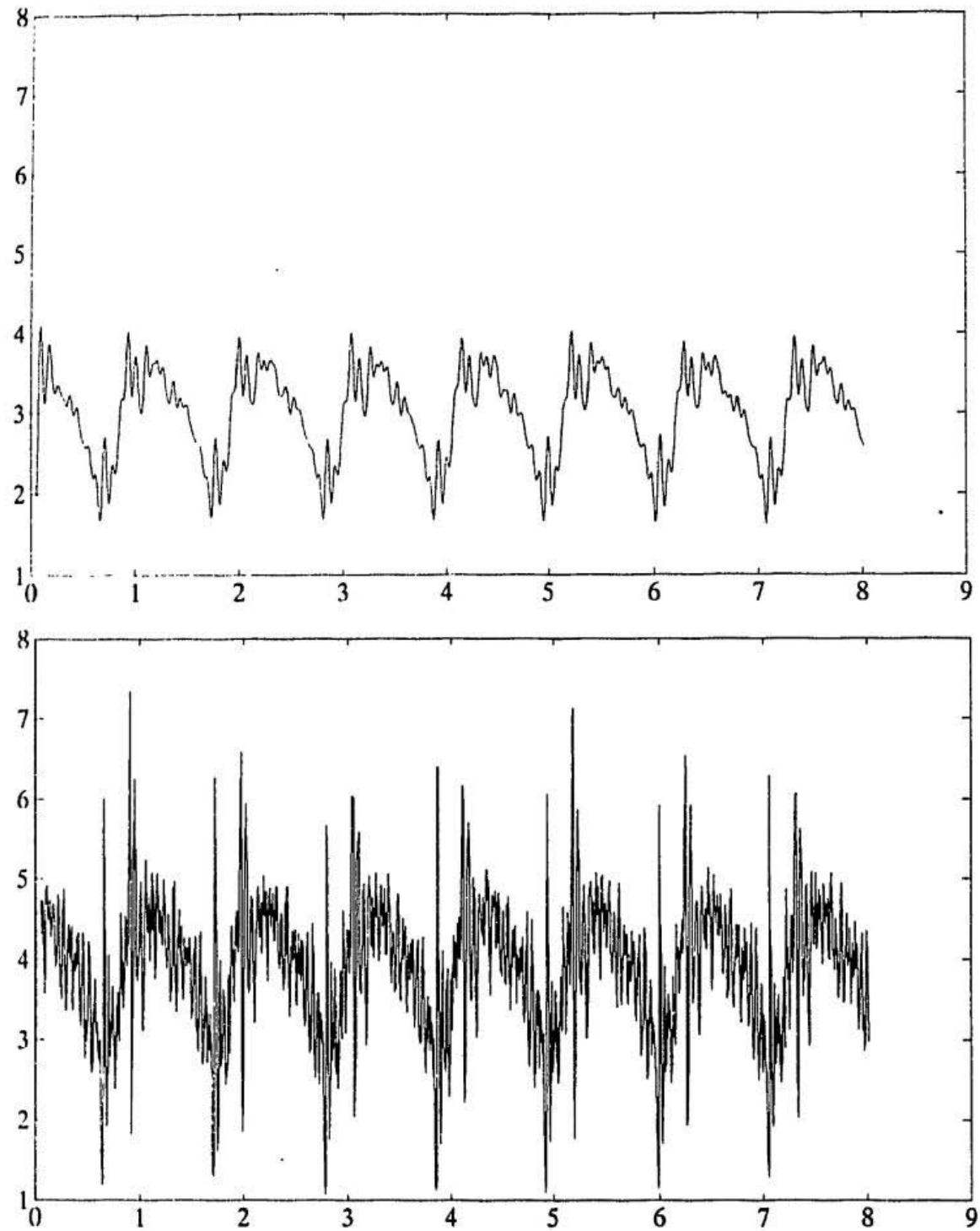

Figure 5.13: A sample run with and without filtering

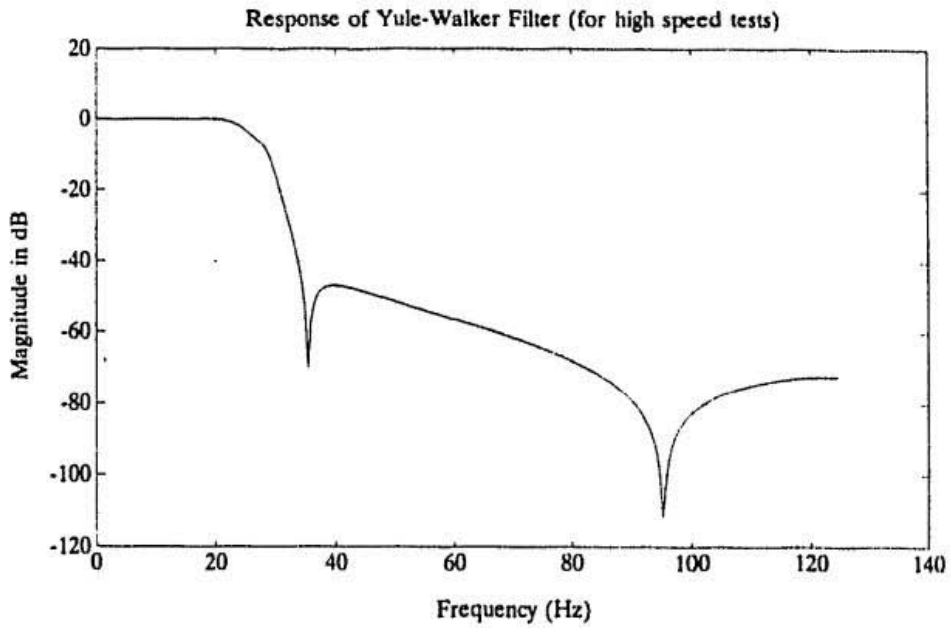

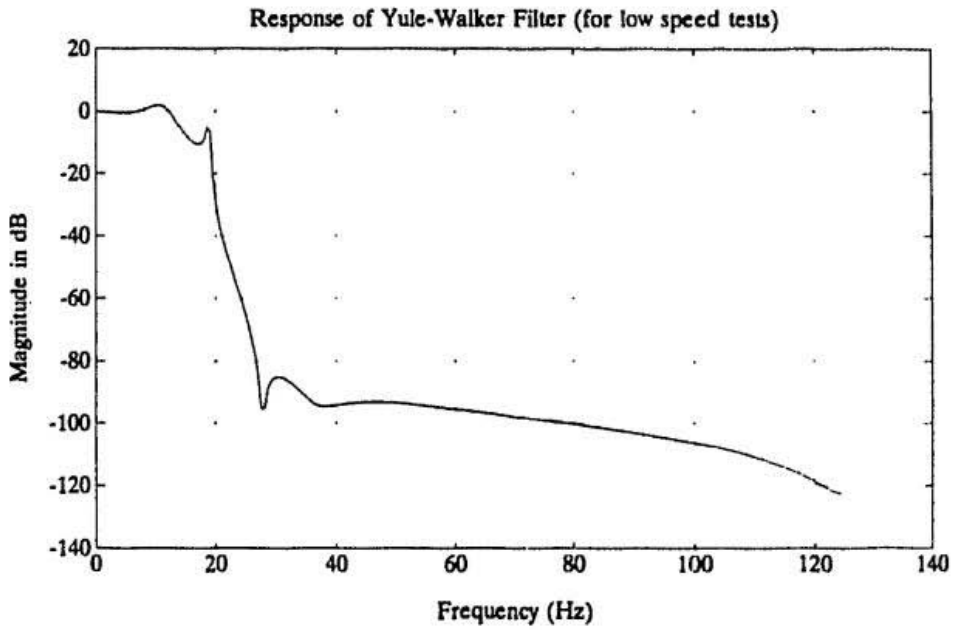

Figure 5.14: The filters used for the data

Chapter 6

Discussion

The discussion in this chapter will be broken into two parts. The first will look at the data from the tests and discuss and draw conclusions from this data. The second section will examine the method and effects of scaling the model tests to a prototype environment.

6.1 Experimental Work

The data from the tests were analyzed and graphs were drawn of force against time for each run. These graphs are shown in Appendix D. From these graphs it was possible to find the dynamic force ratio (DFR). The dynamic force ratio is the ratio of the maximum change in the force (*ie* from trough to crest) to the static value. For example, if the static pretension value was 15 N and the force varied between 10 and 40 N, the DFR would be 2.

Once all the DFR values for the runs were calculated, they were plotted against the frequency for the three different values of pretension and are shown in Figures 6.1 - 6.3. These graphs enable several conclusions to be drawn.

The four conditions first described by Suhara and discussed in Chapter 4 can

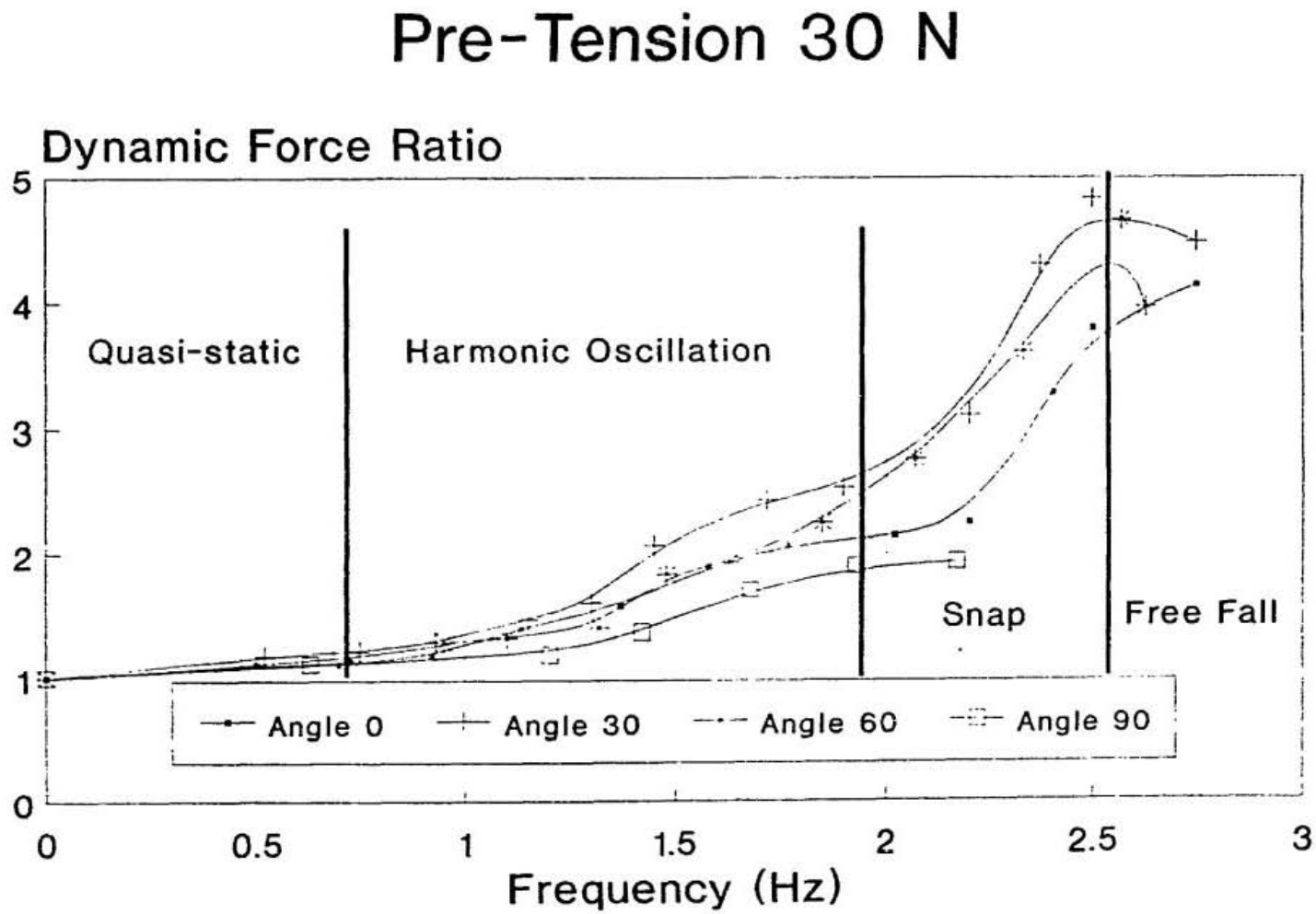

Figure 6.1: The DFR values plotted against frequency for 30N pre-tension

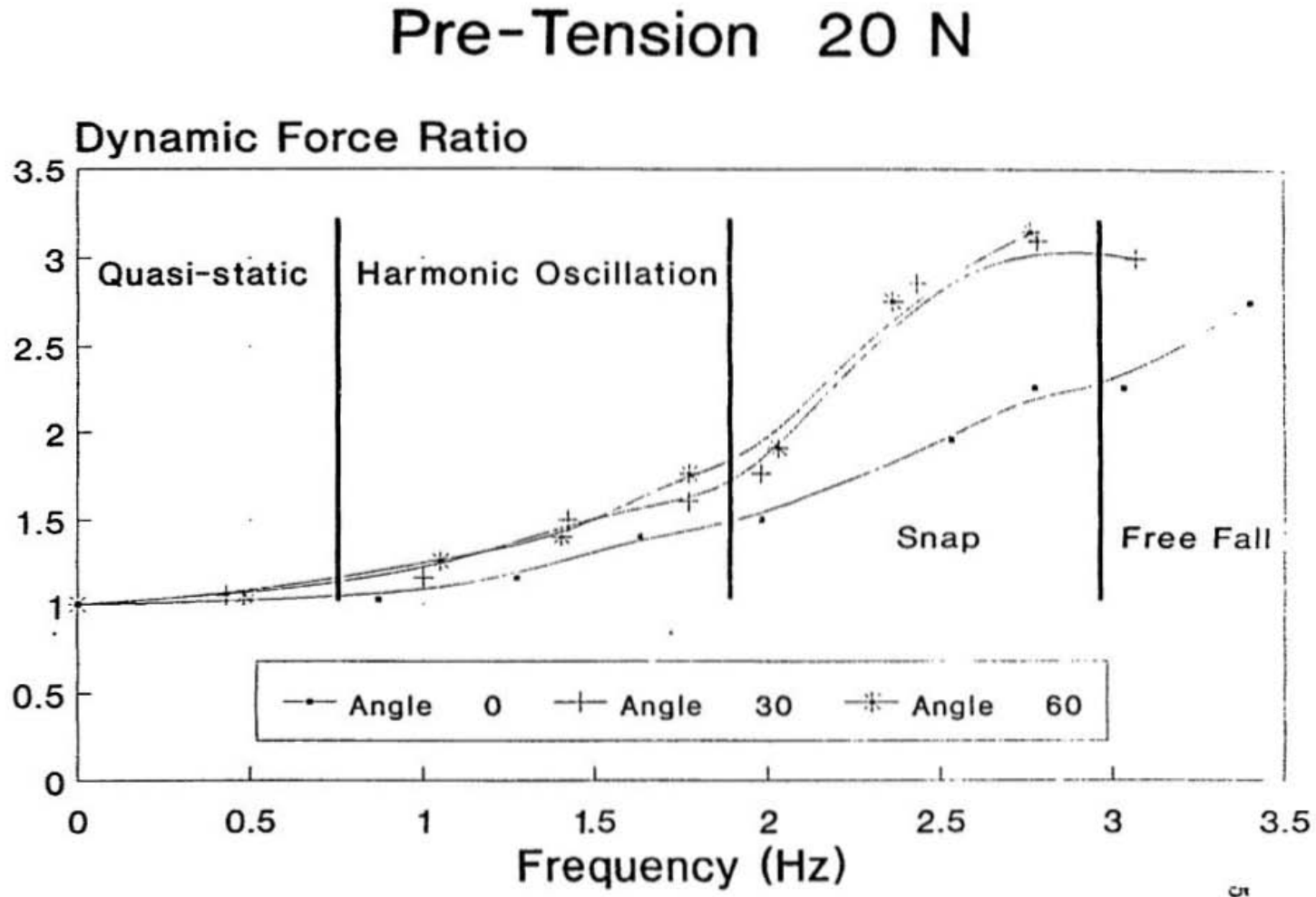

Figure 6.2: The DFR values plotted against frequency for 20N pre-tension

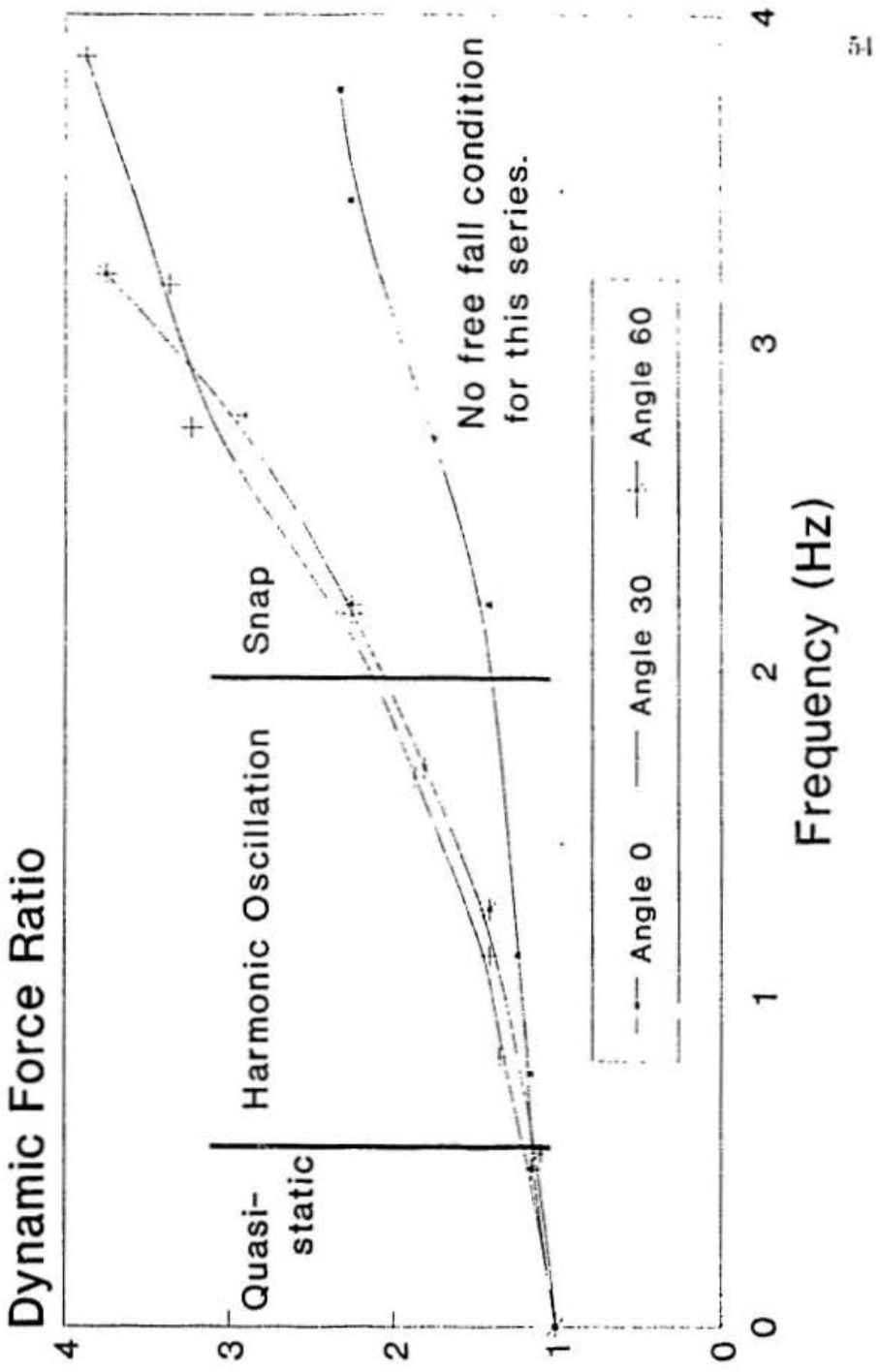

Figure 6.3: The DFR values plotted against frequency for 15N pre-tension

be seen in these graphs. The quasi-static region starts from zero frequency and extends to between about 0.6 Hz and 1 Hz. with the 0.6 Hz. in the small pre-tension condition and the 1 Hz. in the largest pre-tension condition. It should be noted that the end of the quasi-static condition was arbitrarily taken to occur at a DFR of 1.2.

The next condition was the harmonic oscillating condition and it extended from the end of the quasi-static condition to the location at which the slope of the lines from the DFR versus frequency graphs suddenly increases. This point was at about 2 Hz. in the three graphs although for the smallest pre-tension, it was not well defined.

The snap condition was the next region and it was only clearly observed in the large pre-tension graph. The end point of this region is defined as the point at which the DFR starts to drop off and in that graph it ranged from 2 Hz. to about 2.6 Hz. The medium pre-tension graph starts to show some drop off at about 3 Hz. but the small pre-tension graph shows no indication of ending the snap condition.

The last condition is the free fall condition and in this area the DFR starts to decrease. As mentioned, this is only clearly seen in the large pre-tension test. This condition starts at the end of the snap and continues indefinitely.

When these graphs are observed together, it is easy to see the effect of pre-tension on the DFR (which is a non-dimensional indication of the force). In the smallest pre-tension series, there is little indication of the change in the different conditions where as in the large pre-tension case, the sections are well defined.

This is due to the scope of chain in each case. As the pre-tension increases,

the length of chain from top to the contact point with the bottom increases. As well, the length of chain is in place in more of a horizontal condition, or, more importantly, in a direction perpendicular to the force of gravity.

The increase in the length of the chain adds more weight to the suspended portion of the chain. The increase in inertia acts to increase the dynamic forces in the harmonic oscillation condition. The increase in length/weight acts in the snap and free fall conditions and causes larger forces to be experienced.

It would appear that the pre-tension in the chain affected not only the magnitude of the DFR, but the frequency at which the maximum value was detected. The three tests show a trend in that at the pre-tension increases, the frequency of the maximum DFR decreases.

The effect of angle on the maximum force can also be observed in these graphs. In all cases the force from the test at 0° (*ie* when the slider was moving in the horizontal plane) was a minimum. It is also observed from the large-pretension test that the run at angle 90° (*ie* in the vertical plane) produced significantly lower force than the other runs. The tests at the two intermediate angles produced by far the largest dynamic forces.

This is contrary to what has been stated by others. Suhara et al (1981) and Pattison (1974) felt that the maximum forces were to be found by oscillations in the vertical plane, while van Sluijs and Blok (1977) stated that horizontal oscillations induced the major part of the line tensions.

However the results reported here can be supported by looking at how the chain moves. The maximum motion of the chain will take place when the forcing function is applied at an angle tangent to that of the upper link when it is in its

free hanging orientation.

The tests involving starting from zero Hz. and increasing to the maximum also produced interesting results. Some sample results from these tests can be seen in the Figure 6.2. The times taken to reach the different stages were on the order of one cycle for the harmonic oscillating condition and three to five cycles to reach the snap and free-fall conditions. From this the following can be said.

First, it is apparent that no significant transients exist in the system. This is important because transients could have caused larger initial forces. Second, it would appear that the chain reacts very quickly to an imposed displacement and produces the maximum dynamic forces almost immediately. The delay shown in the graphs is caused mainly by waiting for the motor to get up to speed.

6.2 Scaling the Model

It is important to examine how the modelling of catenary mooring cables applies in the ocean environment. The first step in this is to examine scale errors.

The term θ is an angle and thus transforms identically. Geometric similarity can be achieved and thus the terms R/D, S/H and D/S will be modelled correctly. Also, since the experiments take place in water and the material is steel, the ratio m_c/ρ_f will be correct.

The term $\nu^{2/3}/g^{1/3}D$ accounts for the hydrodynamic properties of the cable. In this experiment, the Reynolds number based on the diameter of the chain would be over 10,000 for motions with velocities above about .1 mm/s. This would place operation of the model well into the turbulent range, thus scaling should not have much effect on these properties. This is borne out by the results of van Sluijs and

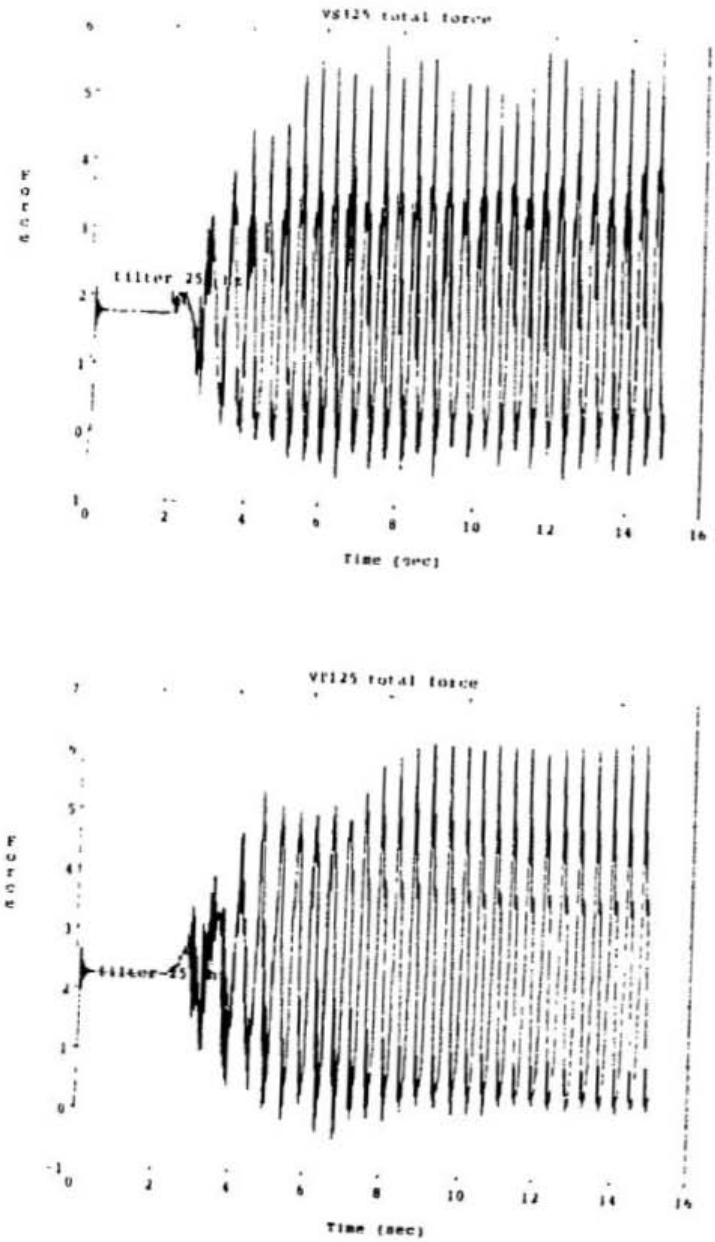

Figure 6.4: Results from the speed up trials

Blok (1977).

The term $E/m_c gS$ accounts for elasticity in the cable. Although for deep water, elasticity is an important parameter, this study is aimed more at waters with a depth measured in tens of meters rather than hundreds. Thus elasticity should not have a great influence on the system.

This leaves the parameter $\omega^2 R/g$ as the most important. This is the ratio of the acceleration that the top end of the chain will undergo to gravitational acceleration. From the tests, non-dimensional graphs of the DFR can be made using this parameter and are shown in Figures 6.5 - 6.7.

It should be noted that there are strict limitations on the use of these graphs. This is due to the fact that the value R was not changed during the tests. In retrospect it would have been useful to change R during the tests, however this would have led to time constraints in the experiment.

Nonetheless, it is possible to work with this limitation. Besides the $\omega^2 R/g$ expression, the only other place that R appears in the dimensionless equation is in the expression for the non-dimensional amplitude of motion R/H. This means that the graphs are valid only for situations with similar R/H values.

To get an idea of what range of frequencies is representative of real ocean data, some values are examined. A period of 10 sec. would correspond to an ω of about .63 rad/sec. This substituted into the $\omega^2 R/g$ expression and combined with g would give a value of $.04R$. Thus, from Figure 6.3a, to get a significant dynamic force, R would need to be on the order of 10 meters.

Ten meters is a long stretch and most moored objects that could move 10 meters such as drill rigs and large ships would take more than 10 seconds to do

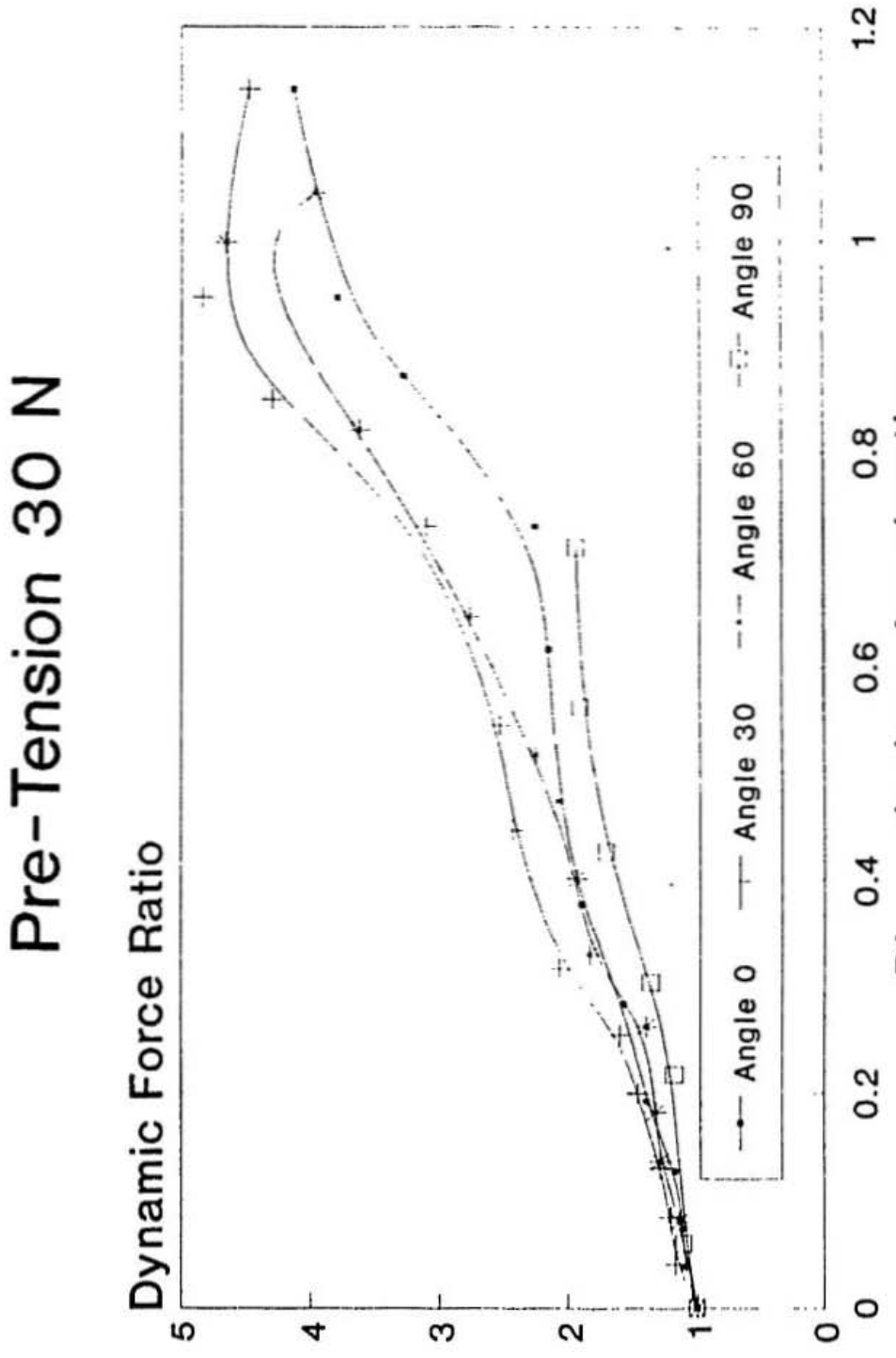

Figure 6.5: Non-dimensional graphs of the results for 30N pre-tension

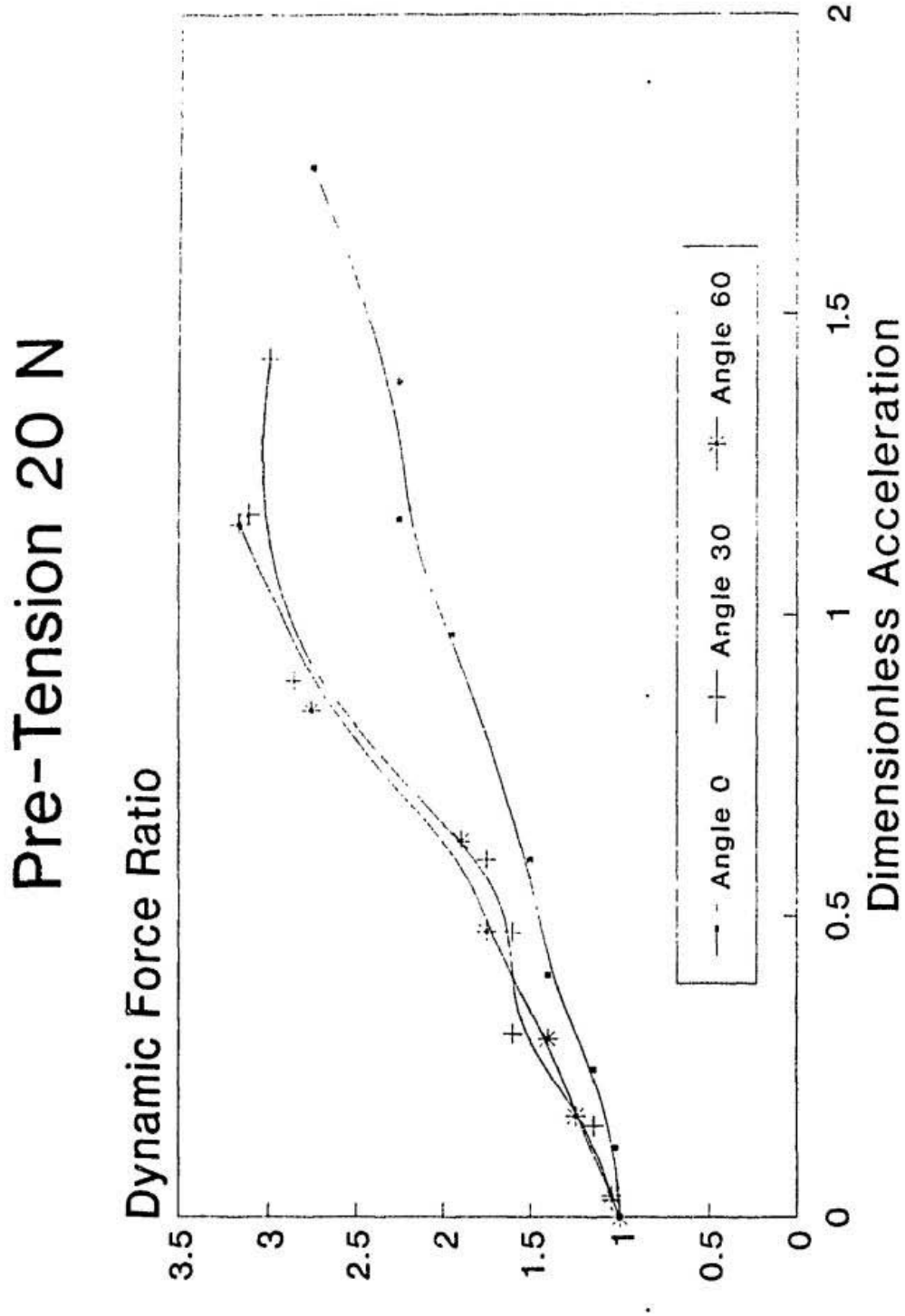

Figure 6.6: Non-dimensional graphs of the results for 20N pre-tension

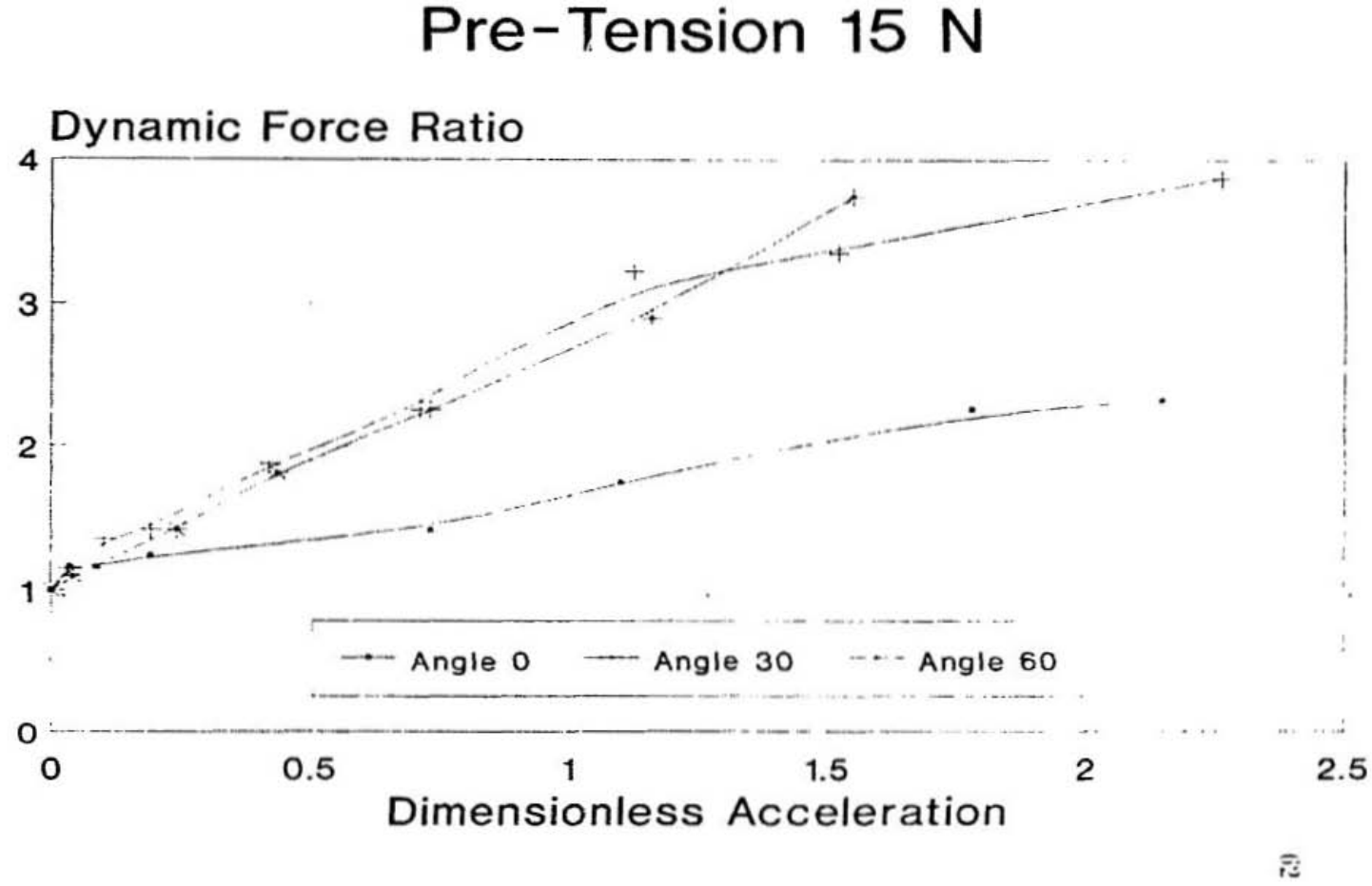

Figure 6.7: Non-dimensional graphs of the results for 15N pre-tension

so. Also, because of the limitations on the R/H value, this would correspond to a depth of several hundred meters which would place operation of the cable in the range where elasticity is important. Thus it would seem that large objects respond in the range where the quasi- static analysis will suffice.

However, there are smaller objects which require mooring (small fishing boats and buoys, for example). An example shows that for a given situation with a similar R/H, significant dynamic forces will occur.

If there is a stretch of wa8Xsimilar R/H, significant dynamic forces will occur.

If there is a stretch of water 10 km long with an average depth of approximately 15 meters and a wind of 70 km/hour blowing for 1 hour, waves with a period of 3.0 seconds and a significant height of 1 meter will be produced as given in the US Army Corps of Engineers' Shore Protection Manual (1984). A can buoy in this wave field would respond at the same frequency with approximately the same amplitude of motion. The $\omega^2 R/g$ parameter for this scenario is 0.23. From Figure 6.3a, it can be seen that this corresponds to a dynamic amplification factor of about 1.5.

This example uses the 1/3 significant wave height. However speed up tests show that the response is very quick, thus in reality a larger R value would be expected.

Another example comes from the design manual that the Canadian Coast Guard uses for buoy design. The criteria that they give for the design conditions of buoys is that the buoy must survive a 2 meter wave with a period of 4 seconds. This corresponds to a DFR of 2.5.

Chapter 7

Conclusions

This work has demonstrated several properties and led to several observations from which conclusions can be drawn. These have been discussed in Chapter 6, however they will be summed up here.

To begin with, the different areas of operation that Suhara first mentioned have been shown. These areas are frequency dependant and are demonstrated best in the test with the 30 N pre-tension, however they are seen to a certain extent in the other tests as well. It is important for the designer to know what area their structure will operate in as this will give an indication of the dynamic forces amplification that would be expected.

If the line responds in the quasi-static range, there is no need to include a safety factor for dynamic forces (although there may be other reasons to use safety factors that still apply such as the temperature changes found in the North Atlantic). However, from this work it is shown that it is possible to have dynamic amplification factors as much as five times the static if the line is forced at a sufficiently high frequency. It should be noted again here that others have reported even larger DFR's (van den Boom (1985), Suhara et al (1981)).

Also, statements about the effects of different forcing functions can be drawn. It was shown that the dynamic force increases with increasing pre-tension. It was also shown that the largest dynamic forces occur at angles between the vertical and the horizontal.

Finally, several conclusions about scaling the experiments can be shown. It was concluded that it is theoretically possible to model mooring experiments. The best parameter for this seems to be the $\omega^2 R/g$ factor. This experiment indicated that for large moored objects, the response of the line places the response in the quasi-static regime. However with smaller objects such as buoys, dynamic forces are significant.

The designer must know the environment in which their design is to be placed and then an idea of the dynamic forces expected and the allowance that should be made for them can be estimated.

Chapter 8

Recommendations

As a result of this work, recommendations for future work can be drawn. It would seem that an important extension to the work would be to do more tests with different R values. However, after doing these tests, it is felt that a different line of experimentation would be more productive.

Having proved that it is possible to scale mooring experiments (both shallow and deep) ways should be found to improve the realism of the experiments. There are two ways that this can be done. The first is to add a current to the experiments. There are many situations in the ocean environment where currents exist and are important to moored objects. Currents could add a strumming phenomena which could change the dynamic forces. However this would involve running the tests in an area where there is flowing water and facilities for this are scarce (although it would be possible to do this work in the flume tank at the Marine Institute in St. John's).

The second way would be to design a new forcing device that could simulate the real motion that a moored object would experience. Two possible means exist for this. The first would be to have a rotating disk on which the mooring line was

attached. Studies have shown that a moored buoy experiences a nearly circular trajectory. Force would be measured between the chain and the disk or along the shaft that runs from the disk. It is anticipated that the measurement of tension would be the major technical difficulty with this experiment.

Another possible method of simulating motions of moored objects would be with two actuators. The actuators would be configured much like the two way force transducer described here. By controlling the actuators, any type of motion could be simulated. Unfortunately, the equipment involved in this method would be quite costly.

Nonetheless, it would be of great benefit to be able to know what dynamic forces would exist, thus avoiding overly conservative or dangerously small safety factors.

References

Adams, R.B.,. (1969) Analysis of Spread Moorings by Dimensionless Functions, *1st Annual Offshore Technology Conference*, Houston, Texas, Paper Number OTC 1077

Collier, M.L. (1972). Jr. Dynamic Similarity Laws Applied to Cables, *Journal of Hydronautics*, Vol. 6, No. 2.

Collipp, B. G. Borgman, and L. E. Miller, C. K. (1962). A Method for Analyzing Mooring Line Catenaries, Report B-2.

Edwards, C.H., and D.E. Penney. (1982) *Calculus and Analytic Geometry*, Prentice-Hall, Inc., Englewood Cliffs, NJ.

Faure, T.D. (1989) Experimental and Numerical investigations of mooring Line Dynamics, Technical Report TR-HY-029, Hydraulics Laboratory, Division of Mechanical Engineering, National Research Council Canada.

Fox, C., (1950) *Calculus of Variations*, Oxford University Press, London.

Hwang, Y.L. (1986) Nonlinear Dynamic Analysis of Mooring Lines, 5th International Symposium of the OMAR, Tokyo.

Johansson, P.I. (1978) Non-linear Dynamic Response of a Mooring Line, Publication No. 106-March 1978, Det Norske Veritas, Hovik, Norway.

Liu, F.C. (1973) Snap Loads in Lifting and Mooring Cable Systems Induced by Surface Wave Conditions, Originator's Report Number - 1288, Naval Civil Engineering Laboratory, Port Hueneme, CA 93043.

Longoria, R.G., J.J. Beaman, and R.W. Miksad, (1991) Nonlinear Hydrodynamic Forces in Random Oscillatory Flow, European Offshore Mechanics Symposium, Trondheim, Norway.

Luo, Y. (1990) Tension Response Statistics and Fatigue Analysis of Catenary Mooring Lines, European Offshore Mechanics Symposium, Trondheim, Norway.

Nakajima, T. (1986) A New Three-Dimensional Quasi-Static Solution for the Multi-Component Mooring System, 5th International Symposium of the OMAR, Tokyo.

Nielsen, S.K.R., (1976) Statical Analysis of Mooring Systems. Danish Ship Research Laboratory, Lyngby, Bulletin No. 41.

Owen, D.G. and B.T. Linfoot (1976) The Development of Mathematical Models of Single-Point Mooring Installations. Eighth Offshore Technology Conference, Huston, Texas.

Ogawa, Y., (1984) Fundamental Analysis of Deep Sea Mooring Line in Static Equilibrium. *Applied Ocean Research*, Vol. 6, No. 3.

Papazoglou, V.J., S.A. Mavrakos, and M.S. Triantafyllou (1990), Non- linear Cable Response and Model Testing in Water, Journal of Sound and Vibration 140, 103-115.

Parnell, J.A. and J.C. Hicks. (1976) Scale Modeling of Large Elastic Undersea Cable Structures, 76-WA/OCE-8, The American Society of Mechanical Engineers, 354 East 47th St. New York, NY.

Pattison, J.H., (1974) Components of Force Generated by Harmonic Oscillations of Small-Scale Mooring Lines in Water, report number SPD 589-01, David W. Taylor Naval Ship Research and Development Center, Bethesda, MD.

Radwan, A., M.C. Chen, and C.W. Leavitt. (1986) Design Curves for Chain Mooring Systems. *5th International Symposium of the OMAE*, Tokyo.

Sharp, J.J., (1981) *Hydraulic Modelling*, Butterworth & Co. Toronto, Canada.

Shaw, P-K. (1989) Statistics of Mooring-Line Tension in Random Waves, 21st Annual Offshore Technology Conference, Houston, Texas.

Sincock, P. and M. Lalani. (1990), Developments in Fatigue Design Guidelines for Anchor Chains as Mooring Lines, 22nd Annual Offshore Technology Conference, Houston, Texas.

Stansby, P.K., Written discussion in The Hydrodynamic Drag of Roughened Circular Cylinders, by B.L. Miller. Royal Institution of Naval Architects.

Suhara, T., Koterayama, W., Tasai, F., Hiyama, H., Sao, K. and Watanabe, K. (1981) Dynamic Behavior and Tension of Oscillating Mooring Chain, *13th Annual Offshore Technology Conference*, Houston, Texas, pp. 415-424.

Suhara, T., W. Koterayama, H. Hiyama, Y. Koga. (1987) Approximate Analyses if Oscillation of Mooring Line. Research Institute for Applied Mechanics, Kyushu University, Japan.

van Sluijs M. F. and J.J. Blok. (1977) The Dynamic Behaviour of Mooring Lines, 9th Annual Offshore Technology Conference, Houston, Texas.

van den Boom (1985) Dynamic Behaviour of Mooring Lines. Behaviour of Offshore Structures, Amsterdam.

Webster, R.L. (1981) SEADYN Mathematical Models, Report Number CR 82,019, Naval Civil Engineering Laboratory, Port Hueneme, CA 93043.

Appendix A
Derivation of the Catenary Equation

Figure 1 shows a catenary mooring system with the origin of the coordinate system at a point where the slope of the line is 0. At the top end there is a tension T, which acts at angle ψ to hold the line in place, and the line has a uniform mass per unit length of w.

The tension can be broken into components in the x and y direction, giving the following equations:

$$\begin{aligned} T_x &= T\cos\psi \\ T_y &= T\sin\psi = wS. \end{aligned} \tag{1}$$

At the point (x - y), we have

$$\frac{dy}{dx} = \tan\psi = \frac{T\sin\psi}{T\cos\psi} = \frac{wS}{T\cos\psi}. \tag{2}$$

Differentiating with respect to x, remembering that S is a function of x we get

$$\frac{d^2y}{dx^2} = \frac{w}{T\cos\psi}\frac{dS}{dx}. \tag{3}$$

We know from elementary calculus that

$$\frac{dS}{dx} = \sqrt{1+\left(\frac{dy}{dx}\right)^2}.$$

Substituting the above equation into Equation 4 gives

$$\frac{d^2y}{dx^2} = \frac{w}{T\cos\psi}\sqrt{1+\left(\frac{dy}{dx}\right)^2}. \tag{4}$$

The above is a standard second order differential equation with a standard method of solution. Let $p = dy/dx$, then $dp/dx = d^2y/dx^2$. Substituting into Equation 5 and rearranging yields,

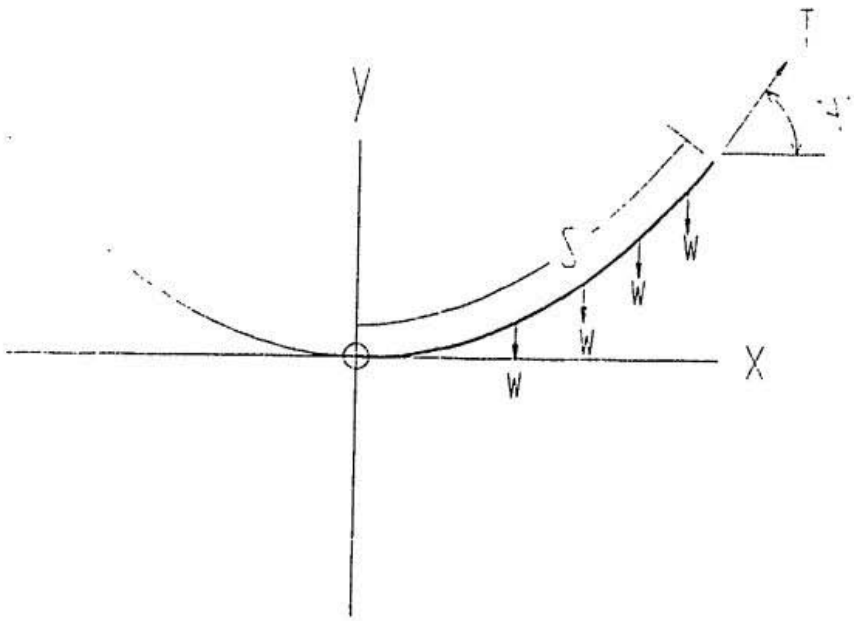

The Catenary Curve

$$\frac{1}{\sqrt{1+p^2}}\frac{dp}{dx} = \frac{w}{T\cos\psi}.$$

Both sides of this equation are integrated to give.

$$\int \frac{1}{\sqrt{1+p^2}}dp = \int \frac{w}{T\cos\psi}dx$$

A standard table of integrals gives as the solution for the left hand side: $\ln(p+\sqrt{p^2+1})+C_1$. This is recognized as the hyperbolic function $\sinh^{-1}p$. Thus,

$$\sinh^{-1}p = \frac{wx}{T\cos\psi} + C_2$$

Since the line has zero slope at the origin, and since $p = dy/dx$; when $x = 0$, $p = 0$. Thus $C_2 = 0$ and we have

$$\sinh^{-1}p = \frac{wx}{T\cos\psi}.$$

Solving for p gives:

$$p = \frac{dy}{dx} = \sinh \frac{wx}{T\cos\psi}. \tag{5}$$

Integration with respect to x of equation 6 gives:

$$\int dy = \int \sinh \frac{wx}{T\cos\psi} dx$$

$$y = \frac{T\cos\psi}{w} \cosh \frac{wx}{T\cos\psi} + C_3$$

When $y = 0$, $x = 0$ and $\cosh wx/T\cos\psi = 1$. Therefore $C_3 = -T\cos\psi/w$. The equation becomes

$$y = \frac{T\cos\psi}{w} \cosh \frac{wx}{T\cos\psi} - \frac{T\cos\psi}{w}. \tag{6}$$

It is desired to solve for the term $T\cos\psi$. Although no explicit formula can be found, this equation is well behaved and is fairly easy to solve iteratively. However the parameters that must be known are x and y. In the model this would correspond to the horizontal distance from the top of the chain to where it touches the bottom and the depth of the water. Depending on the circumstances, it may be easier if the parameters were the scope of chain and the depth of water. Thus the equations will be derived terms of S and y. From before

$$\frac{dS}{dx} = \sqrt{1 + \left(\frac{dy}{dx}\right)^2}$$

$$\frac{dy}{dx} = \sinh \frac{wx}{T\cos\psi}. \tag{7}$$

Combining these two equations gives

$$\frac{dS}{dx} = \sqrt{1 + \sinh^2 \frac{wx}{T\cos\psi}}.$$

Using the identity $1 + \sinh^2 u = \cosh^2 u$ we get

$$\frac{dS}{dx} = \cosh \frac{wx}{T\cos\psi}.$$

For the point $x = a$ the following equation for S is obtained.

$$\begin{aligned} S &= \int_0^a \cosh \frac{wx}{T\cos\psi} dx \\ &= \left[\frac{T\cos\psi}{w} \sinh \frac{wx}{T\cos\psi}\right]_0^a \\ &= \frac{T\cos\psi}{w} \sinh \frac{wa}{T\cos\psi} \end{aligned}$$

Thus for any $x \geq 0$

$$S = \frac{T\cos\psi}{w} \sinh \frac{wx}{T\cos\psi}. \tag{8}$$

Rearranging to solve for x and substituting into Equation 9 gives

$$y = \frac{T\cos\psi}{w} \cosh \sinh^{-1} \frac{Sw}{T\cos\psi} - \frac{T\cos\psi}{w}. \tag{9}$$

Thus $T\cos\psi$ can be found from either Equation 7 or 10 depending on the available information. This, along with Equation 1 provides enough information to find T and ψ.

An alternative method to solving this question is to use an energy approach. The shape is found that contains the minimum potential energy for the system. The resulting equations are identical.

Appendix B

Program for the Static Catenary Analysis

```
C=============================================================
C
C PROGRAM TO ANALYSE THE CATENARY MOORING - BY J.F. CROSS
C   ANALYSIS FOR THE SLACK CASE
C
C    THE PROGRAM SOLVES FOR Z USING A NEWTON-RAPHSON METHOD AND
C    THEN USES Z TO FIND a/h AND CONSEQUENTLY THE TENSIONS.
C
C     SLH = THE VALUE OF (S-L)/h
C       Z = THE VALUE OF THE Z EQUATION THAT GIVES SLH
C     EPS = THE LIMITING DIFFERENCE IN THE NEWTON-RAPHSON ANALYSIS
C  AOVERH = a/h
C   SBARH = S(BAR)/h
C   LBARH = L(BAR)/h
C
C=============================================================
      REAL LBARH
      DATA Z,EPS/.1,.000001/
      OPEN(UNIT=1,FILE='SLACK.OUT',STATUS='UNKNOWN')
      WRITE(1,100)
      WRITE(1,110)
C
C  GO THROUGH SLH VALUES BETWEEN .01 AND .99
      DO 10 I=1,99
      SLH = REAL(I)/100
C
C  FIND Z USING A NEWTON-RAPHSON METHOD
1     CONTINUE
      Z1 = Z - (FUN(SLH,Z)/DFUN(Z))
C  CHECK TO SEE IF SUCESSIVE Z'S DIFFER BY LESS THAN EPS
      IF (ABS(Z-Z1) .GT. EPS) THEN
         Z=Z1
         GOTO 1
```

```
      END IF
C  IF THE Z'S DIFFER BY LESS THAN EPS THE ROOT IS FOUND SO
C  NOW GO ON TO CALCULATE a/h AND THE OTHER EQUATIONS.
      AOVERH = 1/(COSH(Z) - 1)
      T = 1 + AOVERH
      TH = AOVERH
      TV = SQRT((1+AOVERH)**2 - AOVERH**2)
      THETA = ACOS(AOVERH/(1+AOVERH))
      THETA = THETA*180/3.1415927
      SBARH = SINH(Z)/(COSH(Z)-1)
      LBARH = SBARH - SLH
      P1= .5*(SBARH - SBARH*AOVERH + AOVERH*LBARH -1)
      P2= .5*(SBARH + SBARH*AOVERH + AOVERH*LBARH)
      WRITE(1,120) SLH,Z,T,TH,TV,THETA,P1,P2
10    CONTINUE
100   FORMAT(1X,20X,'SLACK CASE TABLE OF VALUES',/)
110   FORMAT(1X,'(S-L)/H',4X,'Z',8X,'T',8X,'Th',8X,'Tv',4X,'THETA',
     +                                    3X,'Pgrav',4X,'Pstr',/)
120   FORMAT(1X,2X,F4.2,2X,F7.5,2X,F8.2,2X,F8.2,2X,F6.2,2X,F5.2,1X,
     +                                              F7.3,1X,F10.2)
      STOP
      END
C=====================================================================
C FUNCTION FOR FINDING Z FOR SLACK LINES
C=====================================================================
      FUNCTION FUN(SLH,Z)
      FUN=SLH - (SINH(Z) - Z) /(COSH(Z) -1)
      RETURN
      END
C=====================================================================
C  DERIVATIVE OF THE FUNCTION FOR FINDING Z
C=====================================================================
      FUNCTION DFUN(Z)
      DFUN= -((COSH(Z)-1)**2-SINH(Z)*(SINH(Z)-Z))/((COSH(Z)-1)**2)
      RETURN
      END


C=====================================================================
C
C PROGRAM TO ANALYSE THE CATENARY MOORING - BY J.F. CROSS
C  ANALYSIS FOR THE TAUT CASE
C
```

```
C   THE PROGRAM ACCEPTS AN S/h RATIO AS DATA.  IT THEN CALCULATES
C   THE MINIMUM AND MAXIMUM POSSIBLE L/h VALUES.  THE VARIABLES
C   ARE CALCULATED AT 30 POINTS BETWEEN THE MAX AND MIN L/h.
C   ALL ROOT SOLVING USE THE NEWTON-RAPHSON METHOD.  BECAUSE
C   SOME OF THE FUNCTIONS ARE VERY SENSITIVE, DOUBLE PERCISION
C   IS USED.
C
C
C  SOVERH = S/h
C  LOVERH = L/H
C       Z = THE VALUE OF THE Z EQUATION
C     EPS = THE LIMITING DIFFERENCE IN THE NEWTON-RAPHSON ANALYSIS
C  AOVERH = a/h
C      LL = LOWER LIMIT FOR L/h
C      UL = UPPER LIMIT FOR L/h
C
C=================================================================
      IMPLICIT REAL*8 (A-H,L,O-Z)
      DATA Z,EPS,I/.1,.0000000000001,0/
      DATA S,H/6.0,1.0/

      OPEN(UNIT=1,FILE='TAUT.OUT',STATUS='UNKNOWN')
      WRITE(1,100) (S/H)
      WRITE(1,110)
C
C  FIND THE RANGE FOR THE VARIABLE L/h
      SOVERH = S/H
      CALL LOWLIM(S,H,LL)
      CALL UPLIM(S,H,LU)
      RANGE = LU-LL
      PLUS = RANGE/31.
C  CALCULATE THE VALUES FOR THIS RANGE
      DO 10 I=1,30
         L = LL + REAL(I)*PLUS
         LOVERH = L/H
         CONST = DSQRT((SOVERH)**2 -1.)/LOVERH
         CALL SOLVE(CONST,Z)
         AOVERH = LOVERH/(2.*Z)
         XOOVRH = AOVERH*(.5*DLOG((1.+H/S)/(1.-H/S))-Z)
         YOOVRH = AOVERH*DCOSH(XOOVRH/AOVERH)
         T = 1. + YOOVRH
         TH = AOVERH
```

```
          TV = DSQRT((1+AOVERH)**2 - AOVERH**2)
          THETA = DACOS(AOVERH/(1.+YOOVRH))
          THETA = THETA*180/3.14159
          RH = AOVERH
          WRITE(1,120) SOVERH,LOVERH,T,TH,TV,THETA
10     CONTINUE
100    FORMAT(1X,5X,'TAUT CASE TABLE OF VALUES FOR S/h = ',F4.1,/)
110    FORMAT(1X,2X,'S/h',5X,'L/h',8X,'T',8X,'Th',8X,'Tv',3X,
     +                                                    'THETA')
120    FORMAT(1X,2X,F4.2,2X,F7.5,2X,F8.4,2X,F8.4,2X,F6.2,2X,F5.2)
       STOP
       END
C=======================================================================
C  SUBROUTINE LOWLIM - FINDS THE LOWER LIMIT FOR THE VARIABLE L/h
C       THE NEWTON-RAPHSON METHOD IS USED TO FIND L/h.  THE
C       FUNCTION AND ITS DERIVATIVE ARE CALCULATED IN LINE 1
C
C=======================================================================
       SUBROUTINE LOWLIM(S,H,L)
       IMPLICIT REAL*8 (A-H,L,O-Z)
       Z = 1.
       EPS = .0000000000001
1      Z1 = Z - (H/S-(DCOSH(Z)-1.)/DSINH(Z))
     + /(-1.*((DSINH(Z)**2-DCOSH(Z)*(DCOSH(Z)-1.))/DSINH(Z)**2))
       IF(DABS(Z1-Z) .GT. EPS) THEN
           ABC = DABS(Z1-Z)
           Z = Z1
           GOTO 1
       END IF
       L = S*Z/DSINH(Z)
       RETURN
       END
C=======================================================================
C  SUBROUTINE UPLIM TO FIND THE UPPER LIMIT OF L/a
C=======================================================================
       SUBROUTINE UPLIM(S,H,L)
       IMPLICIT REAL*8 (A-H,L,O-Z)
       L = DSQRT(S**2 - H**2)
       RETURN
       END
C=======================================================================
C  SUBROUTINE SOLVE - FINDS THE Z FROM THE Z EQUATION
```

```
C=======================================================================
      SUBROUTINE SOLVE(C,Z)
      IMPLICIT REAL*8 (A-H,L,O-Z)
      Z = 3.0
      EPS = .0000000000001
1     Z1 = Z - ((C-DSINH(Z)/Z)/(-1*(DCOSH(Z)*Z-DSINH(Z))/Z**2))
      IF(DABS(Z1-Z) .GT. EPS) THEN
         Z = Z1
         GOTO 1
      END IF
      L = S*Z/DSINH(Z)
      RETURN
      END
```

Appendix C

Drawings for the Experimental Equipment

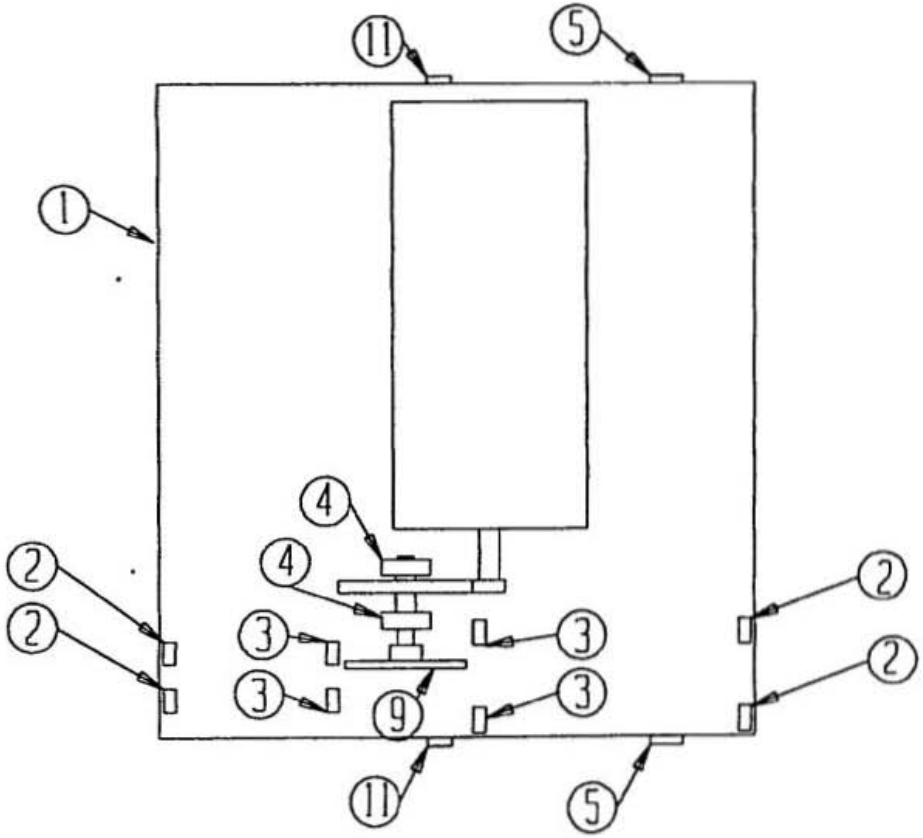

Part Number	Part Name	Quantity
1	Support	1
2	Rail Support Outside	4
3	Rail Support Inside	4
4	Shaft Support	2
5	Pivot	2
6	Wheel 1	4
7	Wheel 2	4
8	Yoke	1
9	Disk	1
10	Shaft	1
11	Side Support	2
12	Gear CG 2020	1
13	Gear CG 2080	1
14	Bearing SKF 6001	1
15	Shaft 1	1
16	Shaft 2	2
17	Chain Block	1
18	Shaft 3	1

Title: Assembly Drawing # 1
Drawing number 1 of 3.
by: J. Cross Date: 08-08-90
Material:

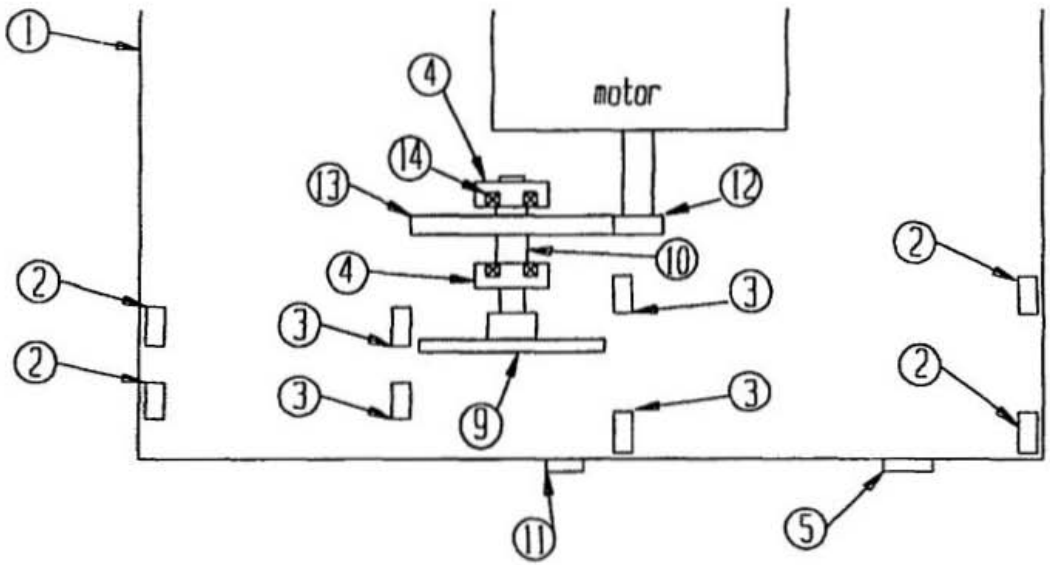

Part Number	Part Name	Quantity
1	Support	1
2	Rail Support Outside	4
3	Rail Support Inside	4
4	Shaft Support	2
5	Pivot	2
6	Wheel 1	4
7	Wheel 2	4
8	Yoke	1
9	Disk	1
10	Shaft	1
11	Side Support	2
12	Gear CG 2020	1
13	Gear CG 2080	1
14	Bearing SKF 6001	1
15	Shaft 1	1
16	Shaft 2	2
17	Chain Block	1
18	Shaft 3	1

Title: Assembly Drawing # 2
Drawing number 2 of 3
by: J. Cross Date: 08-08-90

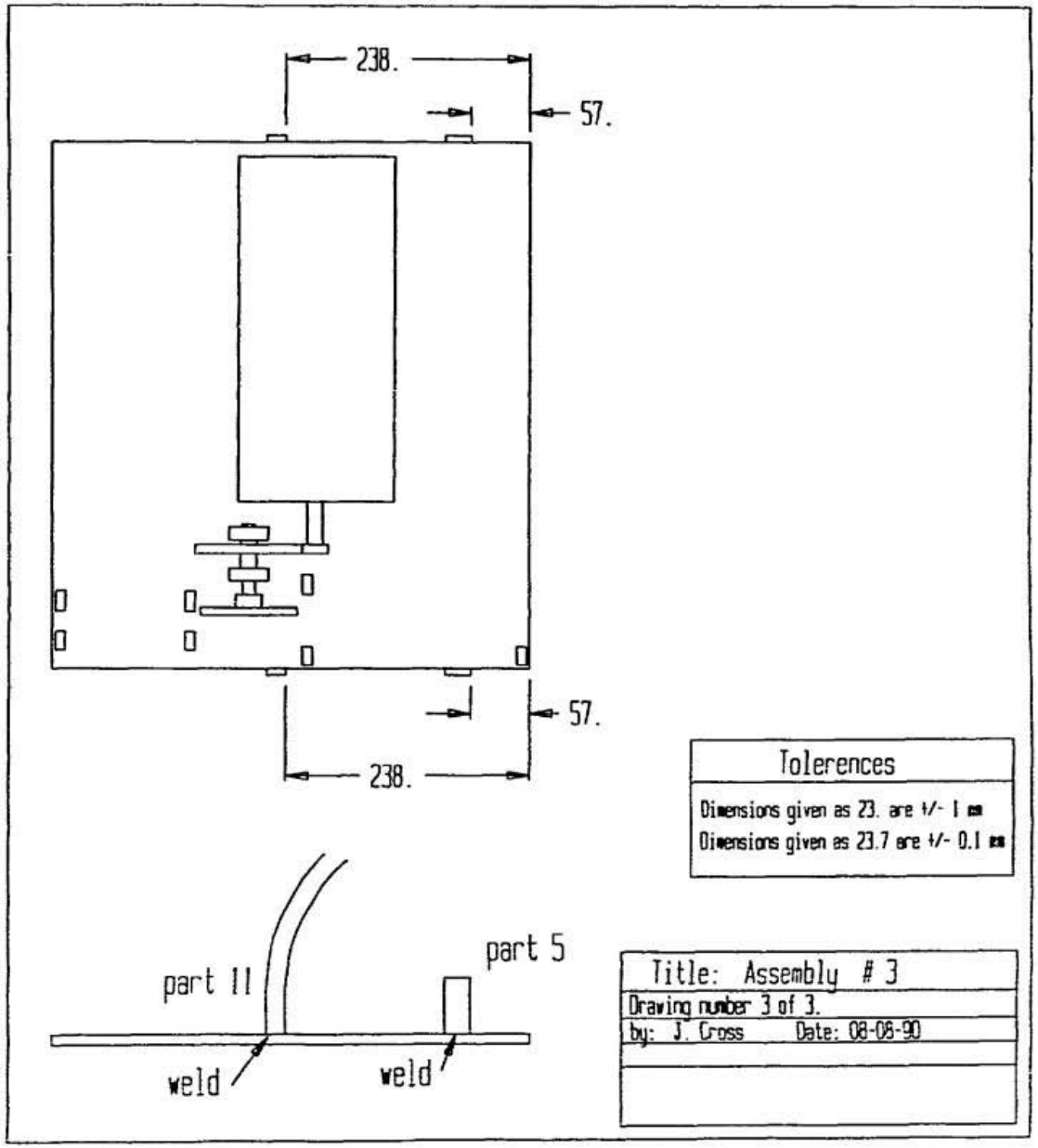
238.
57.
57.
238.
Tolerences
Dimensions given as 23. are +/- 1 mm
Dimensions given as 23.7 are +/- 0.1 mm
part 11
part 5
weld
weld
Title: Assembly # 3
Drawing number 3 of 3.
by: J. Cross Date: 08-05-90

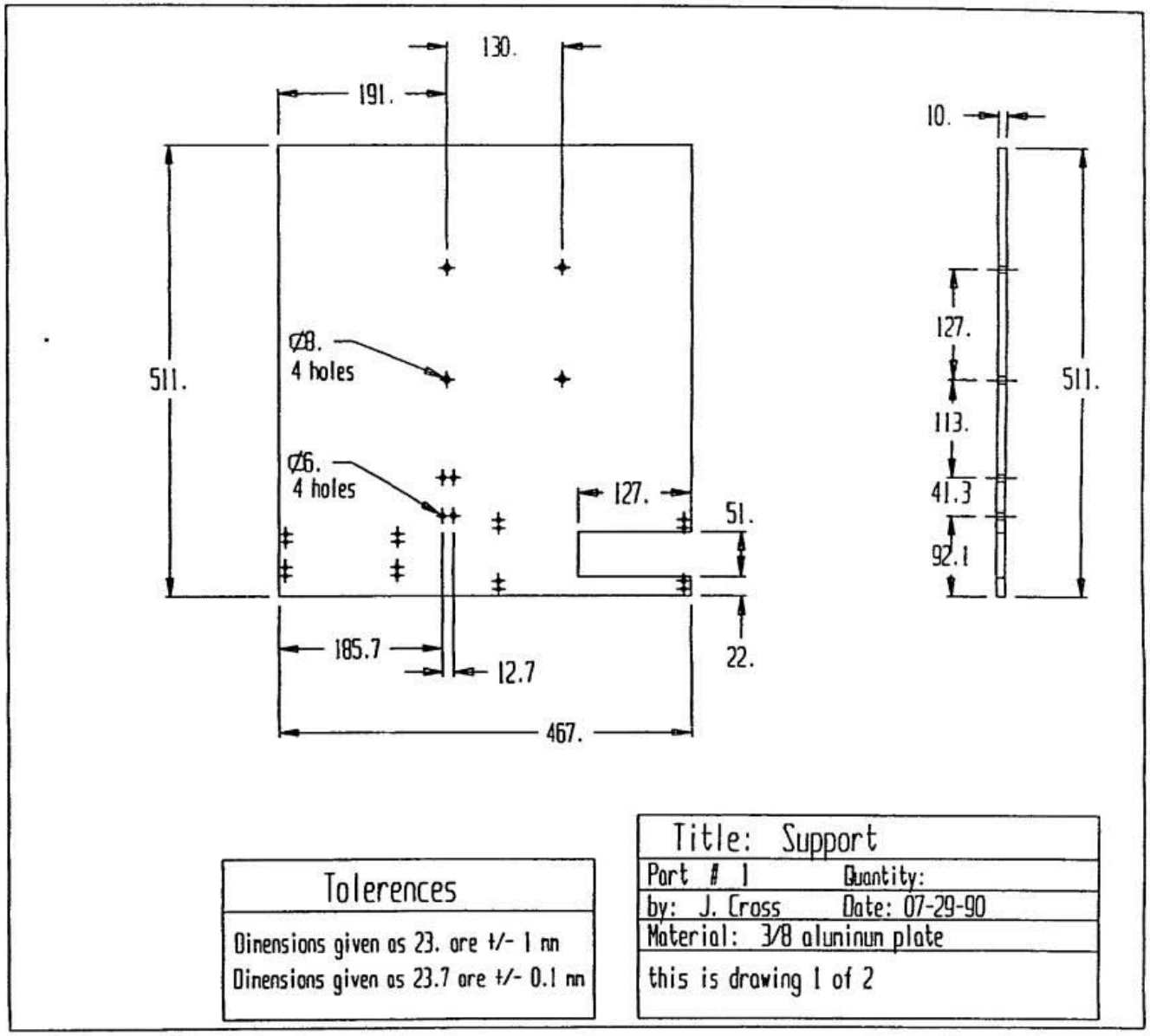

Tolerences
Dinensions given as 23. are +/- 1 nn
Dinensions given as 23.7 are +/- 0.1 nn

Title: Support	
Part # 1	Quantity:
by: J. Cross	Date: 07-29-90
Material: 3/8 aluninun plate	
this is drawing 1 of 2	

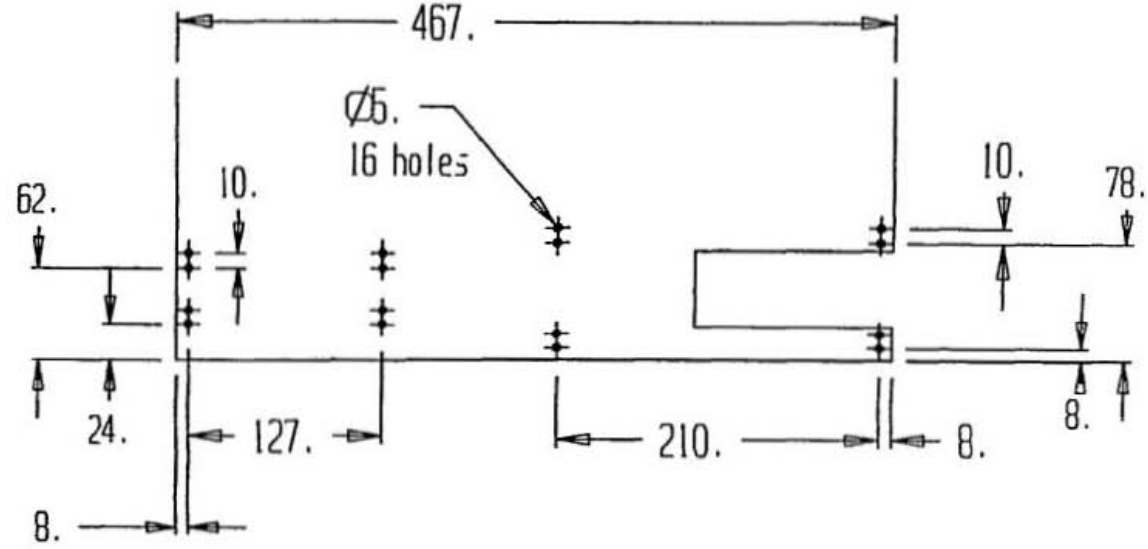

Tolerences
Dimensions given as 23. are +/- 1 mm
Dimensions given as 23.7 are +/- 0.1 mm

Title: Support	
Part # 1	Quantity: 1
by: J. Cross	Date: 07-29-90
Material: 3/8 aluminum	
drawing 2 of 2 top part not shown	

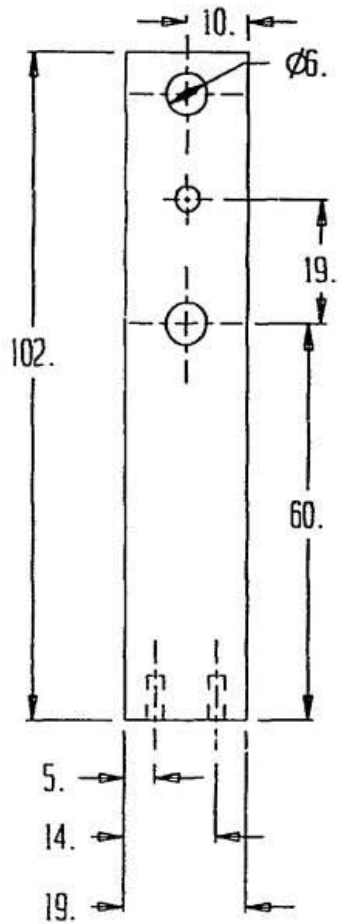

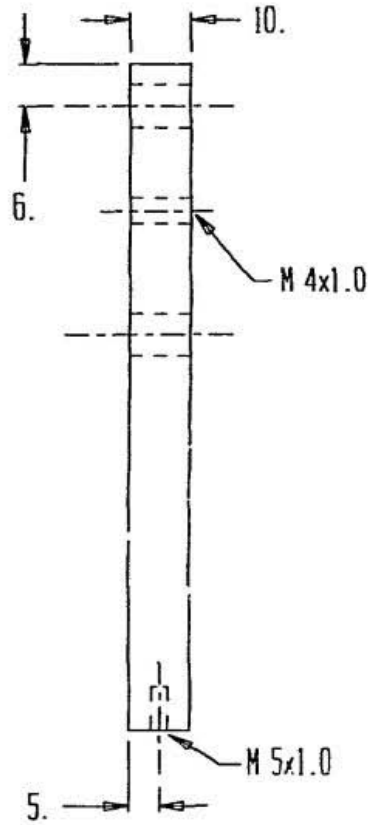

Tolerences
Dimensions given as 23. are +/- 1 mm Dimensions given as 23.7 are +/- 0.1 mm

Title: Rail Support - outside	
Part # 2	Quantity: 4
by: J. Cross	Date: 07-27-90
Material: 3/8 aluminum plate	

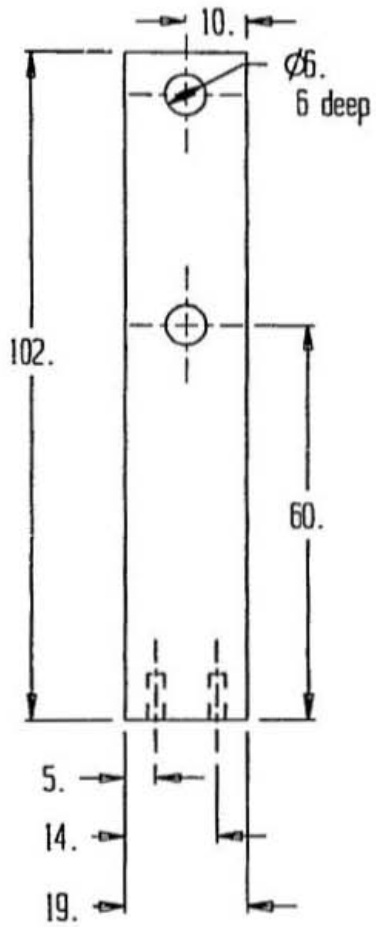

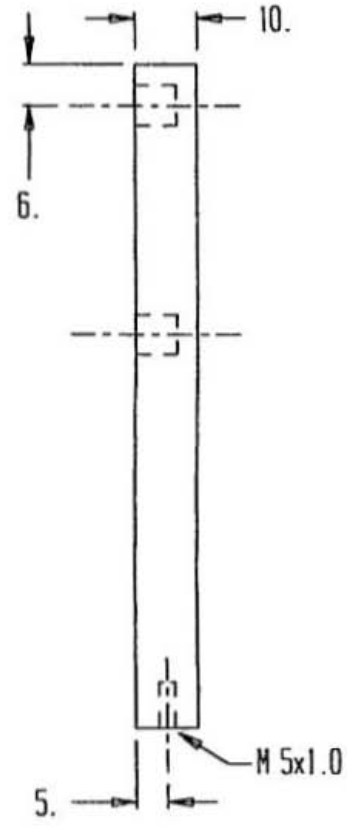

Tolerences
Dimensions given as 23. are +/- 1 mm Dimensions given as 23.7 are +/- 0.1 mm

Title: Rail Support - inside	
Part # 3	Quantity: 4
by: J. Cross	Date: 14-08-90
Material: 3/8 aluminum plate	

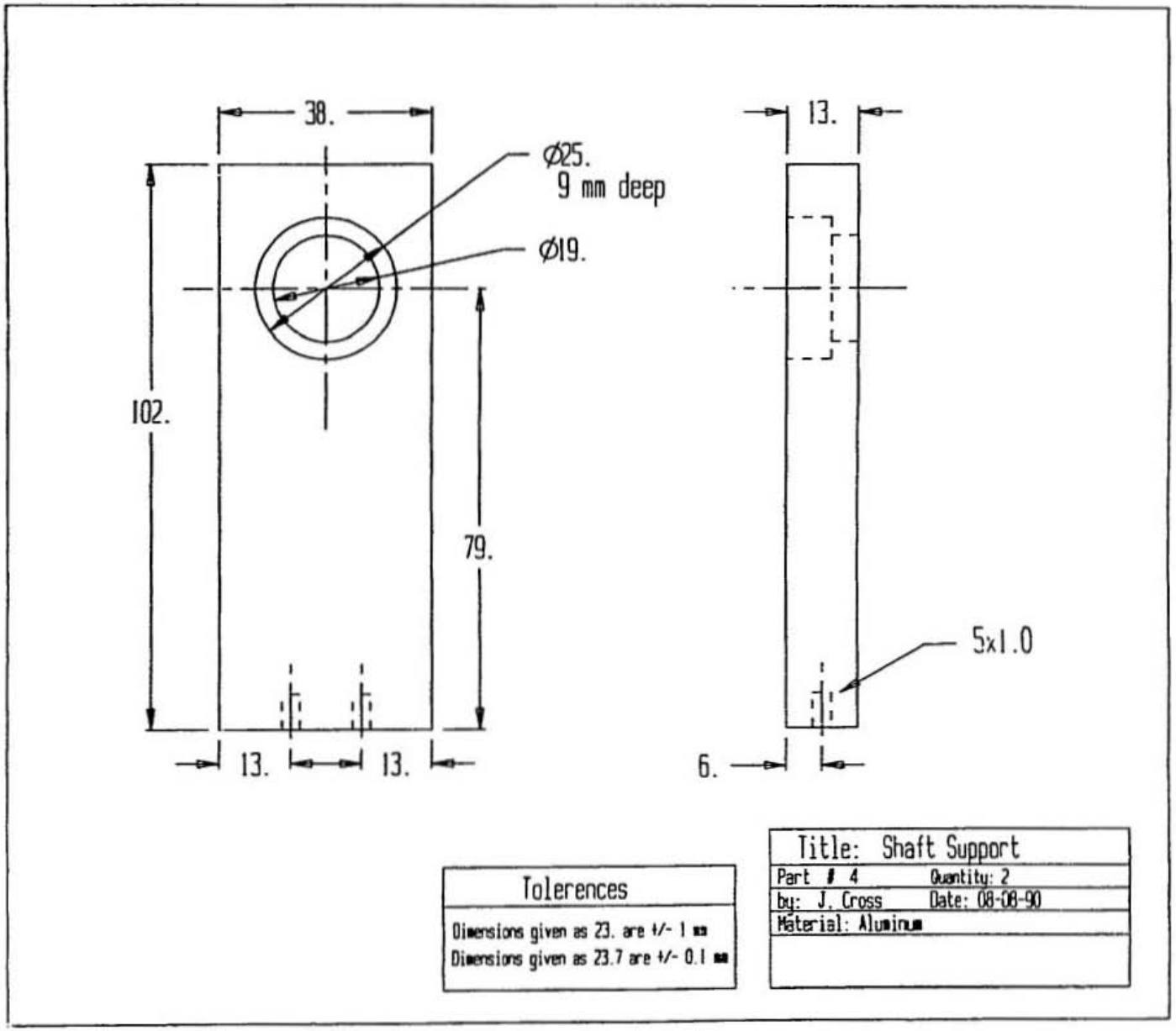
38.
Ø25.
9 mm deep
Ø19.
102.
79.
13.
13.
13.
6.
5x1.0
Tolerences
Dimensions given as 23. are +/- 1 mm
Dimensions given as 23.7 are +/- 0.1 mm
Title: Shaft Support
Part # 4
Quantity: 2
by: J. Cross
Date: 08-06-90
Material: Aluminum

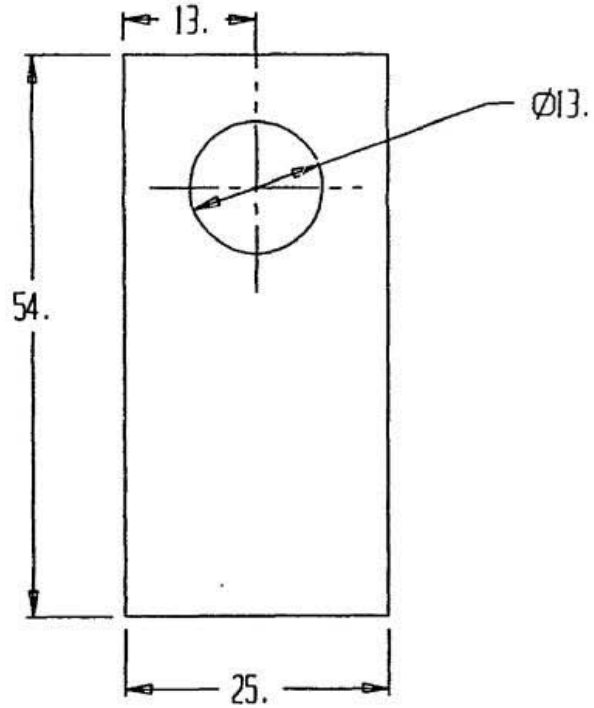

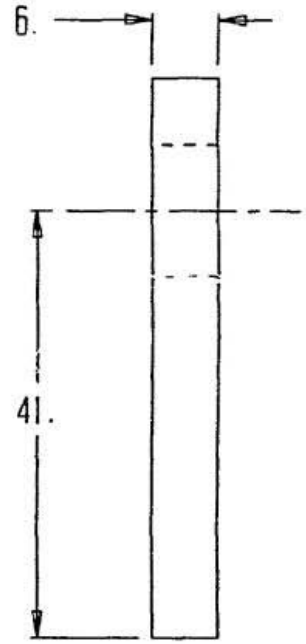

Tolerences
Dinensions given as 23. are +/- 1 nn Dinensions given as 23.7 are +/- 0.1 nn

Title: Pivot	
Part # 5	Quantity: 2
by: J. Cross	Date: 08-02-90
Material: 1/4 aluninun plate	

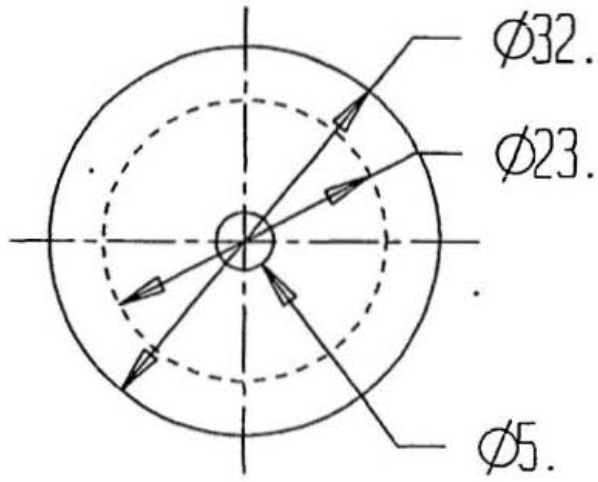

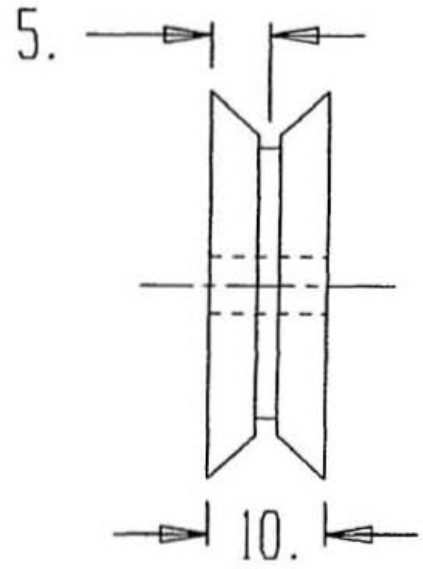

Tolerences
Dimensions given as 23. are +/- 1 mm
Dimensions given as 23.7 are +/- 0.1 mm

Title: Wheel 1	
Part # 6	Quantity: 4
by: J. Cross	Date: 08-08-90
Material: HDPE	

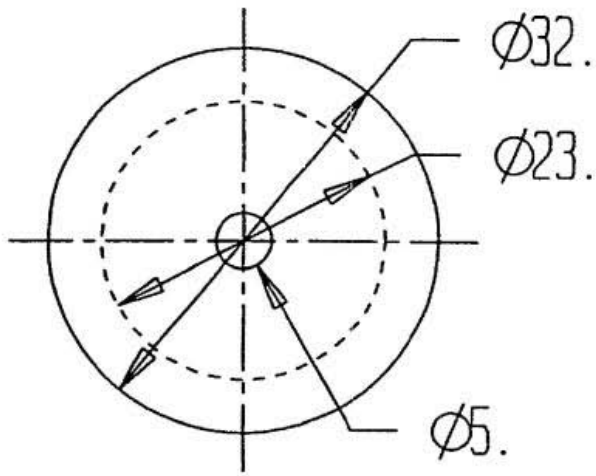

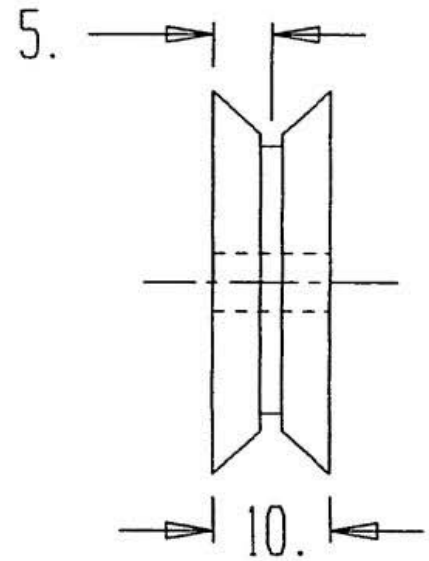

Tolerences
Dimensions given as 23. are +/- 1 mm Dimensions given as 23.7 are +/- 0.1 mm

Title: Wheel 2	
Part # 7	Quantity: 4
by: J. Cross	Date: 08-08-90
Material: HDPE	

06

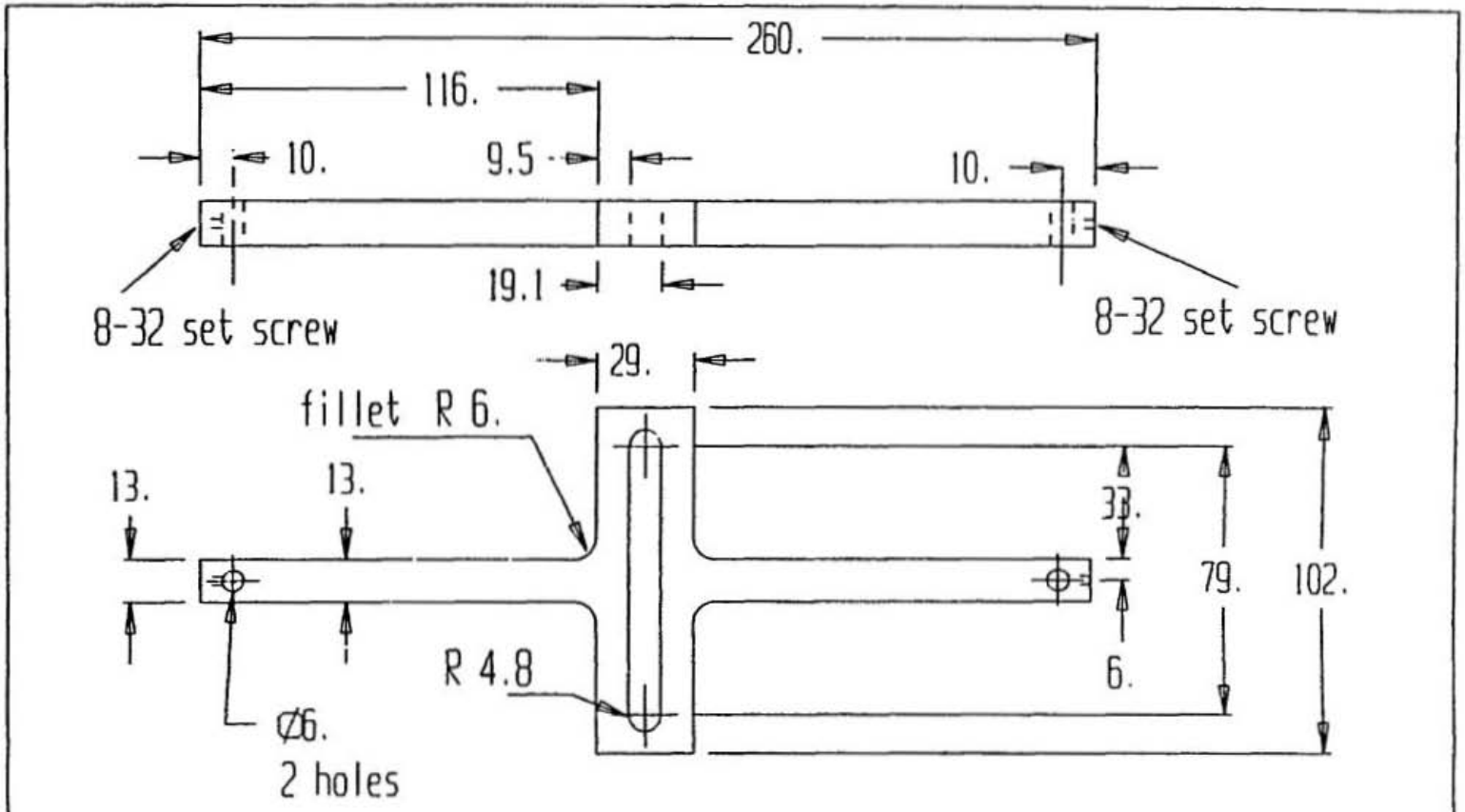

Tolerences
Dimensions given as 23. are +/- 1 mm Dimensions given as 23.7 are +/- 0.1 mm

Title: Yoke	
Part # 8	Quantity: 1
by: J. Cross	Date: 08-03-90
Material: 1/2 aluminum plate	
setscrew designation in imperial units	

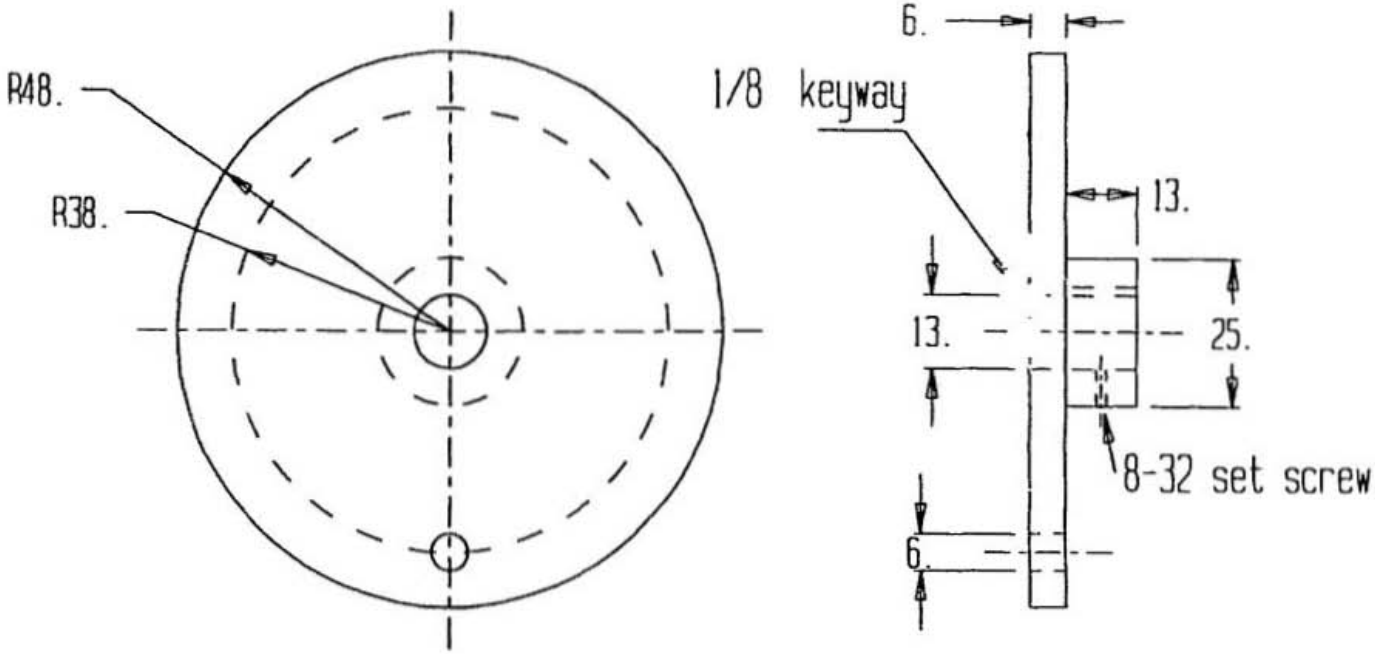

Tolerences
Dimensions given as 23. are +/- 1 mm Dimensions given as 23.7 are +/- 0.1 mm

Title: Disk	
Part # 9	Quantity: 1
by: J. Cross	Date: 29-07-90
Material: Steel	
Keyway and setscrew in imperial units.	

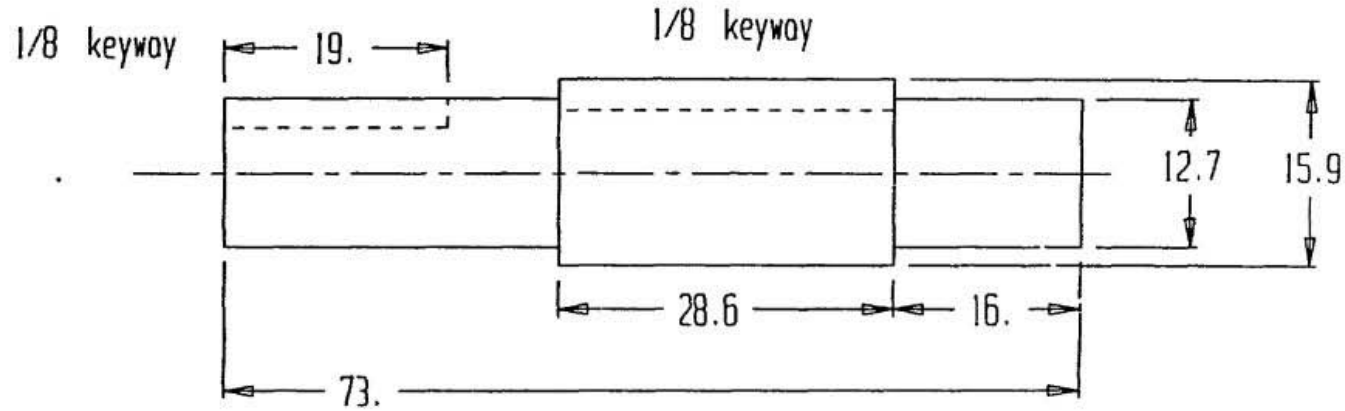

Tolerences
Dimensions given as 23. are +/- 1 mm
Dimensions given as 23.7 are +/- 0.1 mm

Title: Shaft	
Part # 10	Quantity: 1
by: J. Cross	Date: 08-10-90
Material: mild steel	
keyway dimensions are in imperial units	

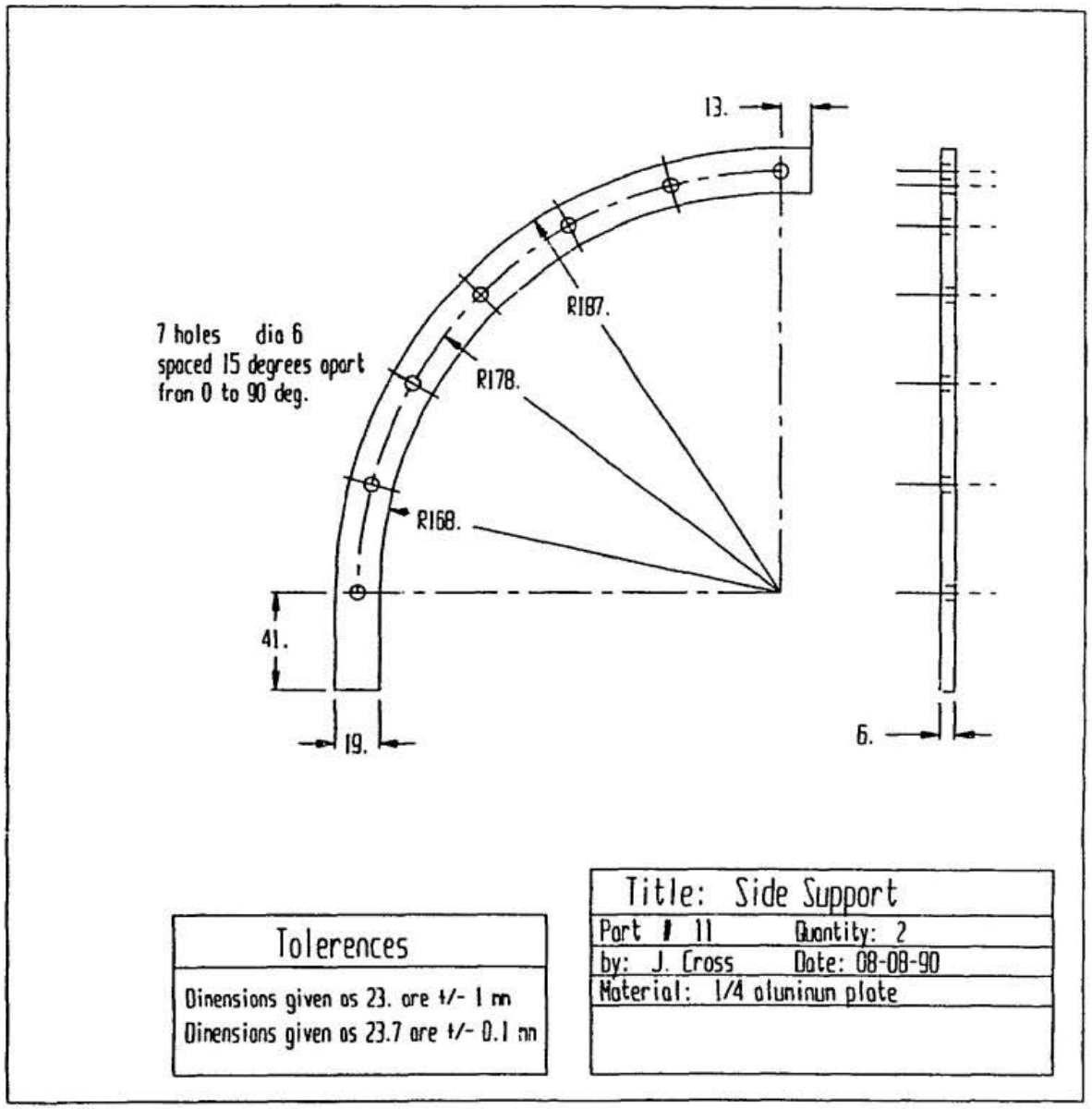

Tolerences
Dinensions given as 23. are +/- 1 nn
Dinensions given as 23.7 are +/- 0.1 nn

Title: Side Support	
Part # 11	Quantity: 2
by: J. Cross	Date: 08-08-90
Material: 1/4 aluninun plate	

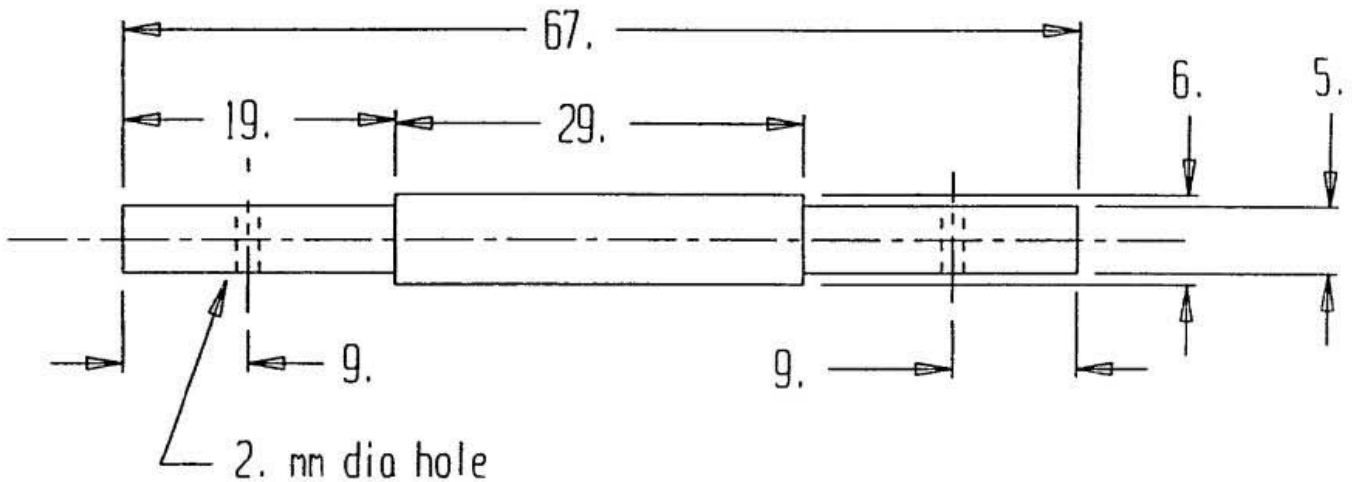

Tolerences
Dimensions given as 23. are +/- 1 mm
Dimensions given as 23.7 are +/- 0.1 mm

Title: Shaft - 1	
Part # 15	Quantity: 1
by: J. Cross	Date: 08-16-90
Material: Mild steel	

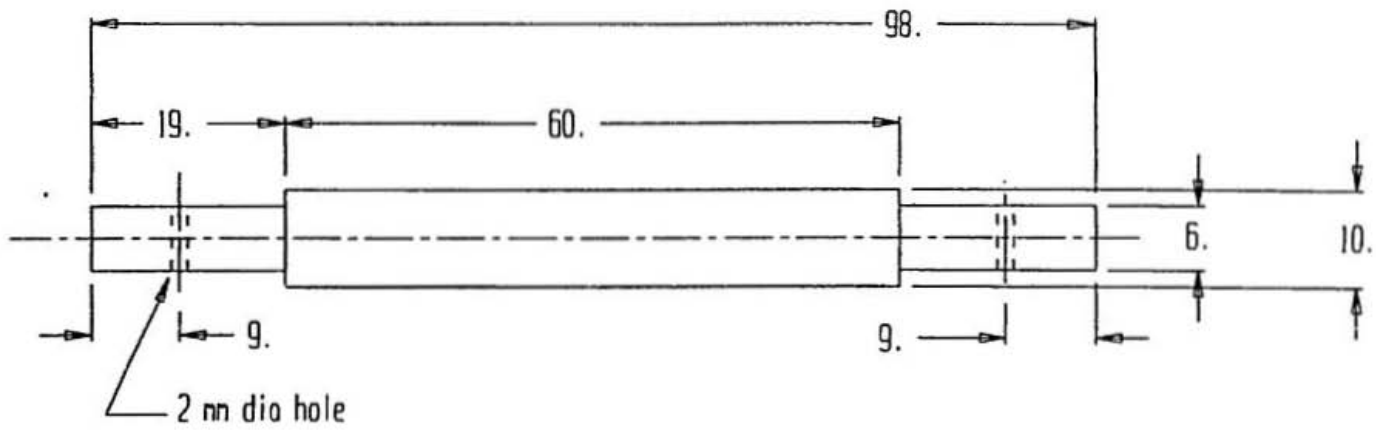

Tolerences
Dimensions given as 23. are +/- 1 mm Dimensions given as 23.7 are +/- 0.1 mm

Title: Shaft - 2	
Part # 16	Quantity: 2
by: J. Cross	Date: 08-12-90
Material: mild steel	

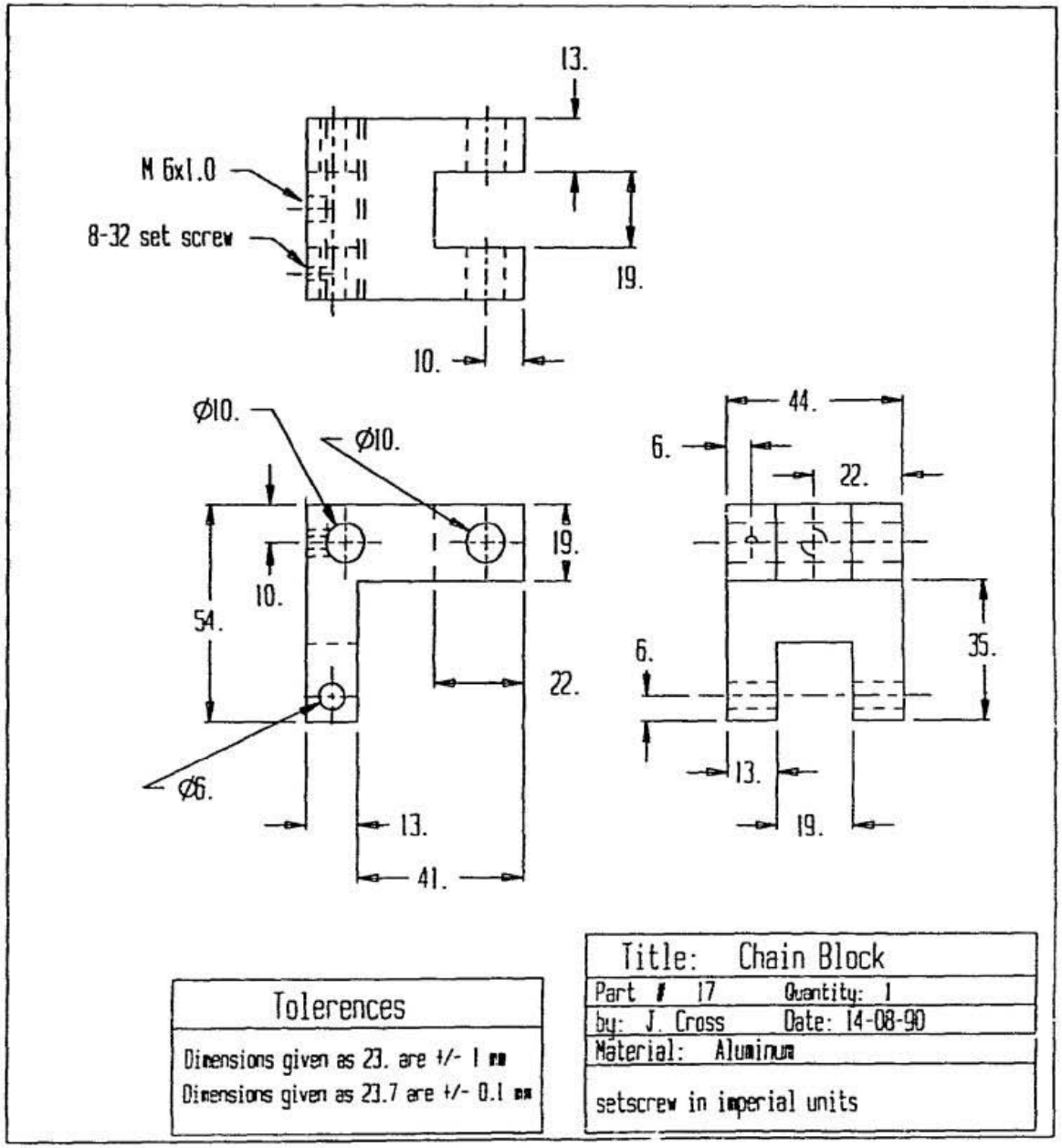

Tolerences
Dimensions given as 23. are +/- 1 mm
Dimensions given as 23.7 are +/- 0.1 mm

Title: Chain Block	
Part # 17	Quantity: 1
by: J. Cross	Date: 14-08-90
Material: Aluminum	
setscrew in imperial units	

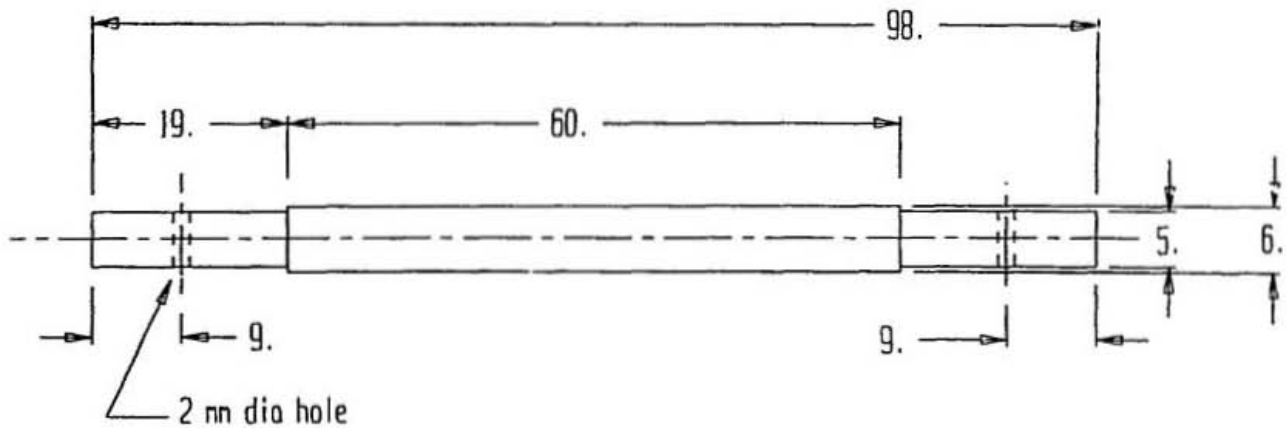

Tolerences
Dinensions given as 23. are +/- 1 nn
Dinensions given as 23.7 are +/- 0.1 nn

Title: Shaft - 3	
Part # 18	Quantity: 1
by: J. Cross	Date: 08-12-90
Material: mild steel	

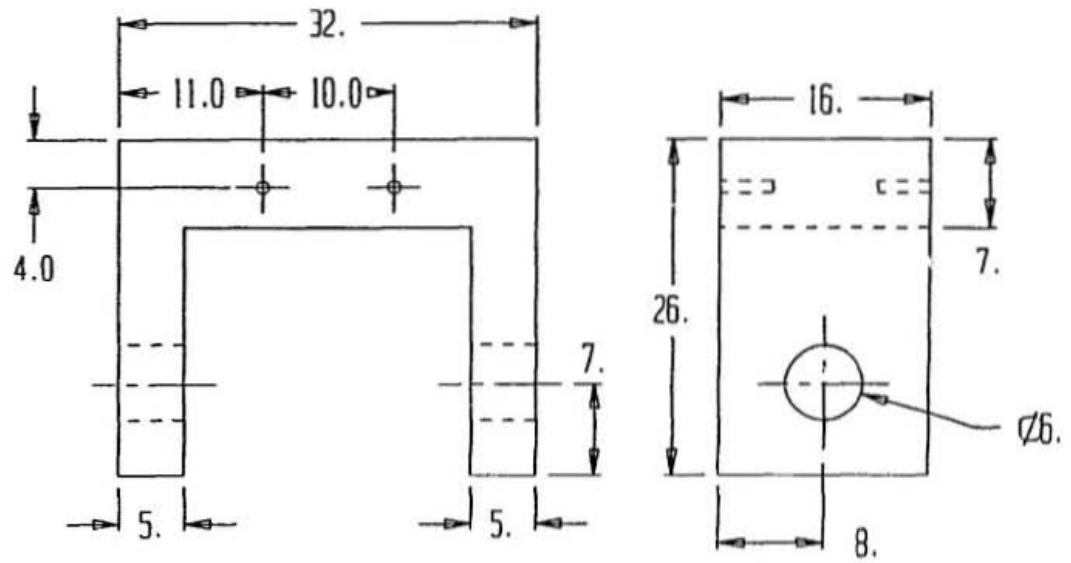

Tolerences
Dinensions given as 23. are +/- 1 nn
Dinensions given as 23.7 are +/- 0.1 nn

Title: Force Trans - botton	
Part # T-1	Quantity: 1
by: J. Cross	Date: 09-10-90
Material: Aluninun	

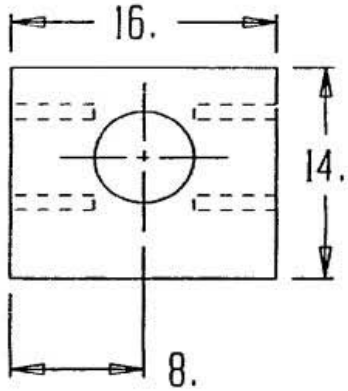

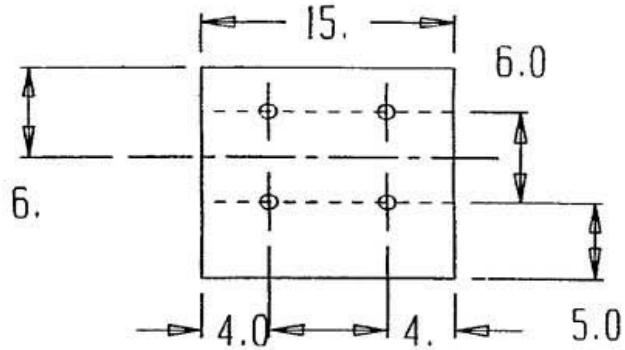

Tolerences
Dinensions given as 23. are +/- 1 nn Dinensions given as 23.7 are +/- 0.1 nn

Title: Force Trans -H -top	
Part # T-2	Quantity: 1
by: J. Cross	Date: 09-11-90
Material:	

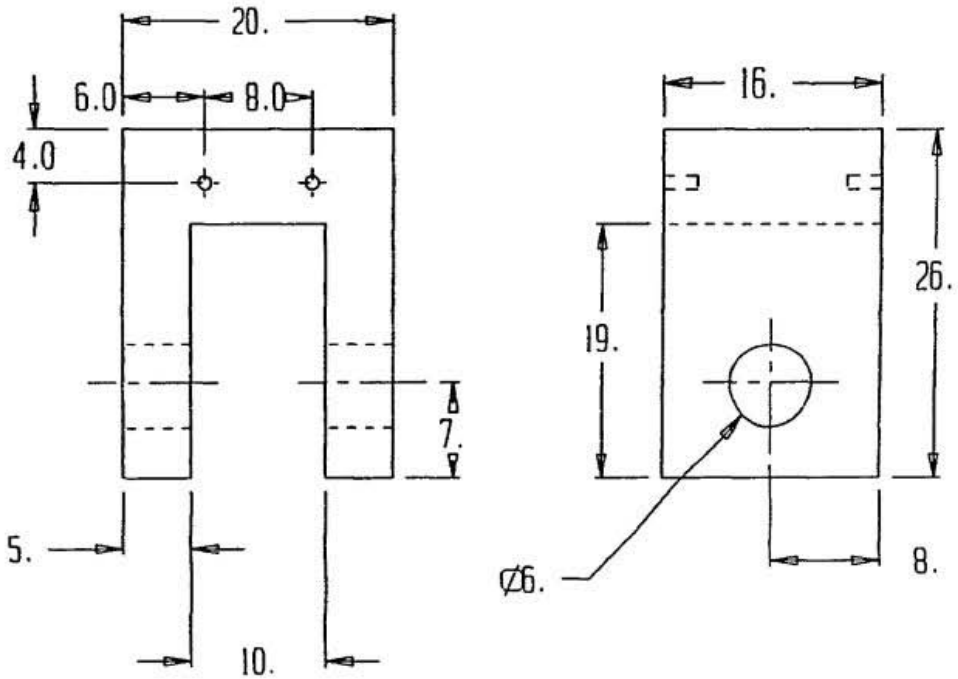

Tolerences
Dimensions given as 23. are +/- 1 mm
Dimensions given as 23.7 are +/- 0.1 mm

Title: Force Trans - botton	
Part # T-3	Quantity: 1
by: J. Cross	Date: 09-10-90
Material: Aluminum	

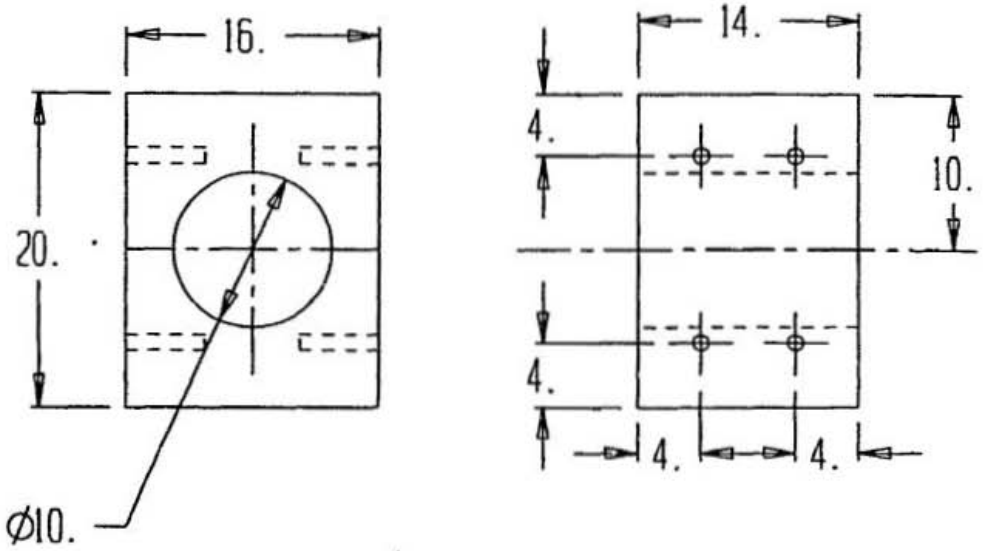

Tolerences
Dimensions given as 23. are +/- 1 mm Dimensions given as 23.7 are +/- 0.1 mm

Title: Force Trans - top	
Part # T-4	Quantity: 1
by: J. Cross	Date: 09-10-90
Material: Aluminum	

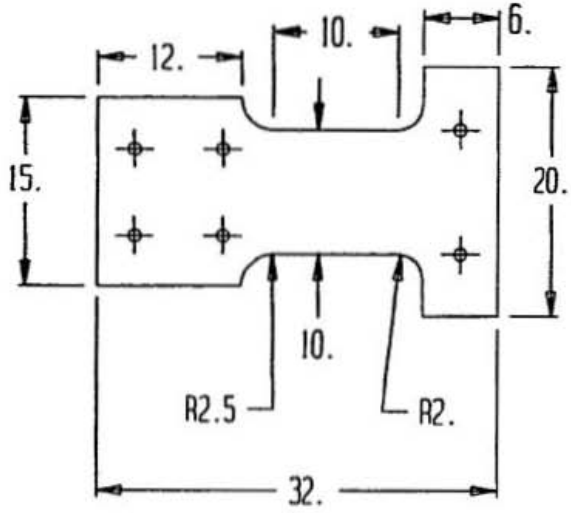

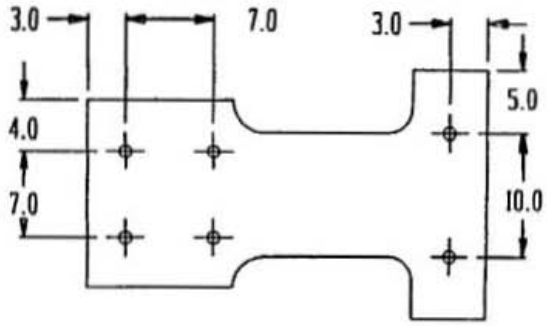

Tolerences
Dimensions given as 23. are +/- 1 mm
Dimensions given as 23.7 are +/- 0.1 mm

Title: horizontal shim	
Part # T-5	Quantity: 2
by: J. Cross	Date: 09-11-90
Material: ten-thou steel shim plate	

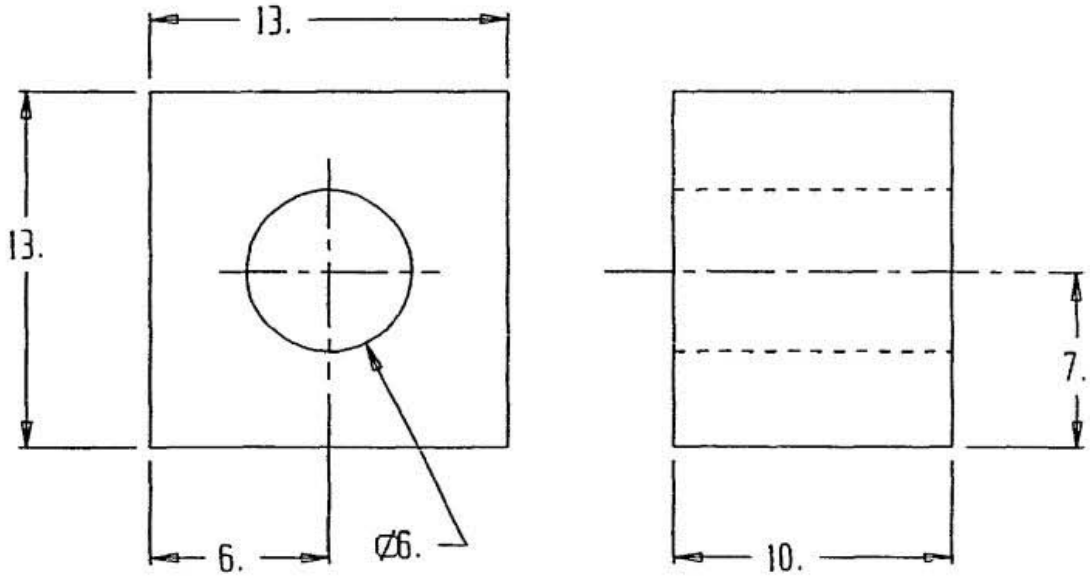

Tolerences
Dinensions given as 23. are +/- 1 mm
Dinensions given as 23.7 are +/- 0.1 mm

Title: Block	
Part #	Quantity: 1
by: J. Cross	Date: 08-08-90
Material: Steel	

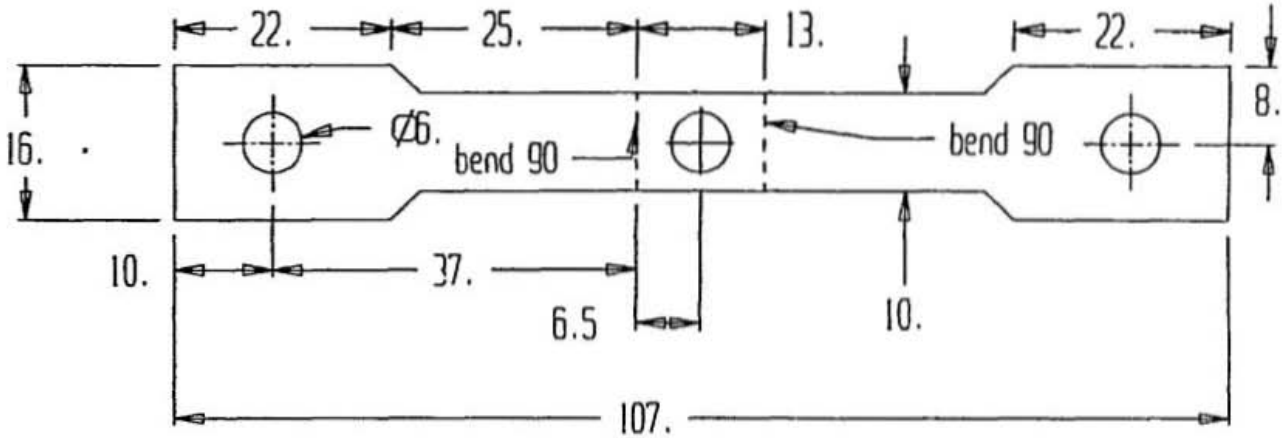

Tolerences
Dimensions given as 23. are +/- 1 mm
Dimensions given as 23.7 are +/- 0.1 mm

Title: Connector	
Part #	Quantity: 1
by: J. Cross	Date: 08-08-90
Material: 1 mm steel plate (or closest)	
Connector to join the yoke and the rail block.	

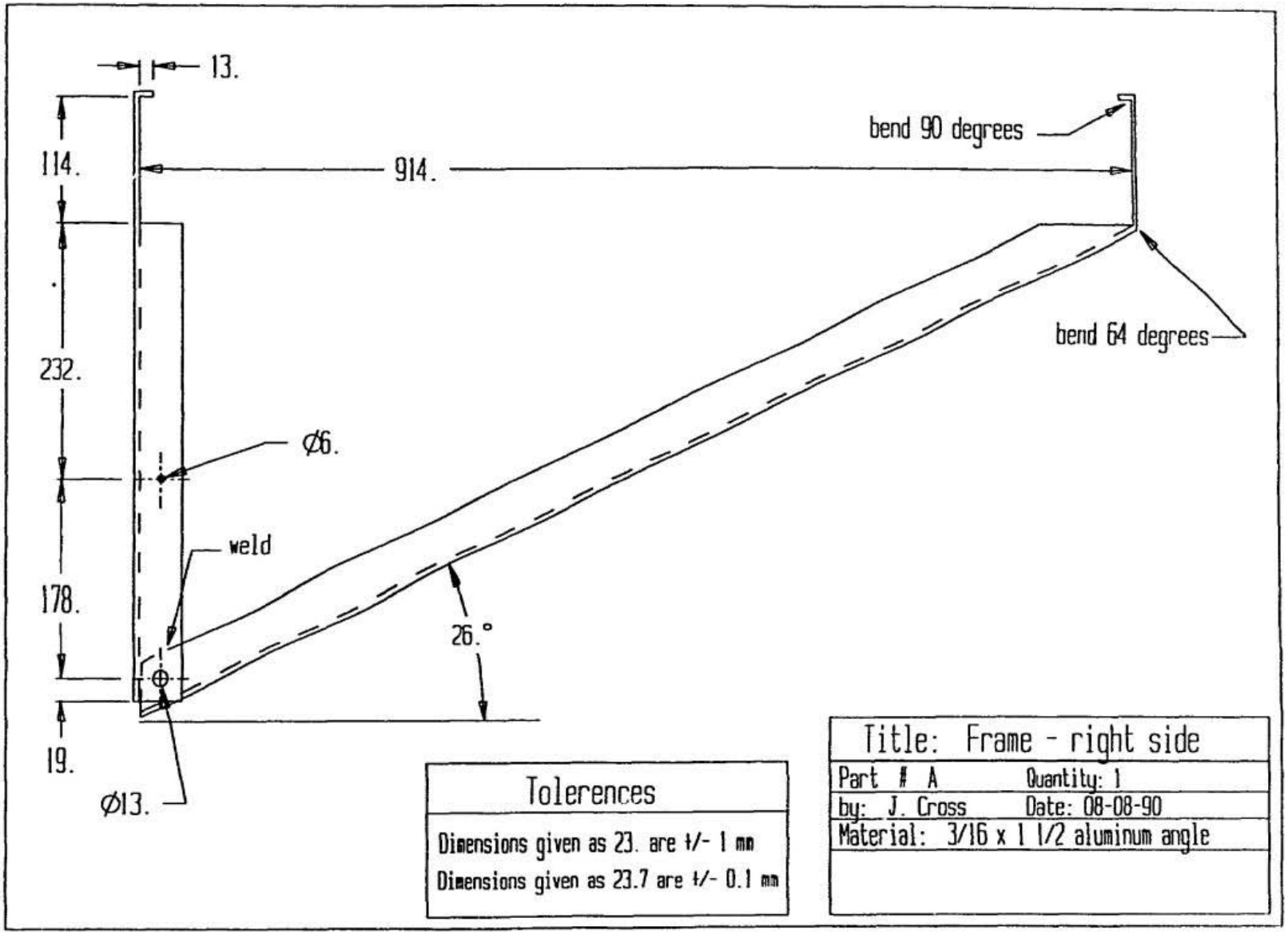

Tolerences
Dimensions given as 23. are +/- 1 mm
Dimensions given as 23.7 are +/- 0.1 mm

Title: Frame - right side	
Part # A	Quantity: 1
by: J. Cross	Date: 08-08-90
Material: 3/16 x 1 1/2 aluminum angle	

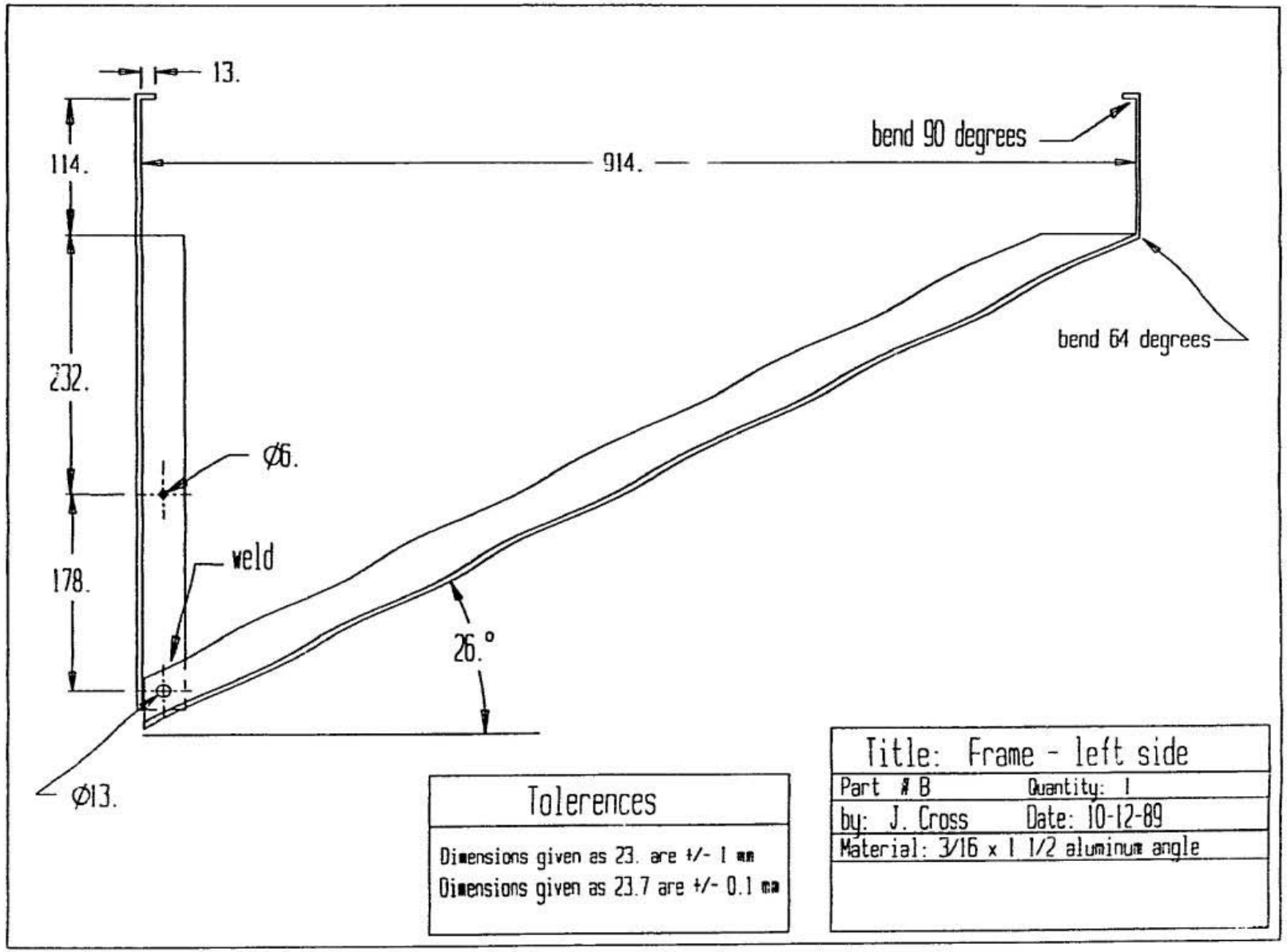

Tolerences
Dimensions given as 23. are +/- 1 mm
Dimensions given as 23.7 are +/- 0.1 mm

Title: Frame - left side	
Part # B	Quantity: 1
by: J. Cross	Date: 10-12-89
Material: 3/16 x 1 1/2 aluminum angle	

Appendix D

Data from the Experimental Runs

This Appendix contain the force-time traces from the experimental runs. The data were filtered before being plotted. Information about the run is contained in the title of the plot. The first letter refers to the pre-tension in the test line. The letter A indicates a pre-tension of 15N, B - 20N and C - 30N. The next number gives information about the angle that the experiment took place with 1 meaning horizontal and 4 vertical. The next letter S is just used as a spacer. The last two numbers are the speed on the controller box and gives a relative measure of the frequency that the experiment took place.

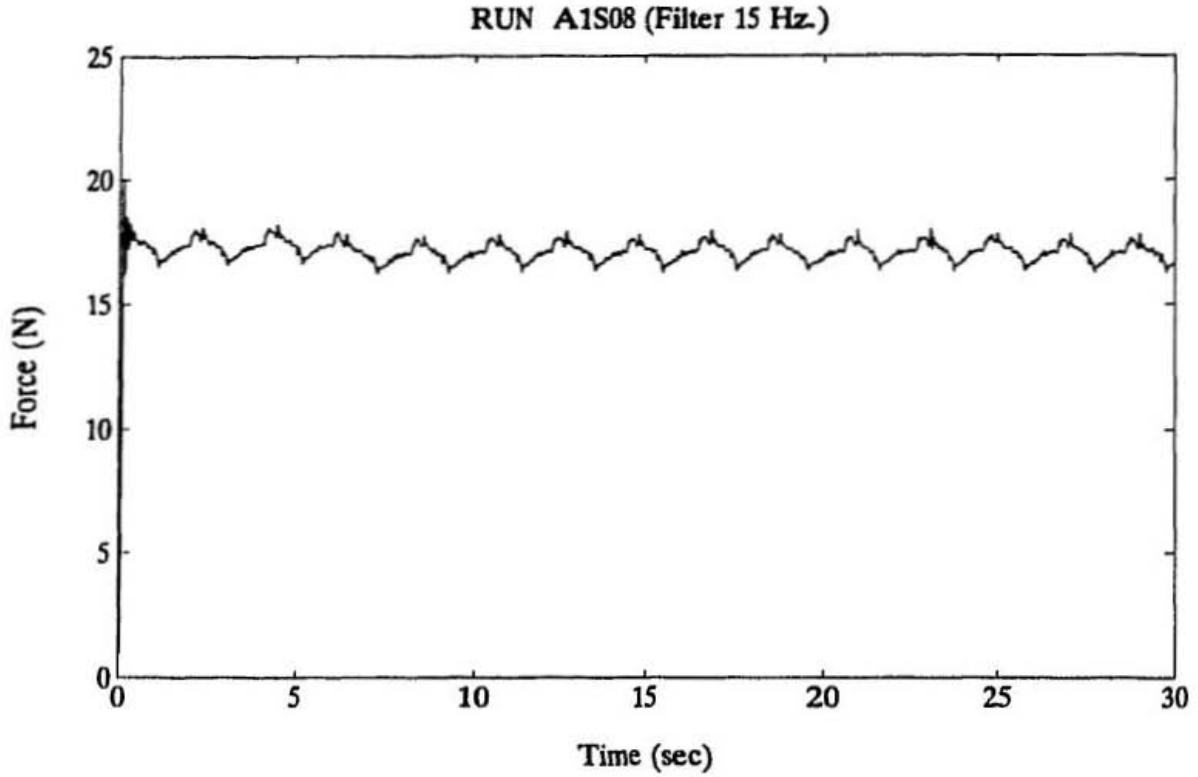
RUN A1S08 (Filter 15 Hz.)
Force (N)
Time (sec)
0
5
10
15
20
25
30

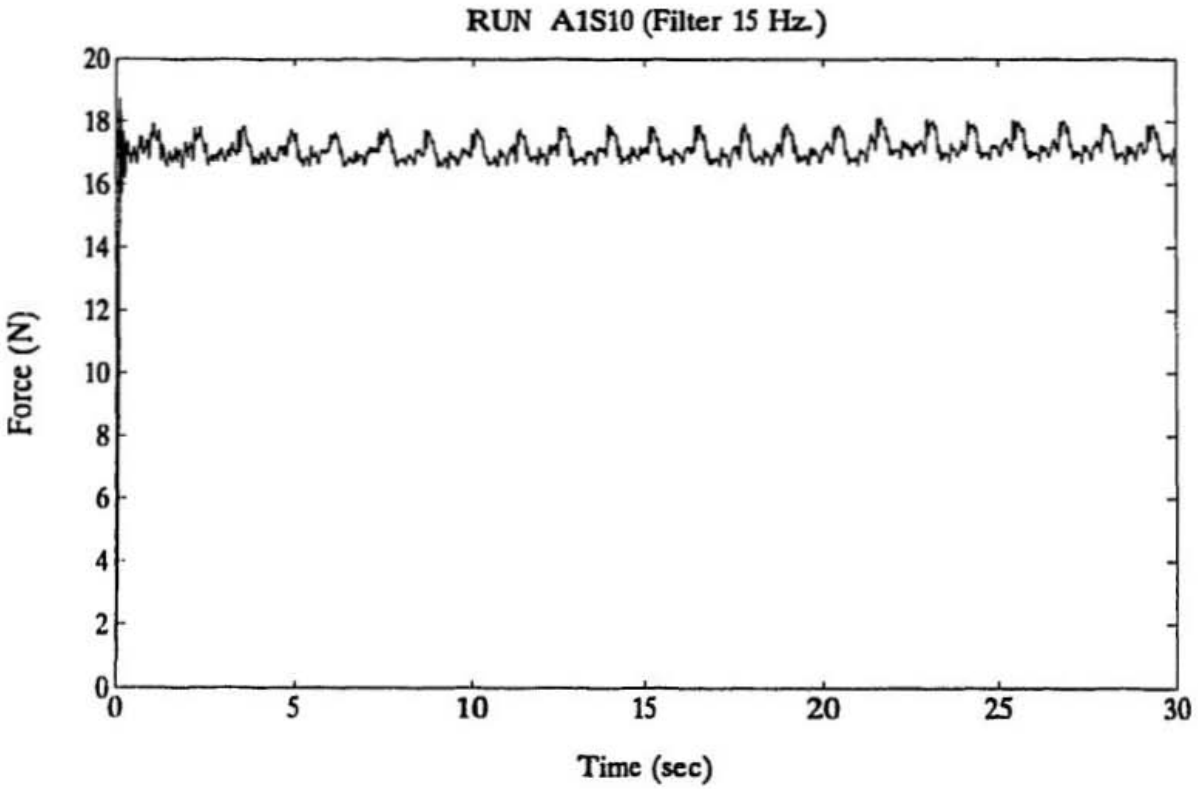
RUN A1S10 (Filter 15 Hz.)
Force (N)
Time (sec)
0
2
4
6
8
10
12
14
16
18
20
5
15
25
30

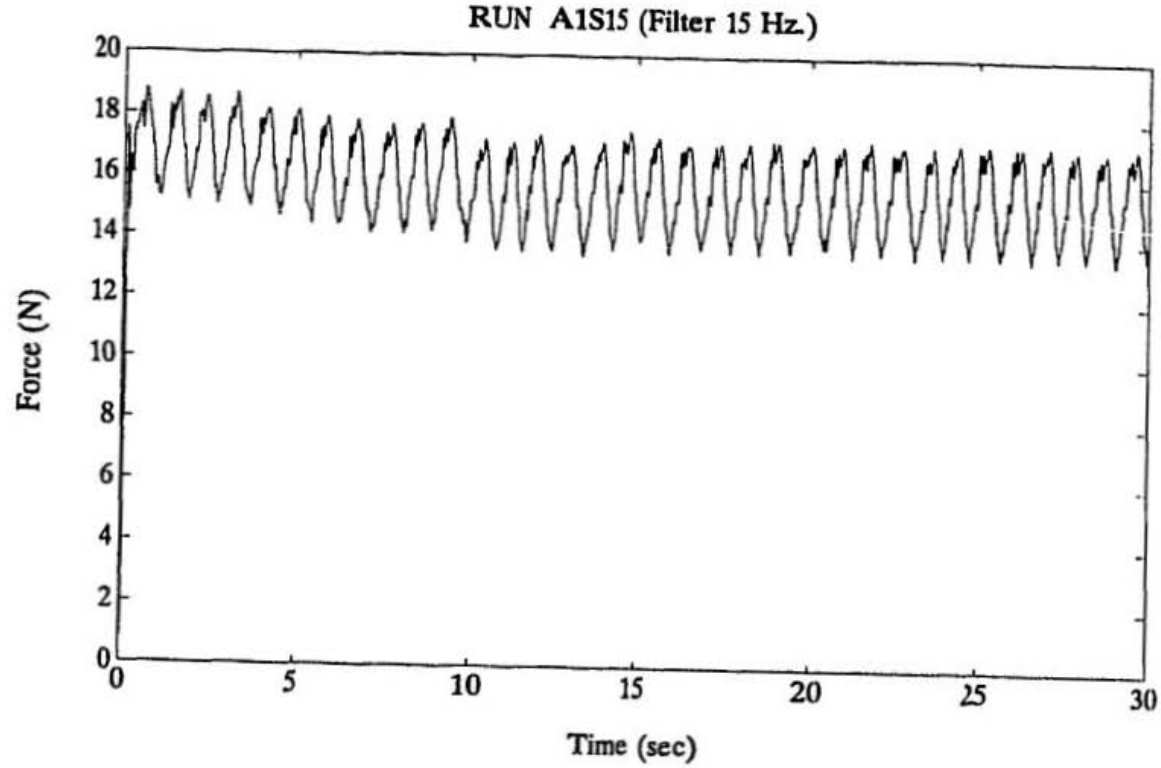
RUN A1S15 (Filter 15 Hz.)
Force (N)
Time (sec)
0
2
4
6
8
10
12
14
16
18
20
0
5
10
15
20
25
30

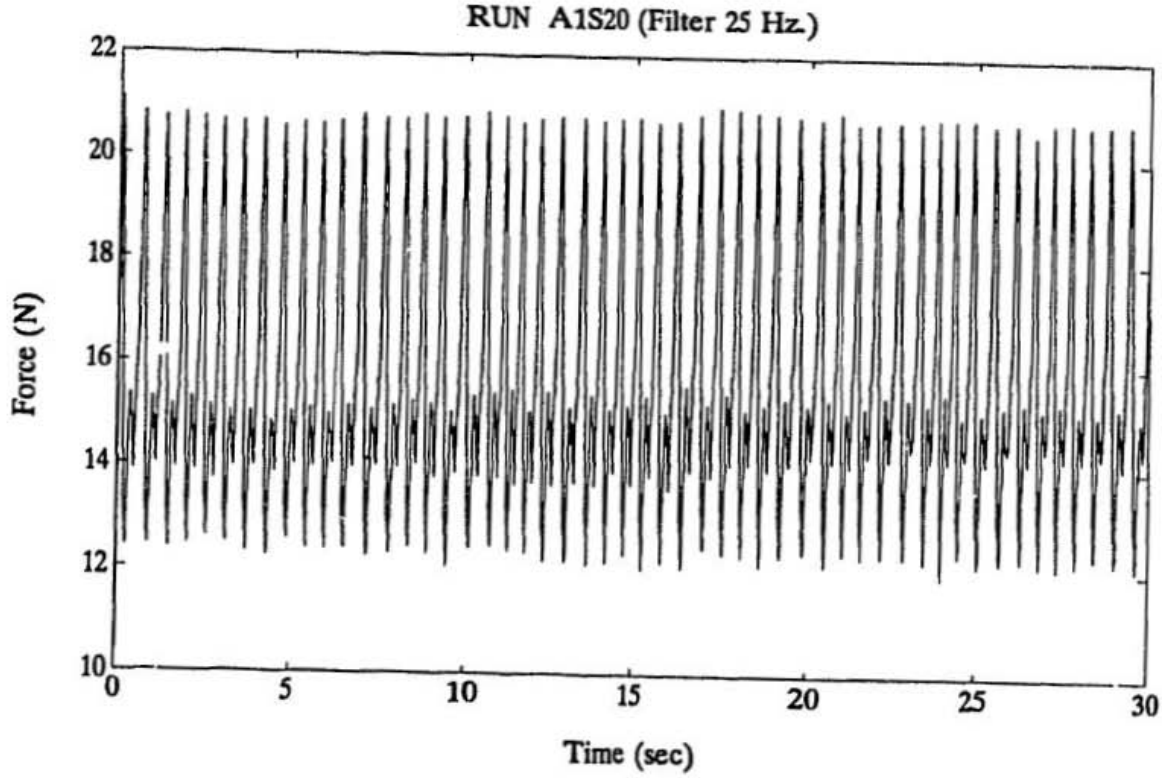
RUN A1S20 (Filter 25 Hz.)
Force (N)
Time (sec)
10
12
14
16
18
20
22
0
5
10
15
20
25
30

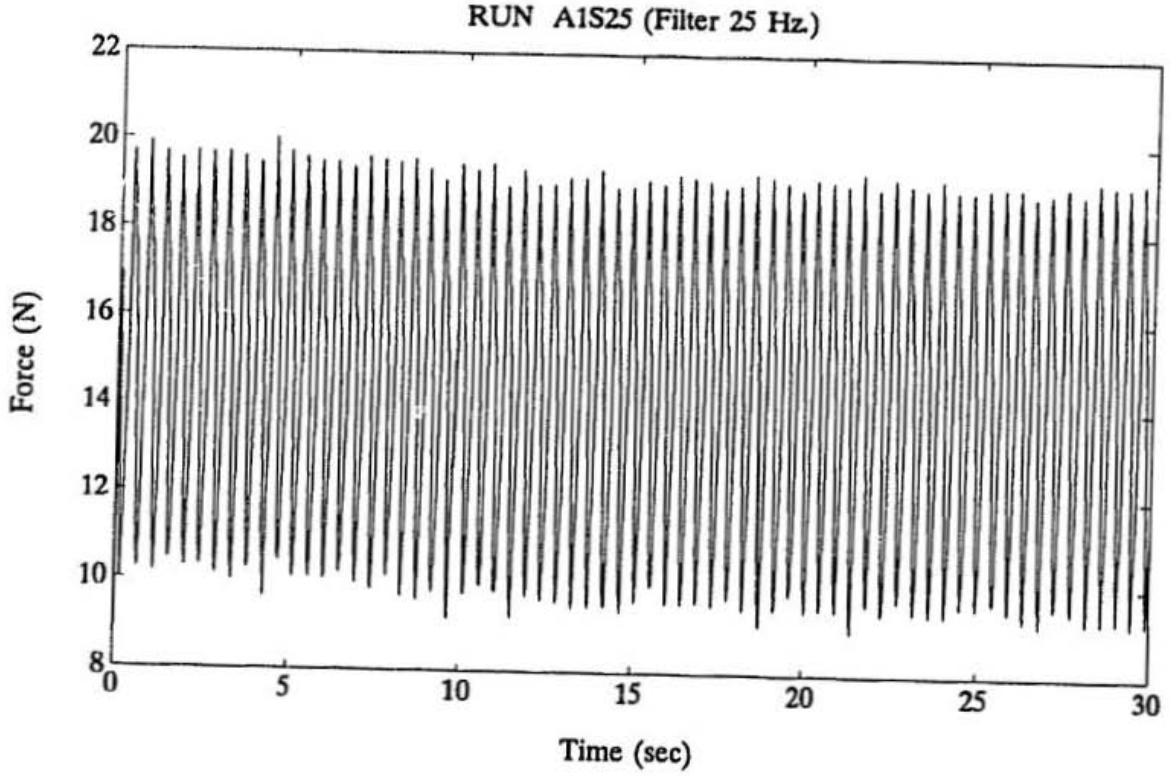
RUN A1S25 (Filter 25 Hz.)
Force (N)
Time (sec)
22
20
18
16
14
12
10
8
0
5
10
15
20
25
30

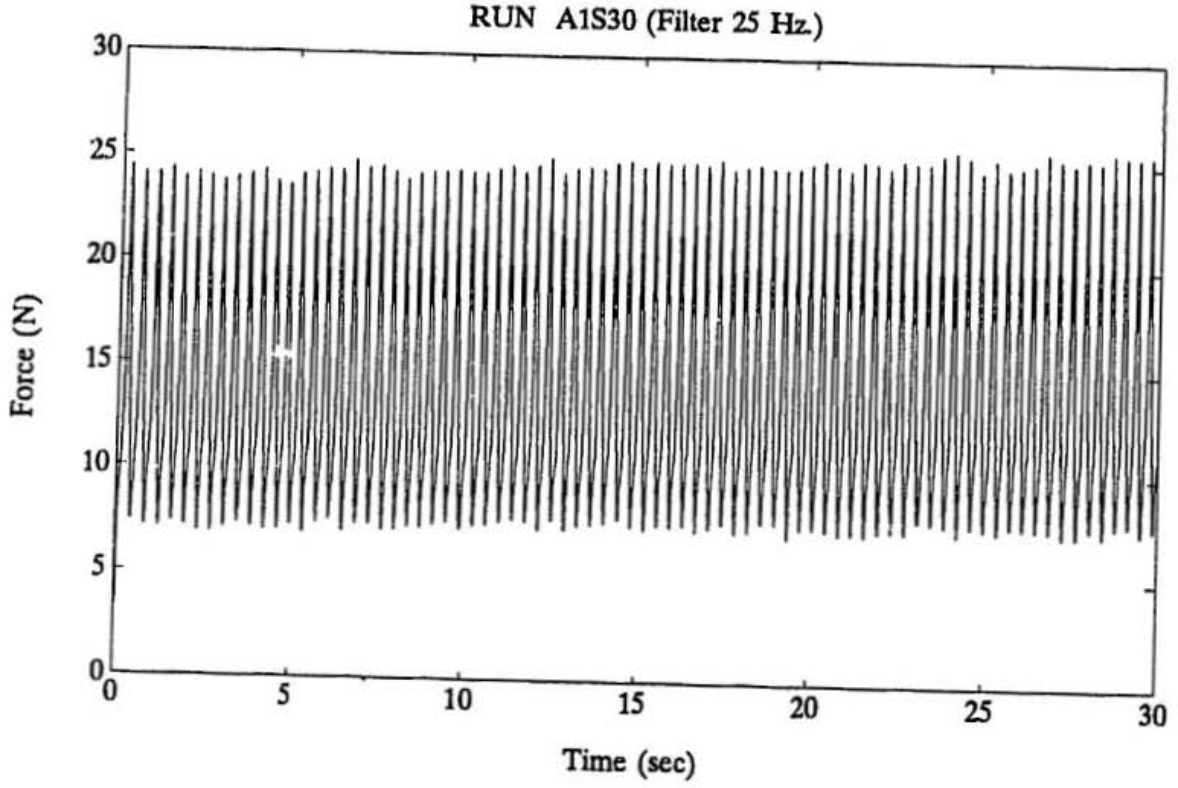
RUN A1S30 (Filter 25 Hz.)
Force (N)
Time (sec)
30
25
20
15
10
5
0
0
5
10
15
20
25
30

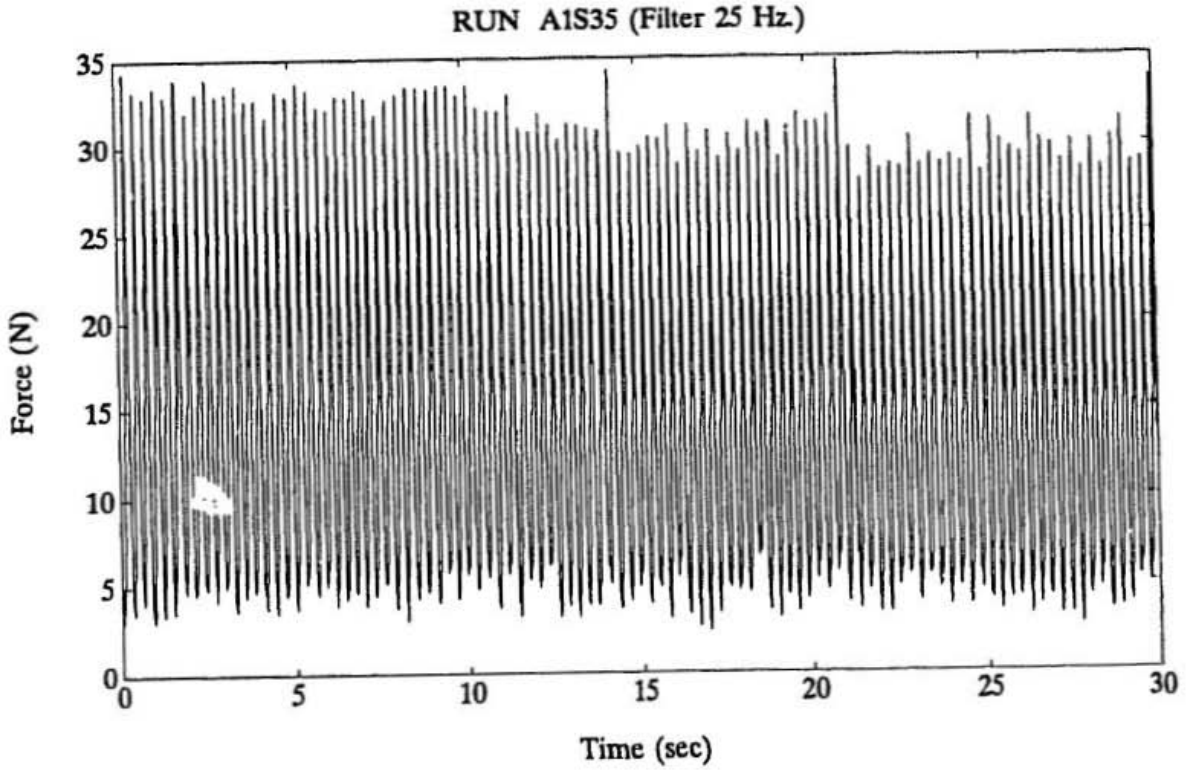
RUN A1S35 (Filter 25 Hz.)
Force (N)
Time (sec)
0
5
10
15
20
25
30
35

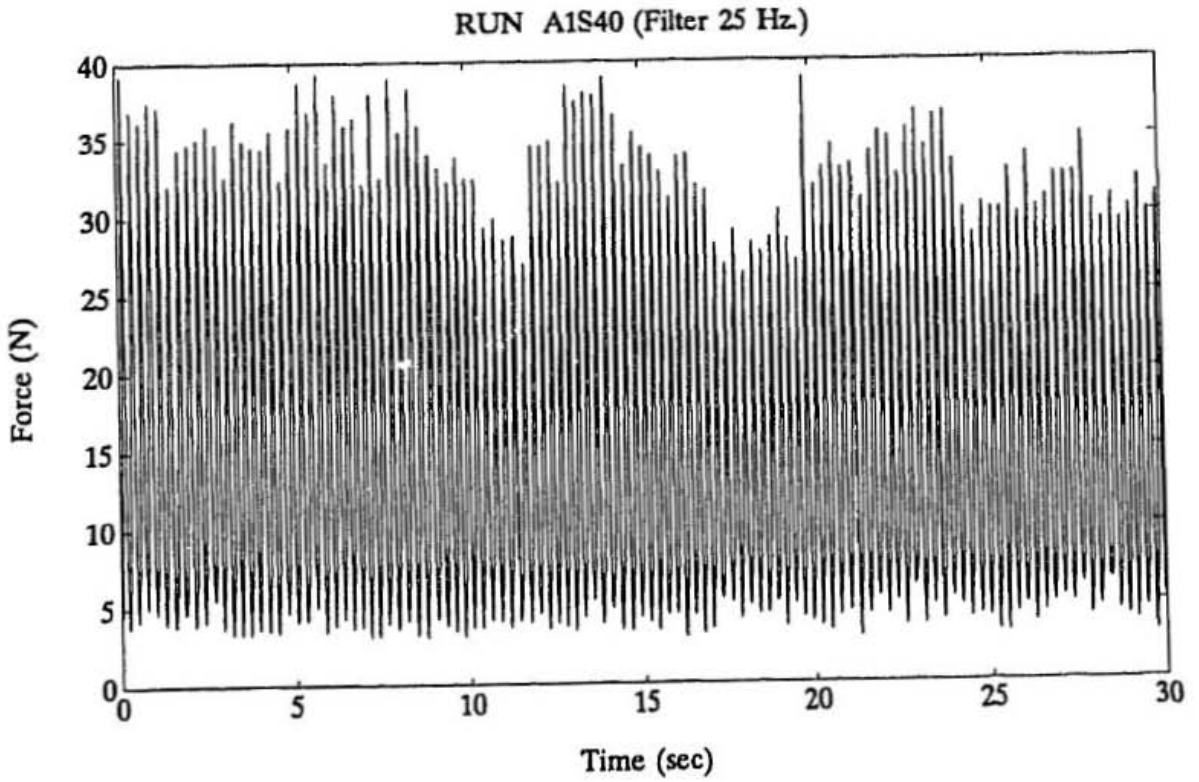
RUN A1S40 (Filter 25 Hz.)
Force (N)
Time (sec)
0
5
10
15
20
25
30
35
40

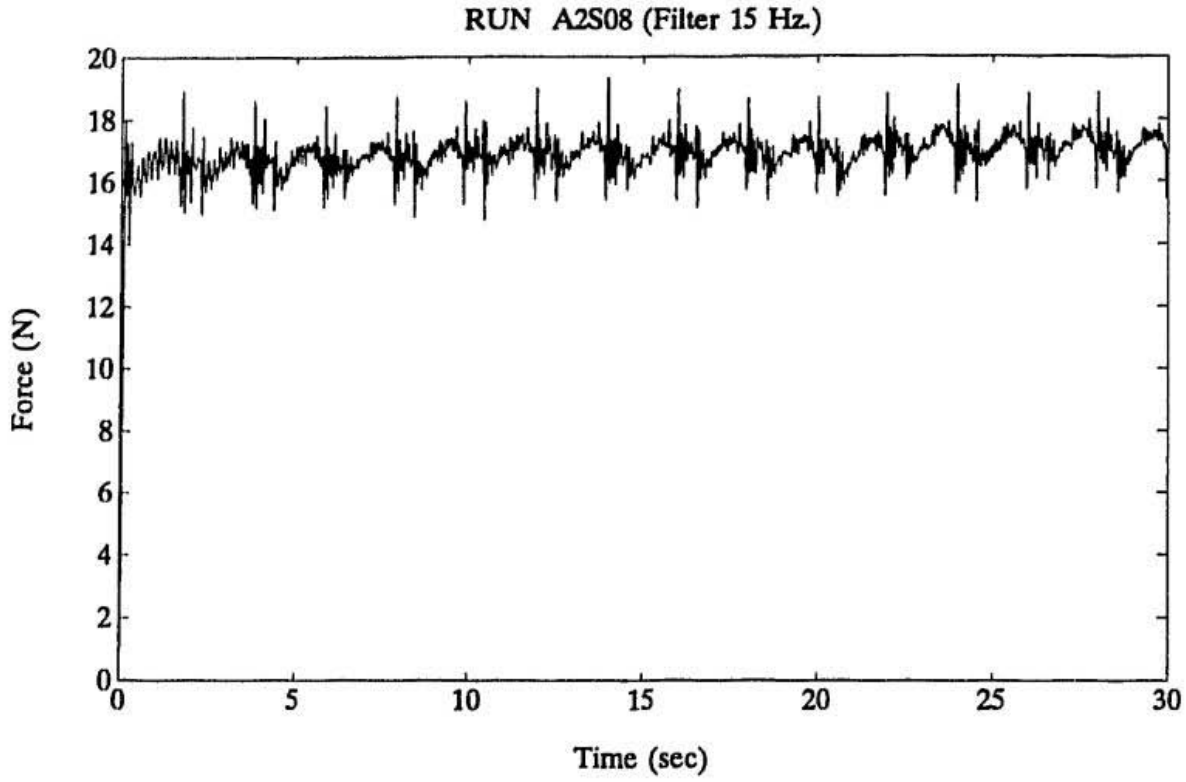
RUN A2S08 (Filter 15 Hz.)
Force (N)
Time (sec)
0
2
4
6
8
10
12
14
16
18
20
0
5
10
15
20
25
30

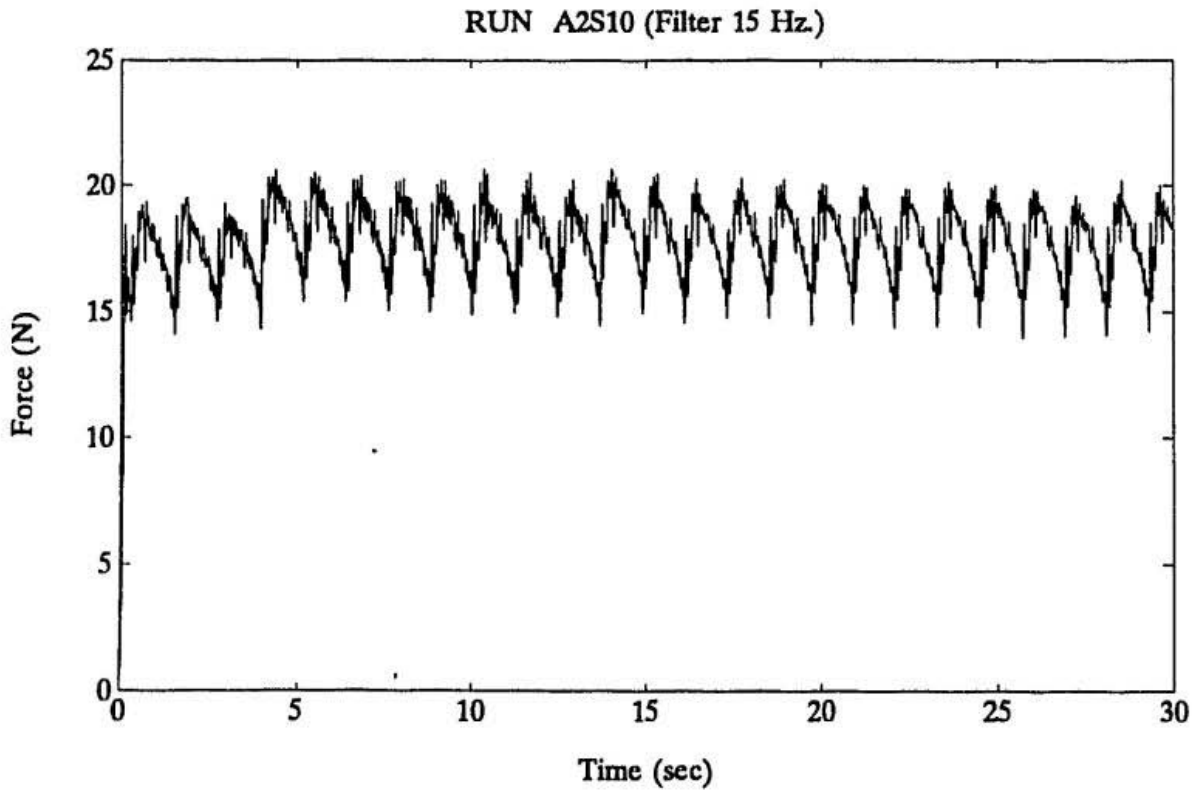
RUN A2S10 (Filter 15 Hz.)
Force (N)
Time (sec)
0
5
10
15
20
25
0
5
10
15
20
25
30

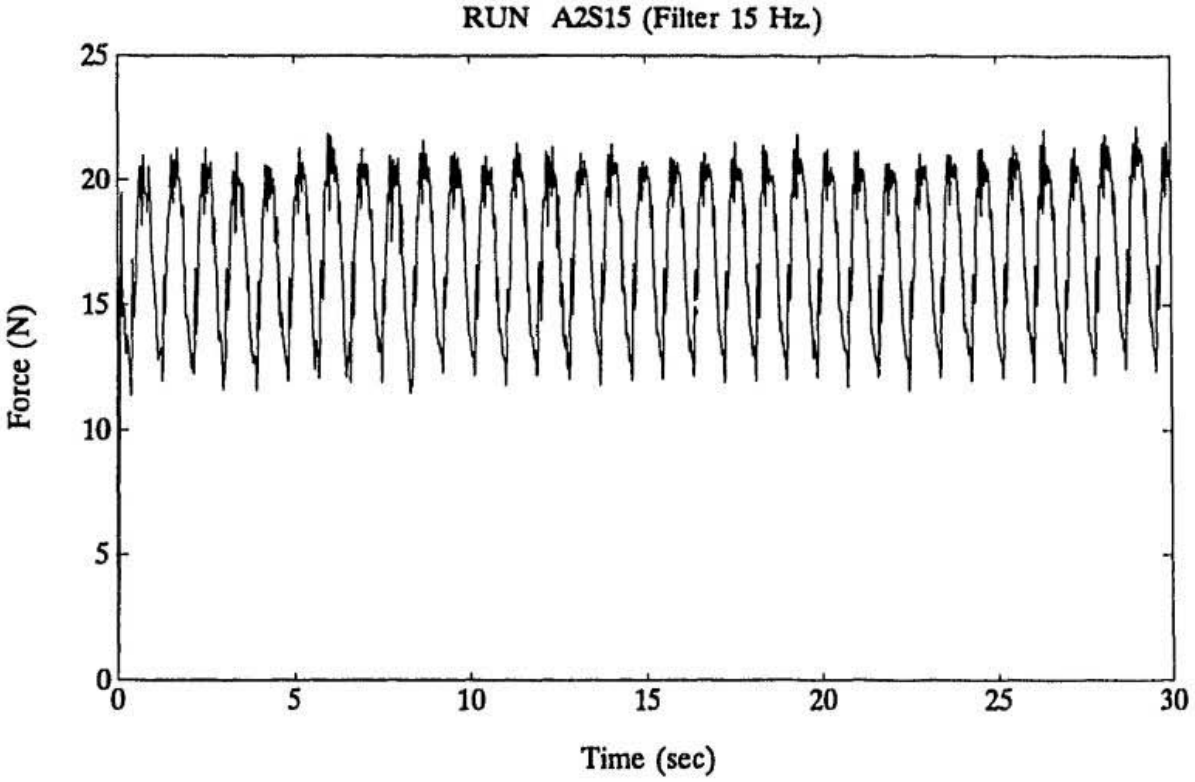
RUN A2S15 (Filter 15 Hz.)
Force (N)
Time (sec)
0
5
10
15
20
25
30

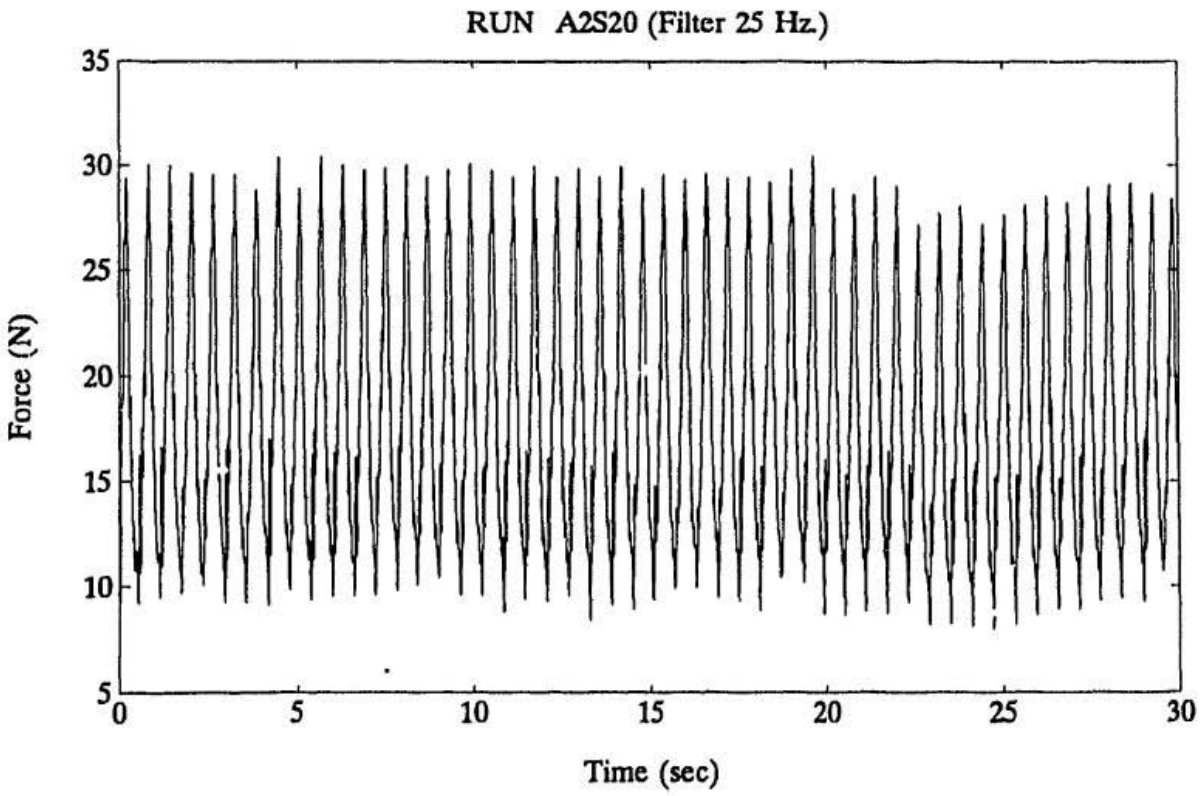
RUN A2S20 (Filter 25 Hz.)
Force (N)
Time (sec)
5
10
15
20
25
30
35

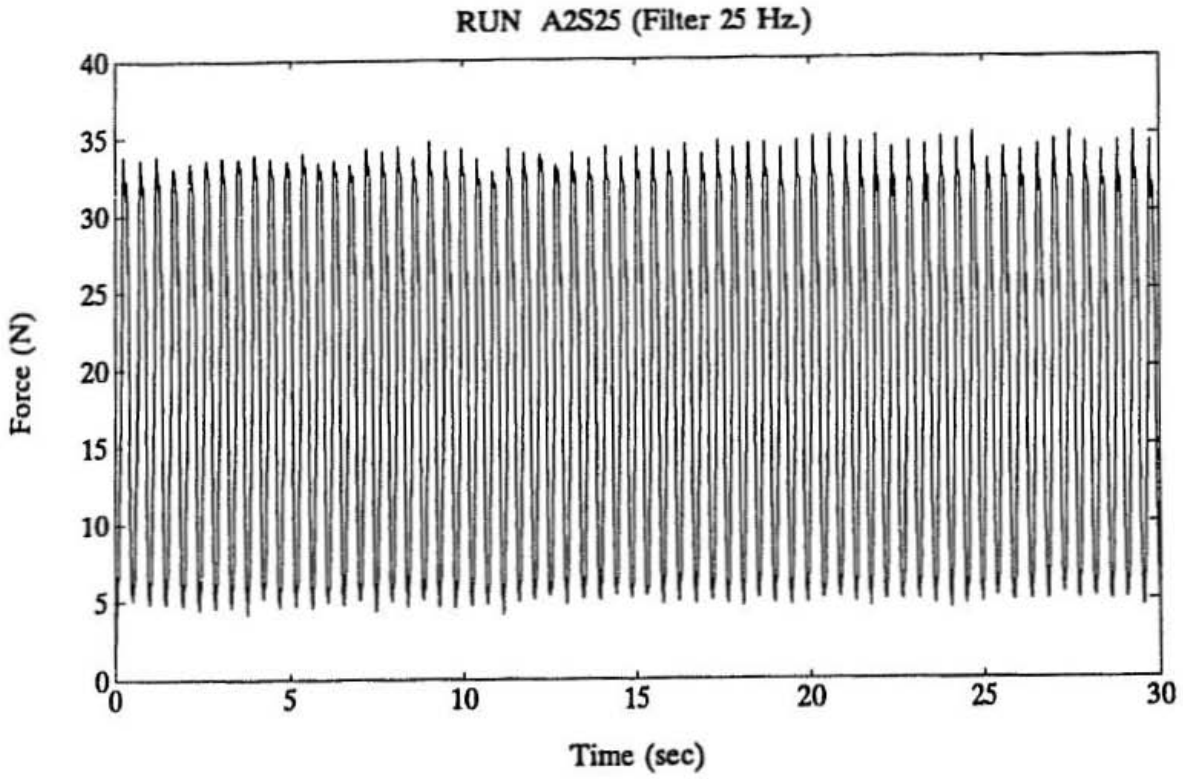
RUN A2S25 (Filter 25 Hz.)
Force (N)
Time (sec)
0
5
10
15
20
25
30
35
40

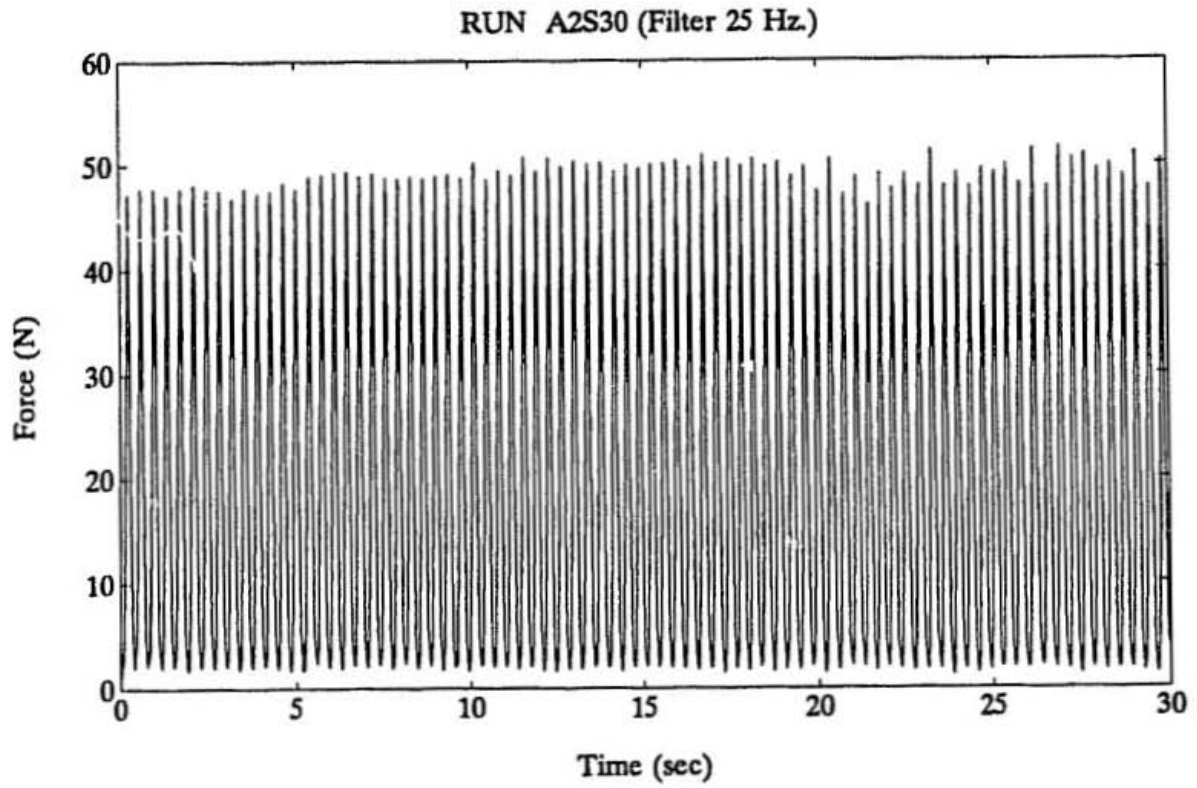
RUN A2S30 (Filter 25 Hz.)
Force (N)
Time (sec)
0
5
10
15
20
25
30
40
50
60

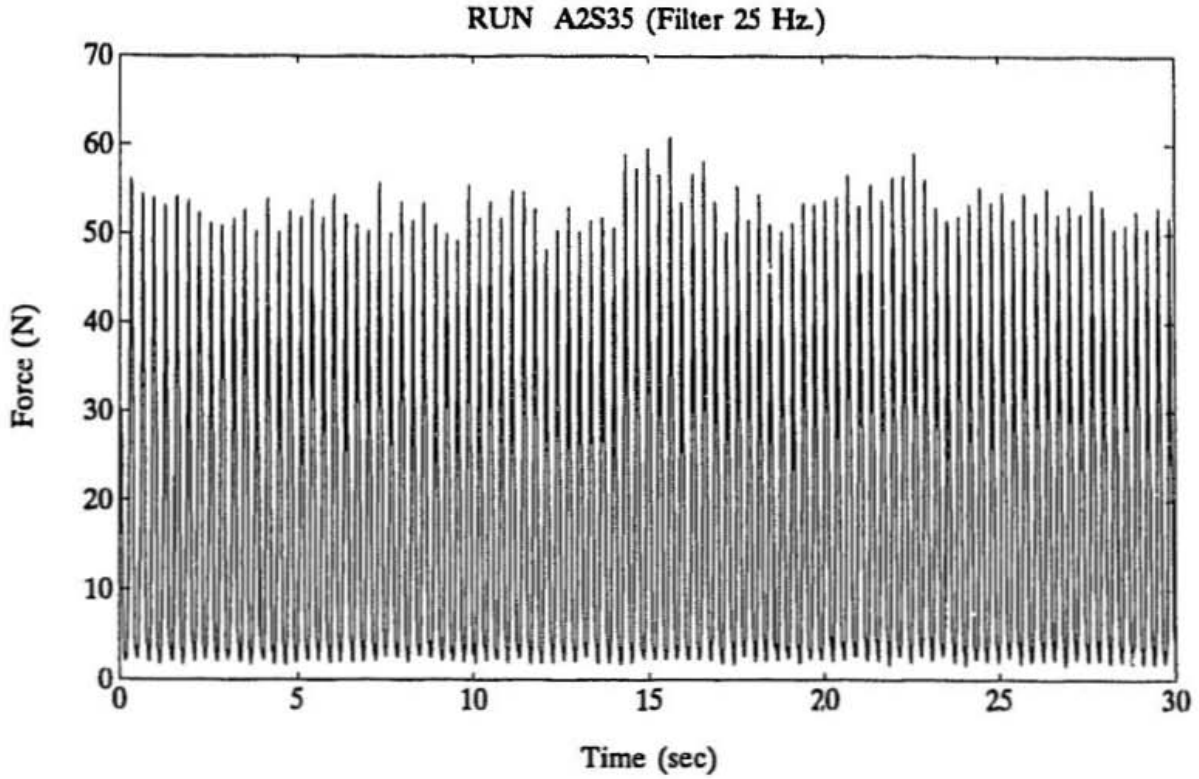
RUN A2S35 (Filter 25 Hz.)
Force (N)
Time (sec)
0
10
20
30
40
50
60
70
0
5
10
15
20
25
30

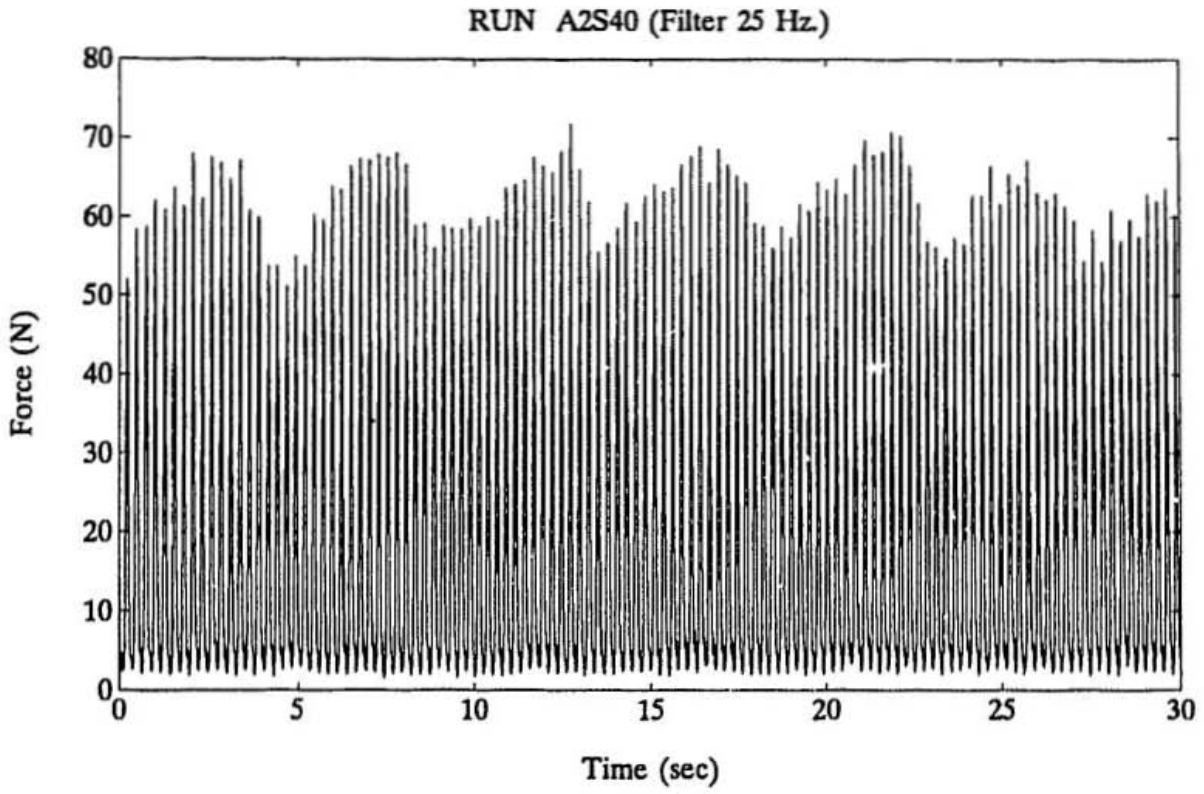
RUN A2S40 (Filter 25 Hz.)
Force (N)
Time (sec)
0
10
20
30
40
50
60
70
80
0
5
10
15
20
25
30

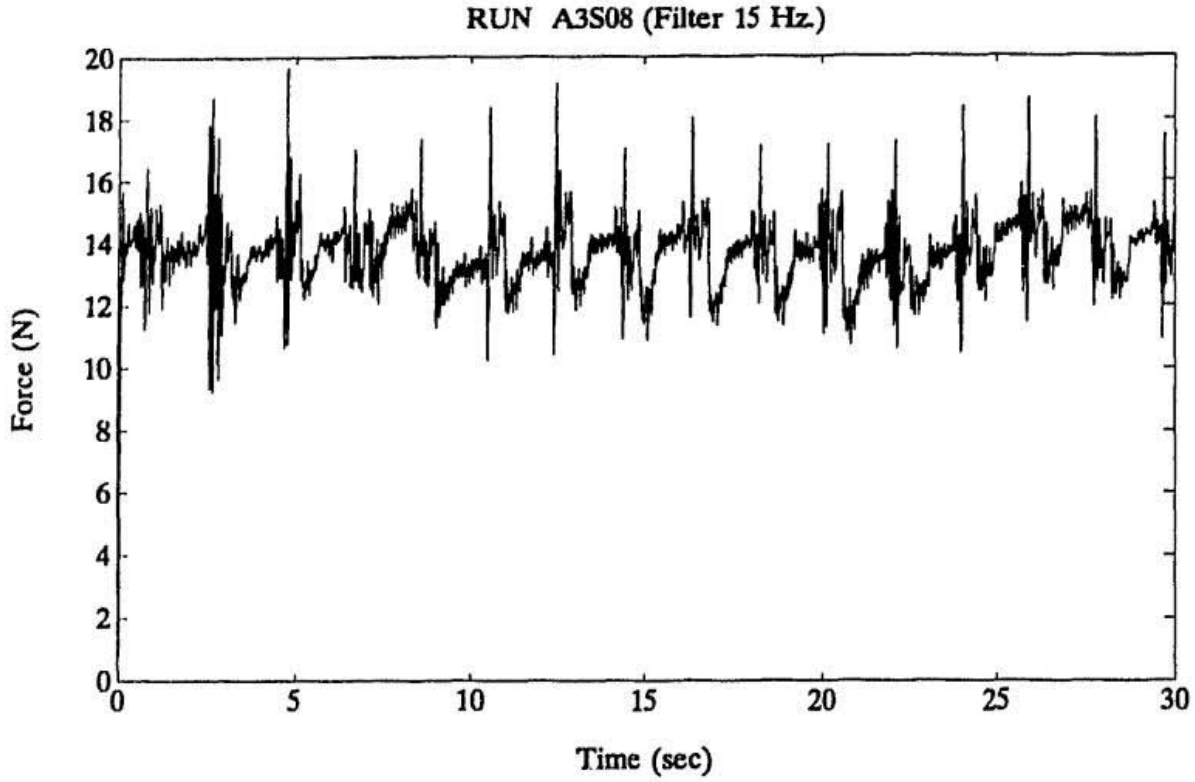
RUN A3S08 (Filter 15 Hz.)
Force (N)
Time (sec)
0
2
4
6
8
10
12
14
16
18
20
0
5
10
15
20
25
30

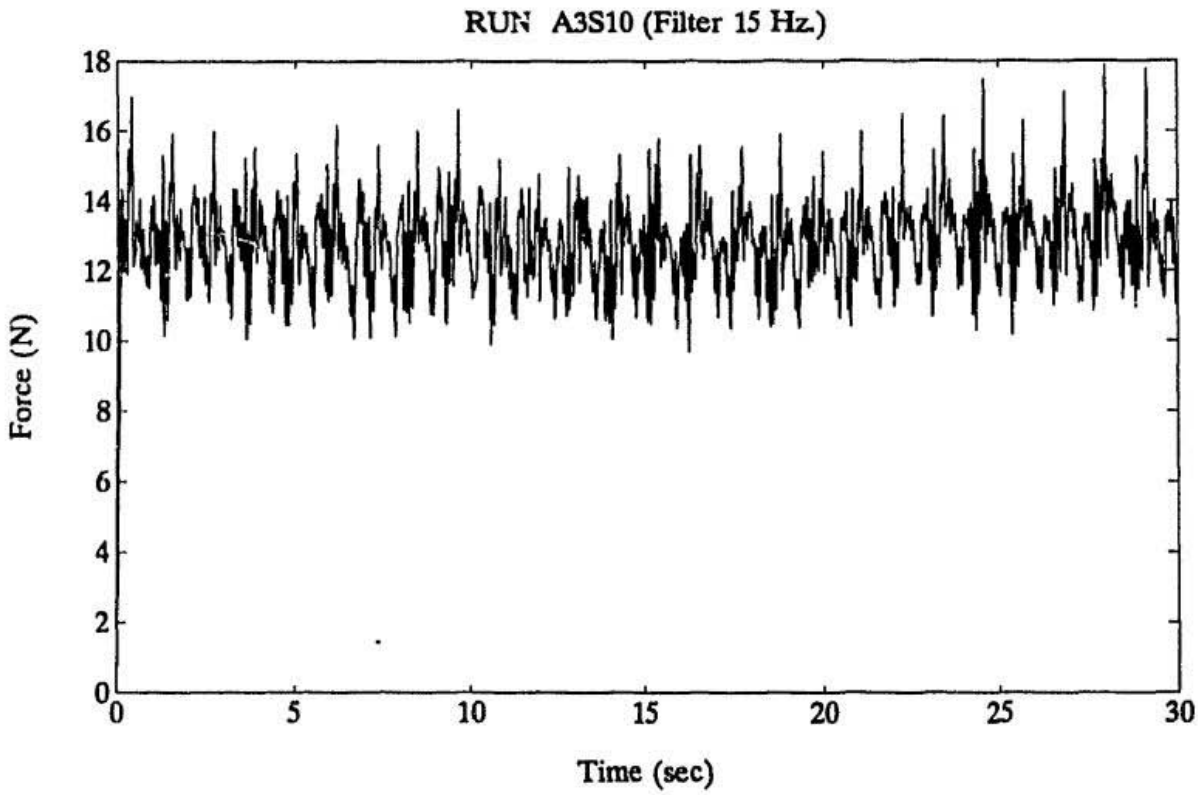
RUN A3S10 (Filter 15 Hz.)
Force (N)
Time (sec)
0
2
4
6
8
10
12
14
16
18
0
5
10
15
20
25
30

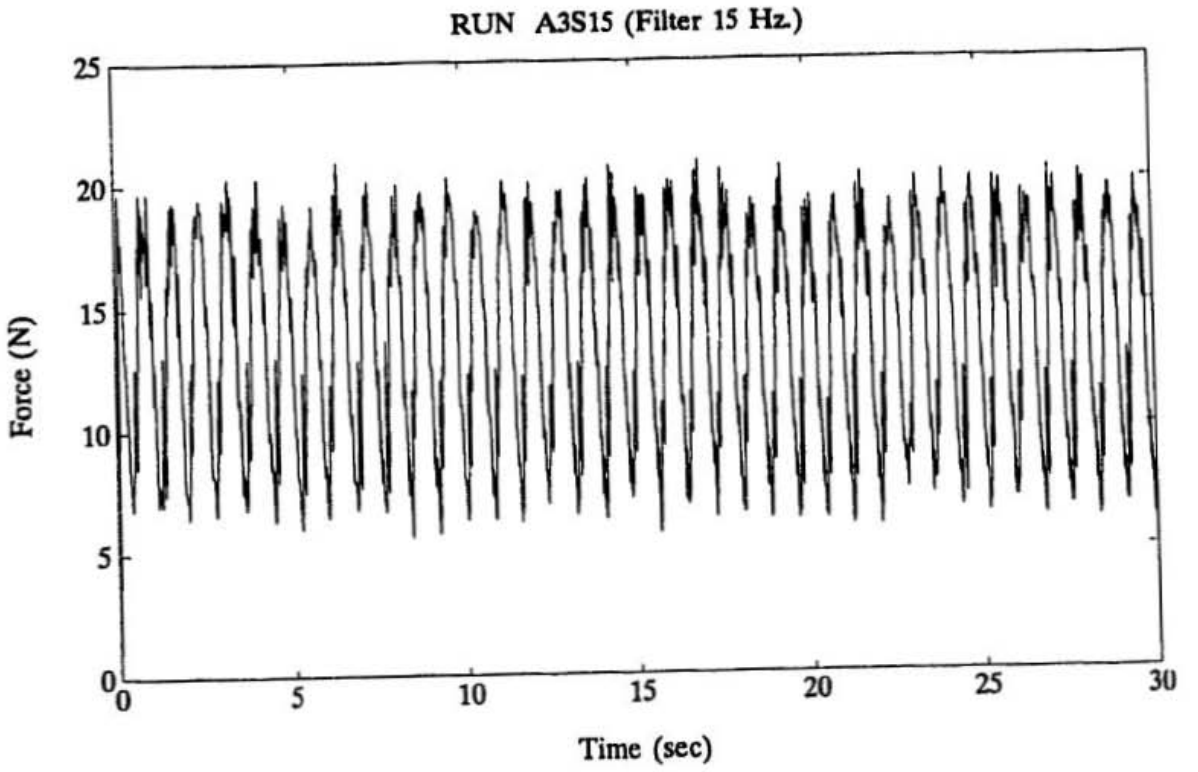
RUN A3S15 (Filter 15 Hz.)
Force (N)
Time (sec)
0
5
10
15
20
25
30

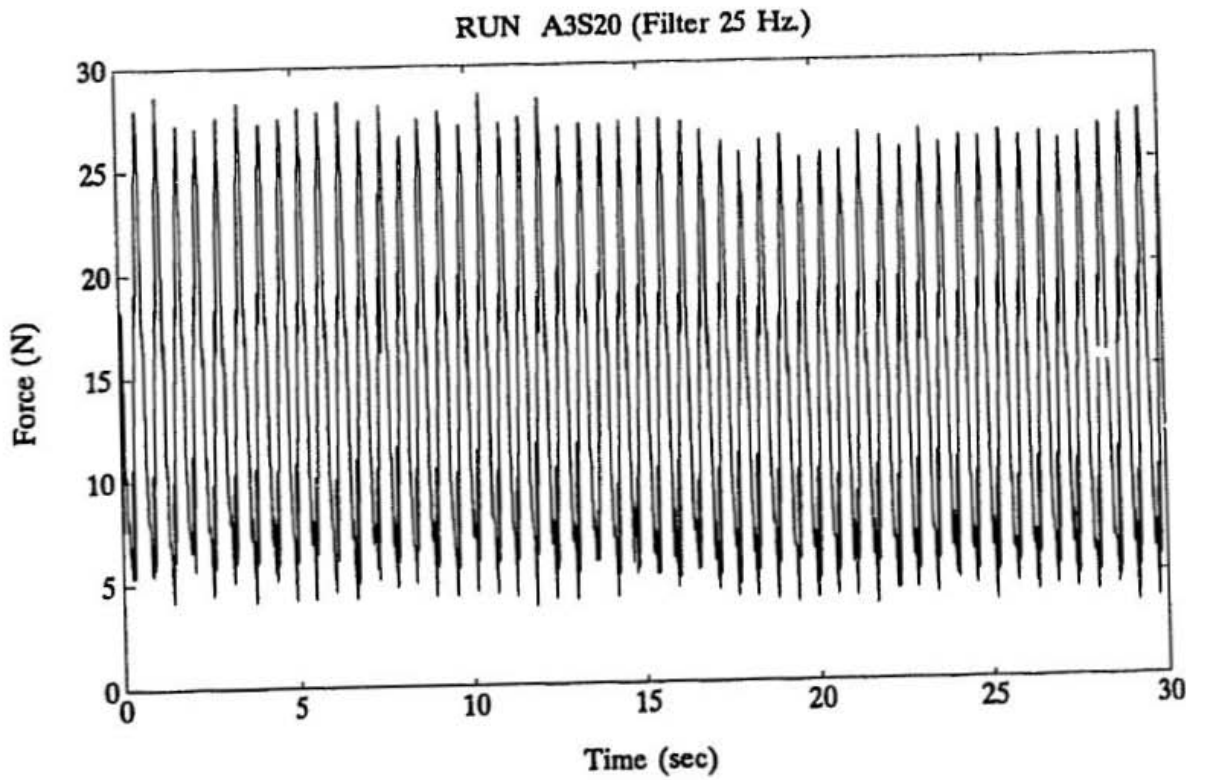
RUN A3S20 (Filter 25 Hz.)
Force (N)
Time (sec)
0
5
10
15
20
25
30

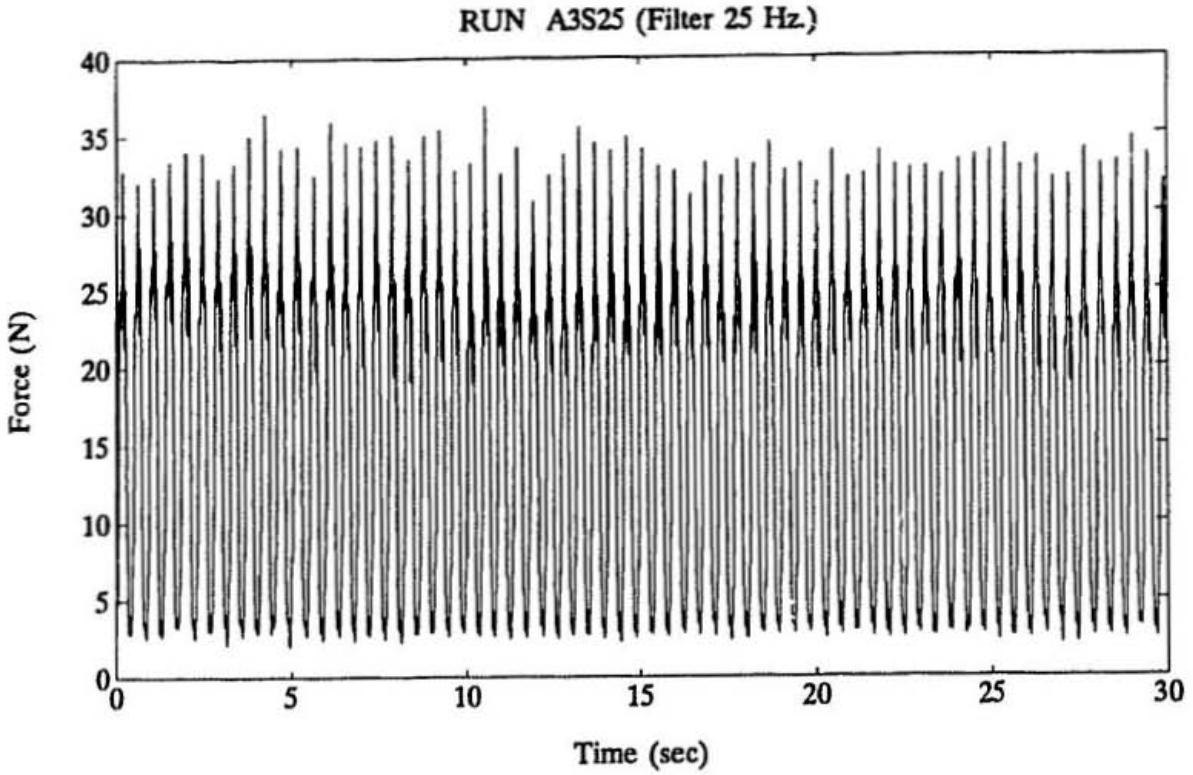
RUN A3S25 (Filter 25 Hz.)
Force (N)
Time (sec)
0
5
10
15
20
25
30
35
40

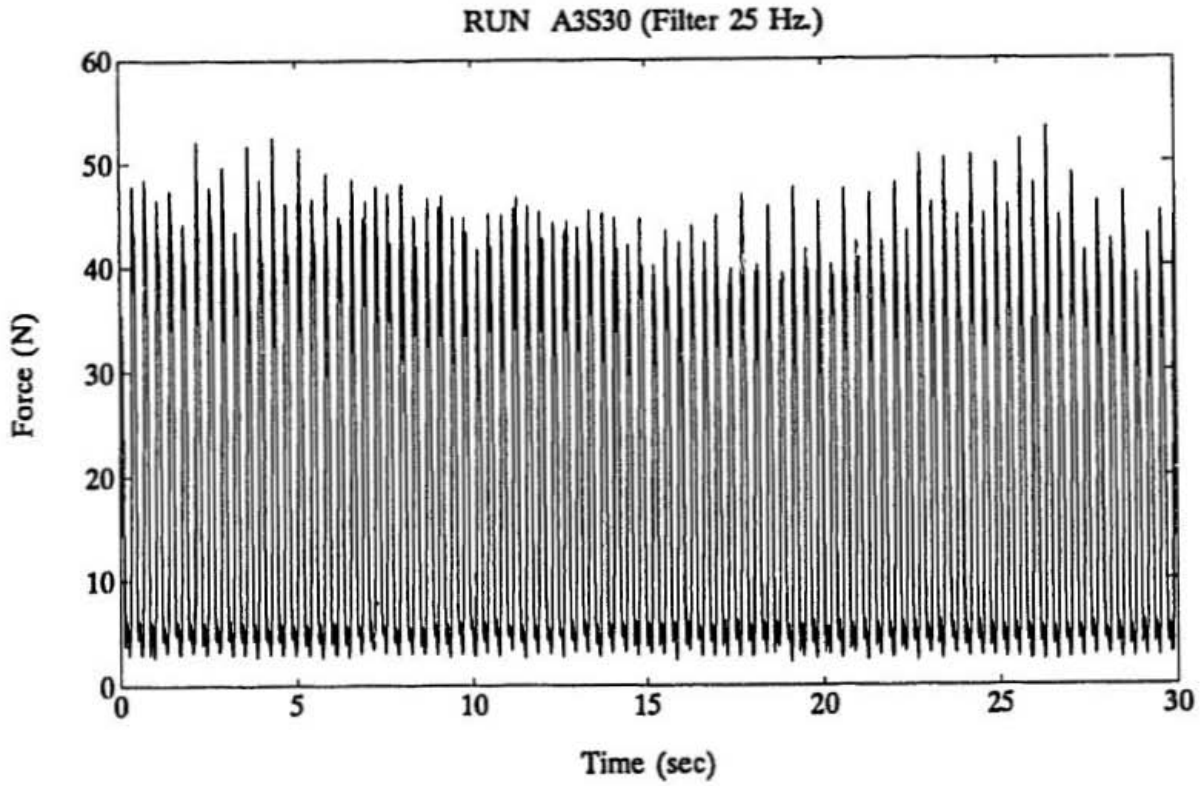
RUN A3S30 (Filter 25 Hz.)
Force (N)
Time (sec)
0
5
10
15
20
25
30
40
50
60

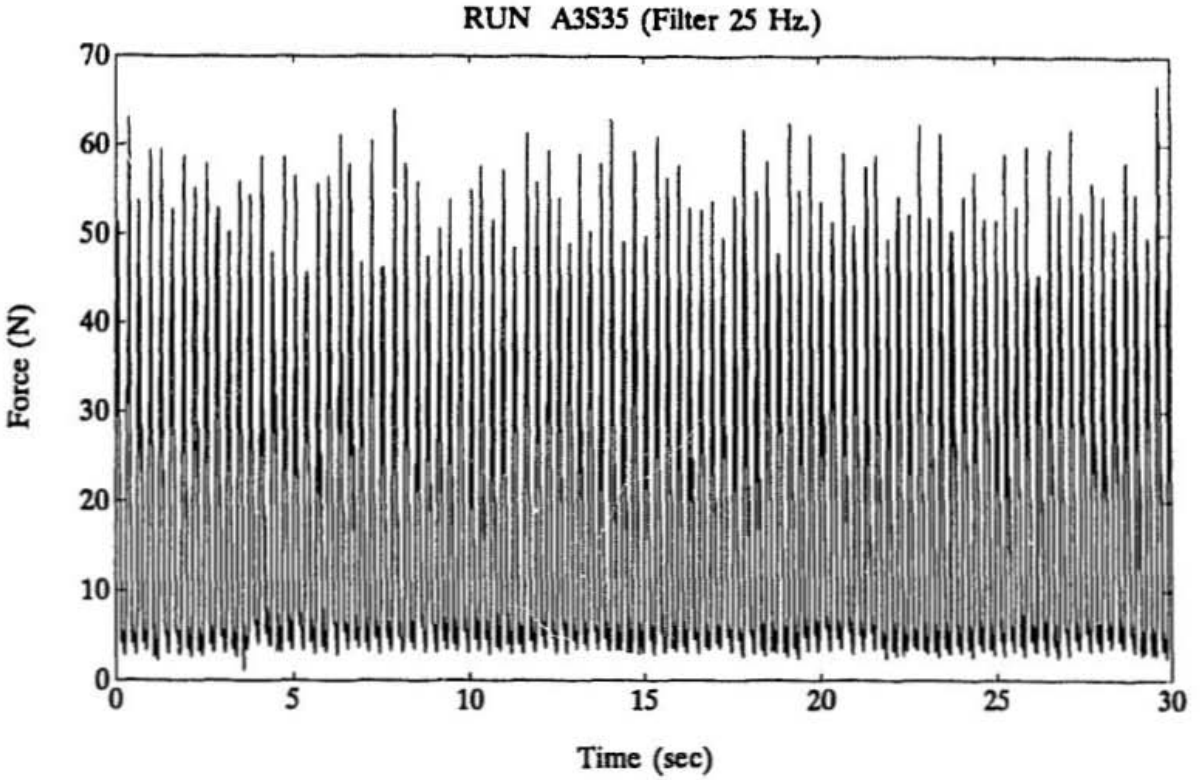
RUN A3S35 (Filter 25 Hz.)
Force (N)
Time (sec)
0
10
20
30
40
50
60
70
0
5
10
15
20
25
30

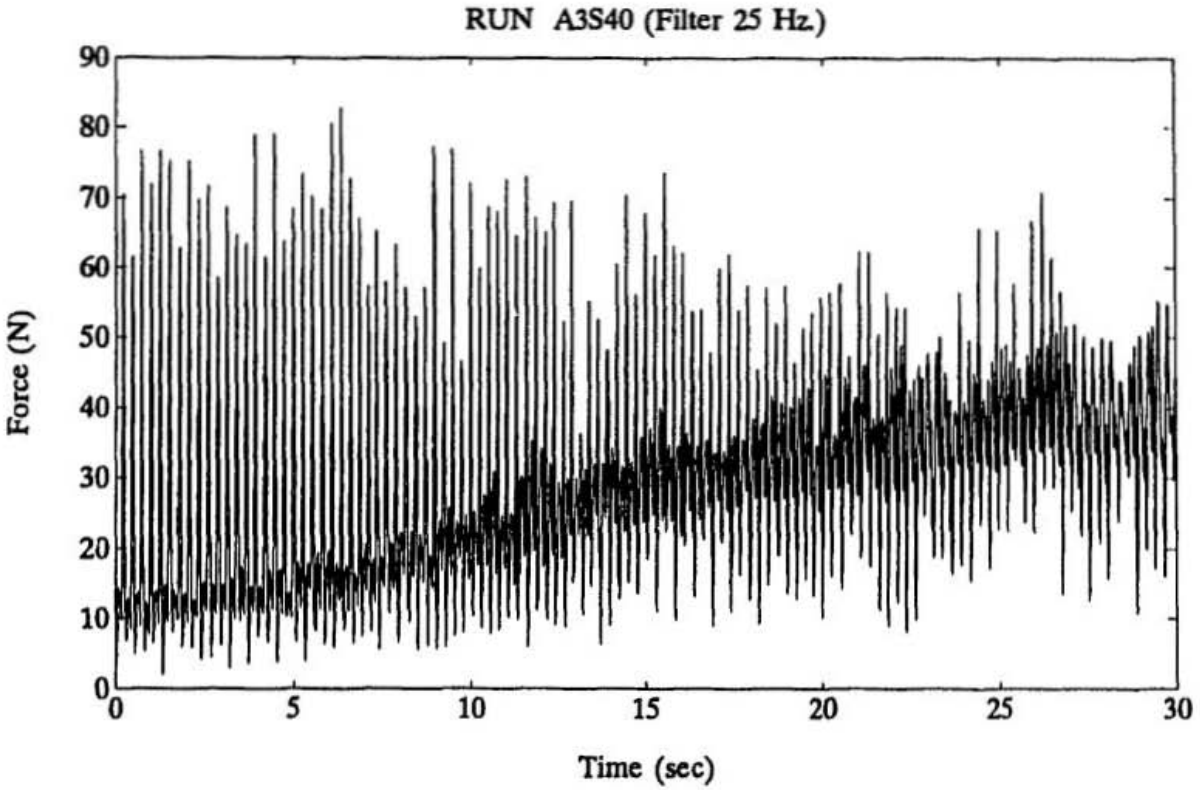
RUN A3S40 (Filter 25 Hz.)
Force (N)
Time (sec)
0
10
20
30
40
50
60
70
80
90
0
5
10
15
20
25
30

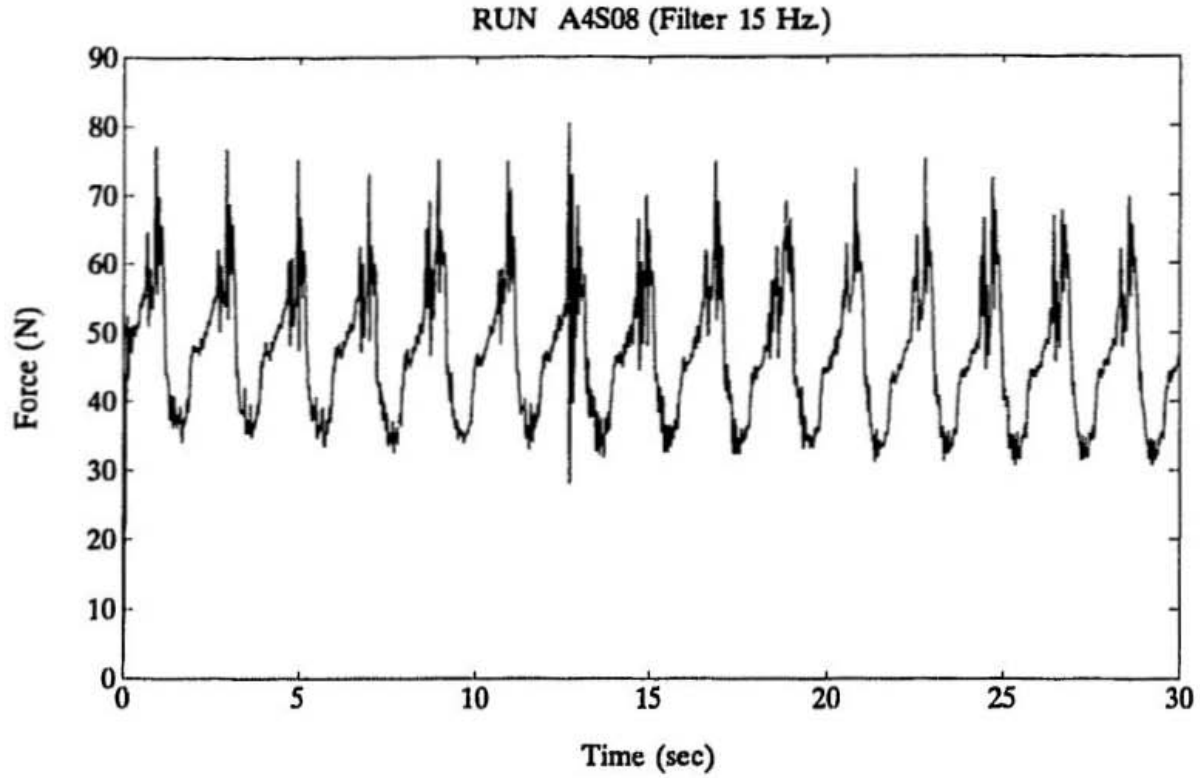
RUN A4S08 (Filter 15 Hz.)
Force (N)
Time (sec)
0
10
20
30
40
50
60
70
80
90
0
5
10
15
20
25
30

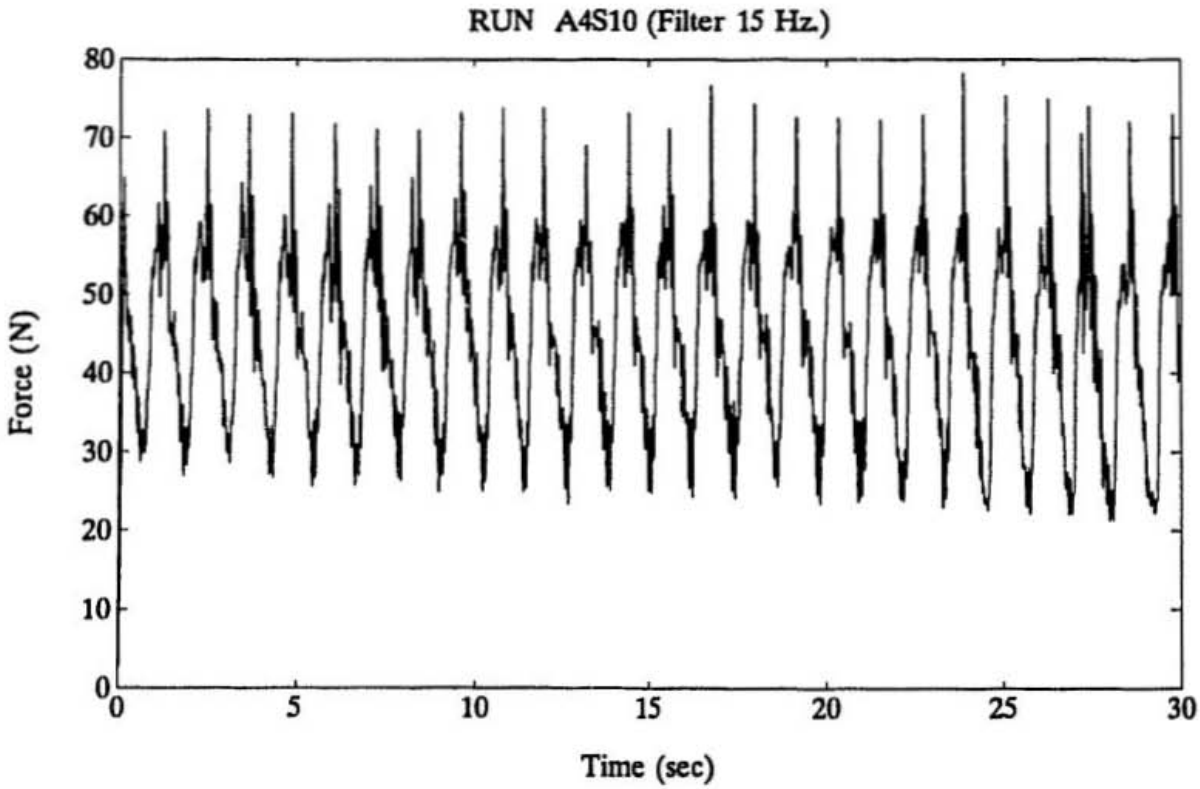
RUN A4S10 (Filter 15 Hz.)
Force (N)
Time (sec)
0
10
20
30
40
50
60
70
80
0
5
10
15
20
25
30

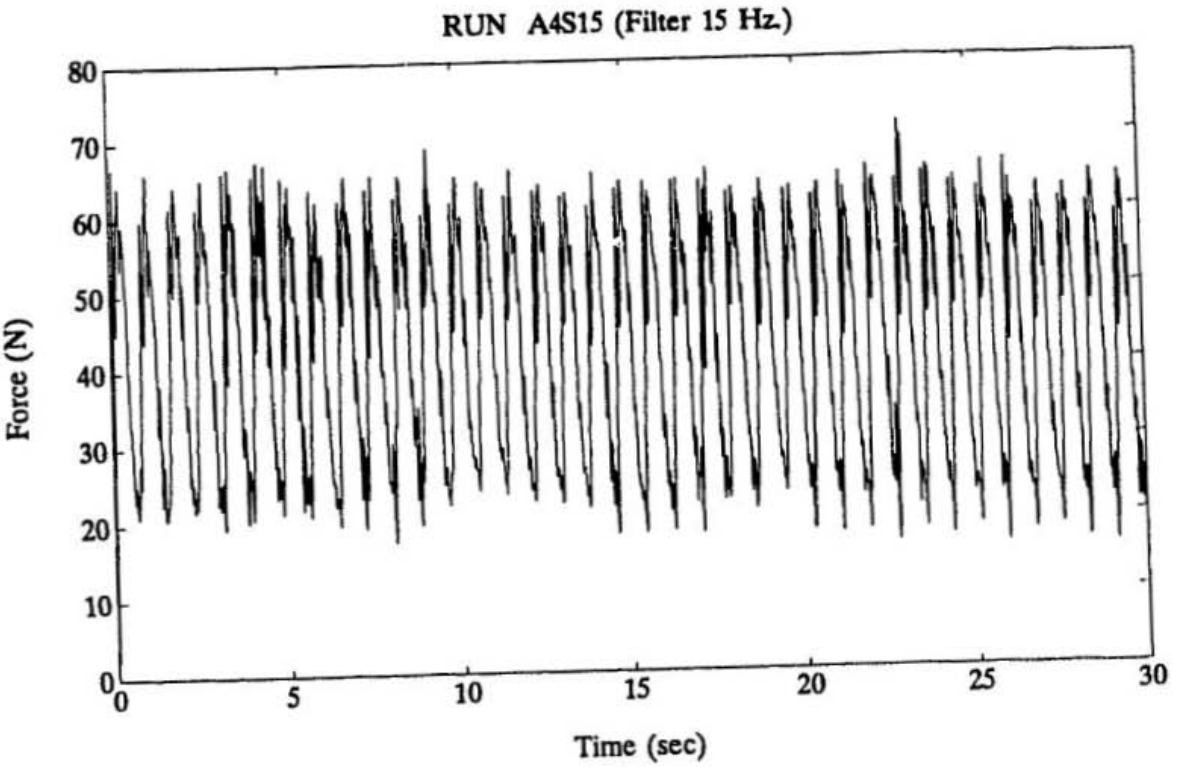
RUN A4S15 (Filter 15 Hz.)
Force (N)
Time (sec)
0
10
20
30
40
50
60
70
80
0
5
10
15
20
25
30

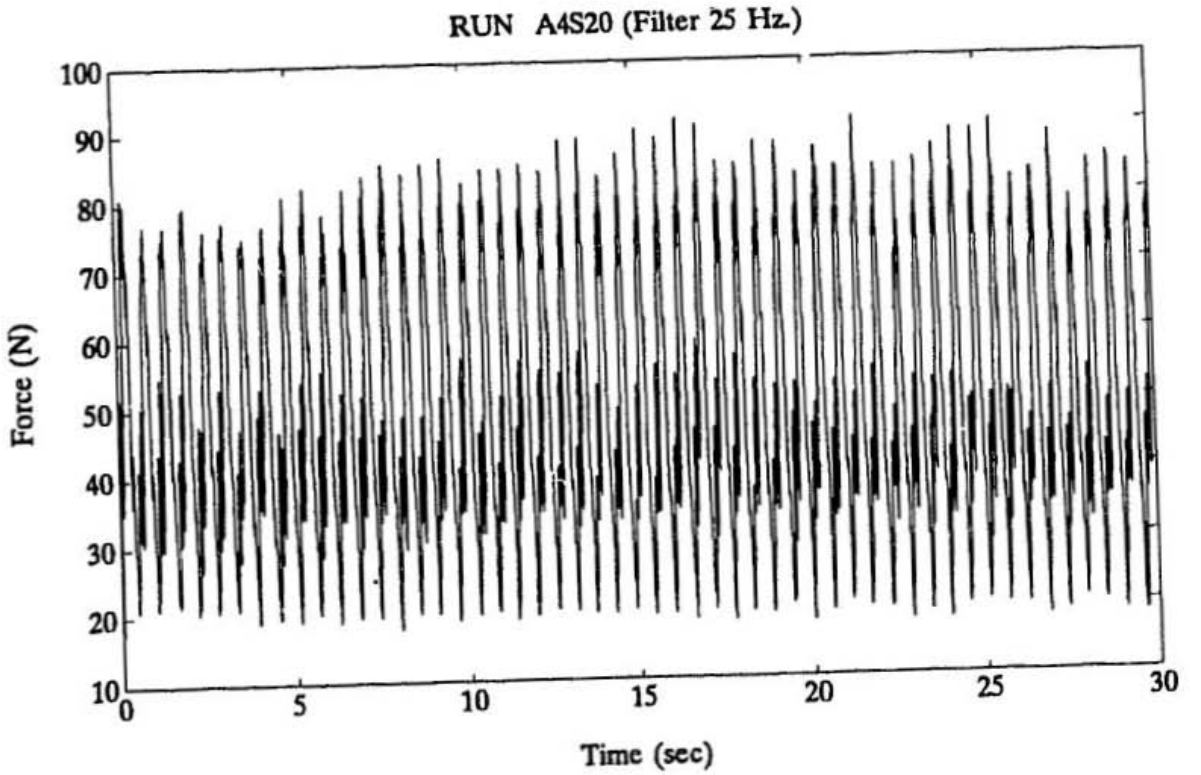
RUN A4S20 (Filter 25 Hz.)
Force (N)
Time (sec)
10
20
30
40
50
60
70
80
90
100
0
5
10
15
20
25
30

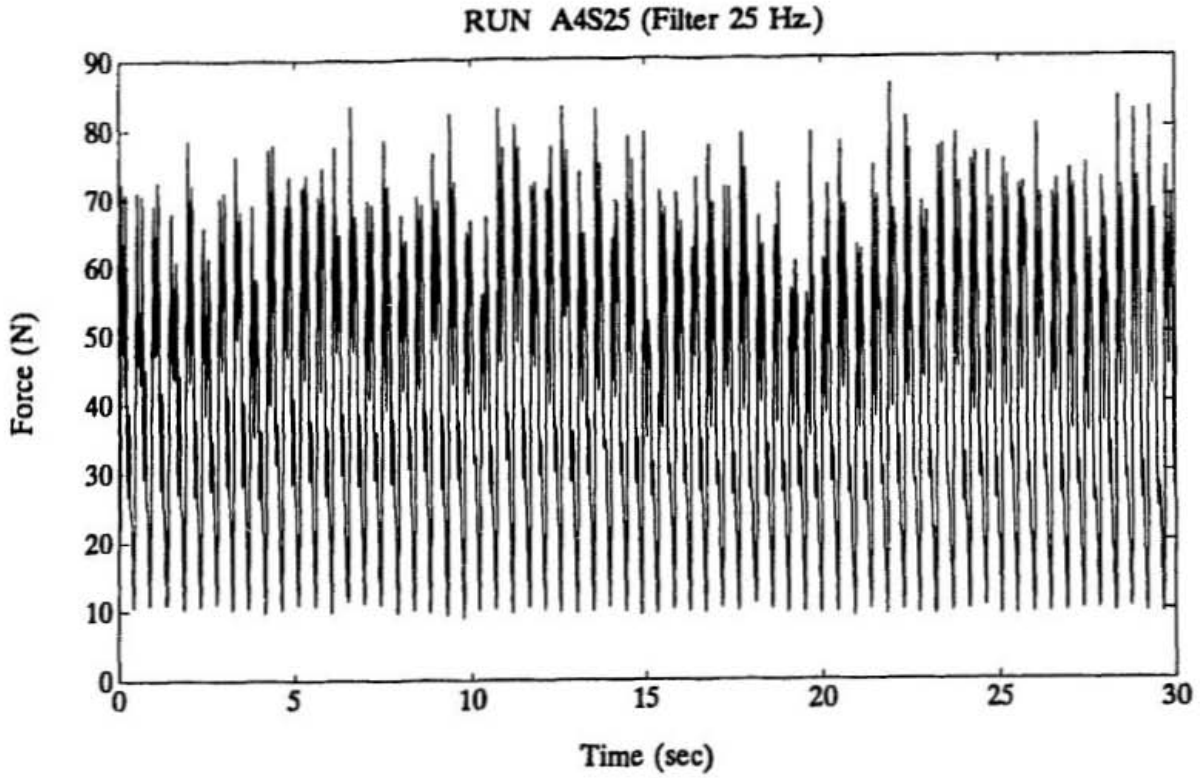
RUN A4S25 (Filter 25 Hz.)
Force (N)
Time (sec)
0
10
20
30
40
50
60
70
80
90
0
5
10
15
20
25
30

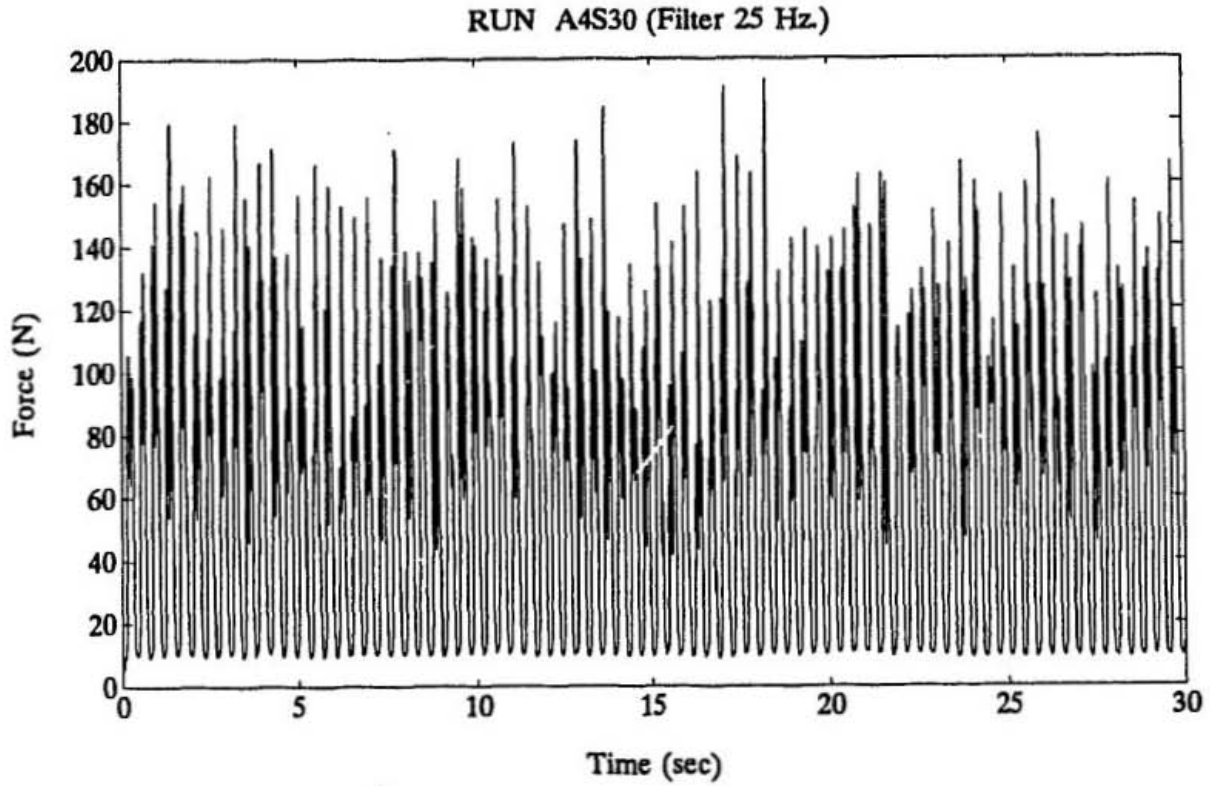
RUN A4S30 (Filter 25 Hz.)
Force (N)
Time (sec)
0
20
40
60
80
100
120
140
160
180
200
0
5
10
15
20
25
30

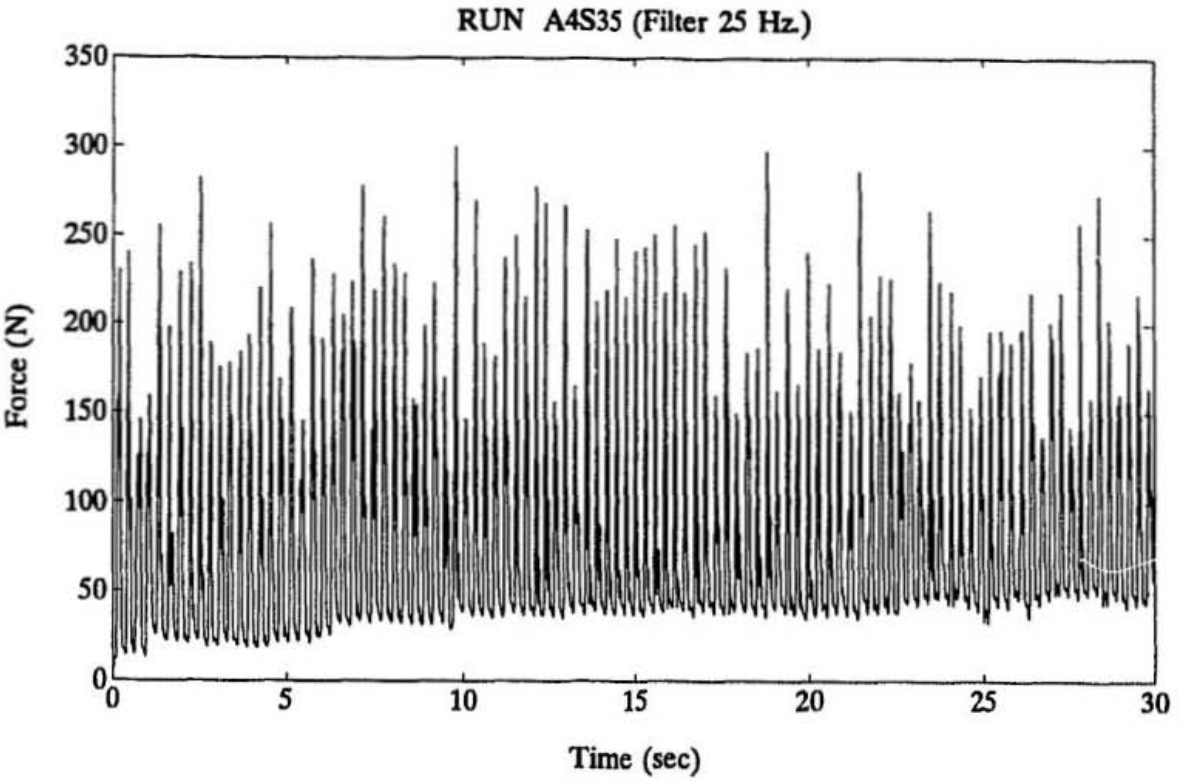
RUN A4S35 (Filter 25 Hz.)
Force (N)
Time (sec)
350
300
250
200
150
100
50
0
0
5
10
15
20
25
30

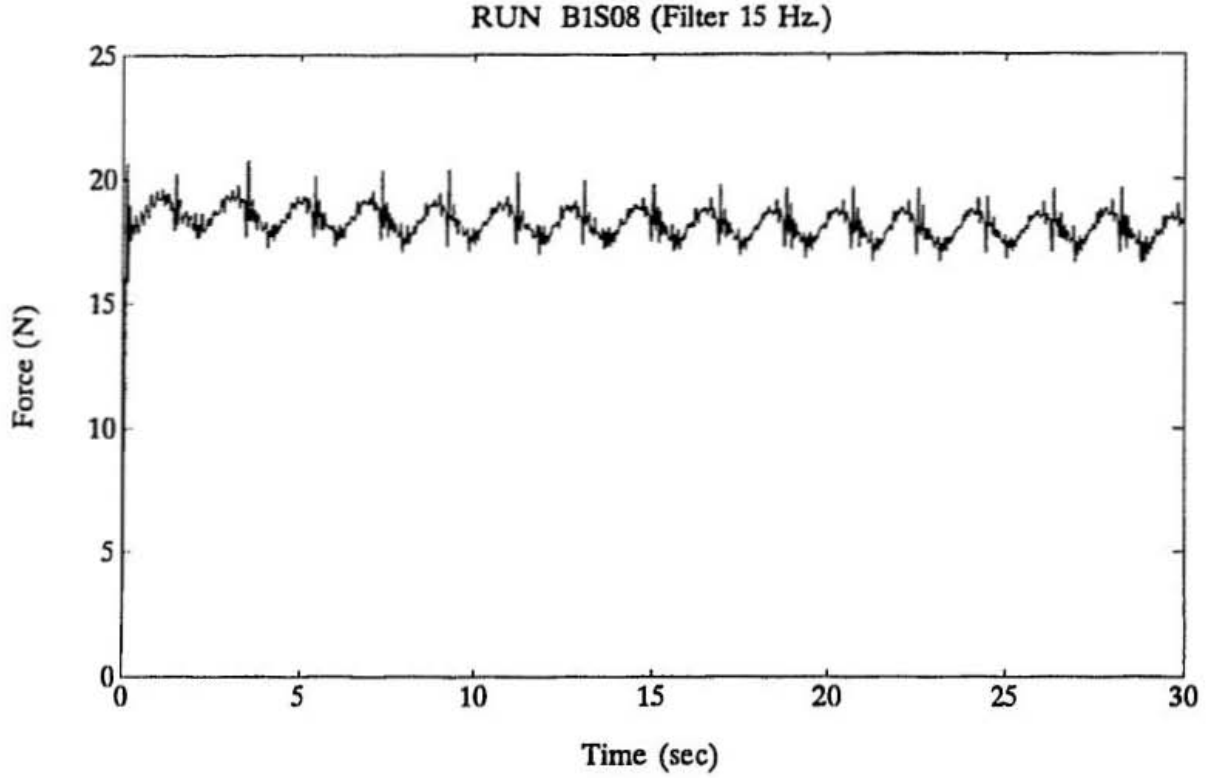
RUN B1S08 (Filter 15 Hz.)
Force (N)
Time (sec)
0
5
10
15
20
25
30

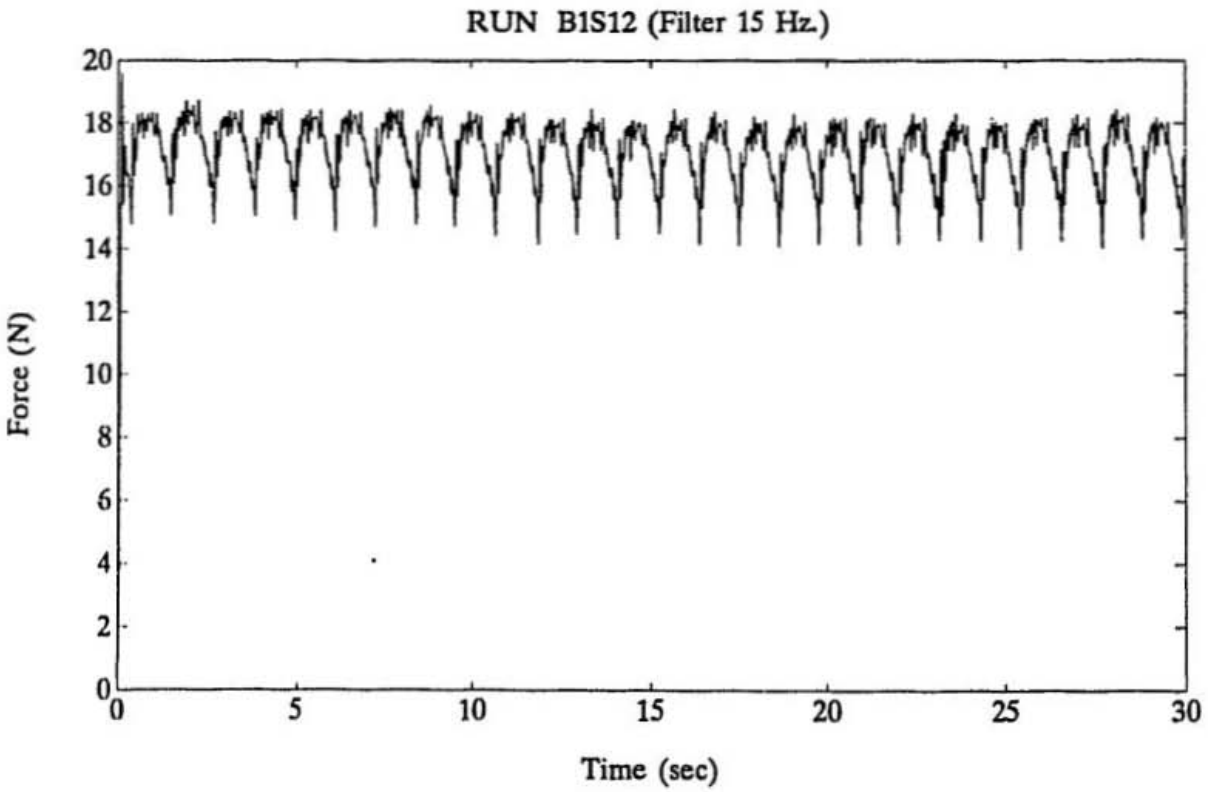
RUN B1S12 (Filter 15 Hz.)
Force (N)
Time (sec)
0
2
4
6
8
10
12
14
16
18
20
25
30

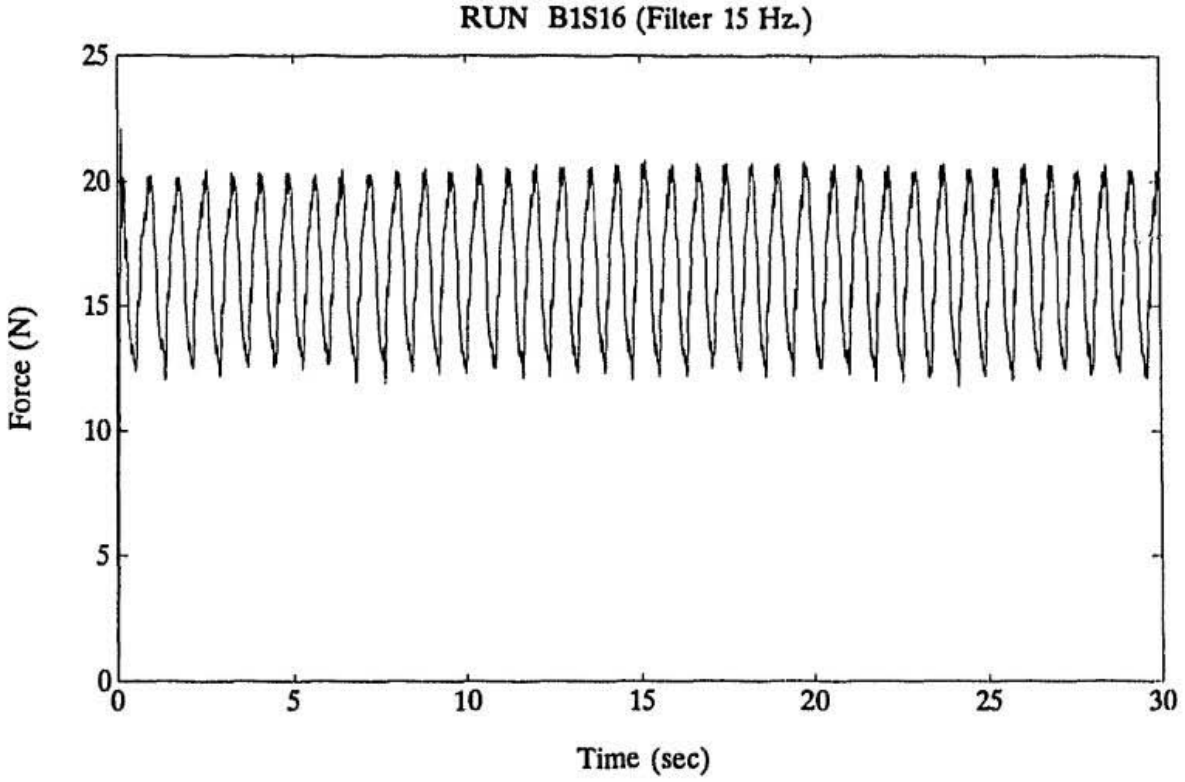
RUN B1S16 (Filter 15 Hz.)
Force (N)
Time (sec)
0
5
10
15
20
25
30

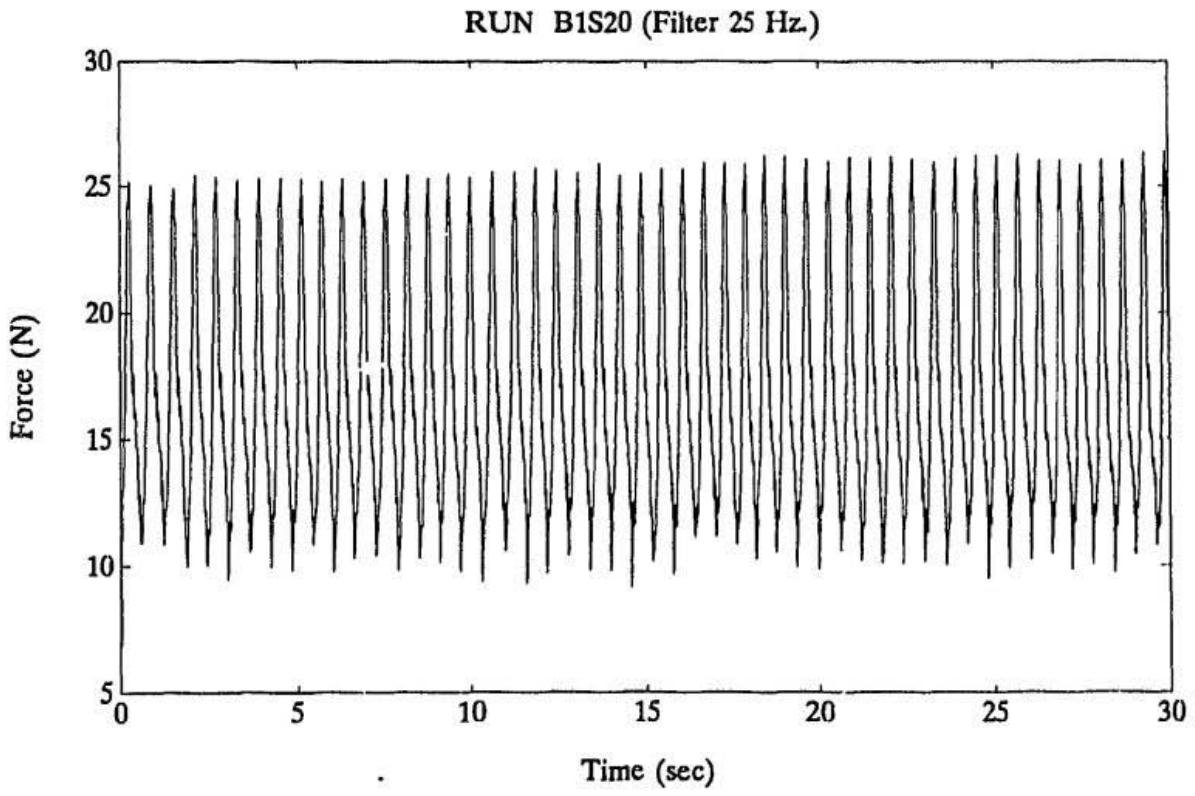
RUN B1S20 (Filter 25 Hz.)
Force (N)
Time (sec)
5
10
15
20
25
30

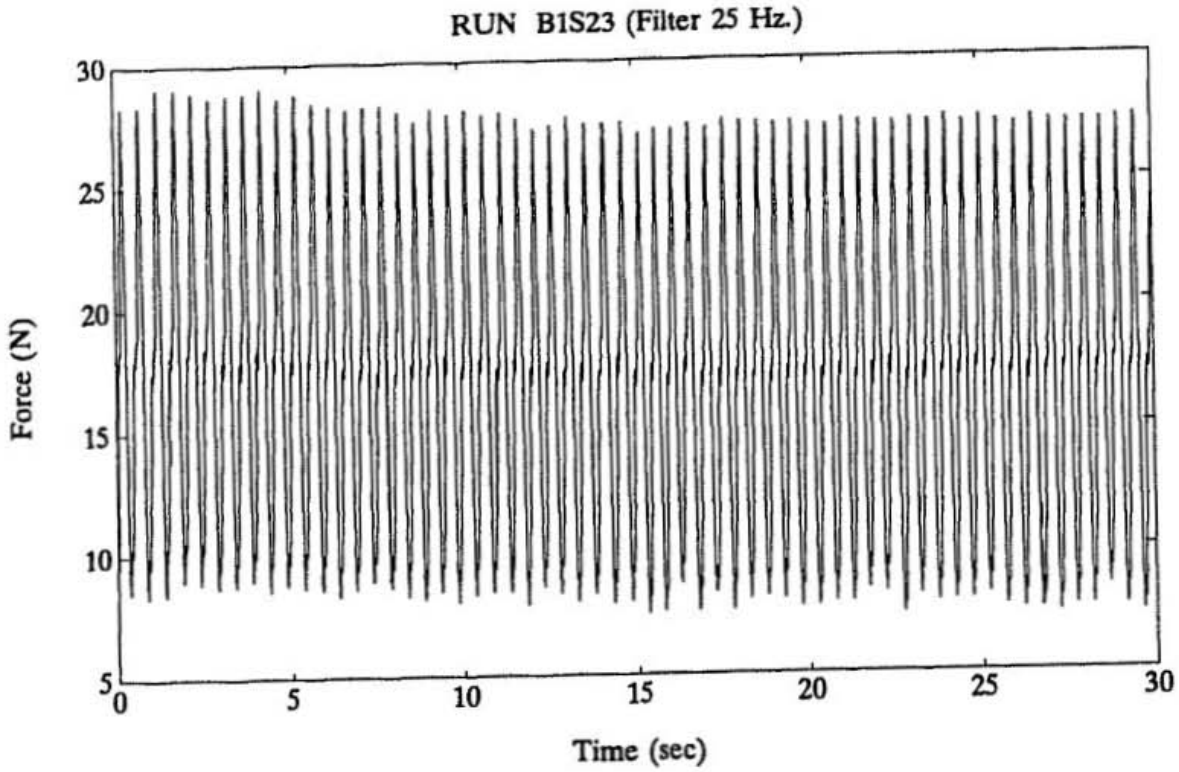
RUN B1S23 (Filter 25 Hz.)
Force (N)
Time (sec)
30
25
20
15
10
5
0
5
10
15
20
25
30

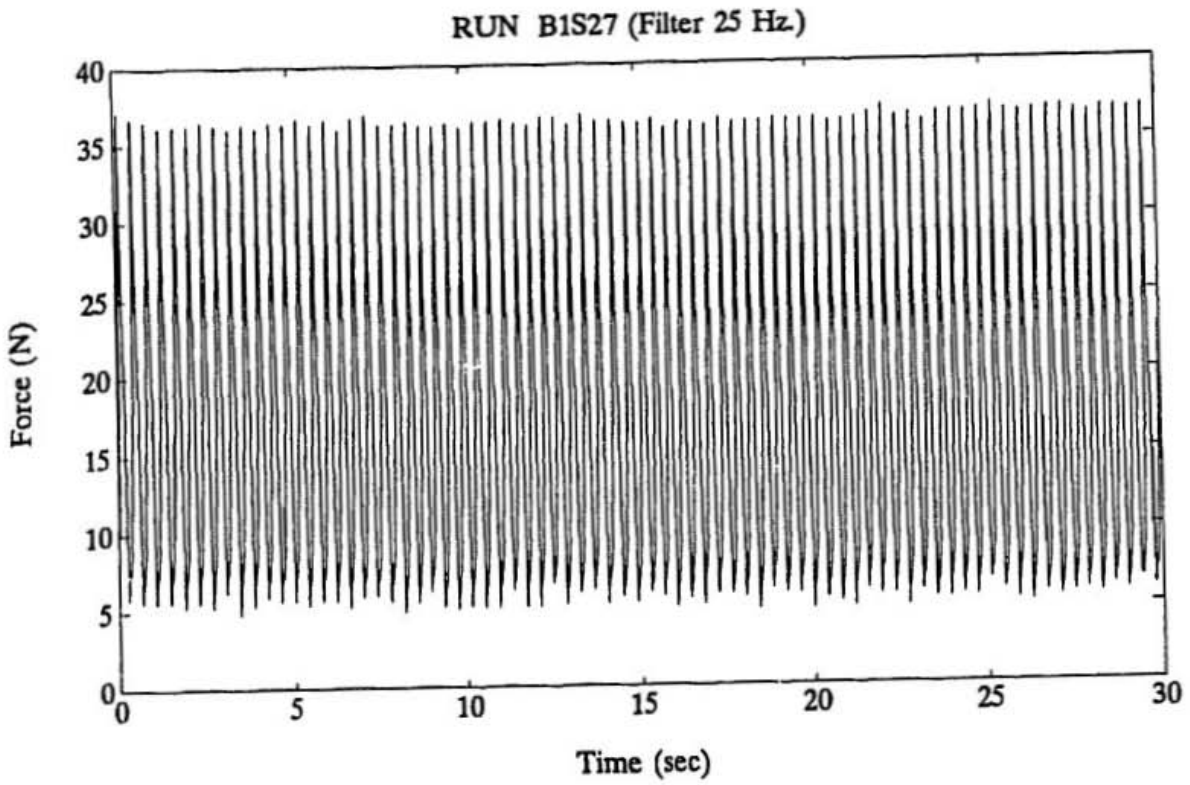
RUN B1S27 (Filter 25 Hz.)
Force (N)
Time (sec)
40
35
30
25
20
15
10
5
0
0
5
10
15
20
25
30

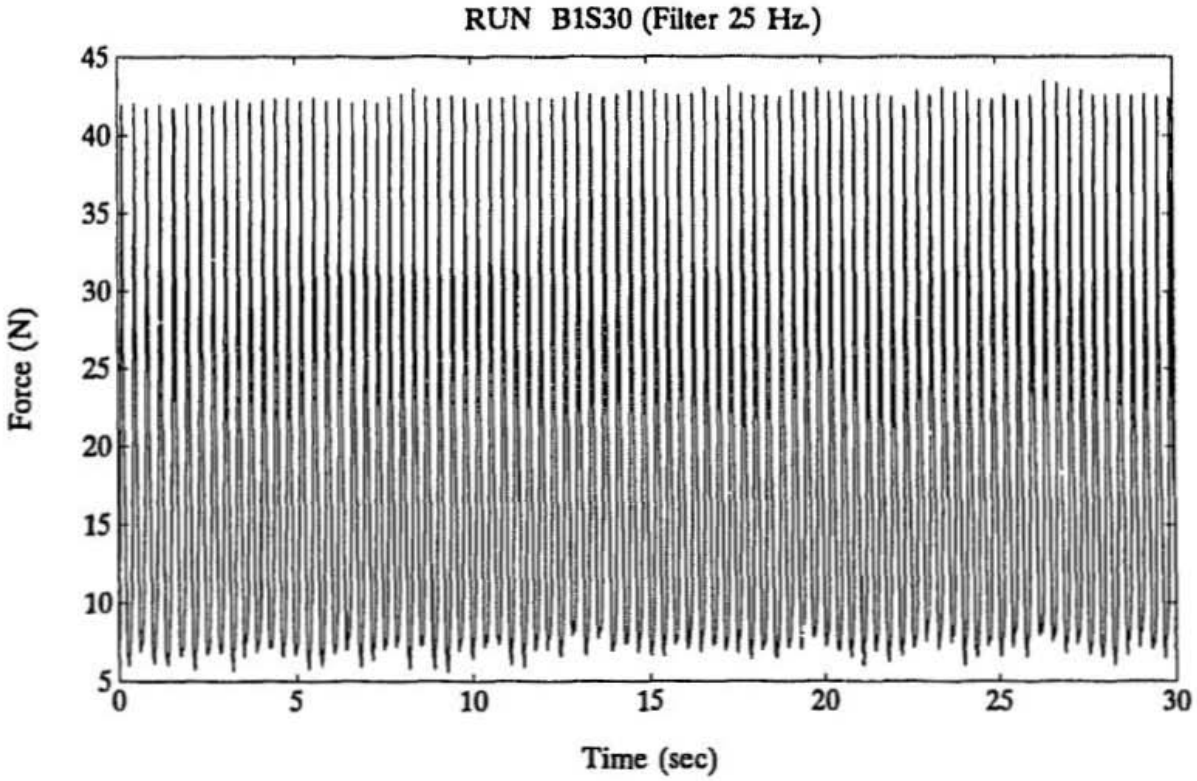
RUN B1S30 (Filter 25 Hz.)
Force (N)
Time (sec)
45
40
35
30
25
20
15
10
5
0
5
10
15
20
25
30

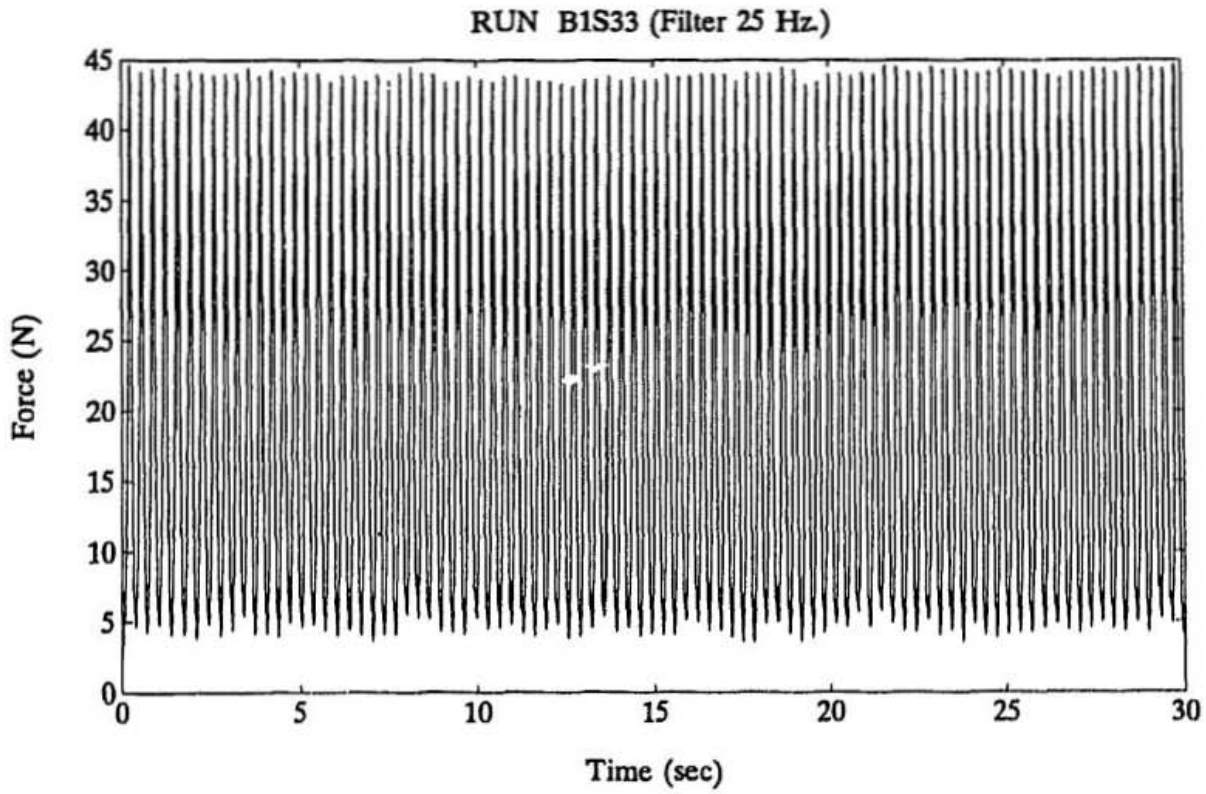
RUN B1S33 (Filter 25 Hz.)
Force (N)
Time (sec)
45
40
35
30
25
20
15
10
5
0
5
10
15
20
25
30

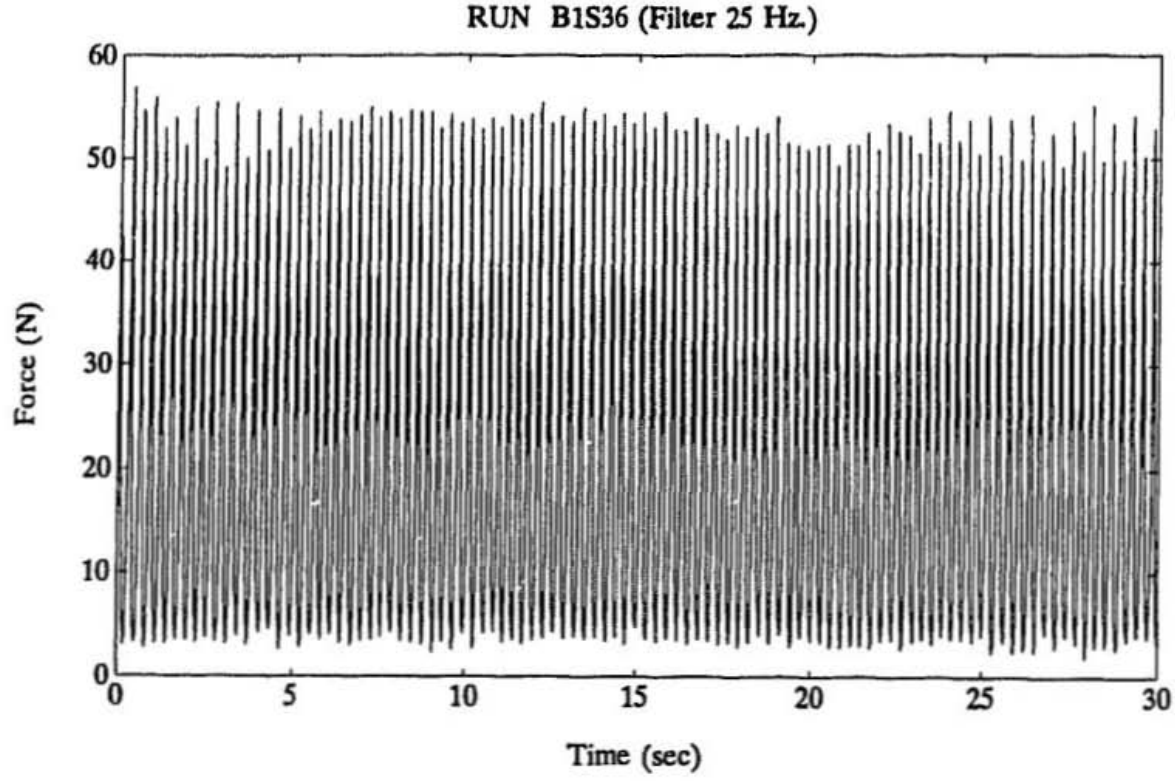
RUN B1S36 (Filter 25 Hz.)
Force (N)
Time (sec)
0
10
20
30
40
50
60
0
5
10
15
20
25
30

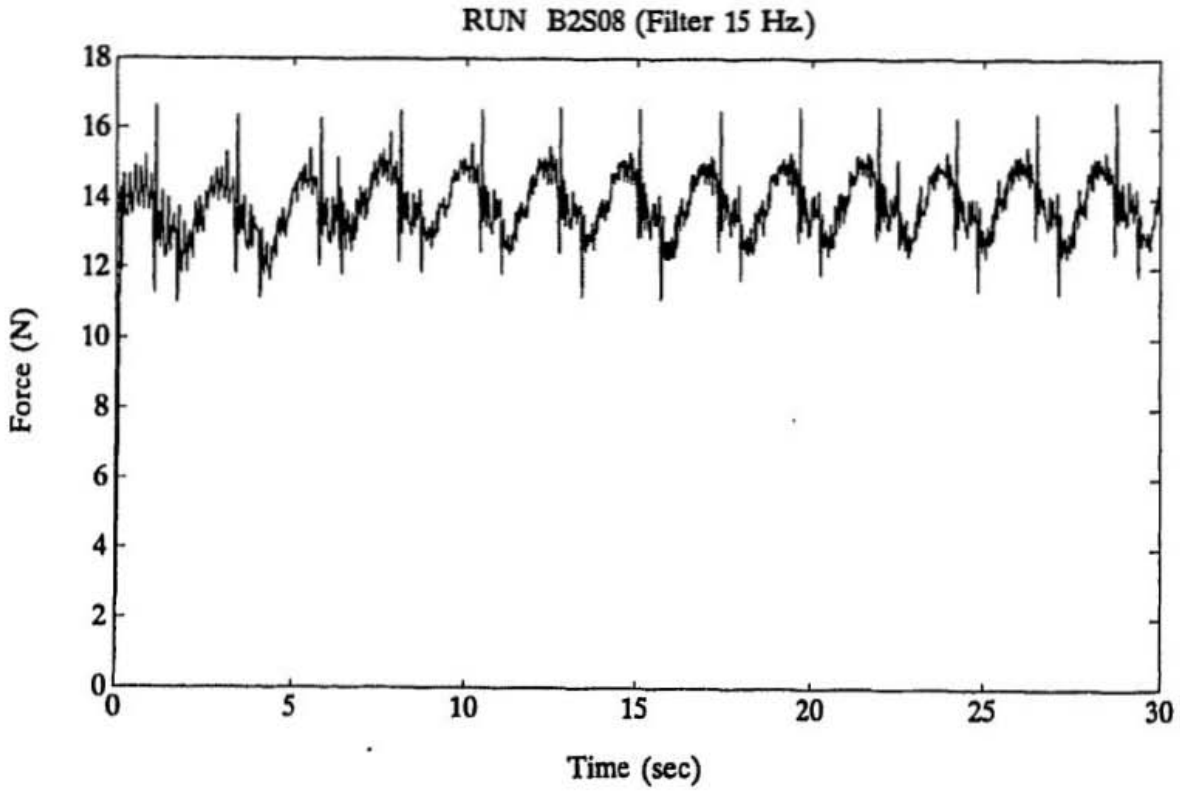
RUN B2S08 (Filter 15 Hz.)
Force (N)
Time (sec)
0
2
4
6
8
10
12
14
16
18
0
5
10
15
20
25
30

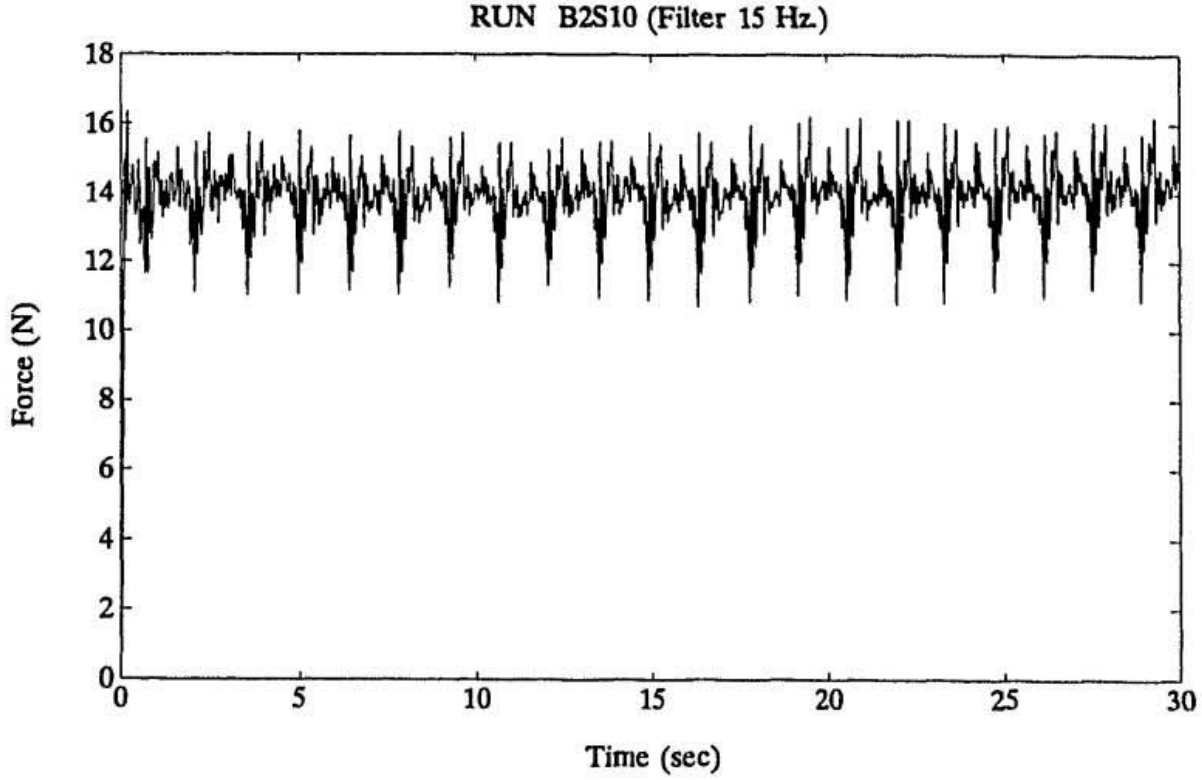
RUN B2S10 (Filter 15 Hz.)
Force (N)
Time (sec)
0
2
4
6
8
10
12
14
16
18
0
5
10
15
20
25
30

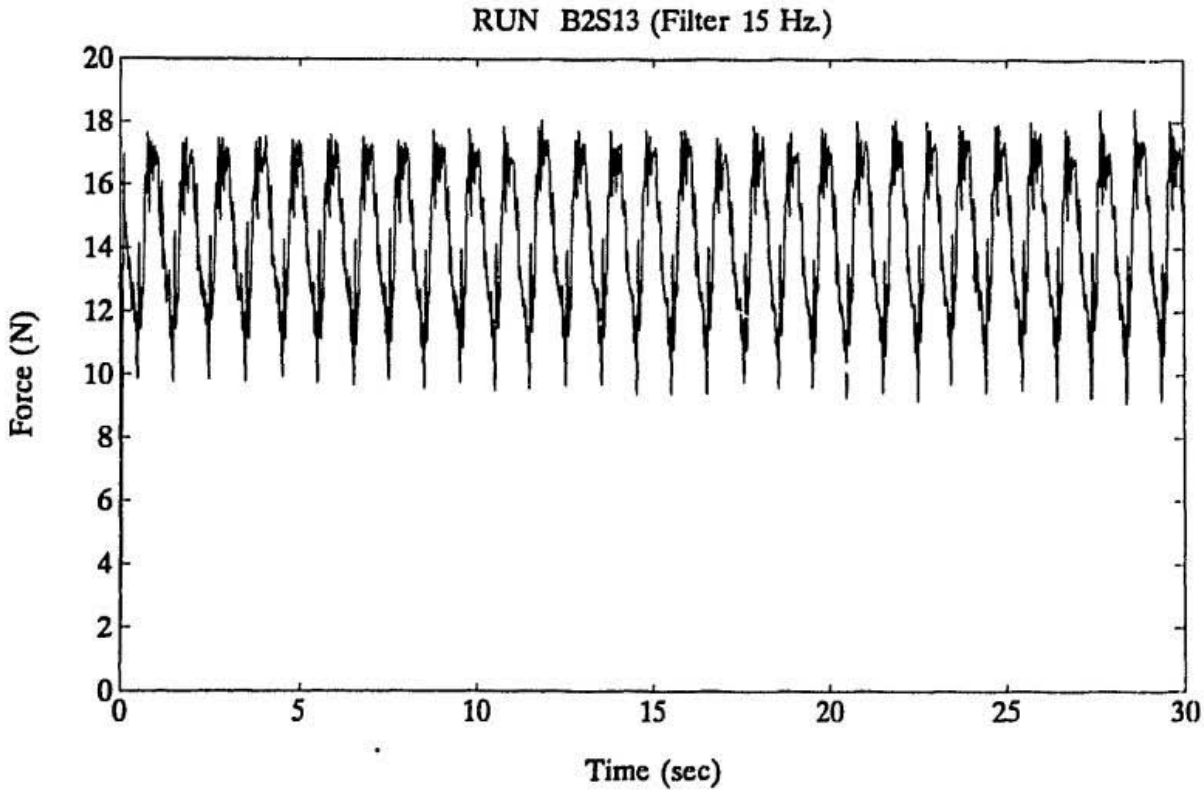
RUN B2S13 (Filter 15 Hz.)
Force (N)
Time (sec)
0
2
4
6
8
10
12
14
16
18
20
0
5
10
15
20
25
30

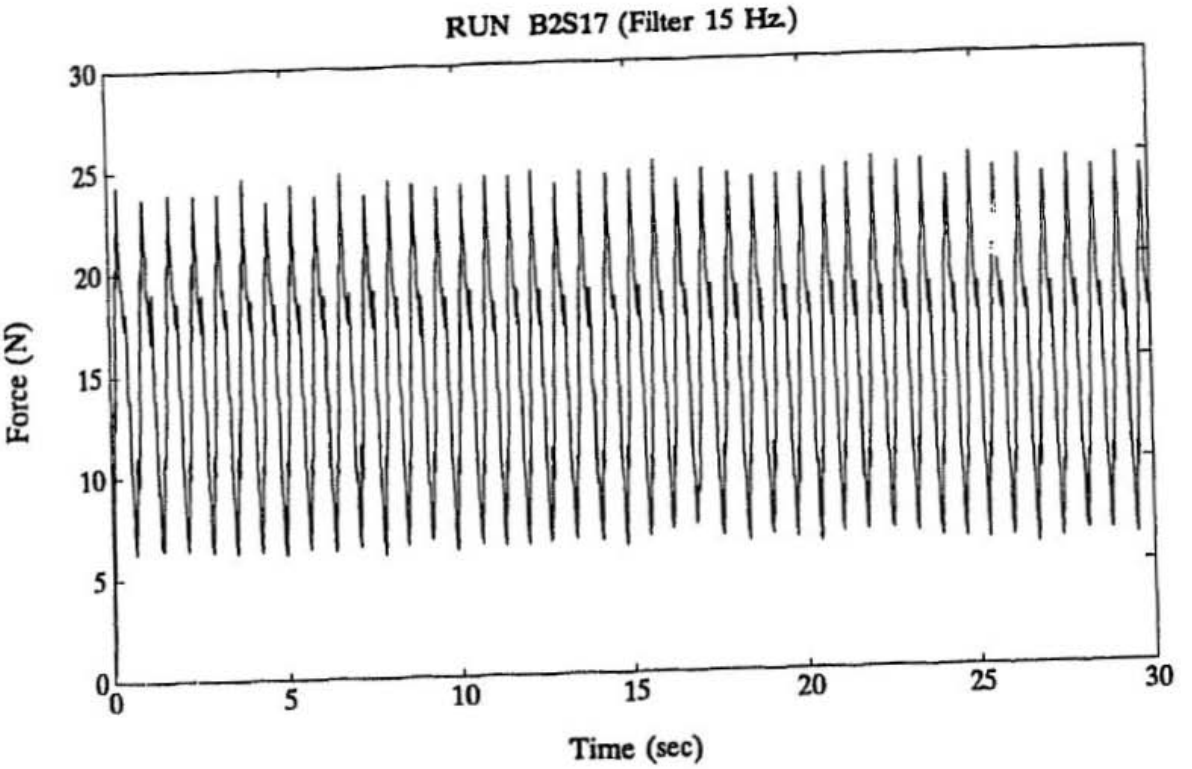
RUN B2S17 (Filter 15 Hz.)
Force (N)
Time (sec)
0
5
10
15
20
25
30

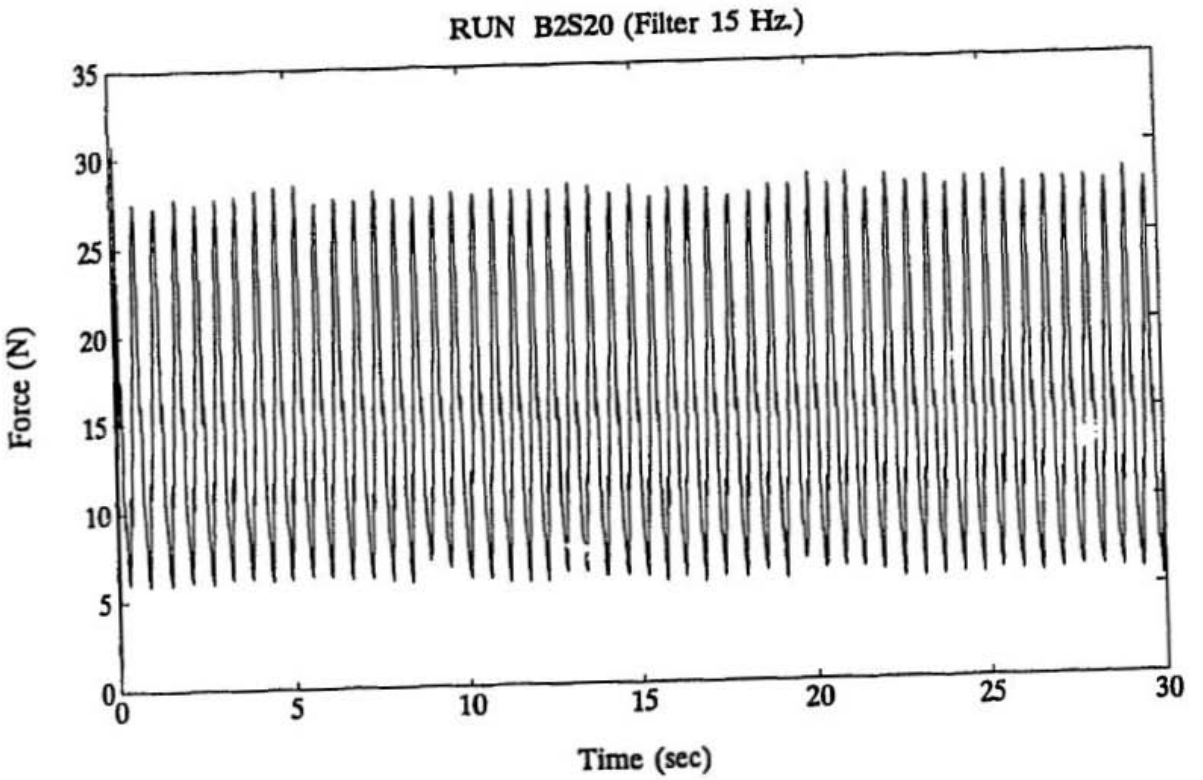
RUN B2S20 (Filter 15 Hz.)
Force (N)
Time (sec)
0
5
10
15
20
25
30
35

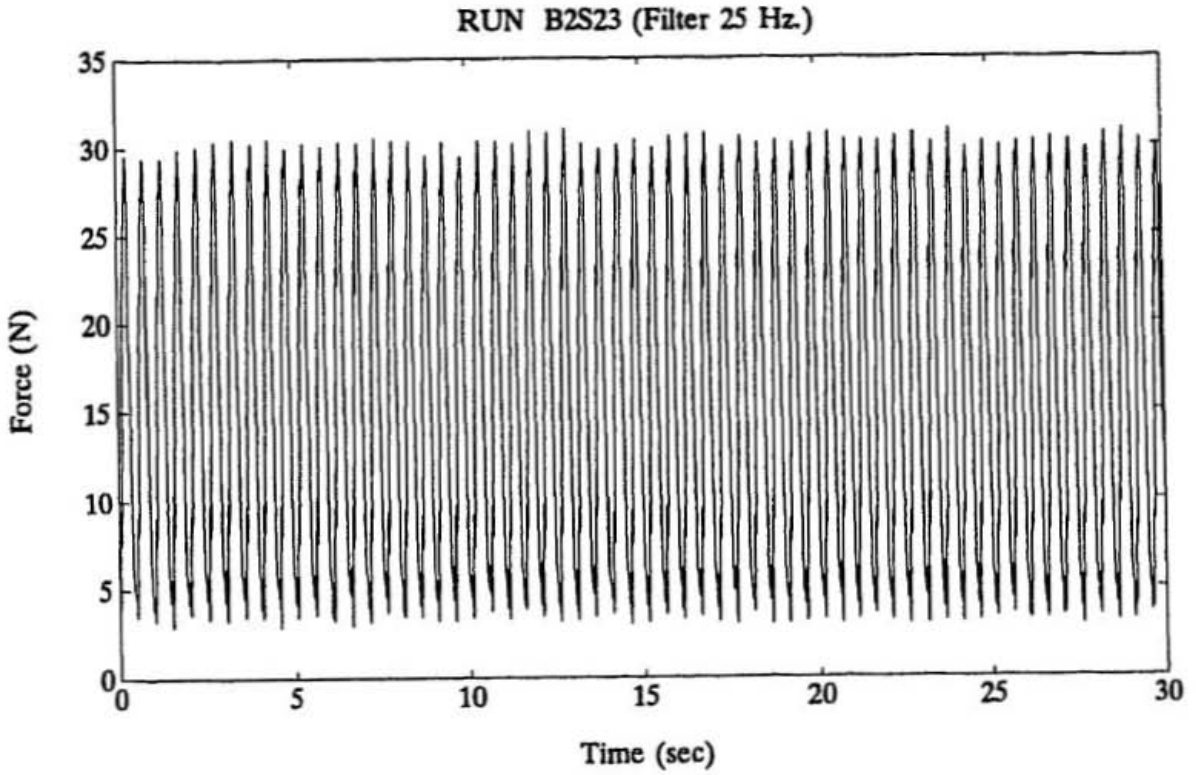
RUN B2S23 (Filter 25 Hz.)
Force (N)
Time (sec)
0
5
10
15
20
25
30
35

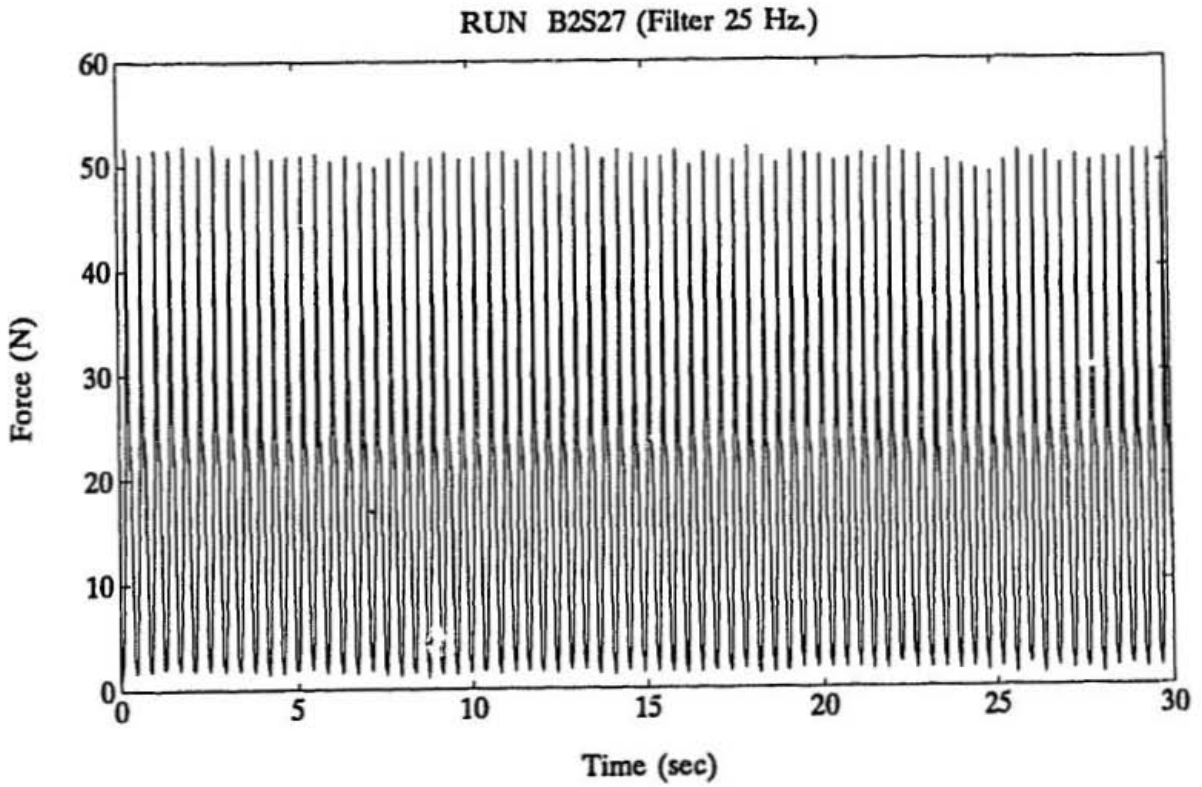
RUN B2S27 (Filter 25 Hz.)
Force (N)
Time (sec)
0
10
20
30
40
50
60

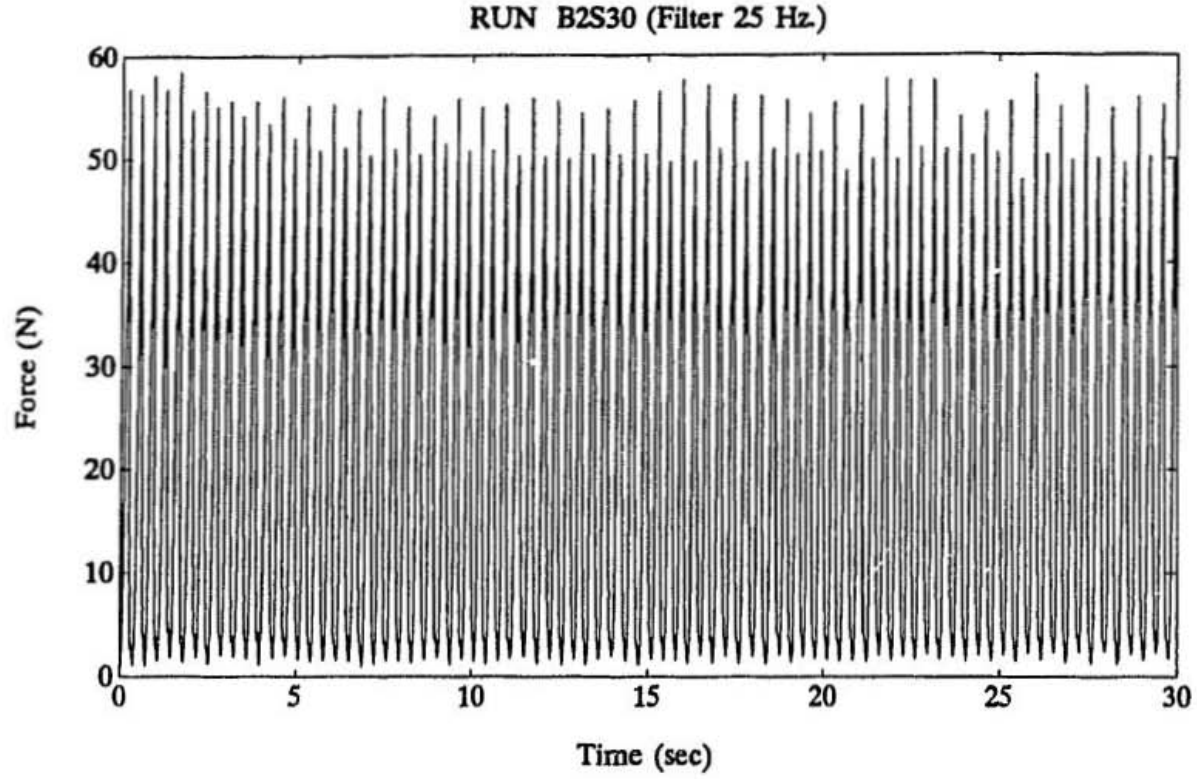
RUN B2S30 (Filter 25 Hz.)
Force (N)
Time (sec)
0
10
20
30
40
50
60
0
5
10
15
20
25
30

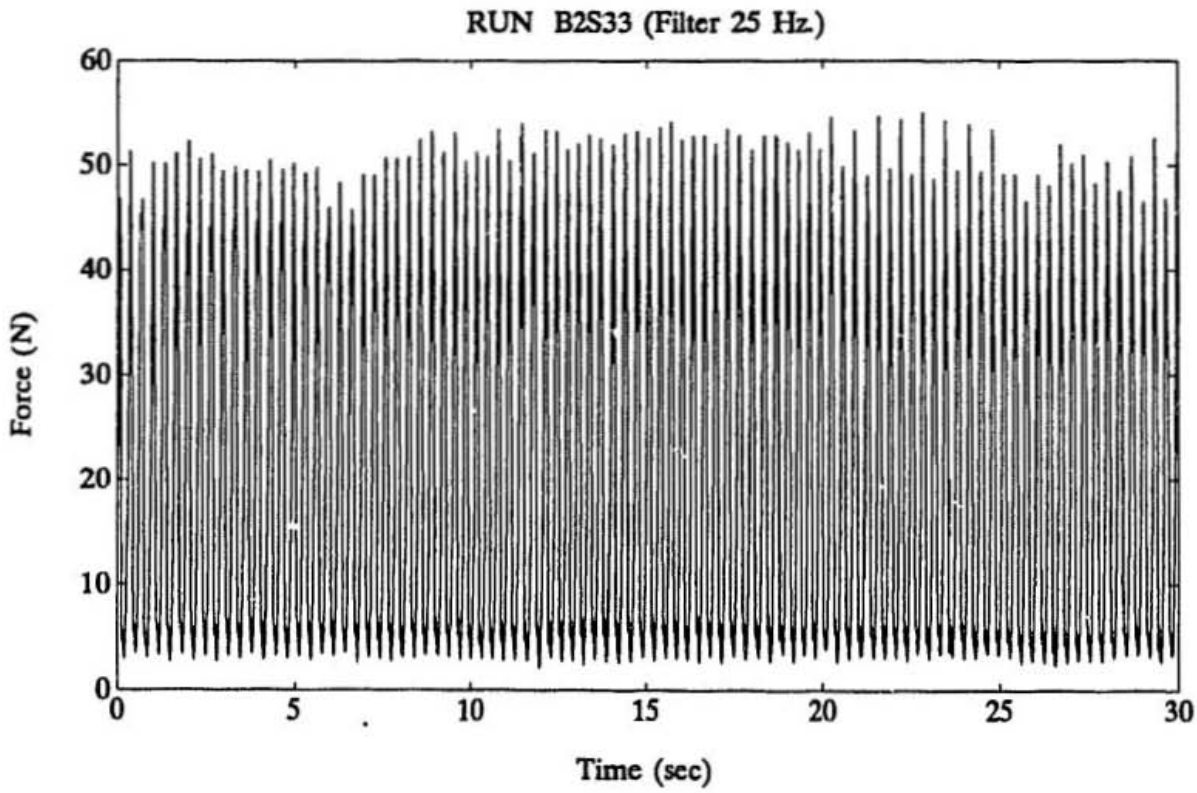
RUN B2S33 (Filter 25 Hz.)
Force (N)
Time (sec)
0
10
20
30
40
50
60
0
5
10
15
20
25
30

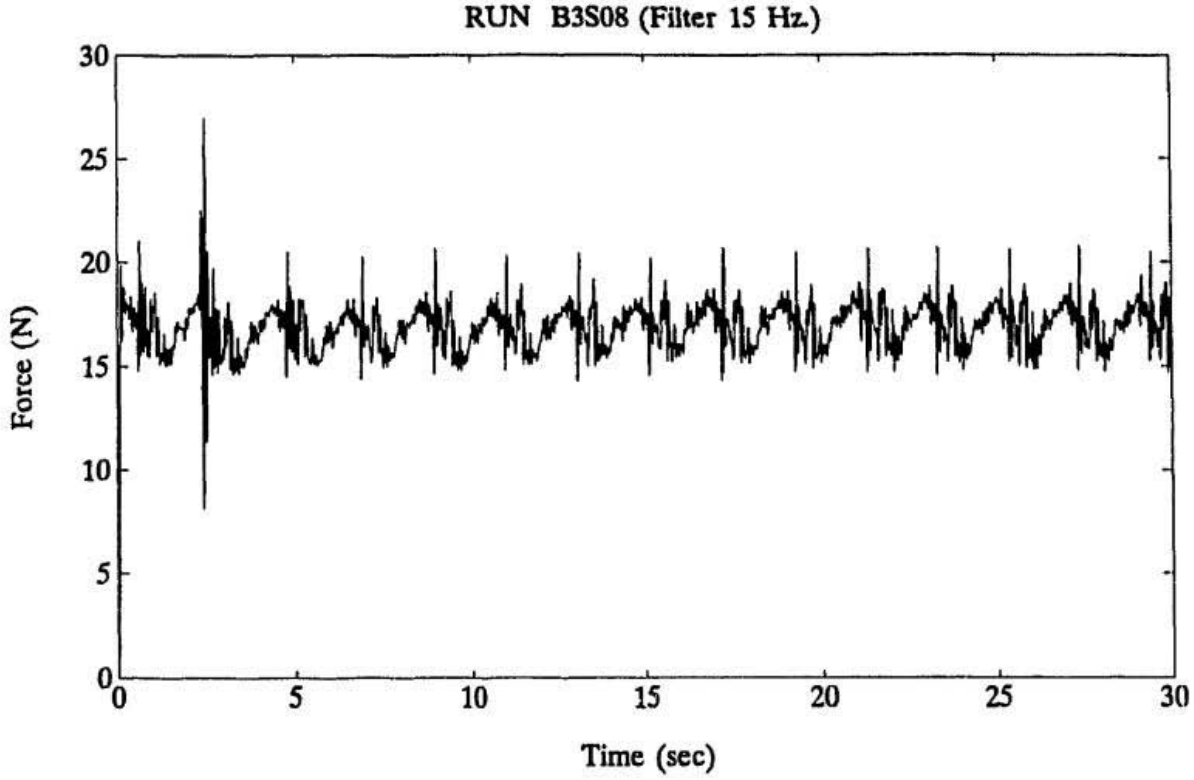
RUN B3S08 (Filter 15 Hz.)
Force (N)
Time (sec)
0
5
10
15
20
25
30

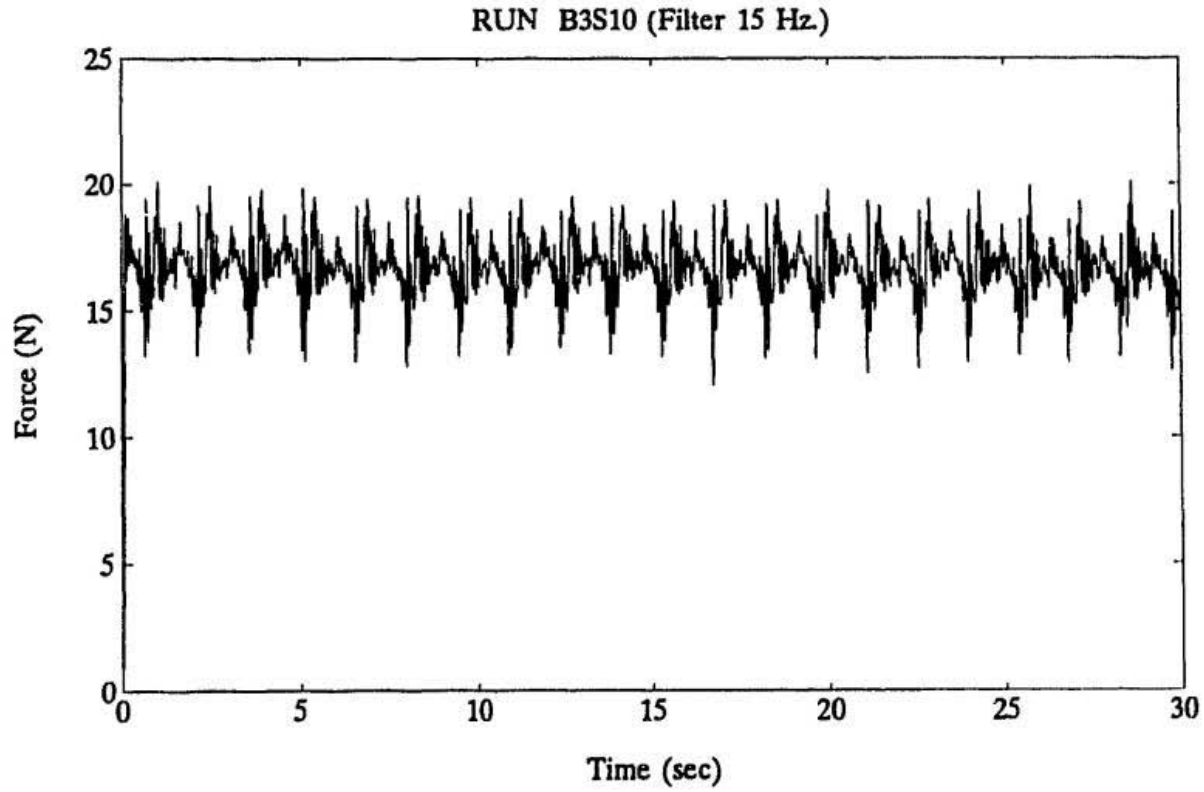
RUN B3S10 (Filter 15 Hz.)
Force (N)
Time (sec)
0
5
10
15
20
25
30

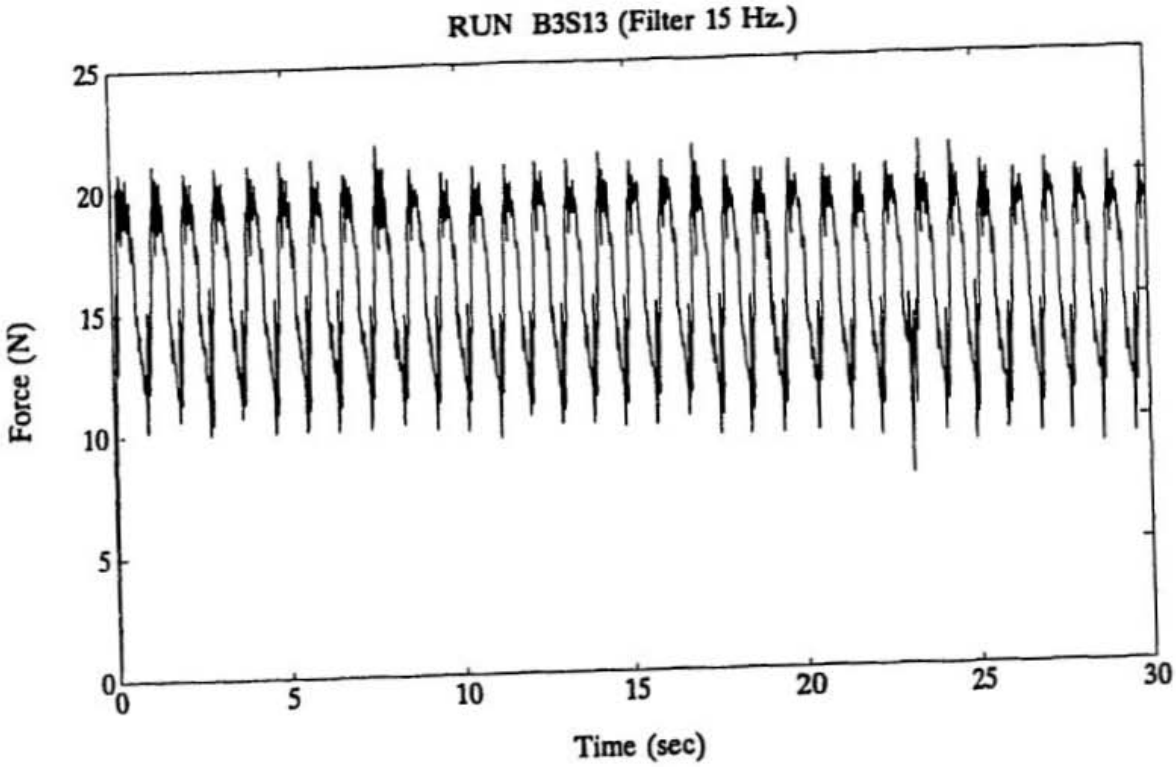
RUN B3S13 (Filter 15 Hz.)
Force (N)
Time (sec)
0
5
10
15
20
25
30

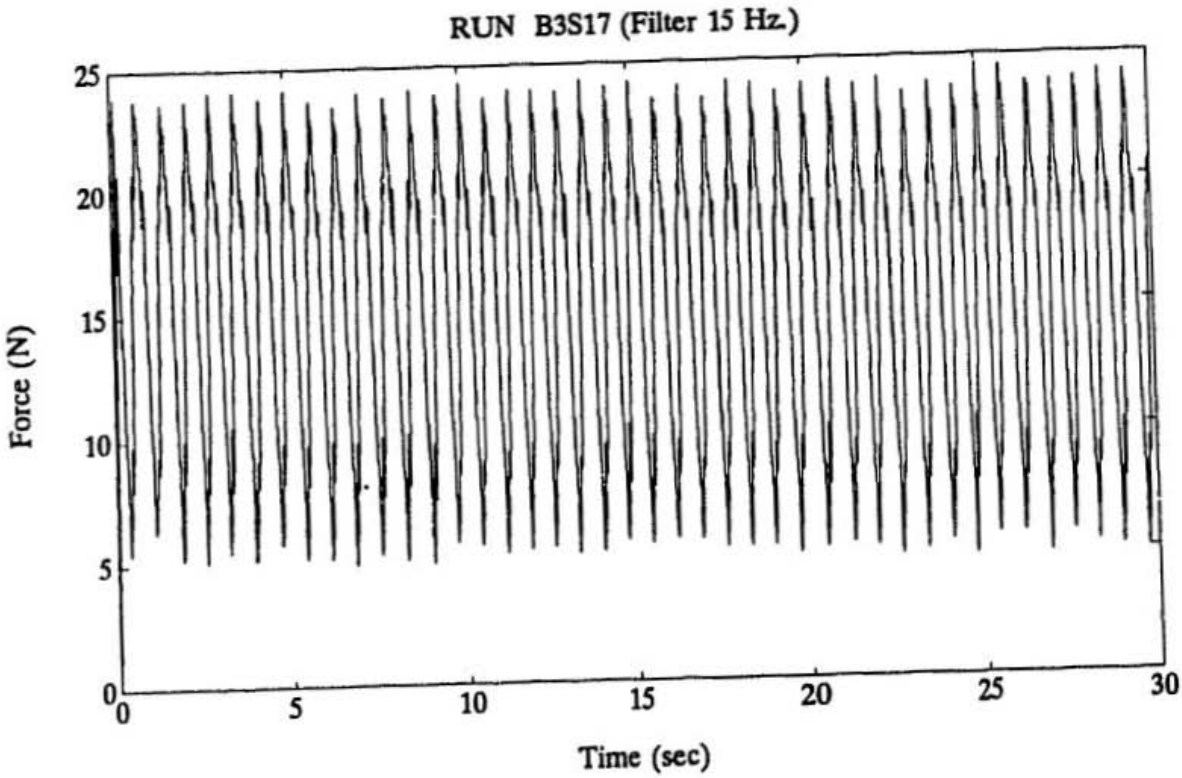
RUN B3S17 (Filter 15 Hz.)
Force (N)
Time (sec)
0
5
10
15
20
25
30

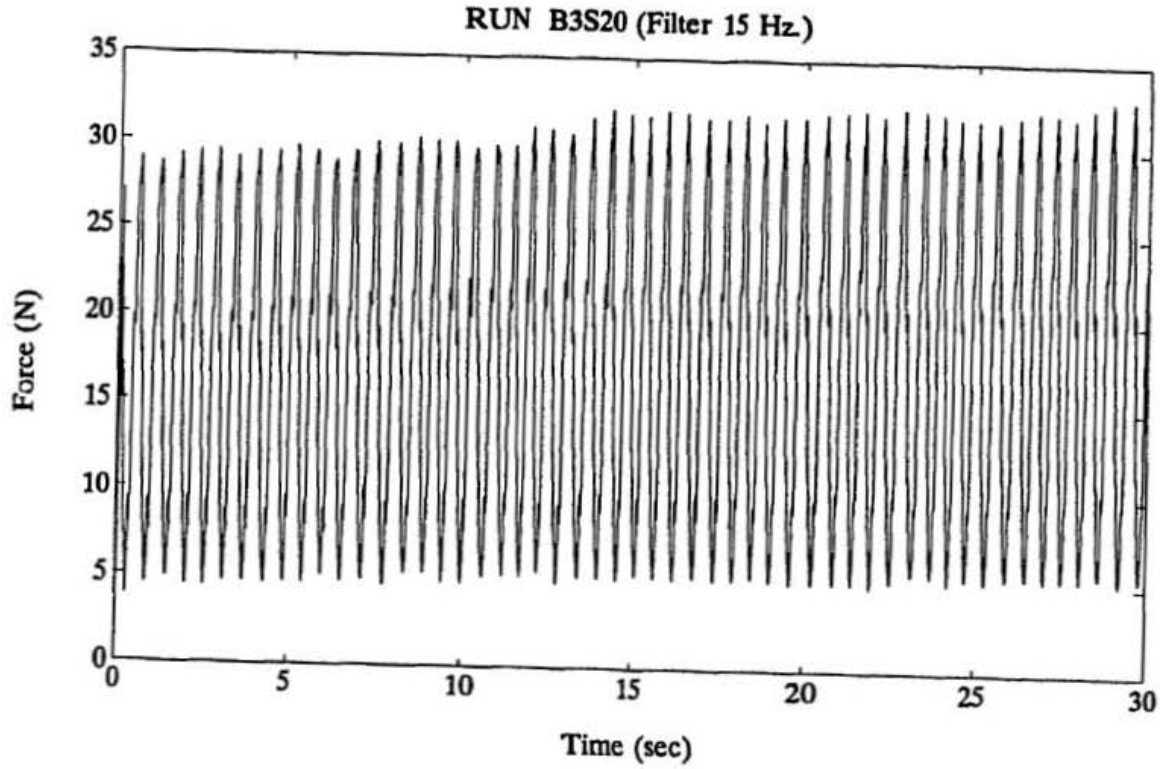
RUN B3S20 (Filter 15 Hz.)
Force (N)
Time (sec)
0
5
10
15
20
25
30
35

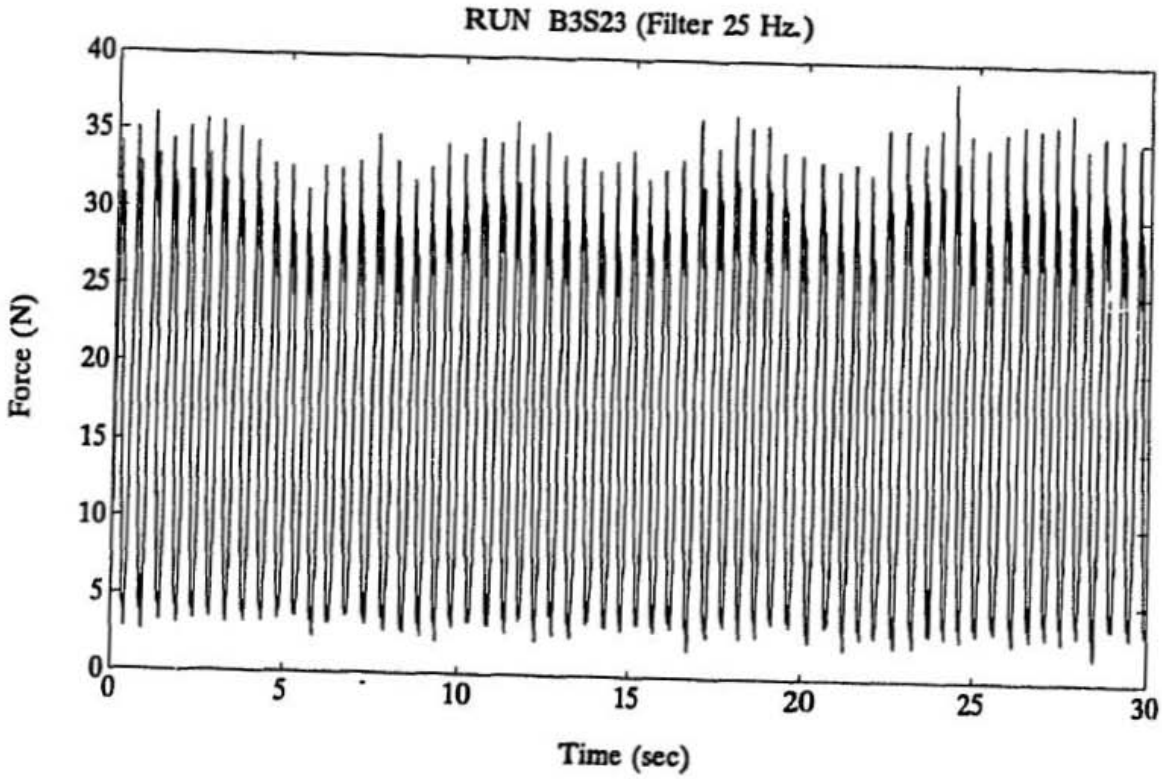
RUN B3S23 (Filter 25 Hz.)
Force (N)
Time (sec)
0
5
10
15
20
25
30
35
40

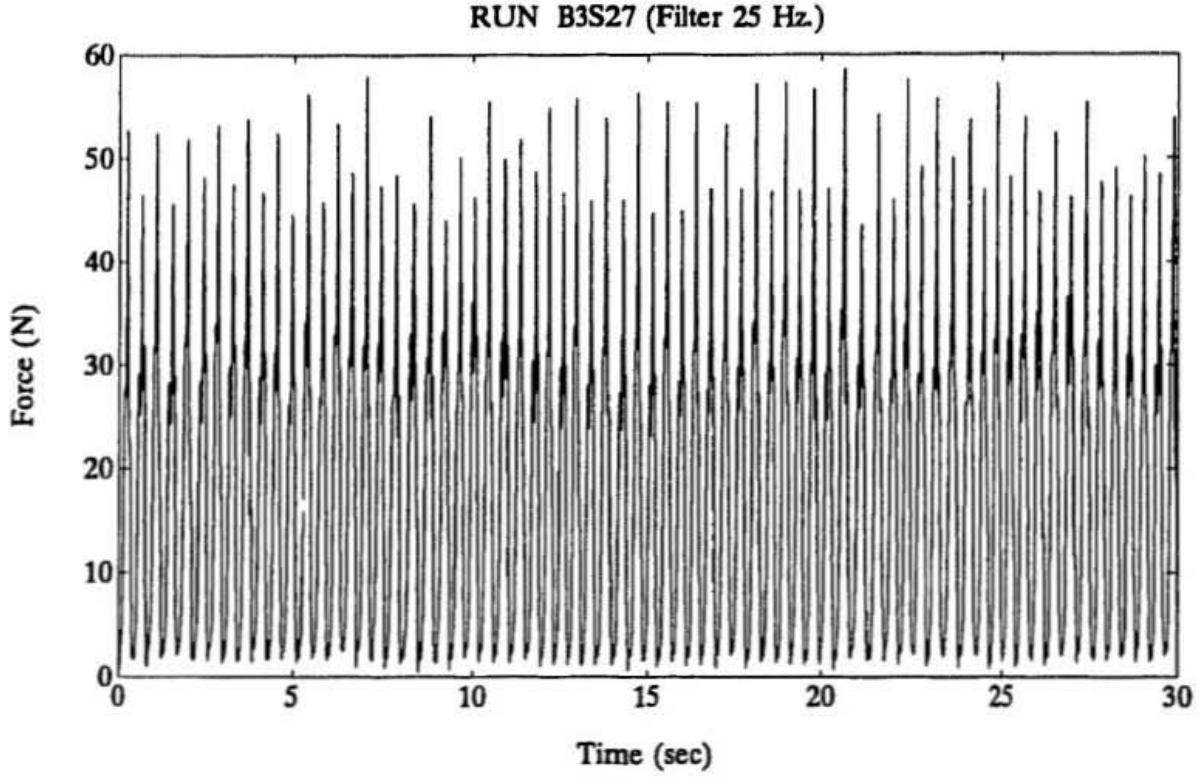
RUN B3S27 (Filter 25 Hz.)
Force (N)
Time (sec)
0
10
20
30
40
50
60
0
5
10
15
20
25
30

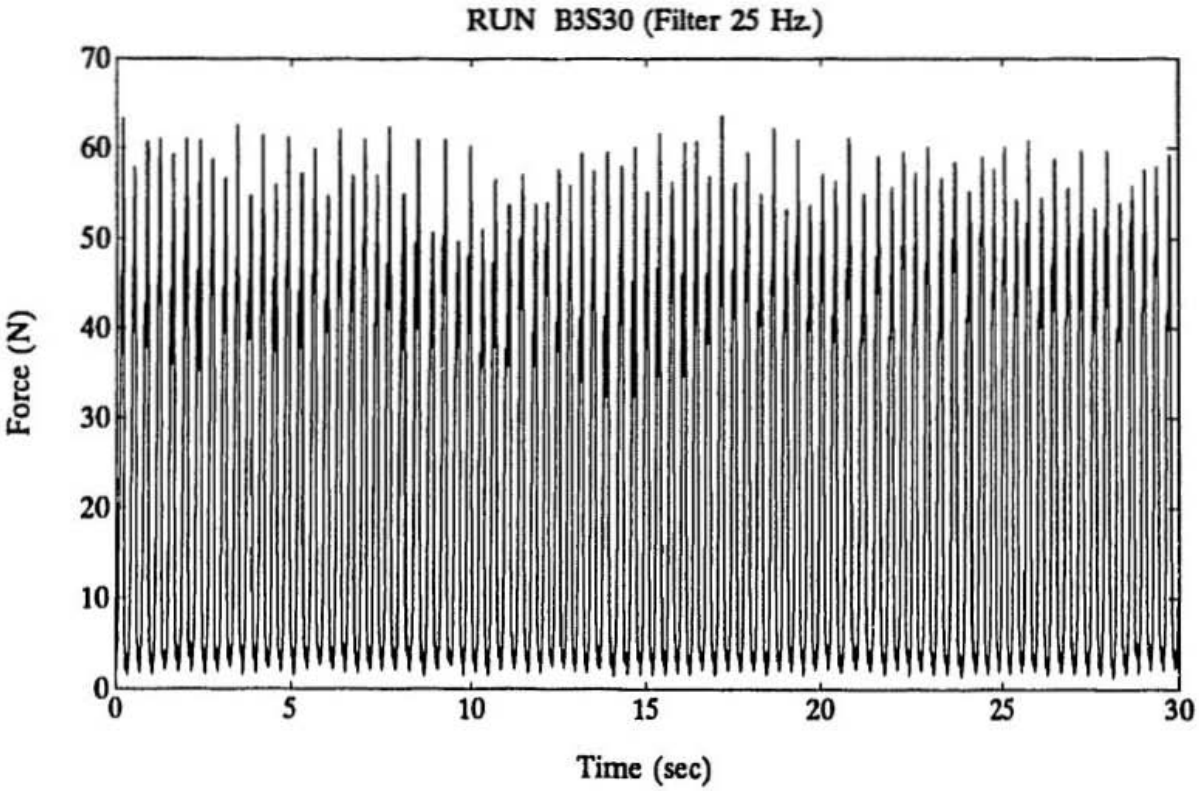
RUN B3S30 (Filter 25 Hz.)
Force (N)
Time (sec)
0
10
20
30
40
50
60
70
0
5
10
15
20
25
30

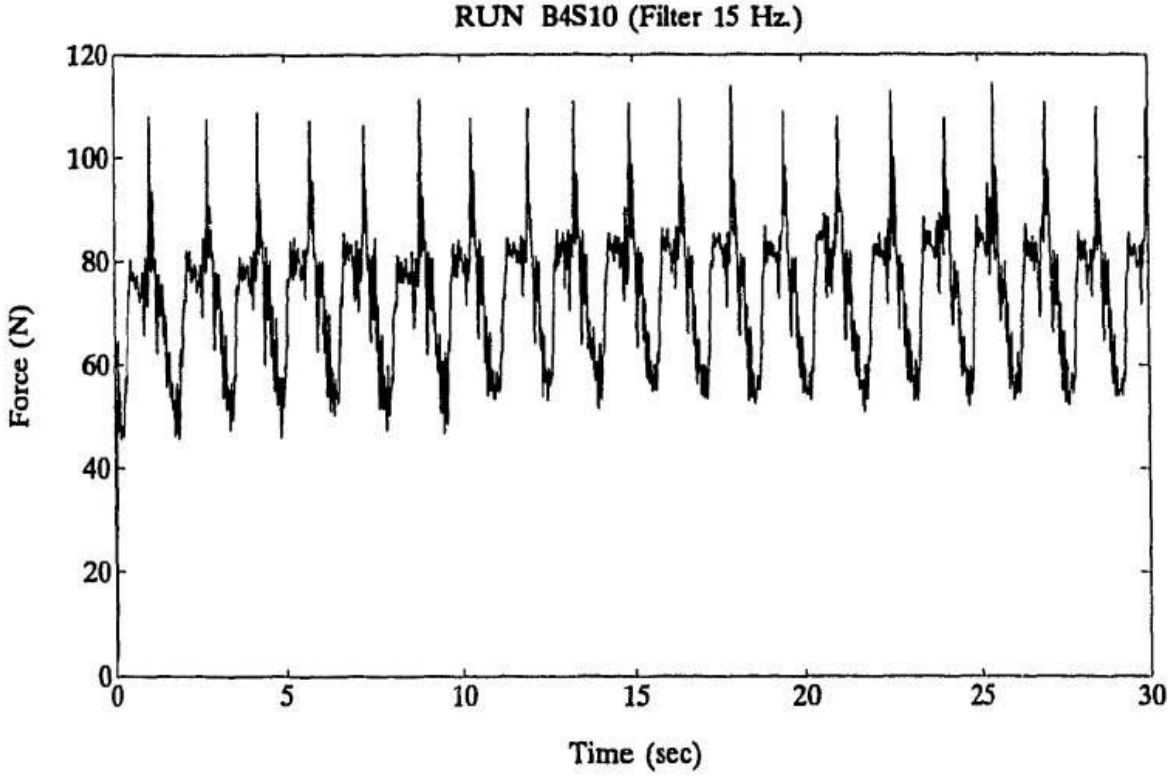
RUN B4S10 (Filter 15 Hz.)
Force (N)
Time (sec)
0
20
40
60
80
100
120
0
5
10
15
20
25
30

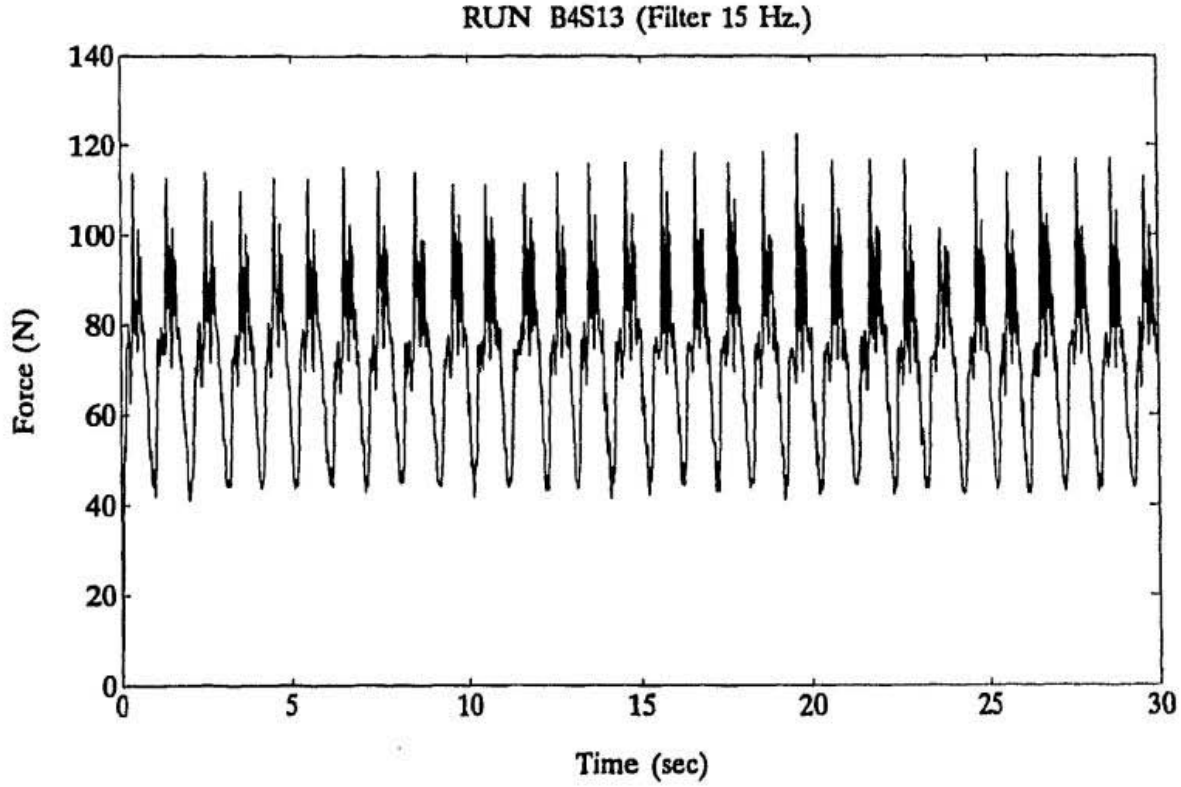
RUN B4S13 (Filter 15 Hz.)
Force (N)
Time (sec)
0
20
40
60
80
100
120
140
0
5
10
15
20
25
30

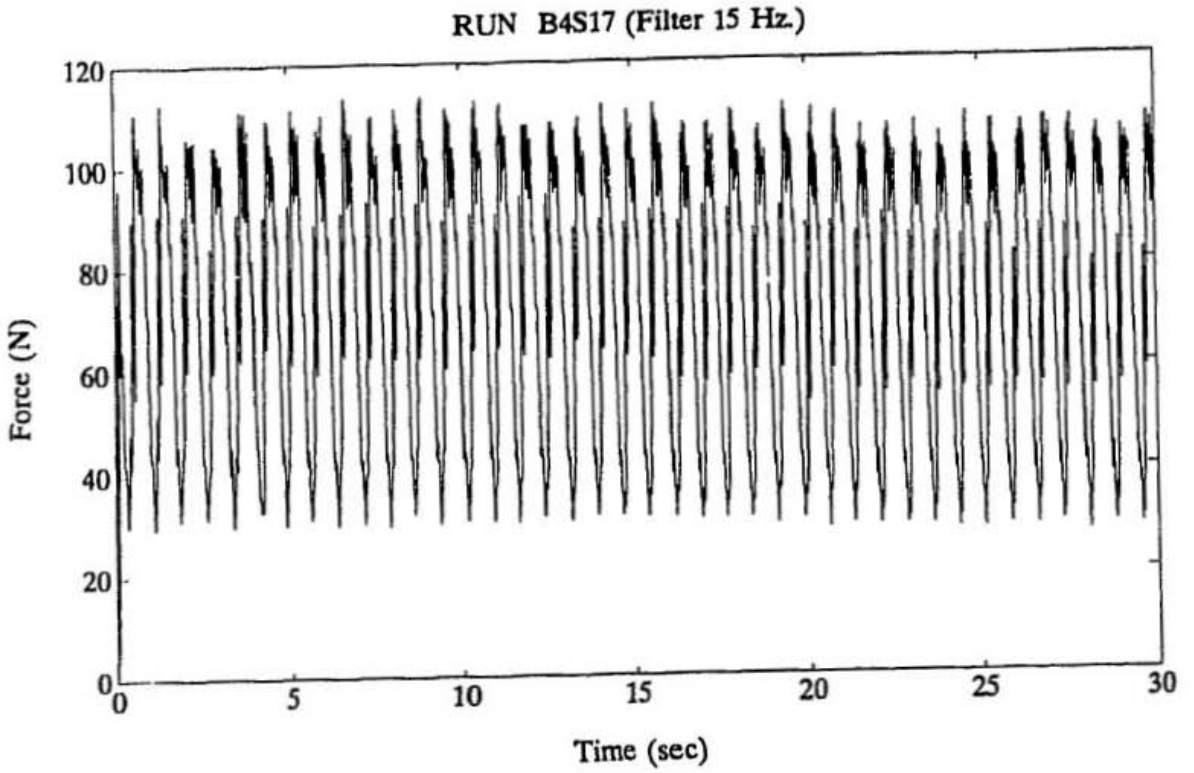
RUN B4S17 (Filter 15 Hz.)
Force (N)
Time (sec)
0
20
40
60
80
100
120
0
5
10
15
20
25
30

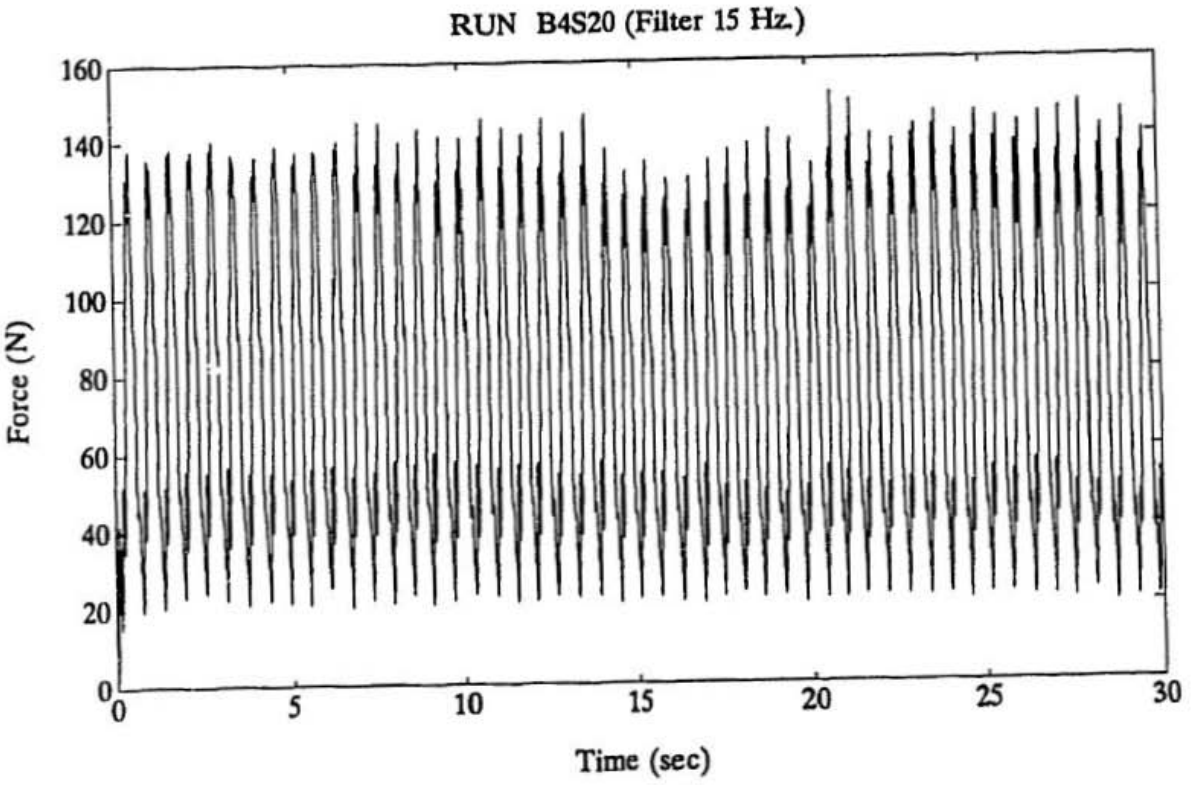
RUN B4S20 (Filter 15 Hz.)
Force (N)
Time (sec)
0
20
40
60
80
100
120
140
160
0
5
10
15
20
25
30

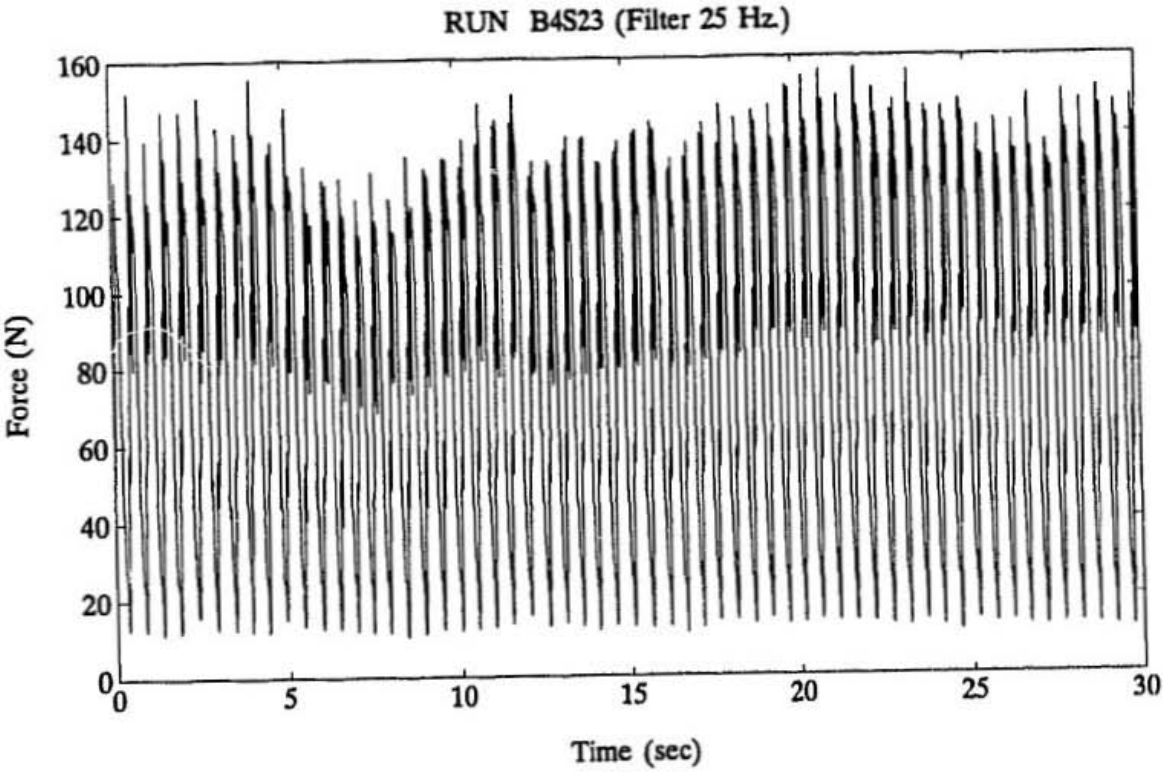
RUN B4S23 (Filter 25 Hz.)
Force (N)
Time (sec)
0
20
40
60
80
100
120
140
160
0
5
10
15
20
25
30

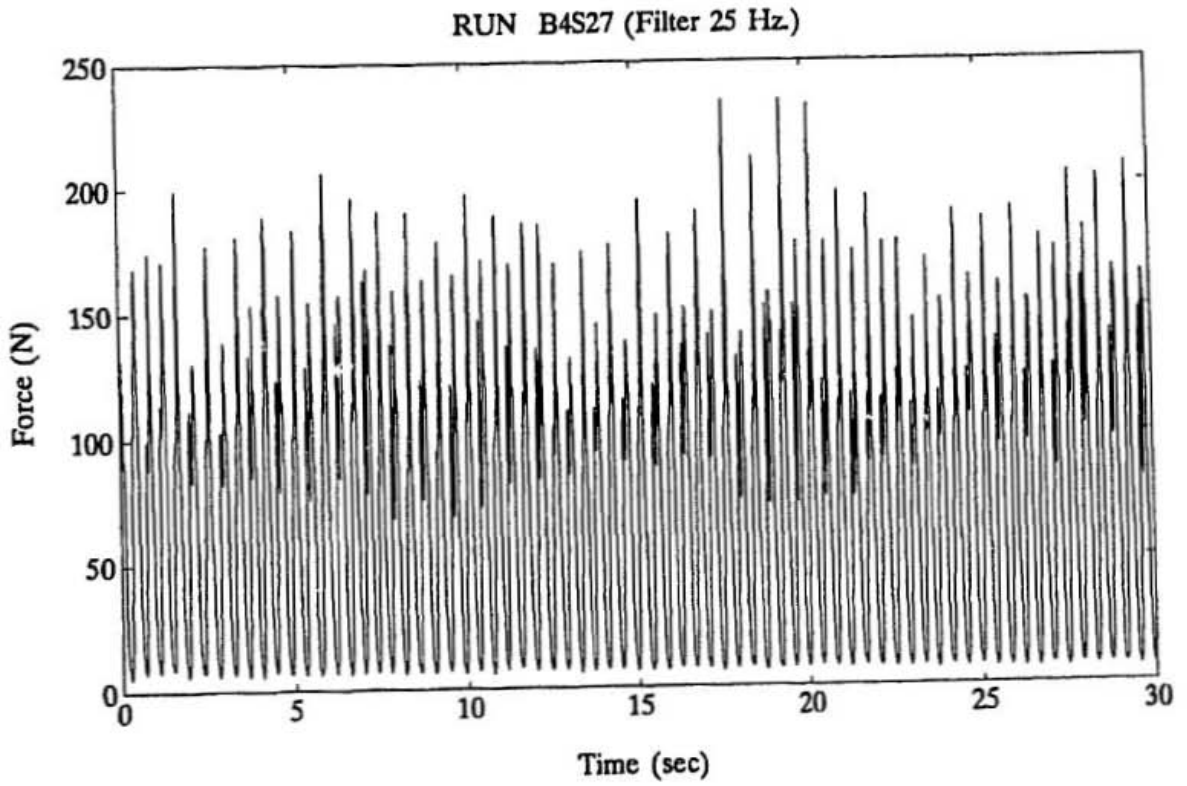
RUN B4S27 (Filter 25 Hz.)
Force (N)
Time (sec)
0
50
100
150
200
250
0
5
10
15
20
25
30

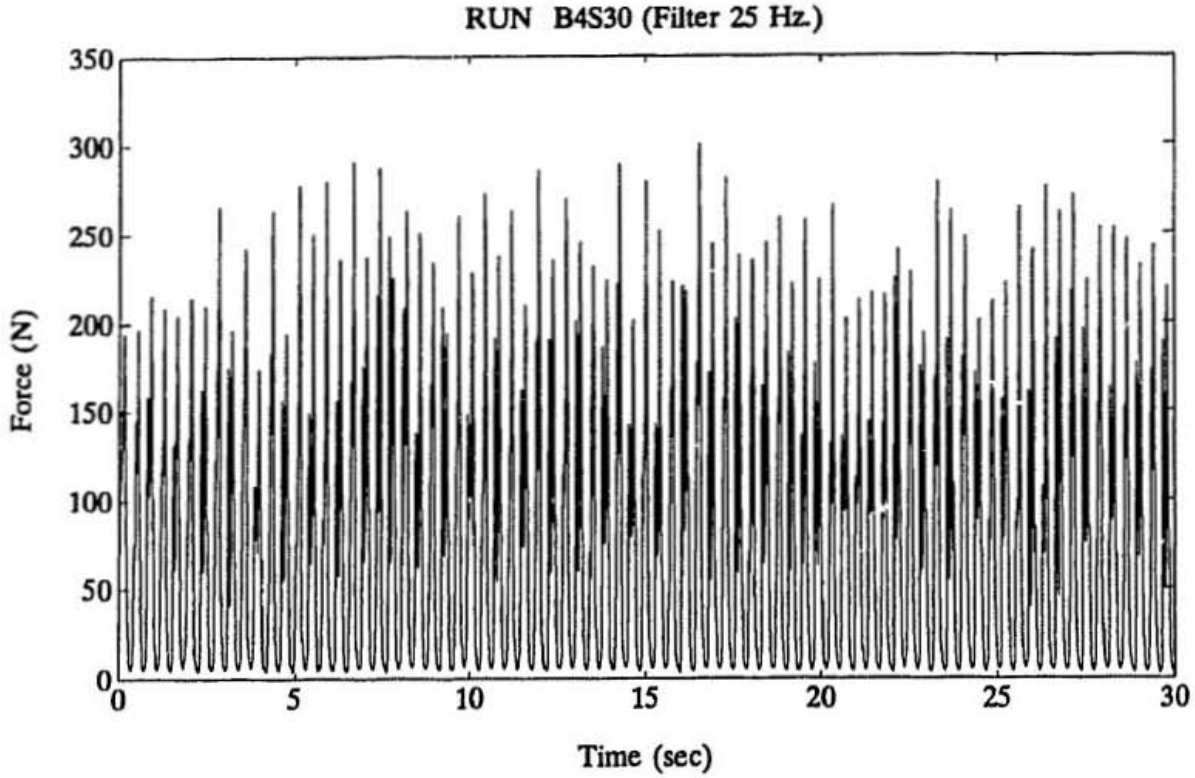
RUN B4S30 (Filter 25 Hz.)
Force (N)
350
300
250
200
150
100
50
0
0
5
10
15
20
25
30
Time (sec)

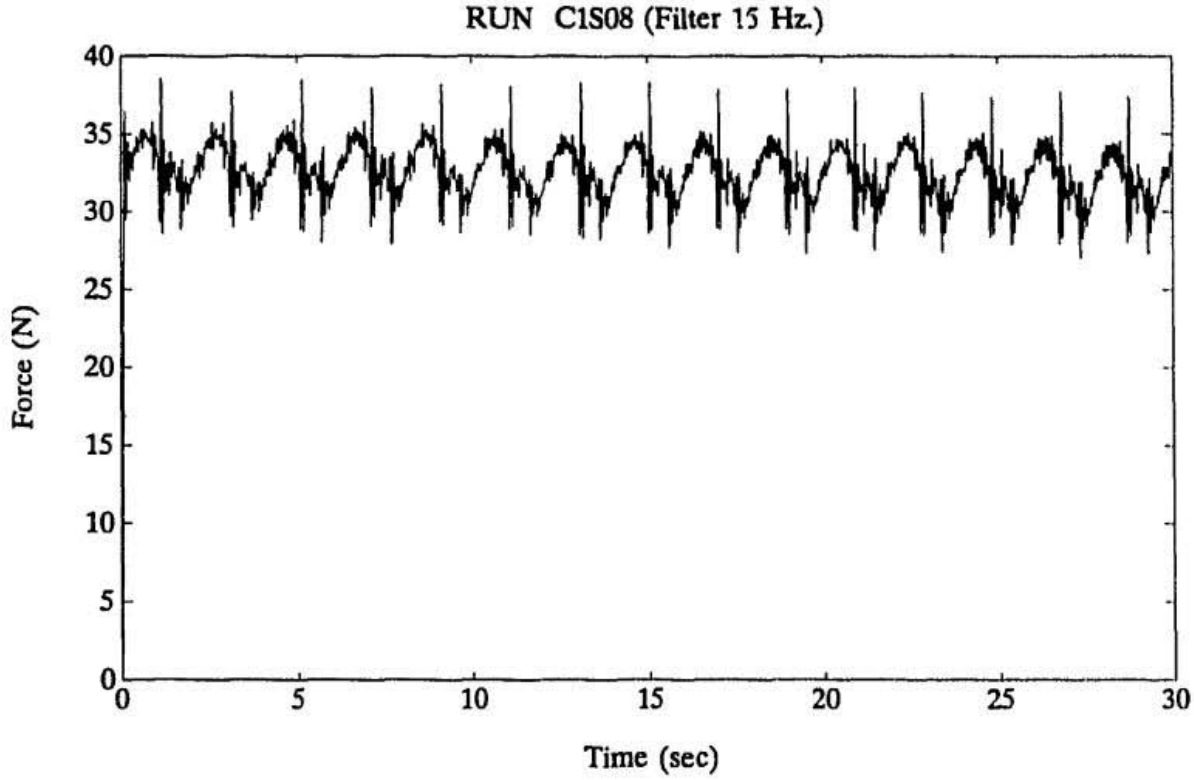
RUN C1S08 (Filter 15 Hz.)
Force (N)
Time (sec)
0
5
10
15
20
25
30
35
40

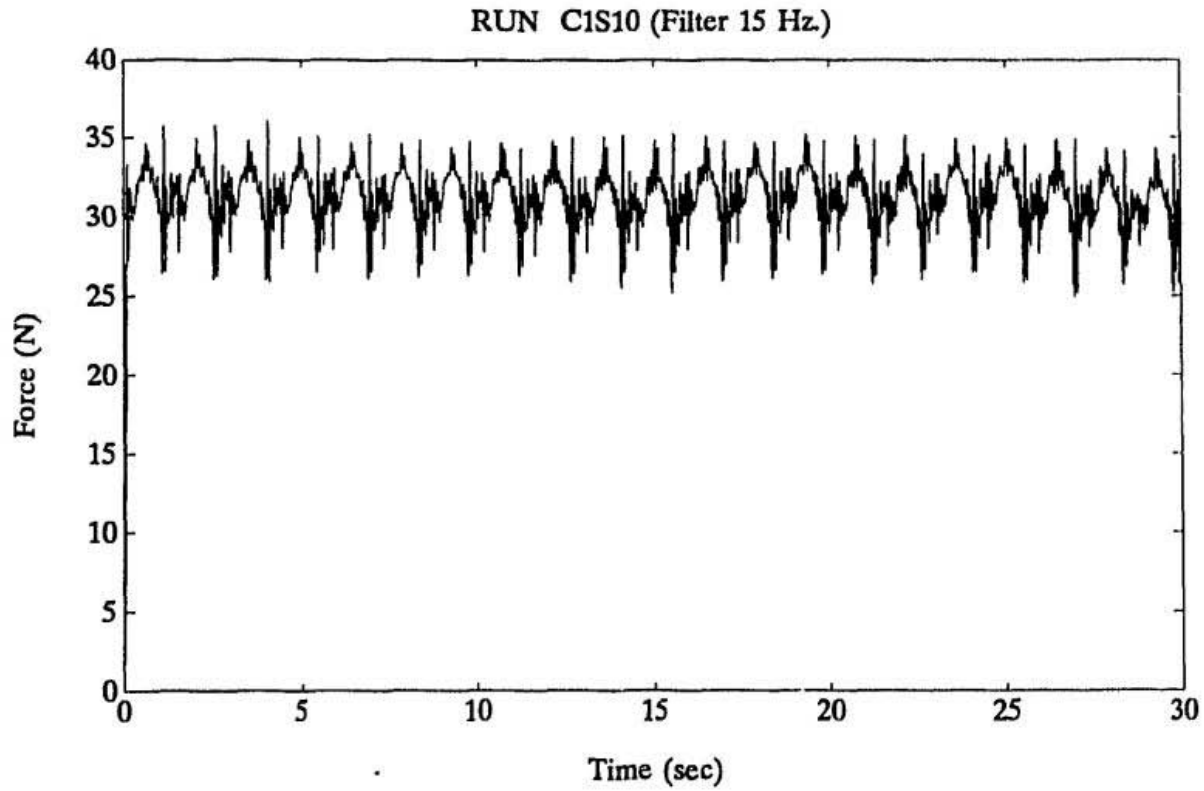
RUN C1S10 (Filter 15 Hz.)
Force (N)
Time (sec)
0
5
10
15
20
25
30
35
40

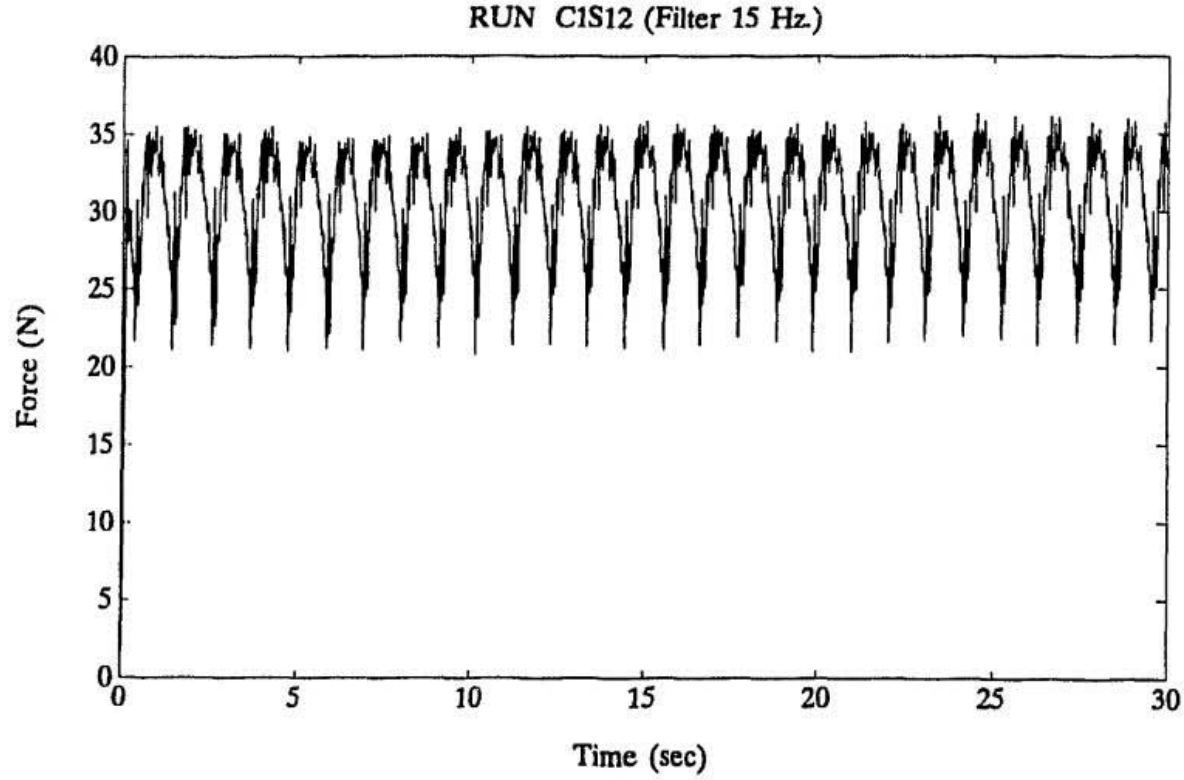
RUN C1S12 (Filter 15 Hz.)
Force (N)
Time (sec)
0
5
10
15
20
25
30
35
40

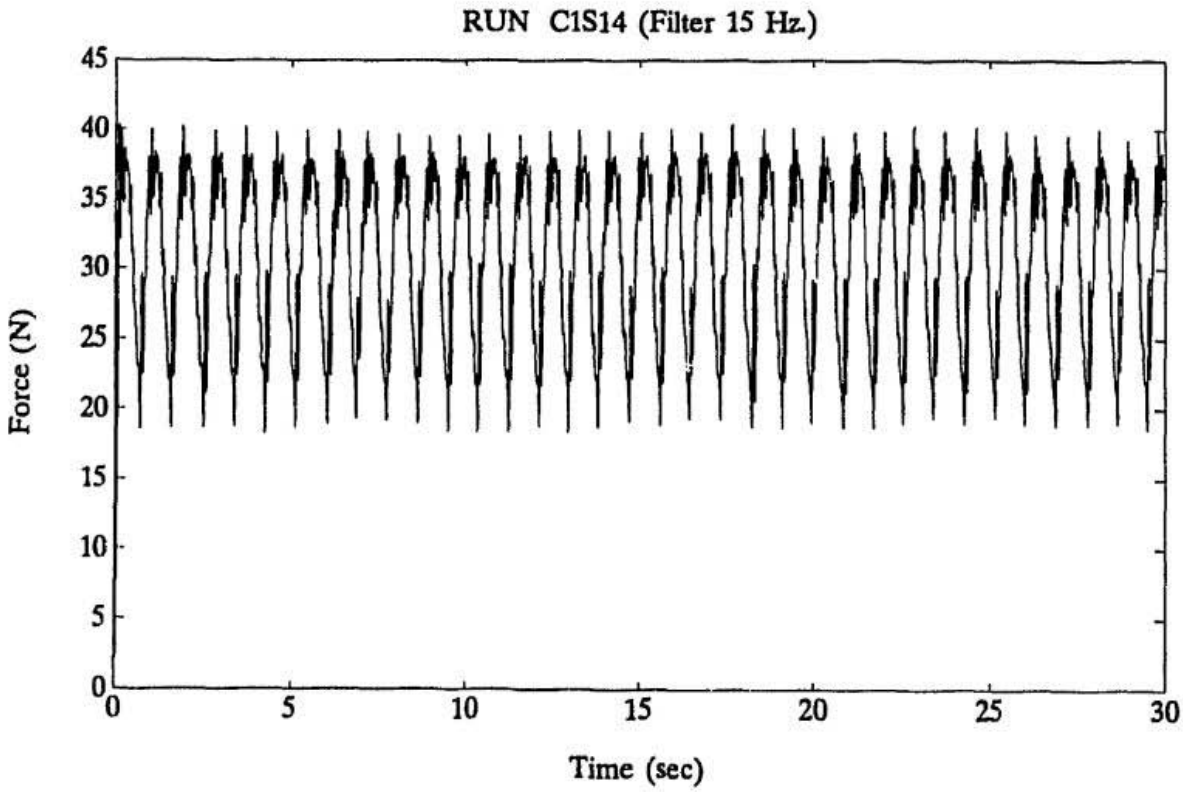
RUN C1S14 (Filter 15 Hz.)
Force (N)
Time (sec)
0
5
10
15
20
25
30
35
40
45

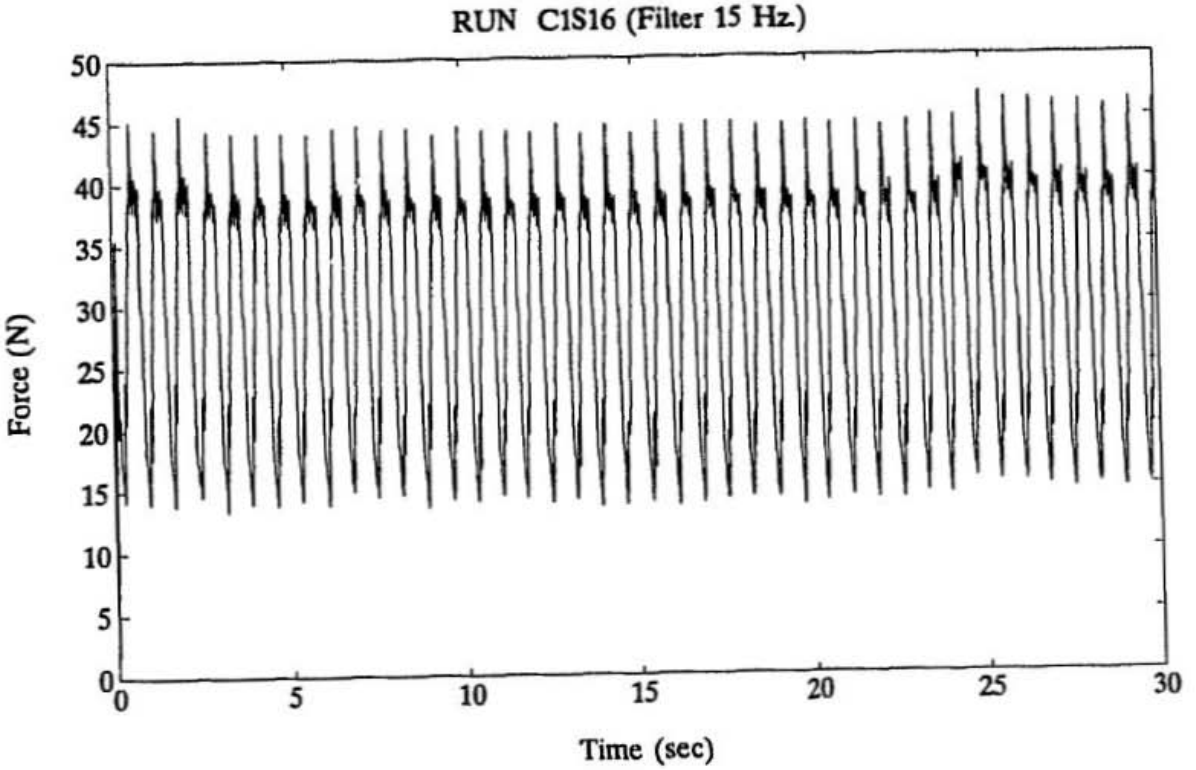
RUN C1S16 (Filter 15 Hz.)
Force (N)
Time (sec)
0
5
10
15
20
25
30
35
40
45
50

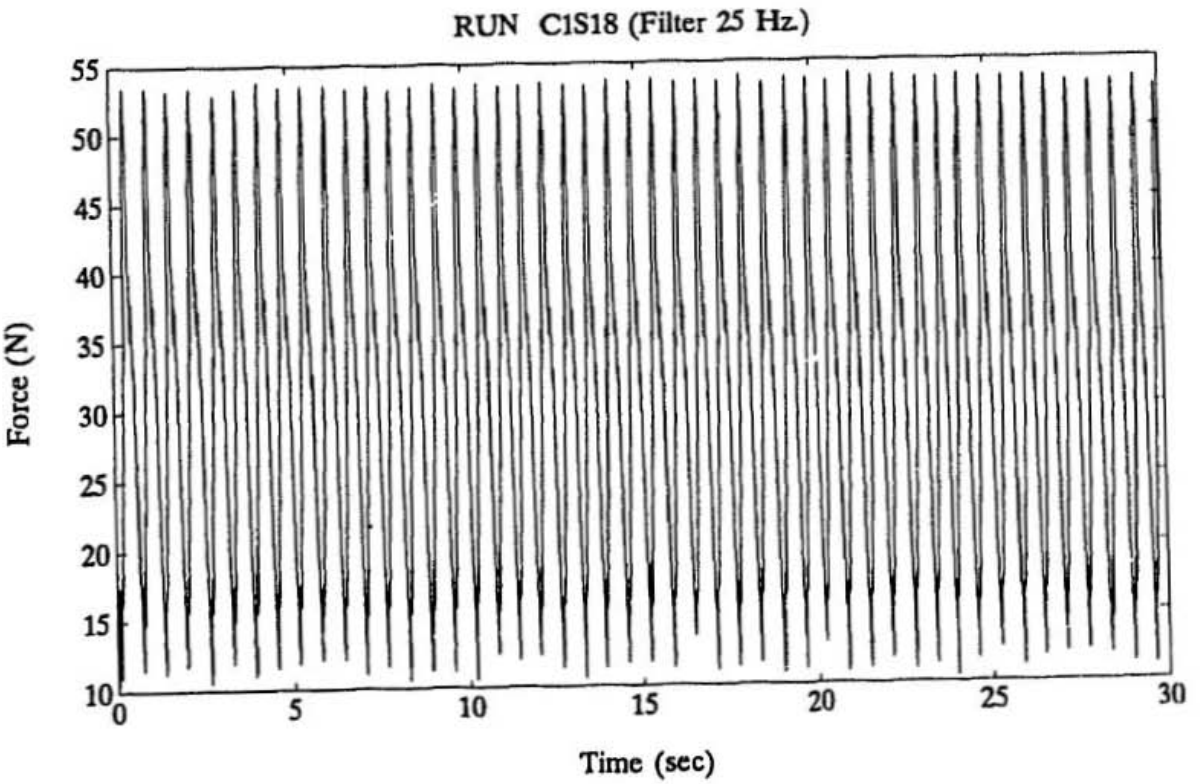
RUN C1S18 (Filter 25 Hz.)
Force (N)
Time (sec)
10
15
20
25
30
35
40
45
50
55

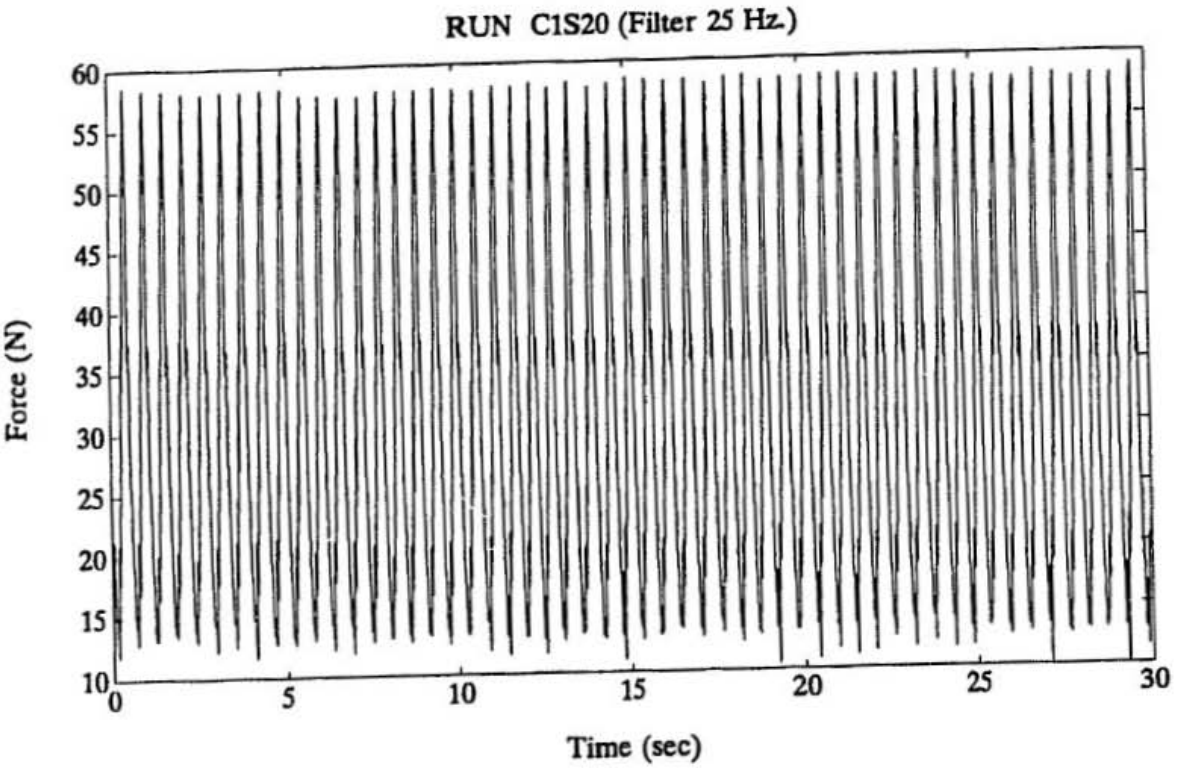
RUN C1S20 (Filter 25 Hz.)
Force (N)
60
55
50
45
40
35
30
25
20
15
10
0
5
10
15
20
25
30
Time (sec)

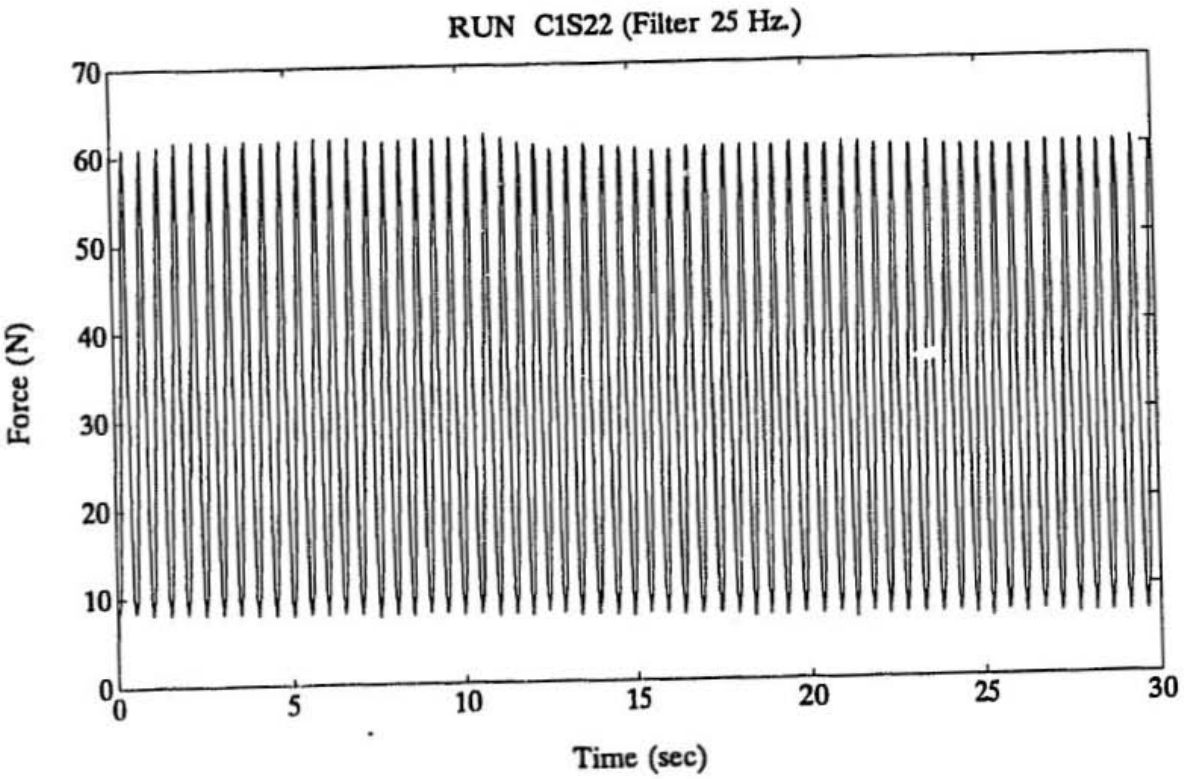
RUN C1S22 (Filter 25 Hz.)
Force (N)
70
60
50
40
30
20
10
0
0
5
10
15
20
25
30
Time (sec)

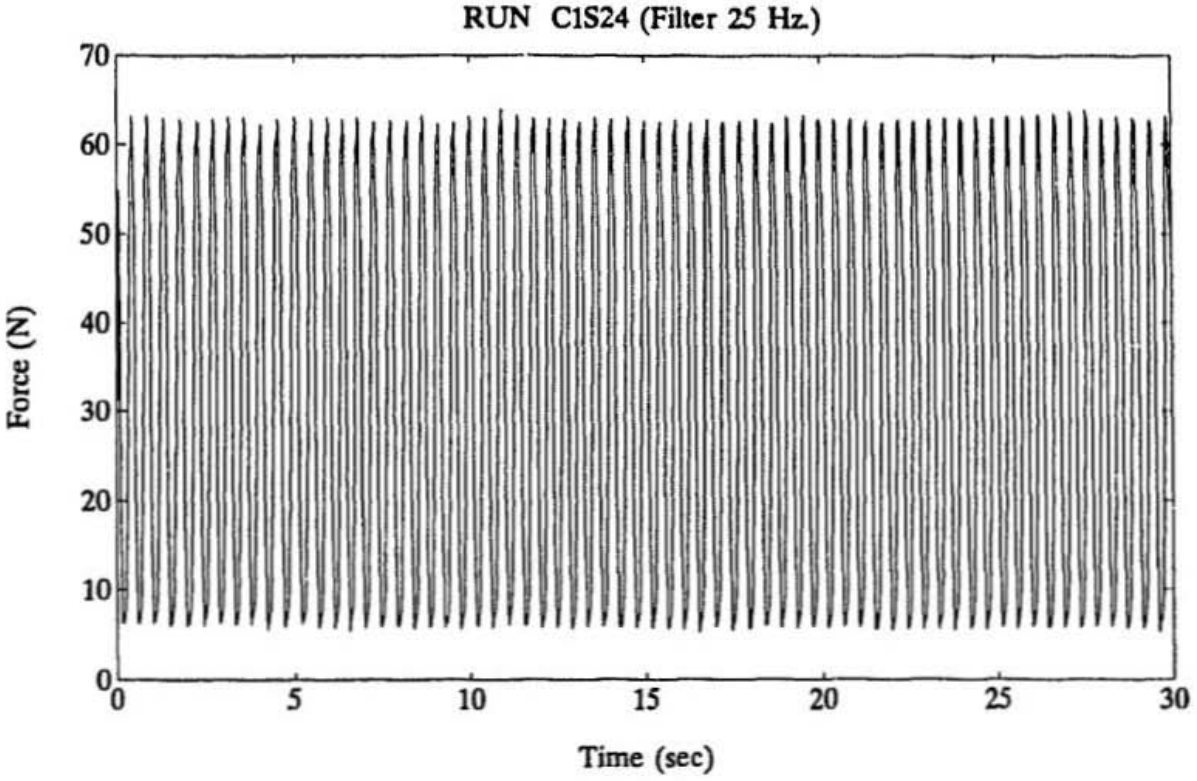
RUN C1S24 (Filter 25 Hz.)
Force (N)
Time (sec)
0
10
20
30
40
50
60
70
0
5
10
15
20
25
30

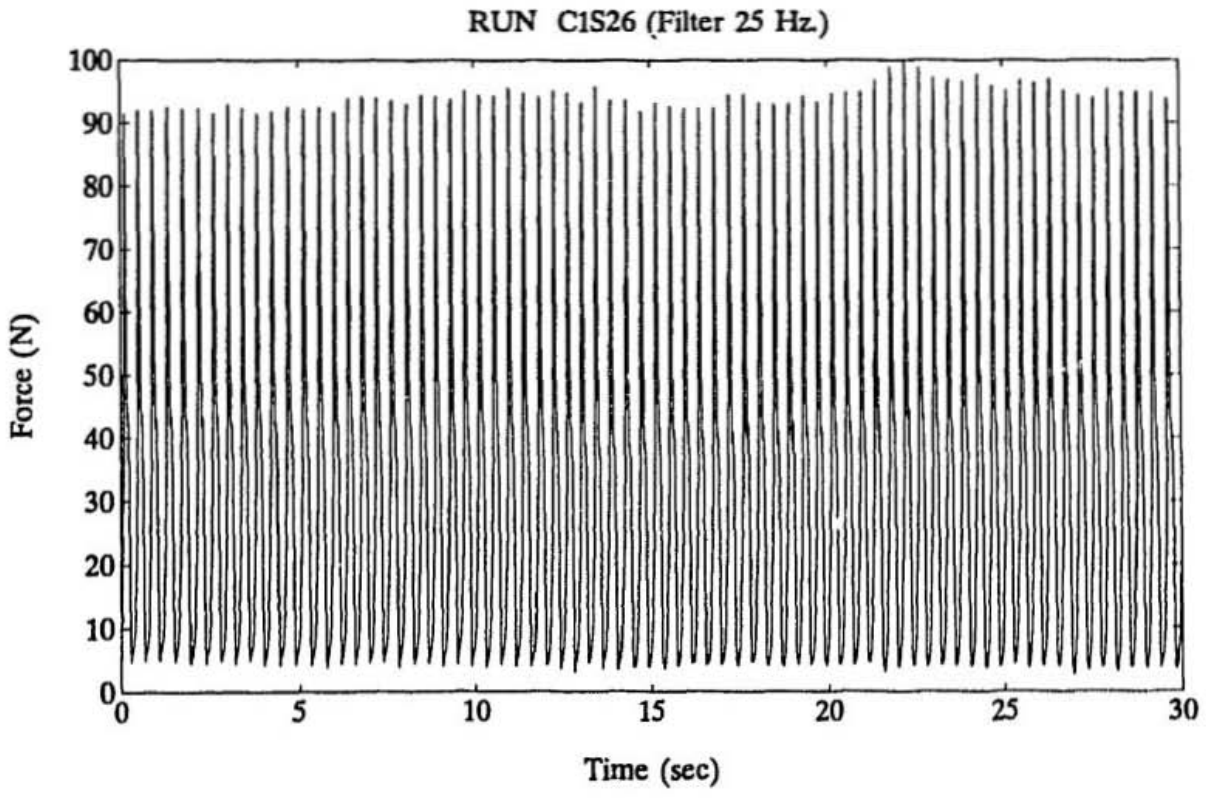
RUN C1S26 (Filter 25 Hz.)
Force (N)
Time (sec)
0
10
20
30
40
50
60
70
80
90
100
0
5
10
15
20
25
30

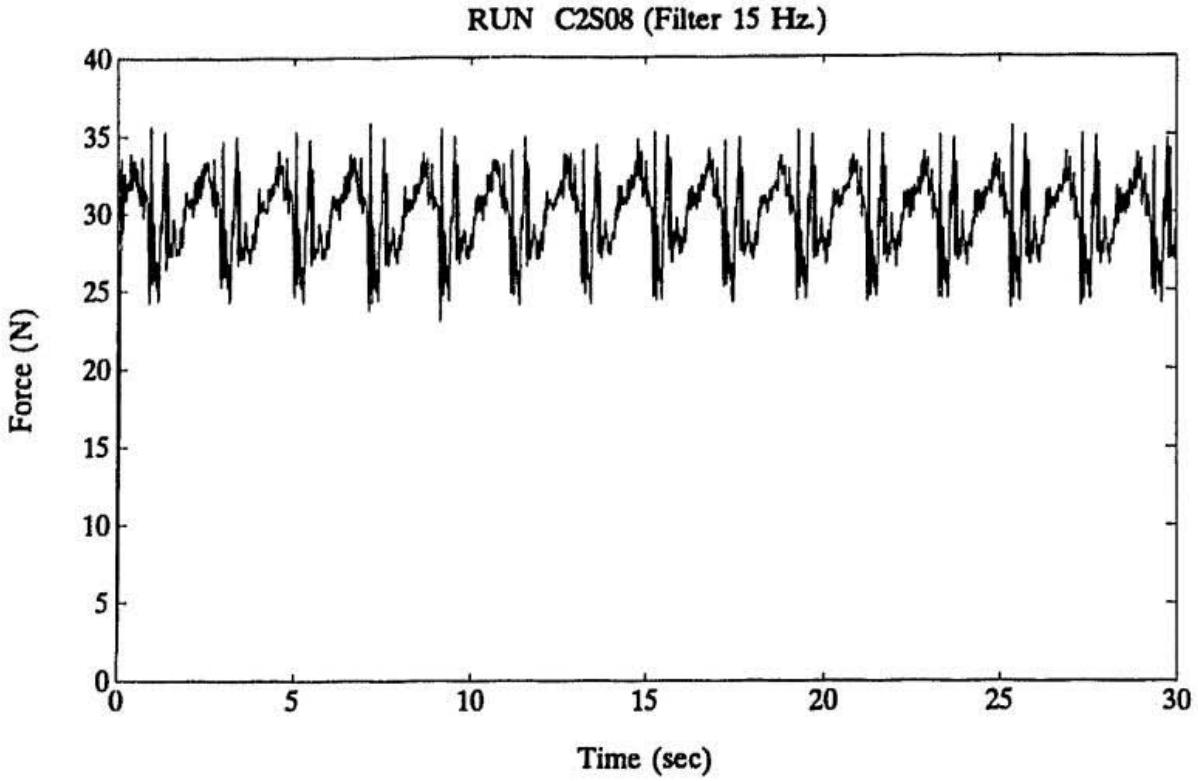
RUN C2S08 (Filter 15 Hz.)
Force (N)
Time (sec)
0
5
10
15
20
25
30
35
40

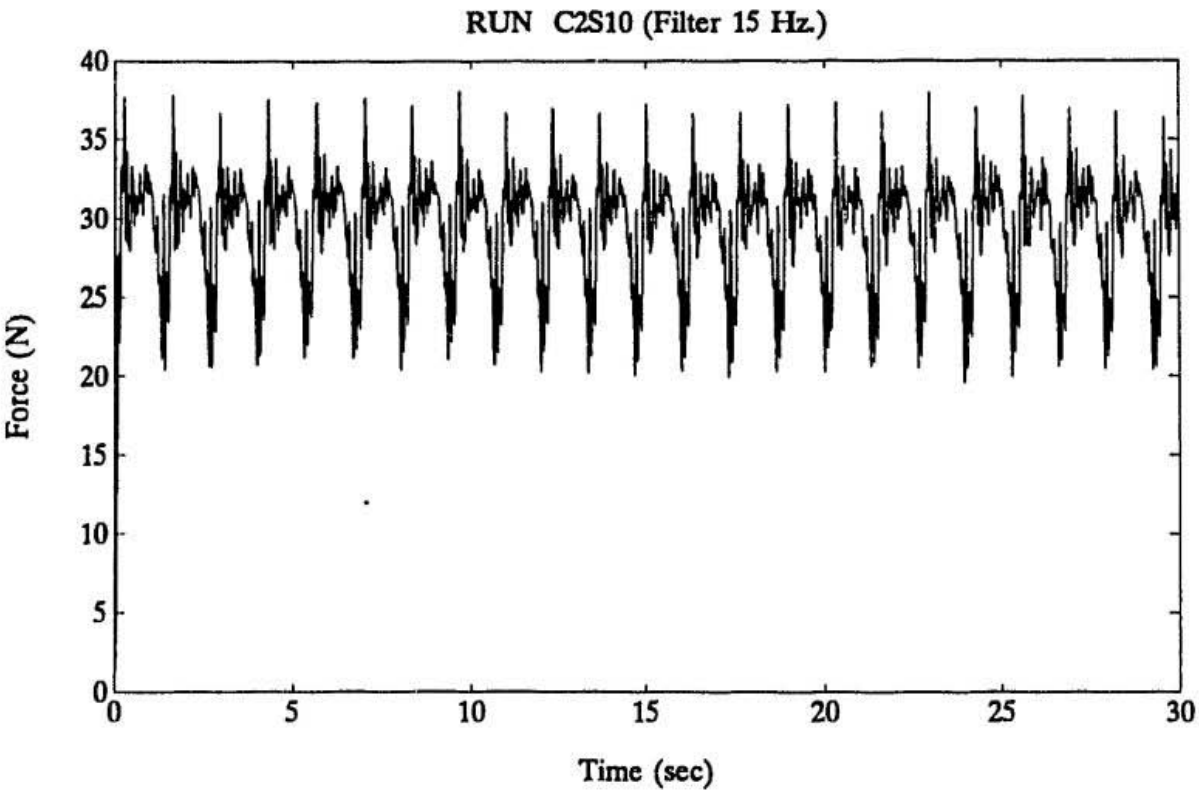
RUN C2S10 (Filter 15 Hz.)
Force (N)
Time (sec)
0
5
10
15
20
25
30
35
40

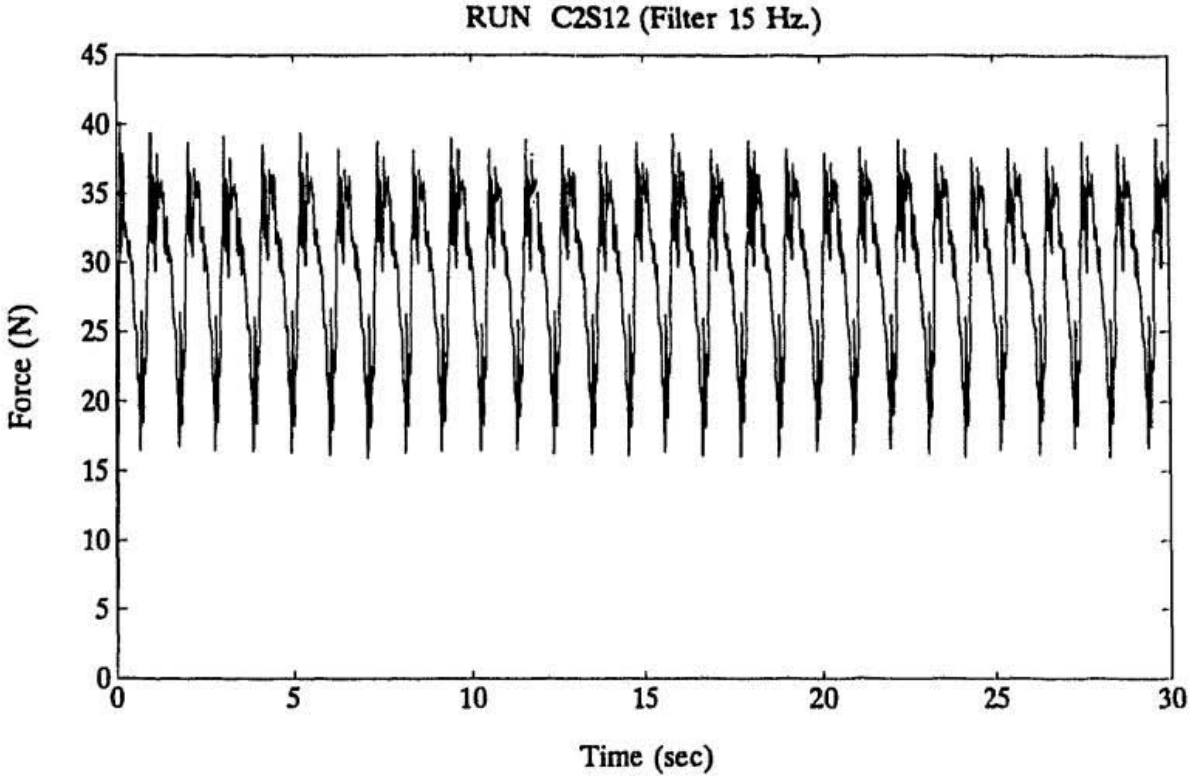
RUN C2S12 (Filter 15 Hz.)
Force (N)
Time (sec)
0
5
10
15
20
25
30
35
40
45

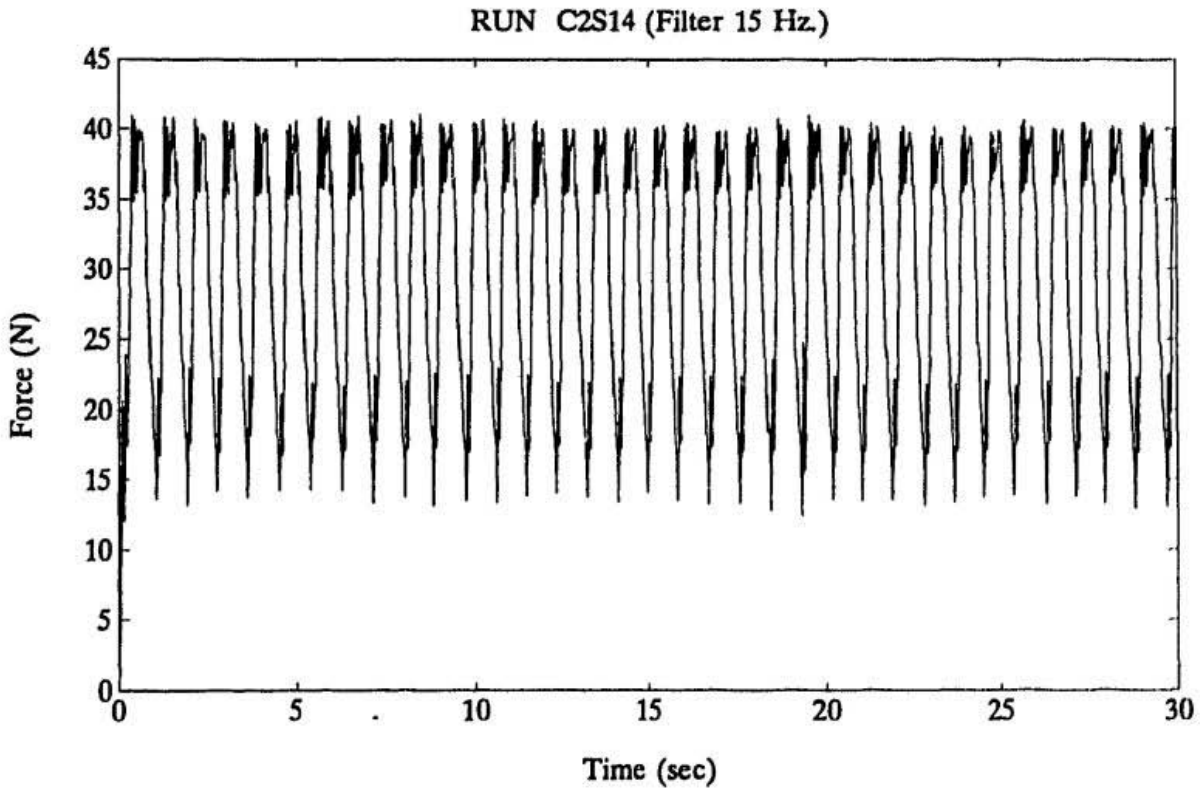
RUN C2S14 (Filter 15 Hz.)
Force (N)
Time (sec)
0
5
10
15
20
25
30
35
40
45

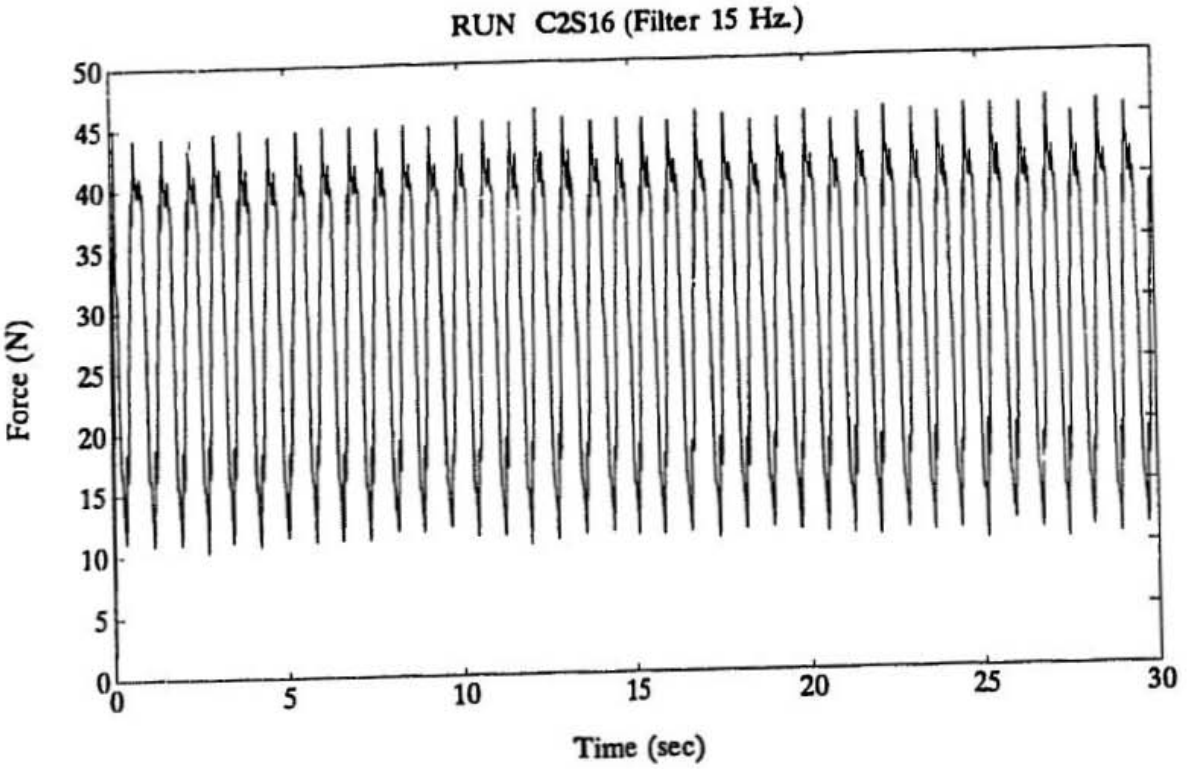
RUN C2S16 (Filter 15 Hz.)
Force (N)
Time (sec)
0
5
10
15
20
25
30
35
40
45
50

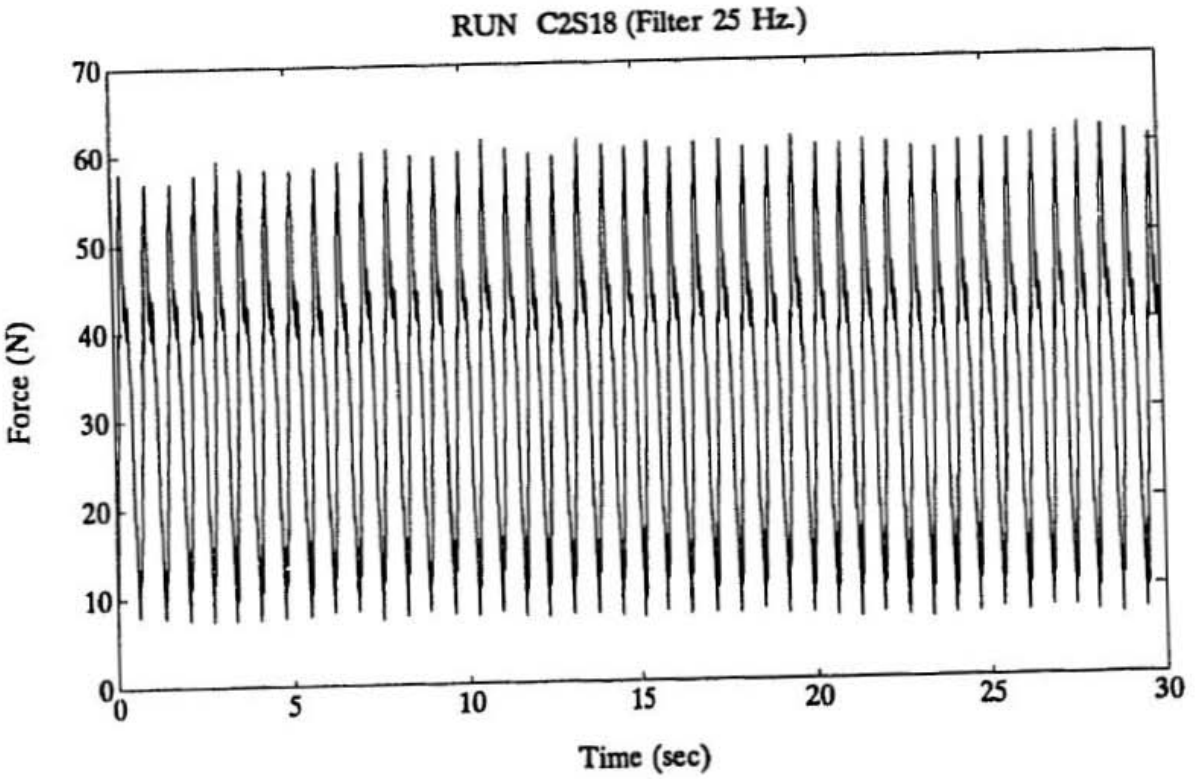
RUN C2S18 (Filter 25 Hz.)
Force (N)
Time (sec)
0
10
20
30
40
50
60
70

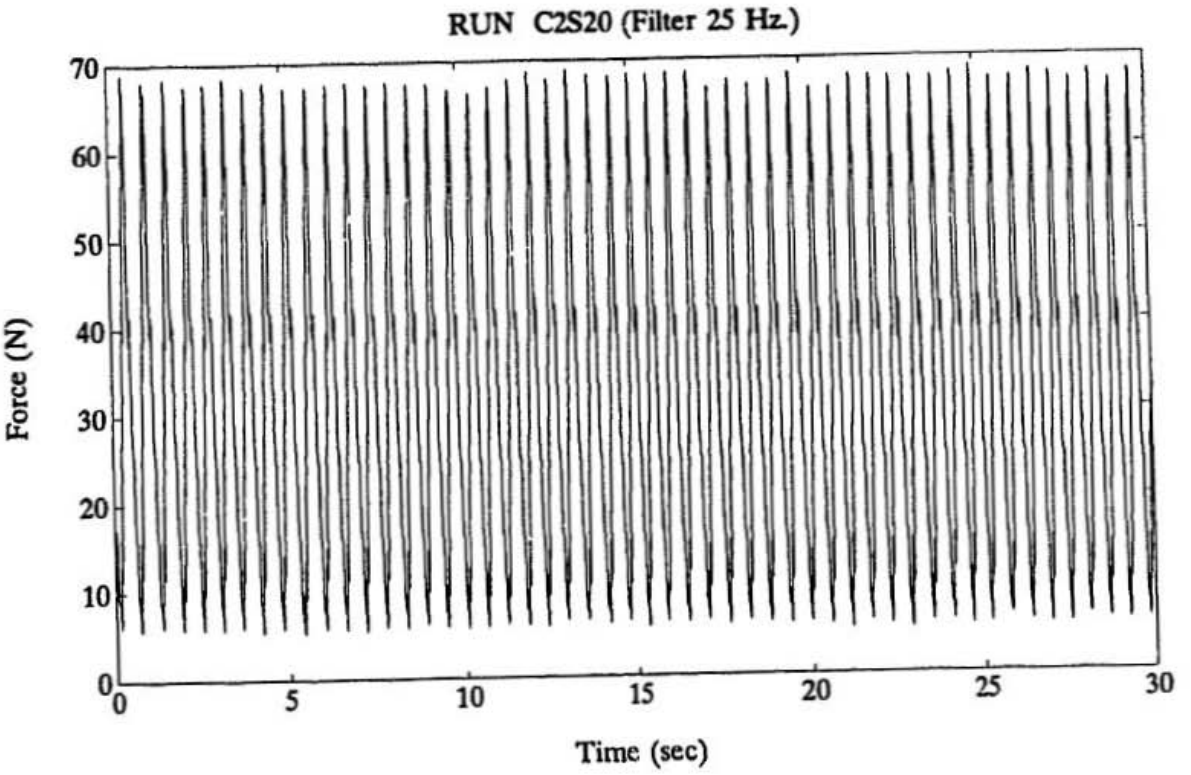
RUN C2S20 (Filter 25 Hz.)
Force (N)
Time (sec)
0
10
20
30
40
50
60
70
0
5
10
15
20
25
30

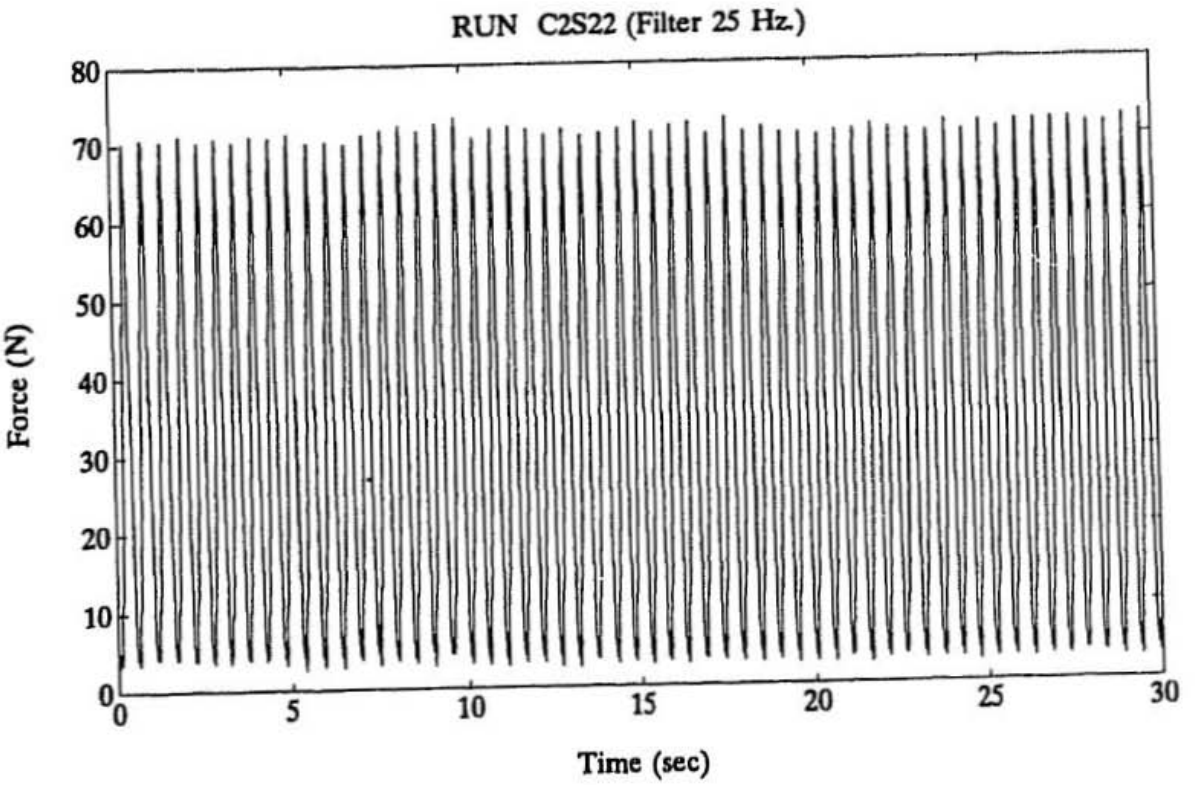
RUN C2S22 (Filter 25 Hz.)
Force (N)
Time (sec)
0
10
20
30
40
50
60
70
80
0
5
10
15
20
25
30

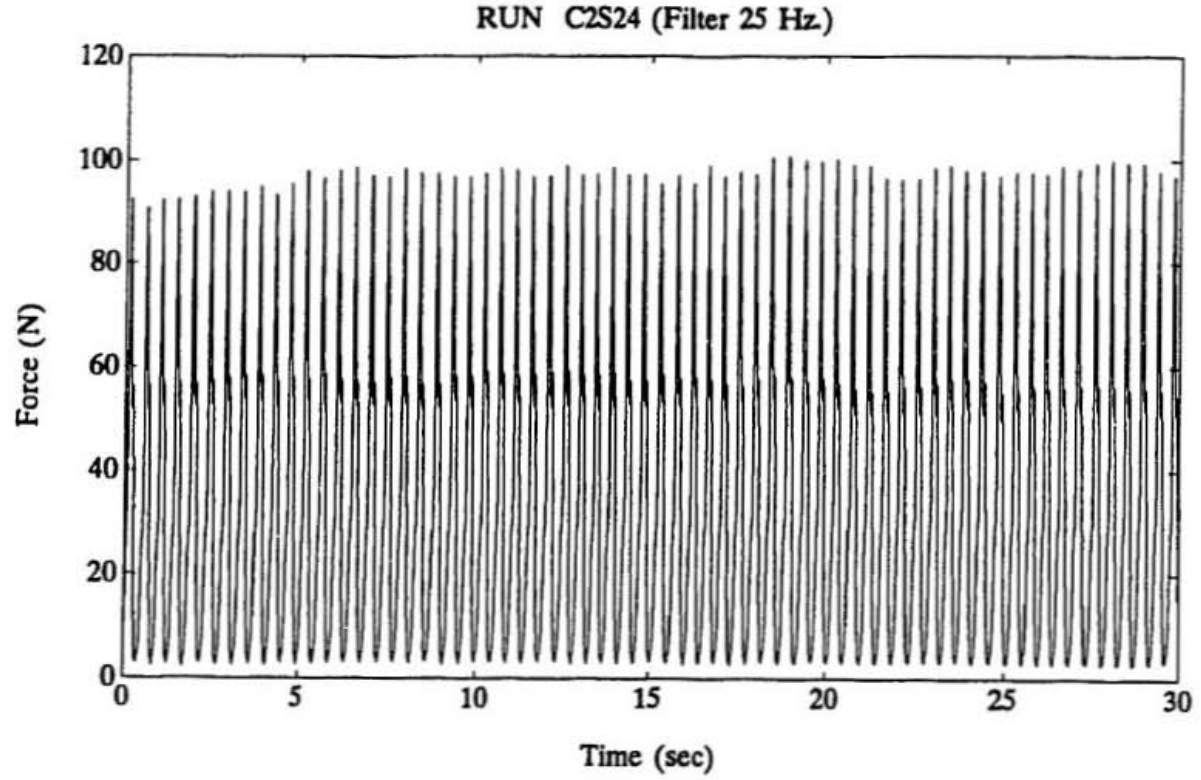
RUN C2S24 (Filter 25 Hz.)
Force (N)
Time (sec)
0
20
40
60
80
100
120
0
5
10
15
20
25
30

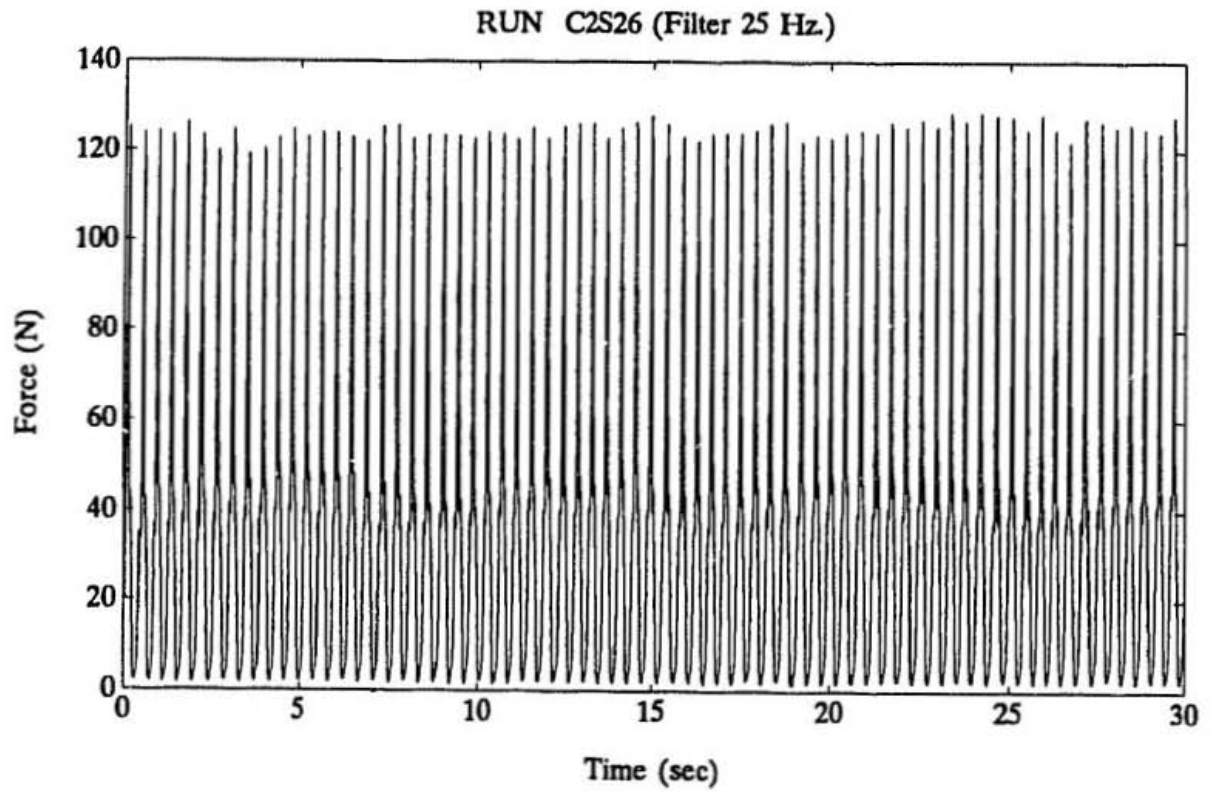
RUN C2S26 (Filter 25 Hz.)
Force (N)
Time (sec)
0
20
40
60
80
100
120
140
0
5
10
15
20
25
30

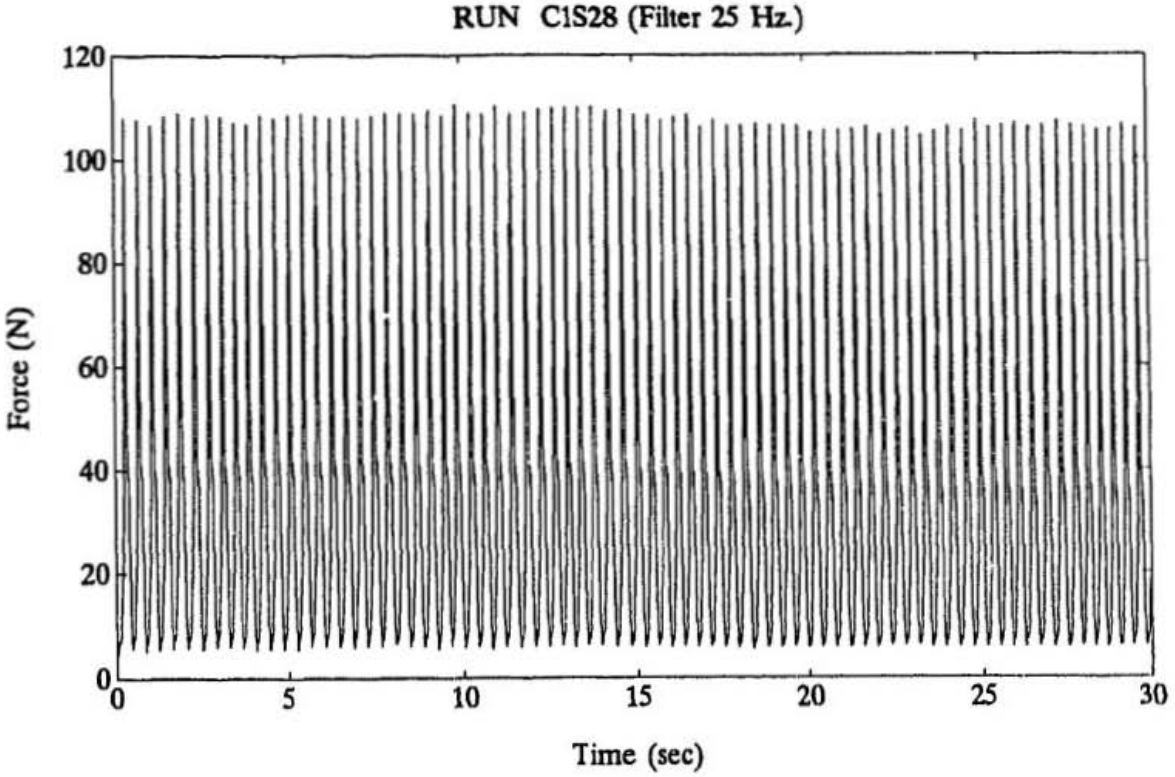
RUN C1S28 (Filter 25 Hz.)
Force (N)
Time (sec)
0
20
40
60
80
100
120
0
5
10
15
20
25
30

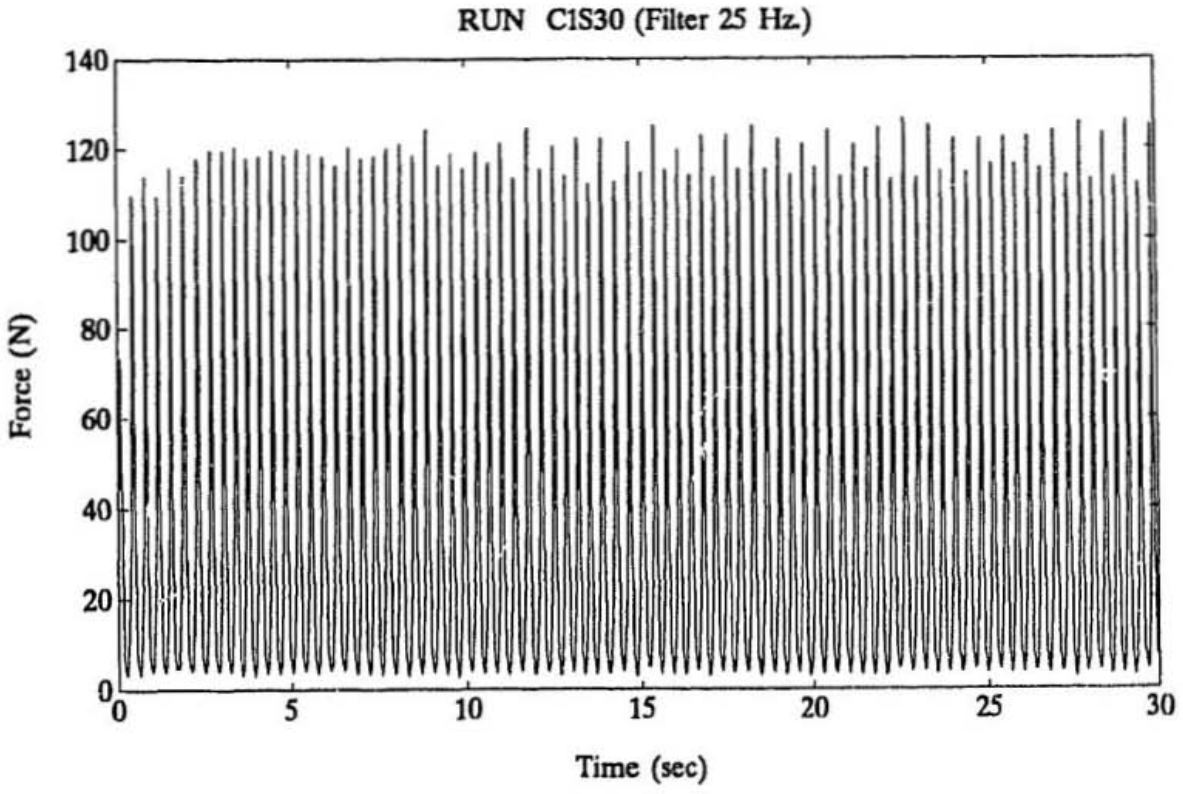
RUN C1S30 (Filter 25 Hz.)
Force (N)
Time (sec)
0
20
40
60
80
100
120
140
0
5
10
15
20
25
30

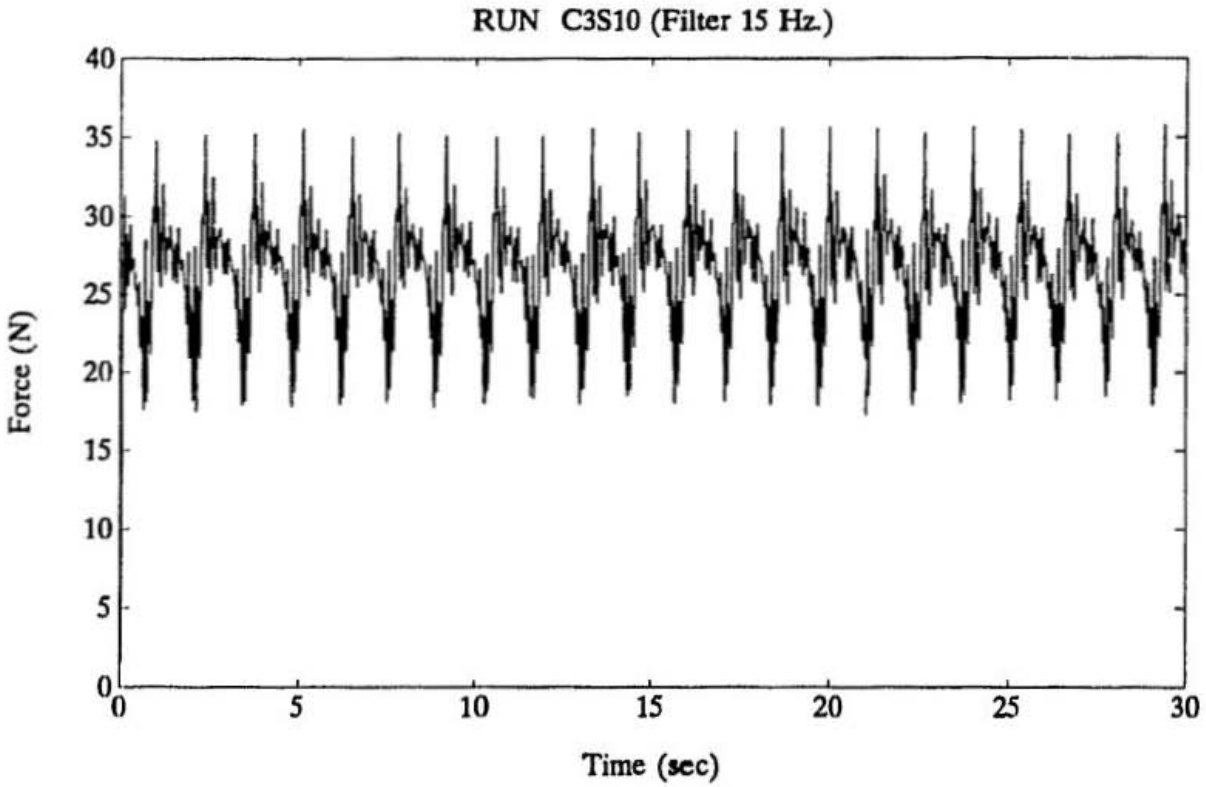
RUN C3S10 (Filter 15 Hz.)
Force (N)
Time (sec)
0
5
10
15
20
25
30
35
40

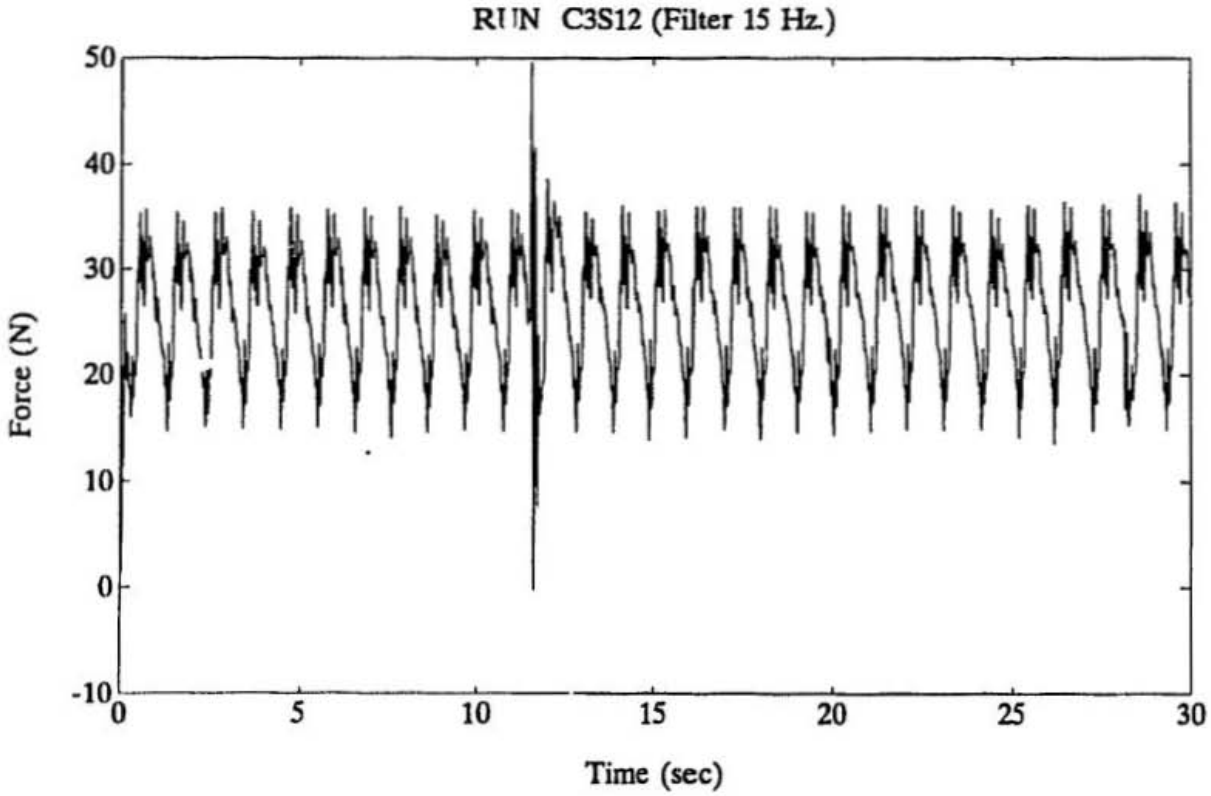
RUN C3S12 (Filter 15 Hz.)
Force (N)
Time (sec)
-10
0
10
20
30
40
50
5
15
25

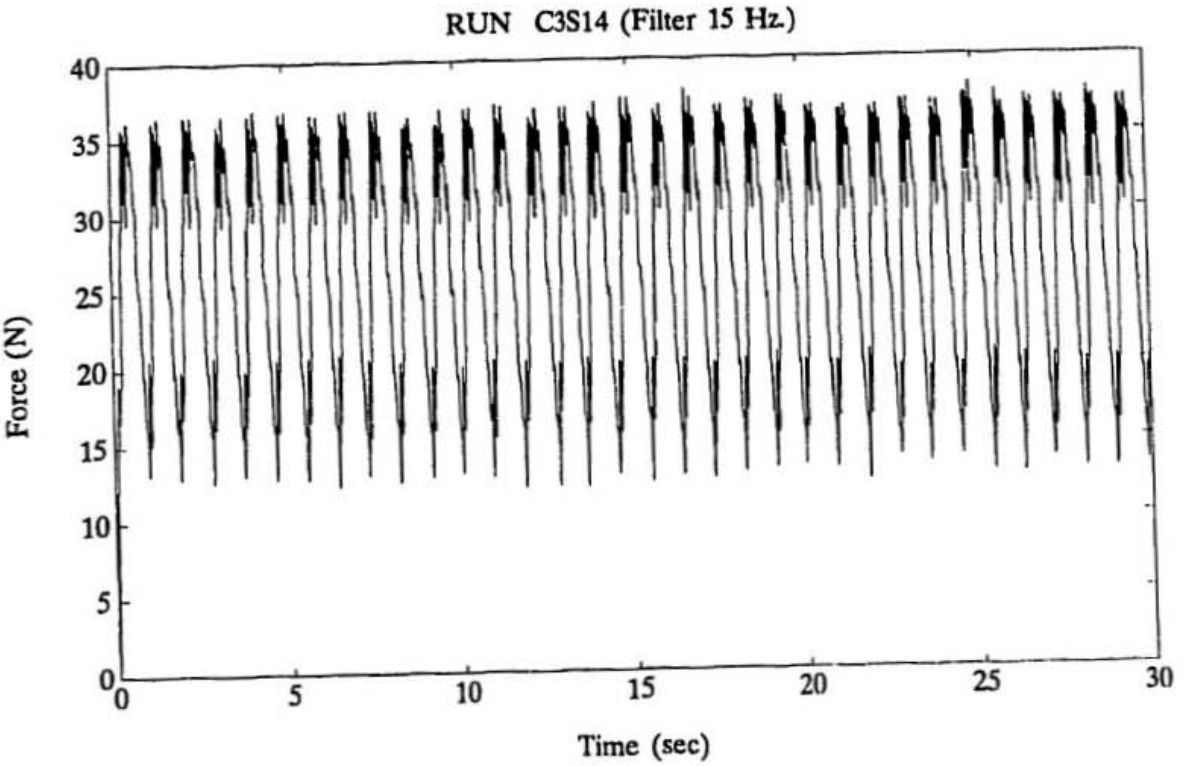
RUN C3S14 (Filter 15 Hz.)
Force (N)
Time (sec)
0
5
10
15
20
25
30
35
40

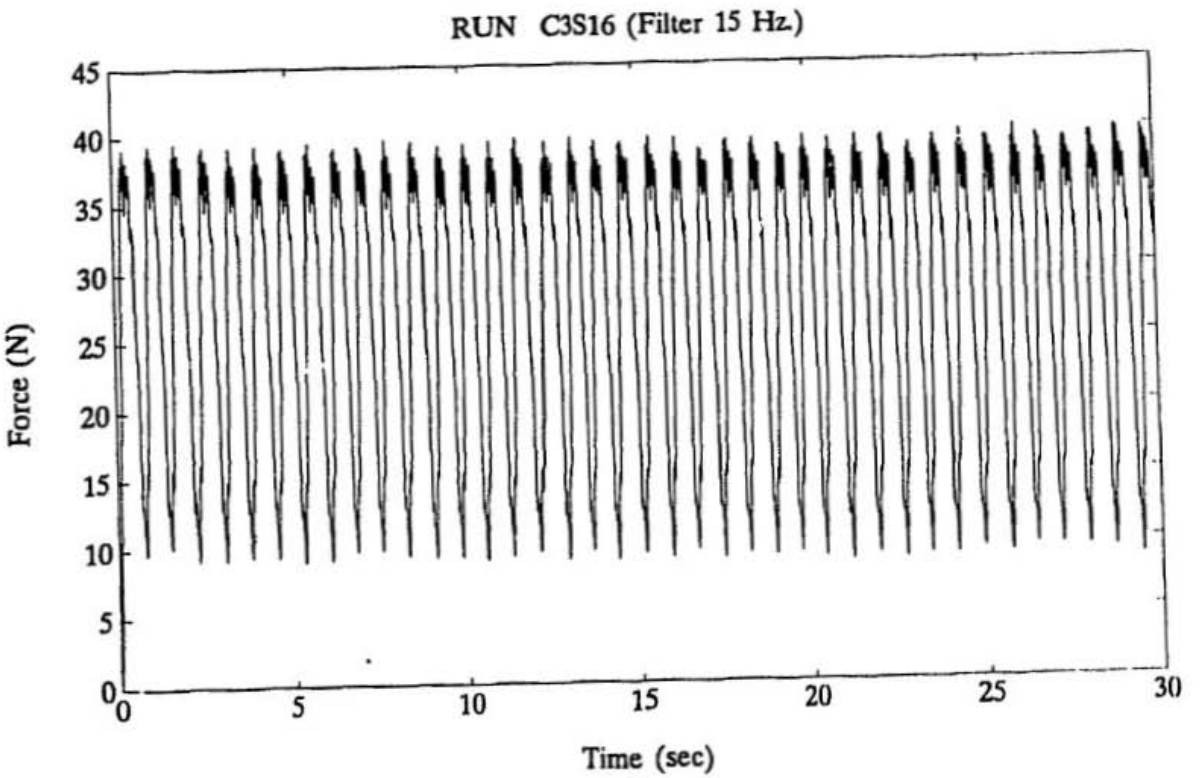
RUN C3S16 (Filter 15 Hz.)
Force (N)
Time (sec)
0
5
10
15
20
25
30
35
40
45

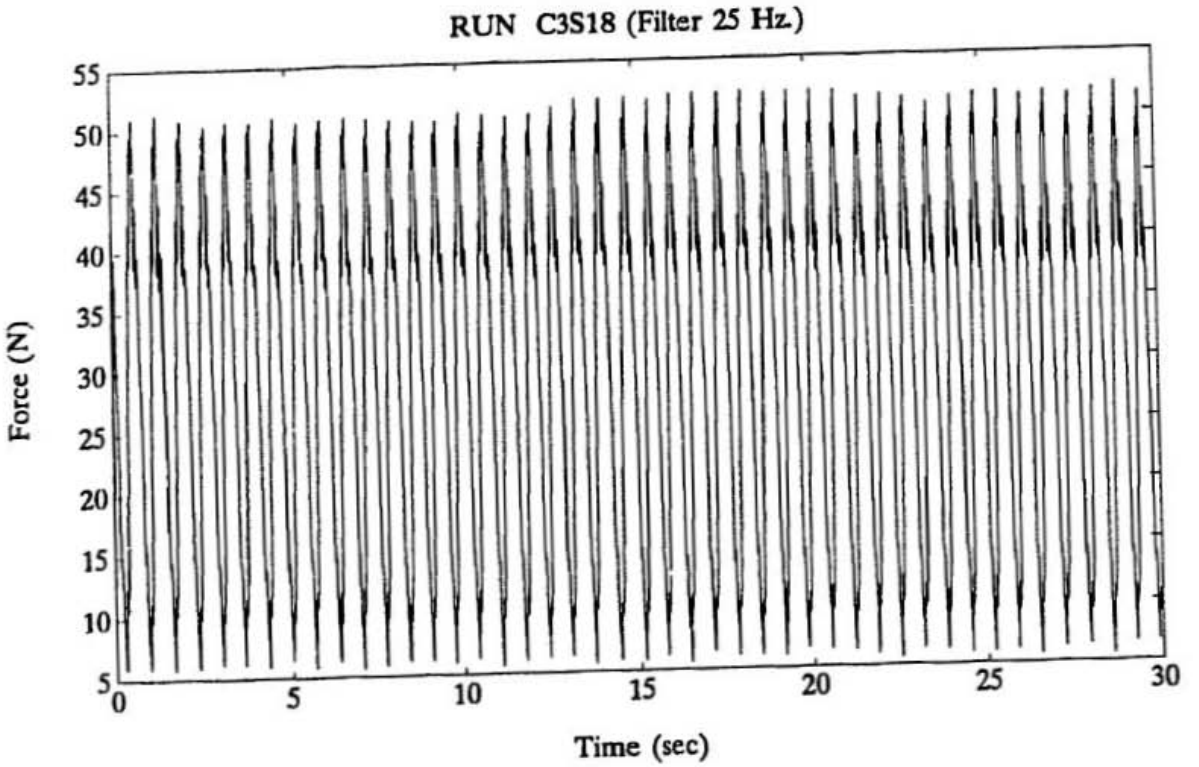
RUN C3S18 (Filter 25 Hz.)
Force (N)
Time (sec)
55
50
45
40
35
30
25
20
15
10
5
0
5
10
15
20
25
30

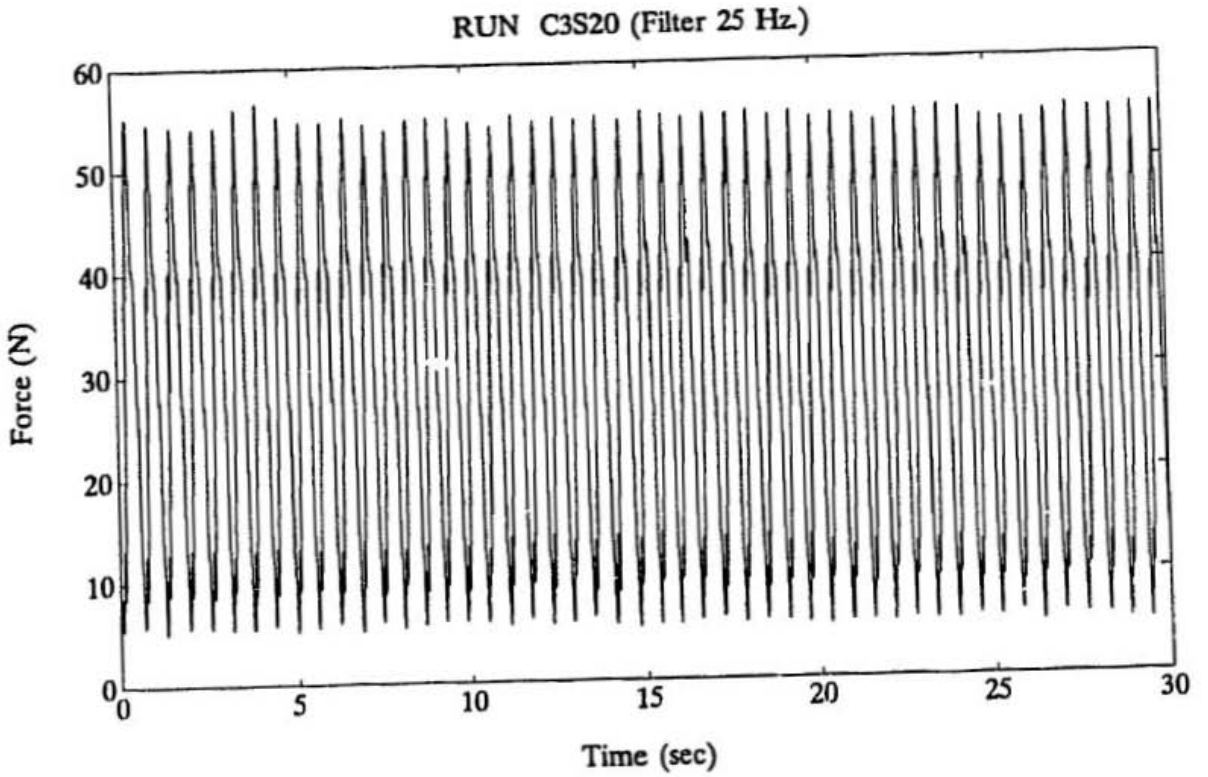
RUN C3S20 (Filter 25 Hz.)
Force (N)
Time (sec)
60
50
40
30
20
10
0
0
5
10
15
20
25
30

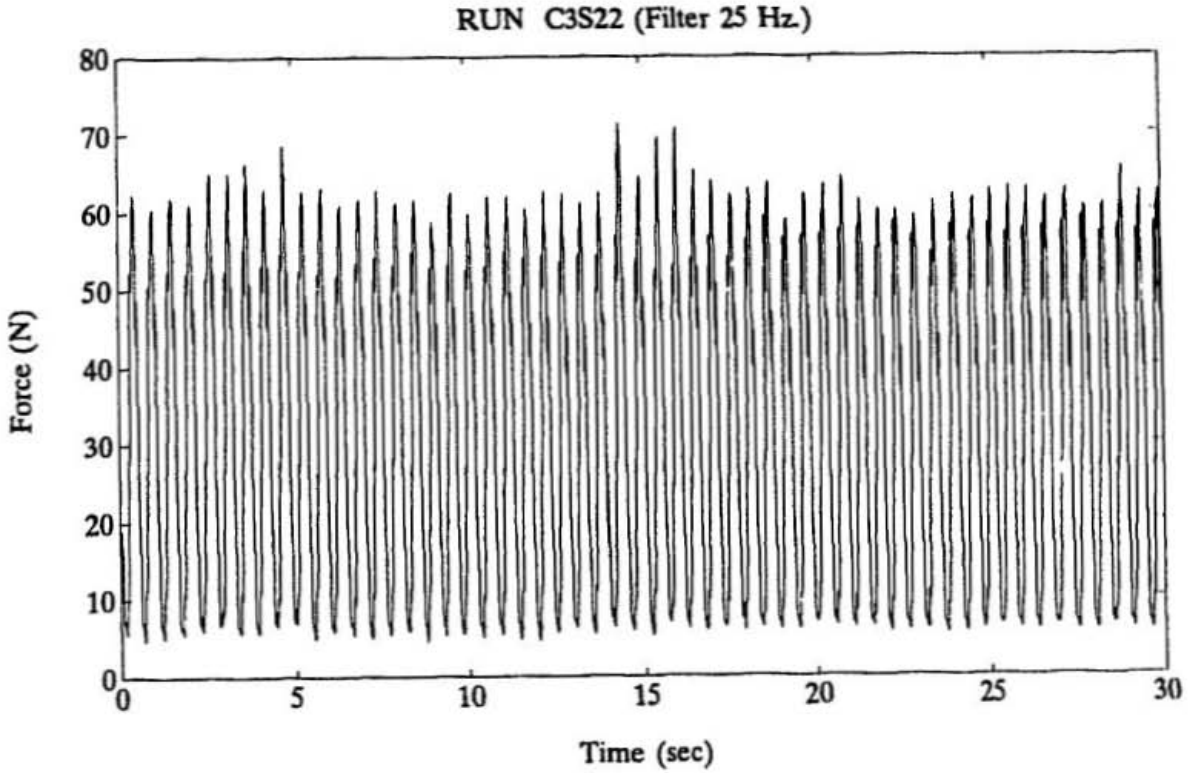
RUN C3S22 (Filter 25 Hz.)
Force (N)
Time (sec)
0
10
20
30
40
50
60
70
80
0
5
10
15
20
25
30

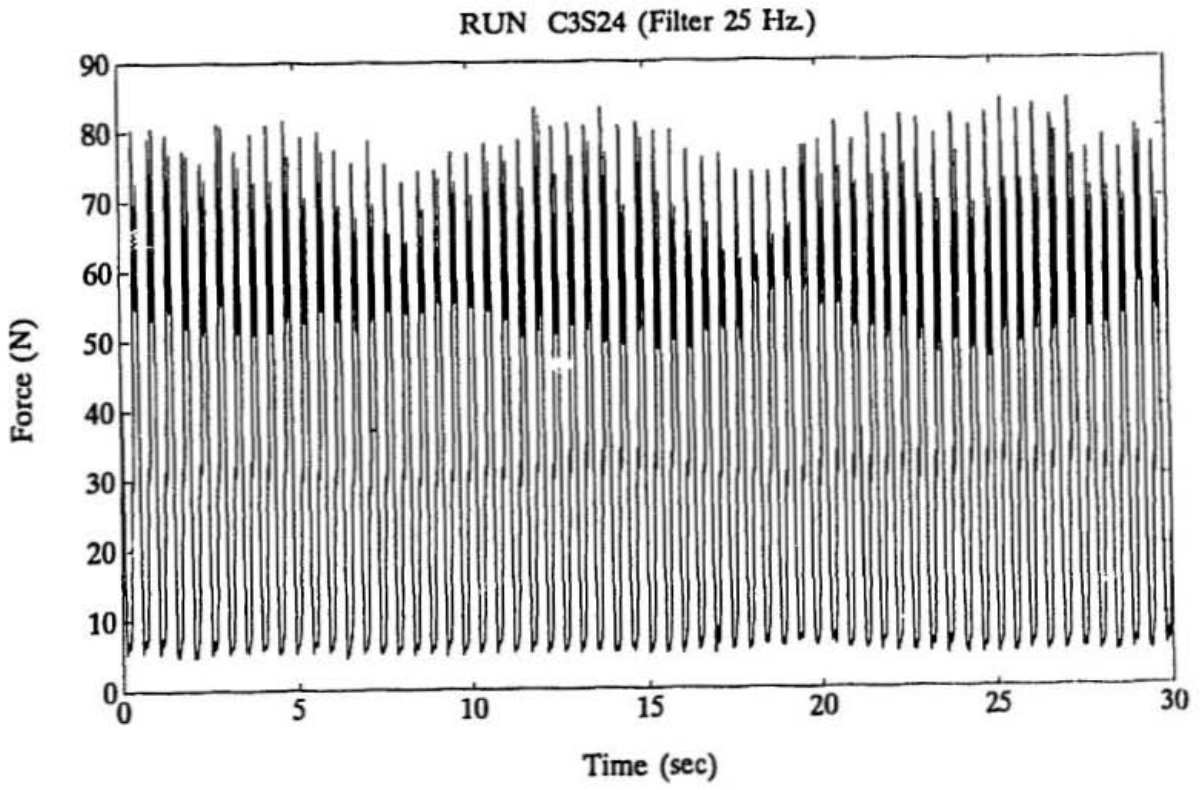
RUN C3S24 (Filter 25 Hz.)
Force (N)
Time (sec)
0
10
20
30
40
50
60
70
80
90
0
5
10
15
20
25
30

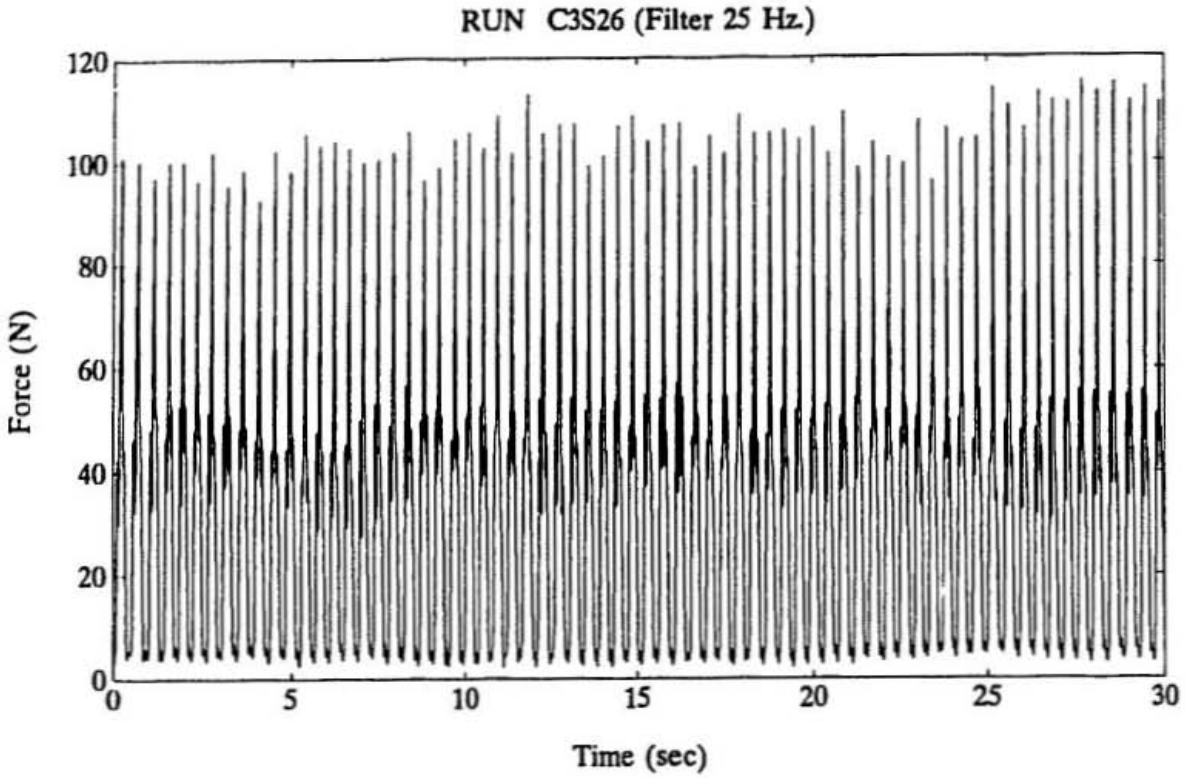
RUN C3S26 (Filter 25 Hz.)
Force (N)
Time (sec)
0
20
40
60
80
100
120
0
5
10
15
20
25
30

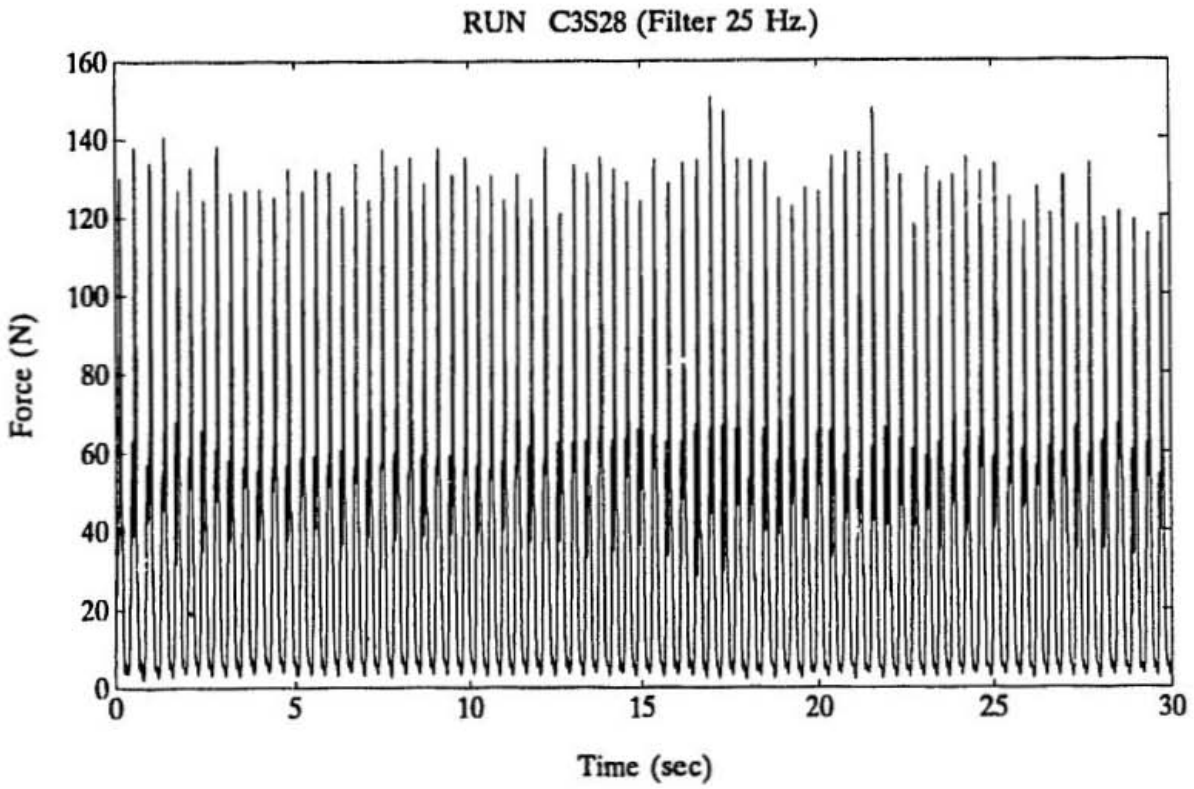
RUN C3S28 (Filter 25 Hz.)
Force (N)
Time (sec)
0
20
40
60
80
100
120
140
160
0
5
10
15
20
25
30

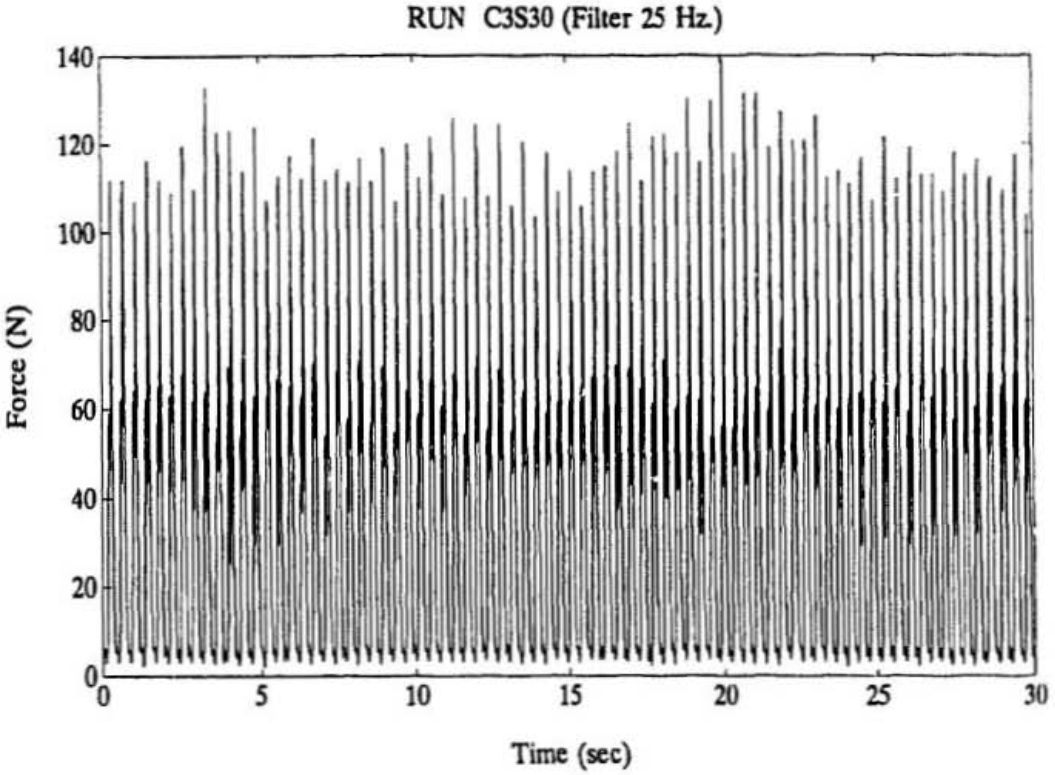
RUN C3S30 (Filter 25 Hz.)
Force (N)
Time (sec)
0
20
40
60
80
100
120
140
0
5
10
15
20
25
30

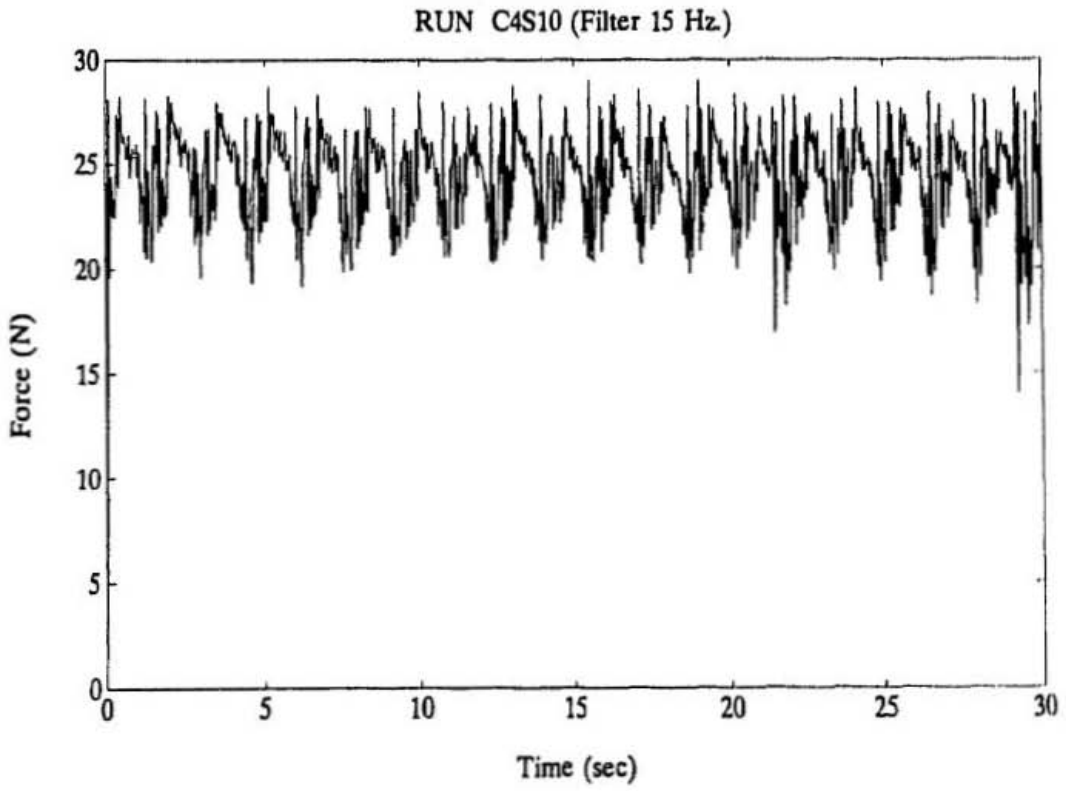
RUN C4S10 (Filter 15 Hz.)
Force (N)
Time (sec)
0
5
10
15
20
25
30
0
5
10
15
20
25
30

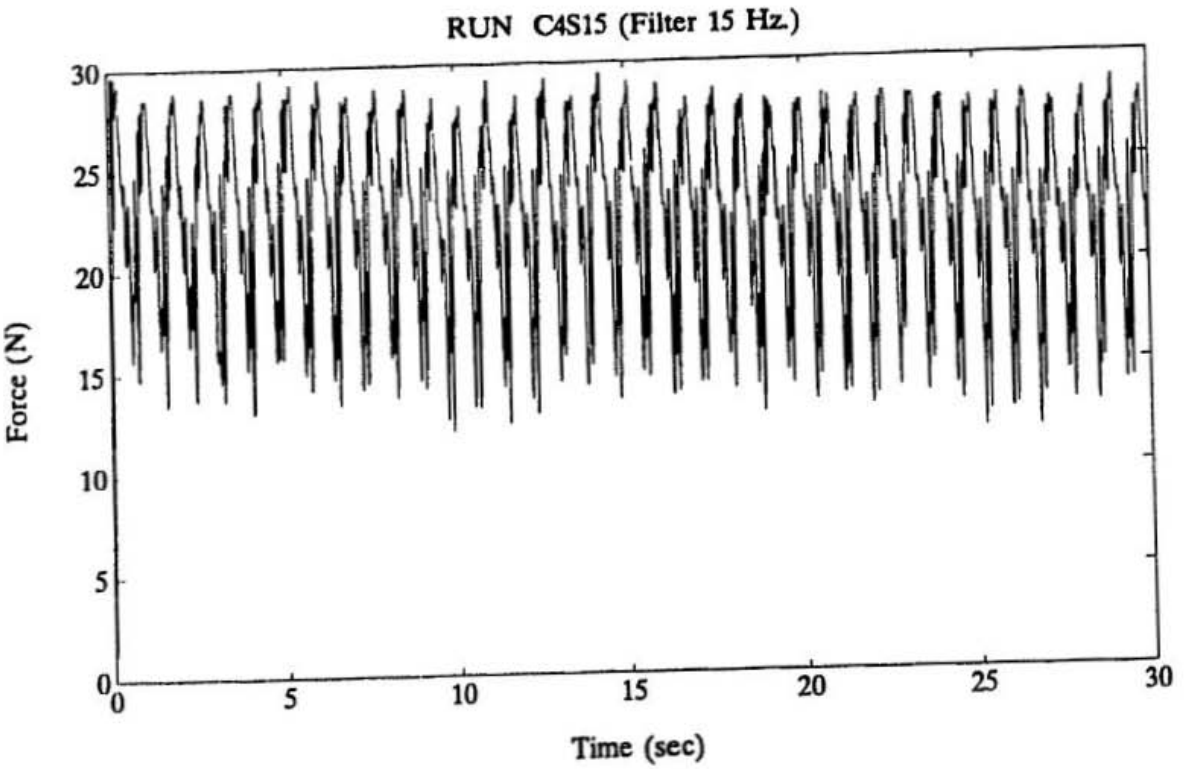
RUN C4S15 (Filter 15 Hz.)
Force (N)
Time (sec)
0
5
10
15
20
25
30

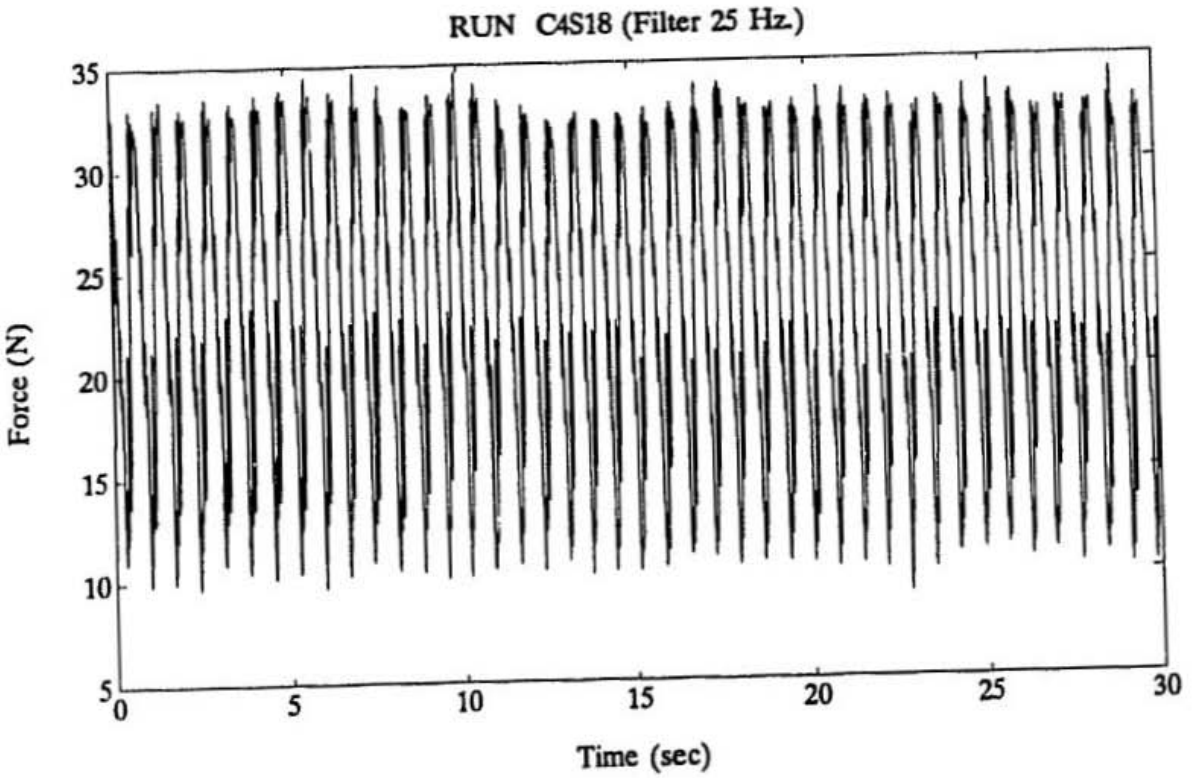
RUN C4S18 (Filter 25 Hz.)
Force (N)
Time (sec)
5
10
15
20
25
30
35

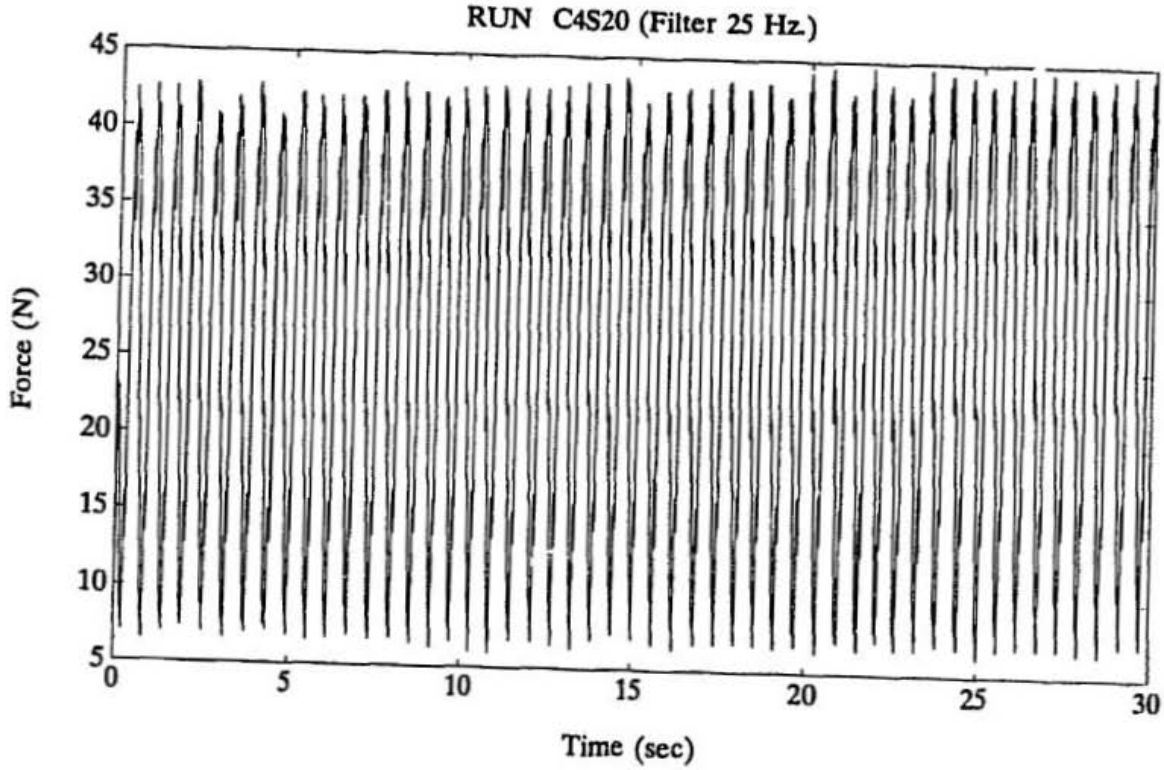
RUN C4S20 (Filter 25 Hz.)
Force (N)
Time (sec)
45
40
35
30
25
20
15
10
5
0
5
10
15
20
25
30

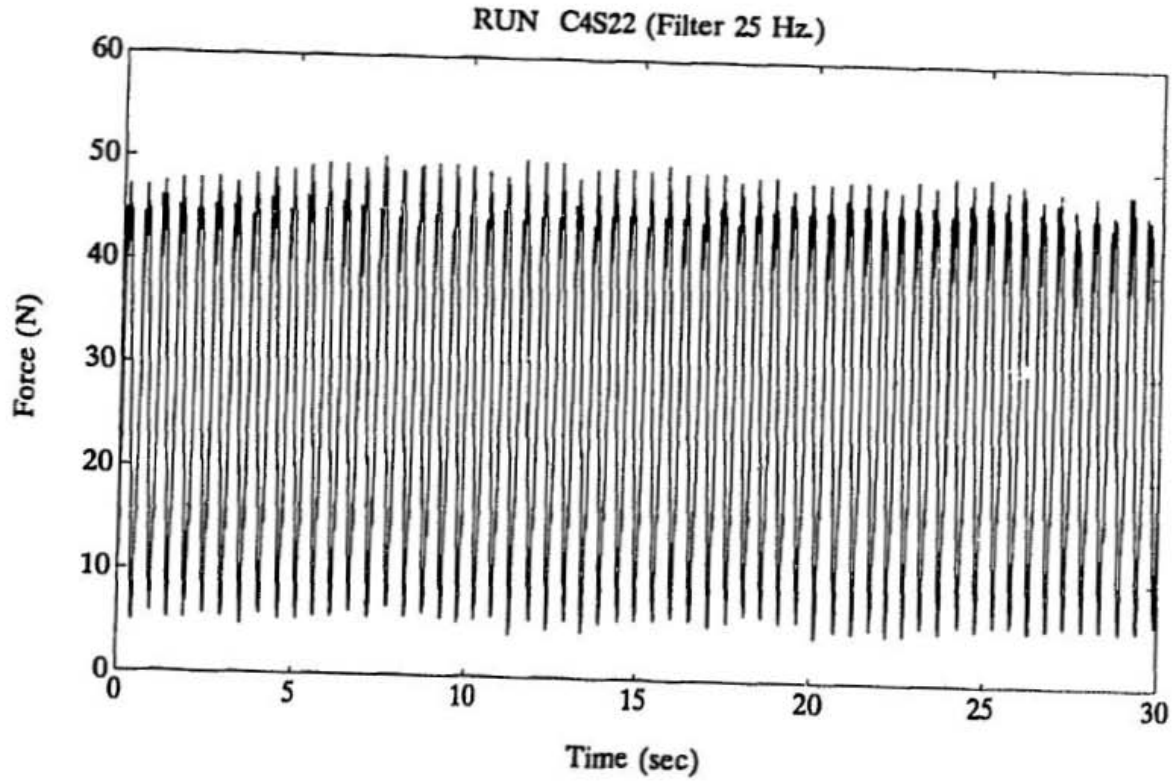
RUN C4S22 (Filter 25 Hz.)
Force (N)
Time (sec)
60
50
40
30
20
10
0
0
5
10
15
20
25
30

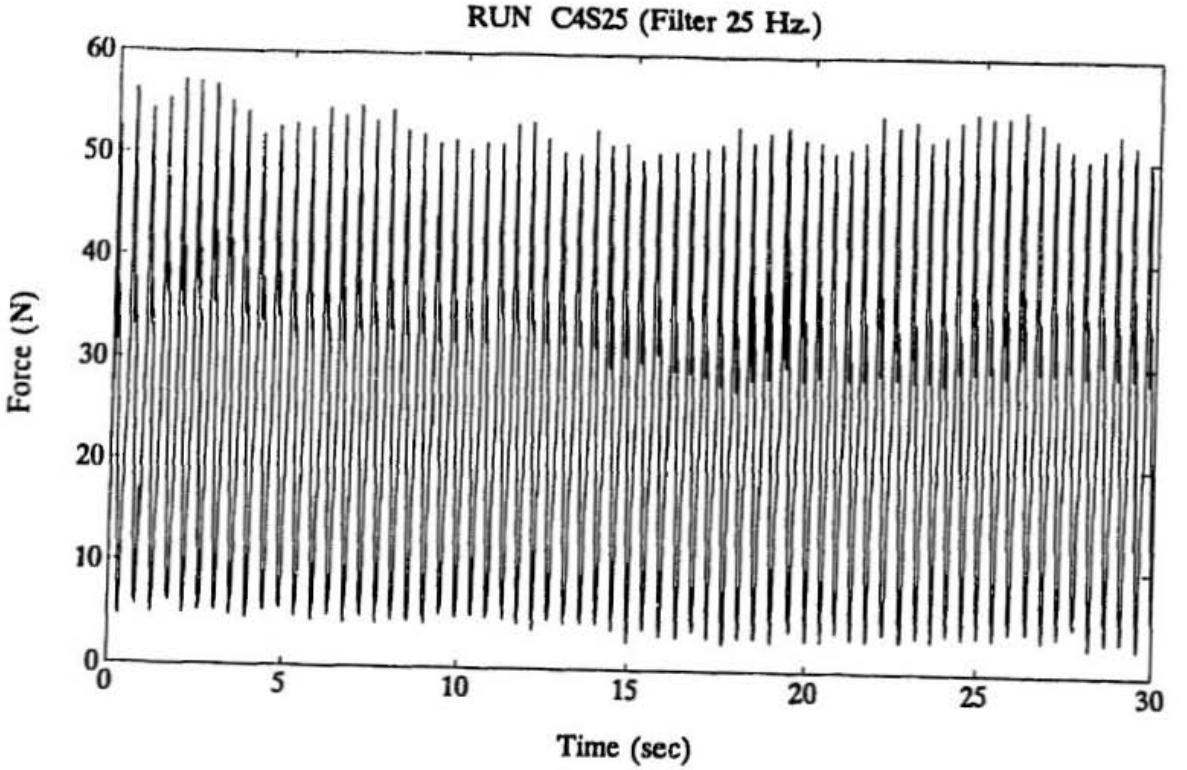
RUN C4S25 (Filter 25 Hz.)
Force (N)
Time (sec)
60
50
40
30
20
10
0
0
5
10
15
20
25
30

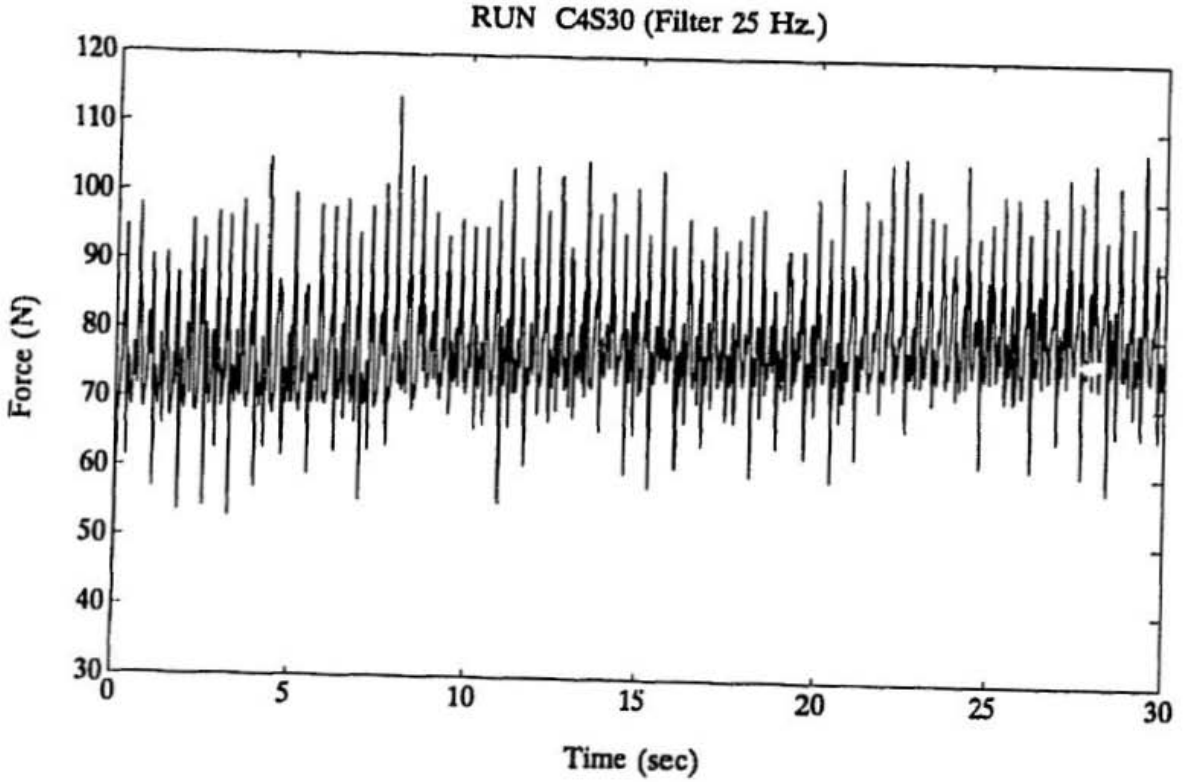
RUN C4S30 (Filter 25 Hz.)
Force (N)
Time (sec)
120
110
100
90
80
70
60
50
40
30
0
5
10
15
20
25
30